

**GADD45 β plays an essential role in the G-CSF
triggered granulocytic differentiation of human
hematopoietic stem cells**

Dissertation

der Mathematisch-Naturwissenschaftlichen Fakultät
der Eberhard Karls Universität Tübingen
zur Erlangung des Grades eines
Doktors der Naturwissenschaften
(Dr. rer. nat.)

vorgelegt von
Perihan Mir (geb. Mardan)
aus Kerkuk/Irak

Tübingen
2020

Gedruckt mit Genehmigung der Mathematisch-Naturwissenschaftlichen Fakultät der Eberhard Karls Universität Tübingen.

Tag der mündlichen Qualifikation: 02.07.2020

Dekan: Prof. Dr. Wolfgang Rosenstiel

1. Berichterstatter/in: Prof. Dr. Julia Skokowa

2. Berichterstatter/in: Prof. Dr. Klaus Schulze-Osthoff

Für meinen Vater

There are no incurable diseases - only the lack of will.

There are no worthless herbs - only the lack of knowledge.

Avicenna (Ibn Sina)

TABLE OF CONTENTS

ABBREVIATIONS	I
SUMMARY	V
ZUSAMMENFASSUNG	VI
LIST OF PUBLICATIONS	VII
PERSONAL CONTRIBUTION	IX
PARTICIPATION IN SCIENTIFIC CONFERENCES	XI
I. INTRODUCTION	1
Hematopoiesis	1
Granulocyte-colony stimulating factor (G-CSF).....	2
Development and clinical application.....	2
G-CSFR signaling cascade	3
Congenital neutropenia (CN)	5
GADD45 stress sensor proteins.....	7
Apoptosis and cell survival	8
Epigenetic role of GADD45 proteins.....	9
Role of GADD45 β in hematopoiesis	11
Role of GADD45 proteins in cancer.....	12
CRISPR/Cas9 technology as a tool to study hematopoiesis.....	14
II. OBJECTIVES OF THE STUDY	16
Mechanism of maturation arrest of granulopoiesis in congenital neutropenia	16

Disease modeling and gene therapy for congenital neutropenia	16
III. RESULTS & DISCUSSION	18
Mechanism of maturation arrest of granulopoiesis in congenital neutropenia	18
Disease modeling and gene therapy for congenital neutropenia	26
OUTLOOK.....	30
DANKSAGUNG	31
REFERENCES	32
APPENDIX I: LIST OF ACCEPTED PUBLICATIONS	A
APPENDIX II: LIST OF SUBMITTED MANUSCRIPTS	B

Abbreviations

ABBREVIATIONS

5caC	5-carboxylcytosine	CDC2	Cyclin dependent kinase
5fC	5-formylcytosine	CFU	Colony forming unit
5hmC	5-hydroxy methylcytosine	ChIP	Chromatin immunoprecipitation
5mC	5-methylcytosine	CHT	Caudal hematopoietic tissue
AID	Activation-induced cytidine deaminase	CLP	Common lymphoid progenitor
AKT	Protein kinase B	CMP	Common myeloid progenitor
AML	Acute myeloid leukemia	CNL	Chronic neutrophilic leukemia
APOBEC	Apolipoprotein B mRNA editing catalytic polypeptide-like	CORO1A	Coronin 1A
ATF	Activating transcription factor	CR6	Cytokine-responsive protein
ATRA	All-trans retinoic acid	CRISPR	Clustered regularly interspaced short palindromic repeats
AZU1	Azurocidin	crRNA	CRISPR RNA
BATF	Basic leucine zipper ATF-like transcription	CSF3R	Receptor for colony stimulating factor 3
BCL-X2	BCL2 associated X protein	CX3CR1	C-X3-C motif chemokine receptor 1
Bdnf 1X	Brain derived neurotrophic factor 1X	CXCR1	C-X-C motif chemokine receptor 1
BER	Base excision repair	DC	Dendritic cell
BIP	Binding immunoglobulin protein	DMP	Differentially methylated probes
BM	Bone marrow	DMR	Differentially methylated regions
BRCA1	Breast Cancer 1	DMS	Differentially methylated site
C/EBP	CCAAT/enhancer-binding protein	DNA	Desoxyribonucleic acid
Cas9	CRISPR associated protein 9	DNA	Desoxyribonucleic acid
CD	Cluster of differentiation	dpf	Days post fertilization

e.g.	For example	HCV	Hepatitis C virus
EB	Embryoid body	HDR	Homology-directed repair
ELANE	Neutrophil elastase	HIV	human immunodeficiency virus
EMP	Erythro-myeloid progenitors	HK3	Hexokinase 3
ER	Endoplasmic reticulum	hpf	Hours post fertilization
Er	Erythrocyte	HS(P)C	Hematopoietic stem (and progenitor) cells
ERa	Estrogen receptor alpha	IL-	Interleukin-
ERK	Extracellular signal-regulated kinase	Indel	Insertion deletion
FACS	Fluorescence activated cell sorting	INFg	Interferon gamma
FOXOA3	Forkhead box O-3	ING1	Inhibitor of growth family member 1
FPR	Formyl peptide receptor	iPSCs	Induced pluripotent stem cells
GADD45B	Growth arrest and DNA-damage-inducible 45, beta	IR	Infrared
G-CSF	Granulocyte-colony stimulating factor	JAK	Janus kinase
G-CSFR	G-CSF receptor	K	Lysine
GFP	Green fluorescent protein	kDa	Kilo dalton
GM-CSF	Granulocyte-monocyte colony stimulating factor	KLF4	Kruppel-like factor 4
GMP	Granulocyte-monocyte progenitor	KO	Knockout
GRB2	Growth factor receptor-bound protein 2	LEF1	Lymphoid enhancer-binding factor 1
gRNA	Guide RNA	LMPP	Lymphoid primed MPP
GvHD	Graft vs. host disease	lncRNA	Long non-coding RNA
h	Hour	LORD-Q	Long-run real-time PCR-based DNA-damage quantification
HAX1	HCLS1-associated protein X-1	LT-HSC	Long-term repopulating HSC
HCK	Hematopoietic cell kinase	LYN	Lck/Yes novel tyrosine kinase
HCLS1	Hematopoietic cell-specific Lyn substrate 1	MAPK	Mitogen-activated protein kinase
M-CSF	Monocyte colony stimulating factor	NLRP12	NLR family pyrin domain containing 12

Abbreviations

MEFV	Mediterranean fever	OCT4	Octamer-binding transcription factor 4
MEKK	Mitogen-activated protein kinase kinase kinase	OSKM	OCT4, SOX2, KLF4, MYC
min	Minutes	PB	Peripheral blood
Mk	Megakaryocyte	PCNA	Proliferating cell nuclear antigen
MKK	Mitogen-activated protein kinase kinase	pg	Picogram
ml	Milliliter	PH	Pleckstrin homology
MLP	Multi-lymphoid progenitor	PI3K	Phosphatidylinositol 3 kinase
MMR	Mismatch repair	PPAR	Peroxisome proliferator-activated receptors
MPO	Myeloperoxidase	PU.1	Purine-rich box
MPP	Multi-potent progenitor	RAR α	Retinoic acid receptor alpha
mRNA	Messenger RNA	RAS	Rat sarcoma
MTK1	Methylthioribose kinase	RNA	Ribonucleic acid
MyD118	Myeloid differentiation primary response 118	RNP	Ribonucleoprotein
MYL6	Myosin Light Chain 6	ROS	Reactive oxygen species
NAD ⁺	Nicotinamide adenine dinucleotide	RUNX1	Runt-related transcription factor 1
NAMPT	Nicotinamide phosphoribosyltransferase	RXR α	Retinoic X receptor alpha
NCF2	Neutrophil cytosolic factor 2	SCN/CN	Congenital neutropenia
NE	Neutrophil elastase	SH2	Src homology 2
NER	Nucleotide excision repair	SIRT	Sirtuin
NF κ B	Nuclear Factor Kappa B	SLPI	Secretory leukocyte peptidase inhibitor
NHEJ	Non-homologous end joining	SOCS3	Suppressor of cytokine signaling 3
NHRs	Nuclear hormone receptor	SOX2	SRY (sex determining region Y)-box 2
NK	Natural killer cell	SPI1	Spi-1 Proto-Oncogene
STAT	Signal transducers and activators of transcription		
ST-HSC	Short-term repopulating HSC		

SYK	Spleen tyrosine kinase
TCR	T-cell receptor
TDG	Thymine-DNA glycosylase
TET	Ten-eleven translocation methylcytosine dioxygenase
TFPI	Tissue factor pathway inhibitor
TGFb	Transforming growth factor beta
Th1	T helper cells
TNFa	Tumor necrosis factor alpha
tracrRNA	Trans-activating CRISPR RNA
UPR	Unfolded protein response
UV	Ultraviolet
W	Tryptophan
XPG	Xeroderma Pigmentosum Complementation Group G
Y	Tyrosine

SUMMARY

Congenital neutropenia (CN) is a bone marrow failure syndrome caused by inherited gene mutations in *e.g.*, *ELANE* or *HAX1* leading to markedly low neutrophil numbers in peripheral blood. The mechanism of the “maturation arrest” of myeloid progenitors in CN patients is not fully elucidated. We aimed to shed light on the pathomechanism of this bone marrow failure. Considering the fact that inherited mutations may disturb the fitness of hematopoietic stem and progenitor cells (HSPCs) and may cause deregulated differentiation, we first investigated the CN HSPC composition and stress levels. Indeed, we found that early HSCs showed higher stress levels than later progenitors. Moreover, despite G-CSF treatment, CN HSPCs were committed towards lymphopoiesis, rather than myelopoiesis. We identified the myeloid differentiation primary response (MyD) and stress sensor gene *GADD45 β* that might play a role in the defective stress-induced granulopoiesis: G-CSF induced the expression of *GADD45 β* in healthy individuals, but not in CN patients. We functionally elaborated the role of *GADD45 β* in stress response and granulopoiesis by CRISPR/Cas9-mediated knockout in iPSCs, primary HSPCs, and zebrafish. Since CRISPR/Cas9 gene-editing in iPSCs and HSPCs is challenging, we established a method that allows the fluorescent labeling of CRISPR/Cas9 RNP and thus the enrichment of gene-edited cells. *GADD45 β* knockout cells were significantly more susceptible to UV-mediated DNA damage compared to control cells. Knockout of *GADD45 β* leads to drastic reduction of granulocytes *in vitro* and *in vivo*. At the same time, the ectopic expression of *GADD45 β* in CN HSPCs restored granulocytic differentiation. We could show that *GADD45 β* is responsible for the demethylation and thus induction of genes essential for granulocytic differentiation. Among others, *GADD45 β* activates the retinoic acid signaling pathway to induce granulopoiesis. Strikingly, the treatment of CN HSPCs with ATRA could bypass the *GADD45 β* activation and rescued diminished neutrophil differentiation. Taken together, we could show that *GADD45 β* regulates granulopoiesis downstream of G-CSF by modulating retinoic acid signaling. To further elaborate the mechanisms of defective granulopoiesis in CN, we established an iPSC model. Research on rare diseases requires valuable patient samples, which are very restricted in the case of pediatric patients. iPSC models may overcome these limitations. This model allows us to study CN pathogenesis, but also to test novel therapies. Using the iPSC model, we were able to set up a CRISPR/Cas9-based *ELANE* knockout to restore granulocytic differentiation. This approach could serve as gene therapy for CN patients.

ZUSAMMENFASSUNG

Kongenitale Neutropenie (CN) ist ein Knochenmarkdefekt verursacht durch vererbte Mutationen in z.B. *ELANE* oder *HAX1*, die zum Mangel an reifen Neutrophilen im Blut führen. Der Mechanismus des Ausreifungsstopps der myeloischen Vorläufer in CN-Patienten ist derzeit nicht aufgeklärt. Ziel der Arbeit war es den Mechanismus dieses Knochenmarkdefekts zu erforschen. Da die vererbten Mutationen die Integrität der hämatopoetischen Stammzellen (HSZ) stören und so die Differenzierung beeinflussen können, untersuchten wir die Zusammensetzung der HSZ und deren Stresslevel. Tatsächlich konnten wir feststellen, dass sehr frühe HSZ höhere Stresslevel aufwiesen als spätere Vorläuferzellen. Darüber hinaus differenzieren CN-HSZ trotz G-CSF-Behandlung eher in lymphatische statt myeloische Zellen. Wir identifizierten das „myeloid differentiation primary response (MyD)“- und Stresssensor-Gen *GADD45 β* als möglichen Grund für die gestörte Stress-induzierte Myelopoese. In gesunden Spendern wird die Expression von *GADD45 β* durch G-CSF induziert, dies ist jedoch nicht der Fall in CN. Wir untersuchten die Rolle von *GADD45 β* in der Granulopoese mit Hilfe von CRISPR/Cas9 vermittelten Gen-Knockout (KO) in iPSZ (induzierte pluripotente Stammzellen) und HSZ *in vitro* sowie in Zebrafisch Embryonen *in vivo*. Da CRISPR/Cas9 Gen-Modifizierung in iPSZ und primären HSZ eine Herausforderung darstellt, entwickelten wir eine Methode, um das CRISPR/Cas9 Ribonucleoprotein (RNP) fluoreszierend zu markieren. Dies ermöglicht die durchflusszytometrische Anreicherung Gen-modifizierter Zellen. Der *GADD45 β* KO führte *in vitro* und *in vivo* zur drastisch reduzierten neutrophilen Differenzierung. Gleichzeitig führte die ektopische Expression von *GADD45 β* in CN-HSZ zur Wiederherstellung der Granulopoese. Wir konnten zeigen, dass *GADD45 β* für die Demethylierung von Neutrophil-assoziierten Genen zuständig ist. Unter anderem aktiviert *GADD45 β* den Retinsäure-Signalweg, um die neutrophile Differenzierung zu induzieren. Interessanterweise, konnten wir durch die Behandlung von CN-HSZ mit ATRA die *GADD45 β* -Aktivierung umgehen und somit die Granulopoese wiederherstellen. Zusammengefasst konnten wir zeigen, dass *GADD45 β* die G-CSF-abhängige Granulopoese durch die Aktivierung des Retinsäure-Signalwegs reguliert.

Um die Mechanismen der gestörten Granulopoese in CN aufzuklären, etablierten wir ein CN-iPSZ-Modell. Die Erforschung von seltenen Erkrankungen erfordert Untersuchungen an primären Patientenproben, die im Fall von pädiatrischen Erkrankungen limitiert sind. Das iPSZ-Modell hilft dabei diese Limitierung zu umgehen, die CN Pathogenese zu verstehen und ggf. neue Therapieansätze zu entwickeln. Mithilfe von CN-iPSZ konnten wir den CRISPR/Cas9 KO von *ELANE* testen, um die Granulopoese wiederherzustellen. Dieser Ansatz könnte in Zukunft als Gentherapie für CN-Patienten angewendet werden.

LIST OF PUBLICATIONS

All relevant publications are listed below. The author contribution is highlighted in bold.

- A. M. Nasri*, **P. Mir***, B. Dannenmann, D. Amend, T. Skroblyn, Y. Xu, K. Schulze-Osthoff, M. Klimiankou, K. Welte and J. Skokowa, '*Fluorescent labeling of CRISPR/Cas9 RNP for gene knockout in HSPCs and iPSCs reveals an essential role for GADD45 β in stress response*', *Blood Advances*, vol. 3, no. 1, p. 63-71, January 2019. (*equal contribution)
- B. **P. Mir**, M. Klimiankou, B. Dannenmann, N. Aghaallaei, M. Nasri, S. Wingert, F. Thalheimer, B. Findik, L. Doll, M. Ritter, T. Thumberger, S. Kandabarau, C. Zeidler, M. Rieger, B. Bajoghli, K. Welte and J. Skokowa, '*GADD45 β -mediated active gene demethylation is essential for G-CSF-triggered granulocytic differentiation*', manuscript in revision.
- C. **P. Mir**, M. Ritter, K. Welte, J. Skokowa and M. Klimiankou, '*Gene Knockout in Hematopoietic Stem and Progenitor Cells Followed by Granulocytic Differentiation*', RNA Interference and CRISPR Technologies, *Methods in Molecular Biology*, vol. 2115, p. 455-469, February 2020
- D. M. Nasri, M. Ritter*, **P. Mir***, B. Dannenmann*, N. Aghaallaei, D. Amend, V. Makaryan, Y. Xu, B. Fletcher, R. Bernhard, I. Steiert, K. Hähnel, J. Berger, I. Koch, B. Sailer, K. Hipp C. Zeidler, M. Klimiankou, B. Bajoghli, D. C. Dale, K. Welte and J. Skokowa, '*CRISPR/Cas9 mediated ELANE knockout enables neutrophilic maturation of primary hematopoietic stem and progenitor cells and induced pluripotent stem cells of severe congenital neutropenia patients*', *Haematologica*, vol. 105, no. 3, p. 598-609, June 2019. (*equal contribution)
- E. B. Dannenmann, A. Zahabi, **P. Mir**, B. Oswald, R. Bernhard, M. Klimiankou, T. Morishima, K. Schulze-Osthoff, C. Zeidler, L. Kanz, N. Lachmann, T. Moritz, K. Welte and J. Skokowa, '*Human iPSC-based model of severe congenital neutropenia reveals elevated UPR and DNA damage in CD34⁺ cells preceding leukemic transformation*', *Experimental Hematology*, vol. 71, p. 51-60, January 2019.

- F. **P. Mir**, M. Klimiankou, B. Findik, K. Haehnel, S. Mellor-Heineke, C. Zeidler, J. Skokowa, K. Welte, '*New insights into the pathomechanism of cyclic neutropenia*', *Annals of the New York Academy of Science*, accepted January 2020.
- G. B. H. Alvarez*, J. Skokowa*, M. Coles* , **P. Mir**, L. Weidmann, K. W. Rogers, K. Welte, A. Lupas, P. Müller, M. ElGamacy, '*Design of novel granulopoietic proteins by topological rescaffolding*', manuscript in revision. (*equal contribution)
- H. B. H. Alvarez*, J. Skokowa*, M. Coles , **P. Mir**, K. W. Rogers, K. Maksymenko, M. Nasri, K. Welte, A. Lupas, P. Müller, M. ElGamacy, '*A topological refactoring design strategy yields highly stable granulopoietic proteins*', manuscript in revision. (*equal contribution)
- I. Y. Xu, M. Nasri, B. Dannenmann, **P. Mir**, A. Zahabi, K. Welte, Tatsuya Morishima*, Julia Skokowa*, '*NAMPT/SIRT2-mediated inhibition of the p53-p21 signaling pathway is indispensable for maintenance and hematopoietic differentiation of human iPS cells*', manuscript in revision. (*equal contribution)

PERSONAL CONTRIBUTION

The following section indicates the personal contribution to each of the above listed publications.

- A. Co-first author, main investigator (together with M. Nasri). Involved in designing the study, performing experiments, analyzing & interpreting the data and preparing the manuscript.
- B. First author, main investigator. Major role in study design (together with J. Skokowa). Performed experiments, analyzed & interpreted the data. Main role in preparing the manuscript (together with J. Skokowa).
- C. First author, role in structural design of book chapter (together with M. Klimiankou and J. Skokowa), wrote sections for CD34⁺ hematopoietic stem cell isolation and expansion, CRISPR/Cas9 RNP nucleofection, estimation of CRISPR/Cas9 gene editing efficiency, characterization of myeloid differentiation of HSPCs. Main role in preparing figures and figure legends.
- D. Co-second author (together with M. Ritter and B. Dannenmann). Performed colony-forming unit (CFU) assay and liquid culture differentiation of CN patient-derived hematopoietic stem and progenitor cells with or without *ELANE* knockout towards neutrophils, analyzed & interpreted the data and was involved in manuscript preparation.
- E. Third author, conducted, analyzed and interpreted DNA damage measurements by LORD-Q. Participated in manuscript preparation.
- F. First author, performed flow cytometric analysis of CyN patient BMMNCs, gH2AX assay, CFU, analyzed and interpreted the data and was involved in manuscript preparation.
- G. Second author, conducted liquid culture differentiation of healthy donor HSPCs treated with modified hG-CSF versions, evaluated and summarized results by flow cytometry and morphologic analysis, was involved in manuscript preparation.

- H. Third author, conducted liquid culture differentiation of healthy donor HSPCs treated with modified hG-CSF versions and neutrophil functional assays, evaluated and summarized the results, was involved in manuscript preparation.

- I. Fourth Author, assisted with the analysis of p53 expression and interpreting the data.

PARTICIPATION IN SCIENTIFIC CONFERENCES

- A. **P. Mir**, M. Klimiankou, B. Dannenmann, N. Aghaallaei, M. Nasri, B. Findik, M. Rieger, C. Zeidler, B. Bajoghli, K. Welte, J. Skokowa, '*GADD45b plays an essential role in the G-CSF triggered granulocytic differentiation of human hematopoietic cells*', Oral presentation, **Best Abstract Award, Best of DGHO 'Translational Medicine'**, Annual meeting of German Society of Hematology and Oncology (DGHO), Berlin, 2019
- B. **P. Mir**, M. Klimiankou, N. Aghaallaei, M. Nasri, B. Findik, F. Thalheimer, S. Wingert, M. Rieger, T. Thumberger, C. Zeidler, B. Bajoghli, K. Welte, J. Skokowa, '*Active DNA demethylation mediated by GADD45 β is essential during G-CSF triggered granulocytic differentiation*', Oral presentation, **winner of ASH Abstract Achievement Award**, Annual meeting of the American Society of Hematology (ASH), Orlando, 2019
- C. **P. Mir**, M. Nasri, B. Dannenmann, M. Klimiankou, B. Findik, R. Bernhard, M. Rieger, L. Kanz, C. Zeidler, K. Welte, J. Skokowa, '*GADD45b plays an essential role in the G-CSF triggered granulocytic differentiation of human hematopoietic cells*', Oral presentation, XXXII. Kind-Philipp meeting on pediatric hematology and oncology research, Wilsede, 2019
- D. **P. Mir**, M. Nasri, B. Dannenmann, M. Klimiankou, B. Findik, R. Bernhard, M. Rieger, L. Kanz, C. Zeidler, K. Welte, J. Skokowa, '*GADD45b plays an essential role in the G-CSF triggered granulocytic differentiation of human hematopoietic cells*', Oral presentation, **winner of ASH Abstract Achievement Award**, ASH annual meeting, San Diego, 2018
- E. **P. Mir**, M. Nasri, B. Dannenmann, K. Haehnel, M. Klimiankou, C. Zeidler, L. Kanz, K. Welte, J. Skokowa, '*Abrogated GADD45b-mediated integrity control of hematopoietic stem cells upon ER stress and DNA damage triggers lymphopoiesis over granulopoiesis in congenital neutropenia*', Oral presentation, **winner of ASH Abstract Achievement Award**, ASH annual meeting, Atlanta, 2017

- F. **P. Mir**, M. Klimiankou, C. Zeidler, L. Kanz, K. Welte, J. Skokowa, '*Deregulated Integrity Control of HSC Pool with Elevated UPR and DNA Damage Responses in Hematopoietic Cells of CN Patients*', Poster presentation, **winner of Travel Grant Award**, Annual meeting of International Society of Experimental Hematology (ISEH), Frankfurt, 2017
- G. **P. Mir**, M. Klimiankou, C. Zeidler, L. Kanz, K. Welte, J. Skokowa, '*Deregulated Integrity Control of HSC Pool with Elevated UPR and DNA Damage Responses in Hematopoietic Cells of CN Patients*', Oral presentation, DGHO, Stuttgart, 2017
- H. **P. Mir**, M. Klimiankou, B. Dannenmann, C. Zeidler, K. Schulze-Osthoff, L. Kanz, K. Welte, J. Skokowa, '*Impaired DNA Damage Repair in Severe Congenital Neutropenia Patients*', Poster presentation, ASH annual meeting, San Diego, 2016

I. INTRODUCTION

Hematopoiesis

The hematopoietic tissue is a highly regenerative and tightly regulated system as it must produce around 5×10^{12} new blood cells daily to maintain proper blood cell functions¹. Hematopoietic stem cells (HSCs) keep the balance between self-renewal and differentiation. HSCs give rise to committed progenitors which differentiate to mature blood cells on the one hand and to a new HSC maintaining the pool size throughout life, on the other. This process is called asymmetric cell division. Multipotent progenitors are sub-divided into three functionally distinct populations, the long-term repopulating HSCs (LT-HSCs), the short-term repopulating HSCs (ST-HSCs), and the multipotent progenitors (MPPs). LT-HSCs are quiescent, self-renewing cells generating ST-HSCs upon commitment, which in turn are restricted in self-renewal^{2, 3}. The classical model of hematopoiesis postulates a developmental hierarchy^{4, 5} with HSCs at the apex that differentiate to MPPs without detectable self-renewal capacity. The earliest fate decision in this model is the divergence into oligopotent common myeloid or common lymphoid progenitors (CMP or CLP, respectively)^{6, 7}. CLPs further differentiate to B-/ T-/ natural killer cell (NK)- and dendritic cell (DC)-progenitors for plasmacytoid, and killer DCs^{6, 8, 9}. CMPs generate granulocyte/monocyte progenitors (GMP), megakaryocyte/erythrocyte progenitors (MEP), and DC progenitors for Langerhans/interstitial/myeloid DCs^{7, 9, 10}. However, recent studies identified lymphoid-primed multipotent progenitors (LMPPs), which lacked the megakaryocyte-erythroid (Mk-Er) potential, suggesting that Mk-Er progenitors branch off before lympho-myeloid specification¹¹⁻¹³. Direct differentiation of HSCs to Mks might indicate the crucial role of Mk cells in HSC regulation. In the murine BM niche, LT-HSCs are in close proximity to Mks which conserve their quiescence¹⁴. However, upon myeloablation, Mks secrete cytokines to induce HSC expansion leading to regeneration of the myeloid lineage^{15, 16}. Among others, Notta et al. challenged the paradigms of hematopoiesis by proving that not only the multipotent HSCs, but also CMPs are heterogeneous and are primarily composed of unipotent myeloid or erythroid progenitors with less megakaryocyte potential¹⁷.

Previously, they showed that multi-lymphoid progenitors (MLPs) could differentiate to the monocytic lineage upon treatment with myeloid cytokines¹⁷⁻¹⁹. In agreement with these findings, Görgens et *al.* described a model in which MPPs give rise to LMPPs and EMPs (erythro-myeloid progenitors) by asymmetric cell division. While LMPPs generate GMPs and MLPs both exhibiting monocytic potential, EMPs obtain the potential to generate Mk-Er, basophils, and eosinophils²⁰.

Based on these observations, hematopoiesis is a complex and highly evolving research field. Future research will exploit the definitive mechanisms regulating hematopoietic differentiation.

Granulocyte-colony stimulating factor (G-CSF)

Development and clinical application

G-CSF is a cytokine that mainly regulates neutrophil differentiation, mobilization, and activation²¹. In healthy individuals, G-CSF levels in serum are relatively low (<30 – 170 pg/ml)²², while upon acute infection, they rise dramatically to a range of 30 – 3199 pg/ml²³. Elevated serum G-CSF levels upon infection induce survival, proliferation, and differentiation of granulocytic progenitor cells in the bone marrow. The capability of the bone marrow to react to the acute demand of neutrophils is called ‘emergency granulopoiesis’. Mice lacking G-CSF show neutropenic phenotype and are more susceptible to infections than their healthy counterparts²⁴. In addition to granulopoiesis-inducing functions, G-CSF was also shown to stimulate proliferation and mobilization of hematopoietic stem/progenitor cells (HSPCs) from the bone marrow to peripheral blood²⁵. The capability of G-CSF to induce proliferation and mobilization of HSPCs into peripheral blood and to increase absolute neutrophil counts within few hours made it essential for clinical applications. Considerable effort was made to resolve the structure and to produce recombinant human G-CSF. Eventually, in 1985 recombinant human G-CSF (rhG-CSF, trade name: *Filgrastim*) was purified and characterized by Welte et *al.*, and in 1991, it was approved in the USA for clinical treatment of chemotherapy-related neutropenia in cancer patients²⁶.²⁷ Since that time, *Filgrastim* has been approved in more than 70 countries for the treatment of acquired and inherited neutropenias, myelodysplastic syndromes (MDS), acute leukemia, myelosuppression after bone marrow transplantation, aplastic anemia, and mobilization of HSPCs into the peripheral blood for

Introduction

transplantations²⁷. The administration of rhG-CSF to neutropenia patients increased blood neutrophil counts, prolonged patient's life-span, and markedly improved quality of life²⁸.

G-CSFR signaling cascade

In the hematopoietic system, the G-CSF receptor (G-CSFR) is expressed on HSCs (low expression levels) and highly expressed on cells of the myeloid lineage. The G-CSFR is a transmembrane protein consisting of 813 amino acids without intrinsic tyrosine kinase activity. Upon ligand binding, the G-CSFR undergoes homodimerization, followed by conformational changes leading to autophosphorylation and the activation of downstream signaling pathways. The intracellular domain of the G-CSFR consists of three distinct box regions. Box1 and box2 are mainly responsible for the transduction of cell proliferation-inducing signal cascades, while box3 is essential for differentiation²⁹. Signaling cascades of activated G-CSFR are mediated by four tyrosine (Y) residues (Y704, Y729, Y744, and Y764) in the intracellular tail, which provide docking sites for intracellular signaling molecules via their SRC homology 2 (SH2) domains. SH2-containing proteins as for example STAT3, SOCS3, the adaptor proteins SHC, GRB2, and the tyrosine phosphatase SHP2, possess docking sites for phosphorylated tyrosines on the G-CSFR³⁰. In addition, the G-CSFR intracellular domain contains conserved lysines (K632, K672, K681, K682, and K762) that serve as ubiquitination sites regulating the receptor routing and recycling³¹.

Activated signal transduction pathways downstream of G-CSFR include the JAK/STAT, PI3K/AKT, and MAPK/ERK pathways. The major kinase group activated upon G-CSF signaling is JAK family of kinases consisting of JAK1, JAK2, TYK2, and SRC kinases (e.g. LYN, HCK). The main functions of G-CSFR rely on the JAK and SRC pathways. Upon G-CSF binding, G-CSFRs dimerize and phosphorylate JAK2 which is mediated by tryptophan (W) 650 residue³². Active JAK2 phosphorylates STAT proteins, which then dimerize and translocate into the nucleus, mediating the expression of their target genes. Among the target genes of STAT3 is the cyclin-dependent kinase inhibitor p27^{kip1} which promotes differentiation by arresting the cell cycle. JAKs also activate STAT5 which induces proliferation and survival. The signal integration of STAT3 and STAT5 is vital in orchestrating myeloid lineage proliferation versus differentiation³⁰. Active G-CSFR has been shown to induce

membrane-proximal phosphatidylinositol-3 kinase (PI3K), which in turn activates pleckstrin homology (PH) domain-containing proteins, for instance, AKT. It is not yet elucidated whether this activation happens in a JAK2-dependent or -independent manner. SRC kinases might stimulate the PI3K/AKT pathway downstream of G-CSFR³³. The PI3K/AKT cascade regulates the cell cycle by directly influencing cellular proliferation and quiescence. It also blocks apoptosis and is crucial for the proliferation of myeloid progenitor cells in a G-CSF dependent manner³⁴. G-CSFR phosphorylation at Y764 induces activation of the MAPK/ERK, p38 and Jun N-terminal kinase (JNK) through the RAS pathway. The RAS pathway promotes the proliferation of myeloid progenitors and attenuates differentiation via ERK1/2³⁵ and p38³⁶. Another critical player in the G-CSF signal transduction cascade is the tyrosine protein phosphatase SHP2 which activates Lyn³⁷. Together with SYK, LYN phosphorylates and thus activates hematopoietic lineage cell-specific protein (HCLS1)³⁸. HCLS1 is an interaction partner of HCLS1 associated protein X1 (HAX1). Our laboratory previously demonstrated that the HCLS1-HAX1 complex interacts with the transcription factor lymphoid-enhancer binding factor 1 (LEF-1), leading to its nuclear translocation³⁹. Nuclear LEF-1 directly binds to the promoter and activates the transcription of the myeloid transcription factor *C/EBPA* (CCAAT/enhancer-binding protein alpha)^{39, 40}. *C/EBPα* is an essential transcription factor regulating 'steady-state' granulopoiesis by transcriptionally activating myeloid differentiation genes, e.g. *G-CSFR*⁴¹. Of note, in granulocytic progenitors of congenital neutropenia (CN) patients *HCLS1*, *LEF-1*, and *C/EBPA* expressions are severely diminished, thus 'steady-state' granulopoiesis is abrogated. Alternatively, G-CSF treatment induces the 'emergency granulopoiesis' in HSPCs of CN patients by activating nicotinamide phosphoribosyltransferase (NAMPT). NAMPT subsequently activates NAD⁺-dependent protein deacetylases, sirtuins (SIRT) that deacetylate and activate *C/EBPβ*⁴².

Negative regulation of the G-CSFR downstream signaling is mediated by receptor internalization, ubiquitination, and degradation⁴³ as well as by SOCS3 (suppressor of cytokine signaling 3). SOCS3 binds to the receptor at phospho-Y729 and prevents JAK-driven STAT activation⁴⁴. G-CSFR that lacks the negative regulatory sites is hyperactive and may promote malignant transformation as is frequently observed in CN-associated AML^{44, 45}.

Introduction

Myeloid disorders that are associated with acquired G-CSFR mutations include CN, MDS, AML⁴⁶, chronic neutrophilic leukemia (CNL) and atypical chronic myeloid leukemia⁴⁷. CN is the most predominant disease related to acquired G-CSFR mutations with a high risk to undergo malignant transformation to MDS or AML⁴⁵. In CN, G-CSFR mutations leading to a premature stop-codon are reported to be the initial drivers of leukemogenesis, providing the HSPC clones with growth advantage and pre-leukemia. Acquisition of additional cooperating mutations in *e.g.* *RUNX1*, ultimately contribute to leukemia progression in CN patients⁴⁸.

Congenital neutropenia (CN)

CN, also referred to as Kostmann syndrome, was described as a pre-leukemic bone marrow failure syndrome characterized by impaired neutrophil maturation. CN patients have a maturation arrest of granulopoiesis in the bone marrow at the level of promyelocytes^{49, 50}. The majority of CN patients respond to daily treatment with relatively high doses of rhG-CSF that results in an increase of neutrophil numbers and markedly diminished frequency of bacterial infections^{28, 51}. The cumulative incidence of MDS or leukemia in CN patients is around 22 % after 10 years^{52, 53}.

Inherited mutations in several genes are associated with CN. The most common cause of CN is an autosomal-dominant mutation in the *ELANE* gene encoding for the neutrophil elastase (NE). Depending on the mutated protein domain, *ELANE* mutations may cause the accumulation of mislocalized⁵⁴ or misfolded NE inducing ER stress and activating the unfolded protein response (UPR)⁵⁵⁻⁵⁸. Interestingly, autosomal dominant *ELANE* mutations are also the main cause of cyclic neutropenia (CyN)⁵⁹. CyN is characterized by oscillating blood neutrophil counts within a period of 21 days⁶⁰. The reason why HSCs of CyN patients cannot maintain a consistent neutrophil count is poorly understood. Treatment of CyN patients with rhG-CSF improves absolute neutrophil counts and shortens the cycle periodicity from 21 to 14 days⁶¹. CyN patients have a lower risk of developing MDS/AML⁶². It is not fully understood why the same *ELANE* mutations activate UPR in CN patients, while this is not the case in CyN patients. One explanation might be the difference in secretory leukocyte protease inhibitor (SLPI) levels, which is the natural inhibitor of NE. In CN, SLPI expression is diminished and thus cannot prevent the induction of UPR by mutated NE⁶³.

Consanguinity is the cause of the autosomal-recessive inheritance of mutations in the *HAX1* (HCLS1-associated protein X-1) gene leading to CN⁶⁴. *HAX1* is a protein with pre-dominant mitochondrial localization involved in the maintenance of the inner mitochondrial membrane potential^{64, 65}. However, it was shown by several studies that *HAX1* also serves as an interaction partner for cellular proteins, including *HCLS1*^{39, 66-69}. Neutropenia in *HAX1*-CN patients probably arises from the abrogated activation of the *HCLS1* due to the absence of functional *HAX1* protein³⁹ and the apoptosis of myeloid progenitors caused by mitochondrial dysfunctions⁶⁴.

Although having different genetic disease backgrounds, the different CN patient groups show similar disease phenotypes suggesting the dysregulation of common transcriptional regulators or signaling pathways⁷⁰. This might be caused by the internal stress in HSCs carrying the inherited mutations. Several studies showed that HSCs, when suffering from ER stress or DNA damage, undergo differentiation or apoptosis to maintain the HSC pool integrity and avoid malignant transformation of 'stressed' HSCs⁷¹⁻⁷³.

Myeloid lineage commitment is regulated by the combinatorial effect of several key transcription factors. *C/EBP α* and *PU.1* are essential regulators of myeloid development. During granulocytic differentiation, *C/EBP α* is upregulated and *PU.1* is repressed, whereas monocytic differentiation requires active *PU.1* and suppressed *C/EBP α* ⁷⁴. Myeloid abnormalities or malignancies are often caused by the aberrant expression or deregulated ratio of these key transcription factors^{75, 76}. Indeed, the myeloid progenitors of CN patients are more committed towards monocytopoiesis rather than granulopoiesis. This results from the disrupted ratio of *PU.1* to *C/EBP α* expression levels with shift towards elevated *PU.1* expression in CN progenitor cells⁷⁰. Additionally, myeloid cells of CN patients, in contrast to patients with other types of neutropenia, show abrogated *LEF-1* expression and thus the lack of its target gene *C/EBP α* ⁴⁰. An additional role for *LEF-1* in regulating granulopoiesis was shown to underlie in the transcriptional inhibition of *PU.1* transcription factor⁷⁷, thus favoring granulopoiesis over monocytopoiesis. While the steady-state granulopoiesis requires *LEF-1* and *C/EBP α* , CN patients respond to G-CSF mainly by activating *NAMPT*⁴². *NAMPT* converts nicotinamide into nicotinamide mononucleotide which in turn is converted to NAD^+ . The levels of NAD^+ regulate functions of NAD^+ -dependent

Introduction

enzymes, sirtuins, linking sirtuin activity to the metabolic activity of the cell. Sirtuins are lysine deacetylases for histones and non-histone proteins, playing an important role in transcriptional regulation⁷⁸⁻⁸⁰. In healthy individuals, SIRT1 induces C/EBP α and C/EBP β expression downstream of G-CSF. In CN patients, however, C/EBP α is severely diminished, thus cytokine-induced 'emergency' granulopoiesis via the NAMPT-NAD⁺-SIRT1-C/EBP β axis compensates the missing C/EBP α functions^{70, 81} (Figure 1).

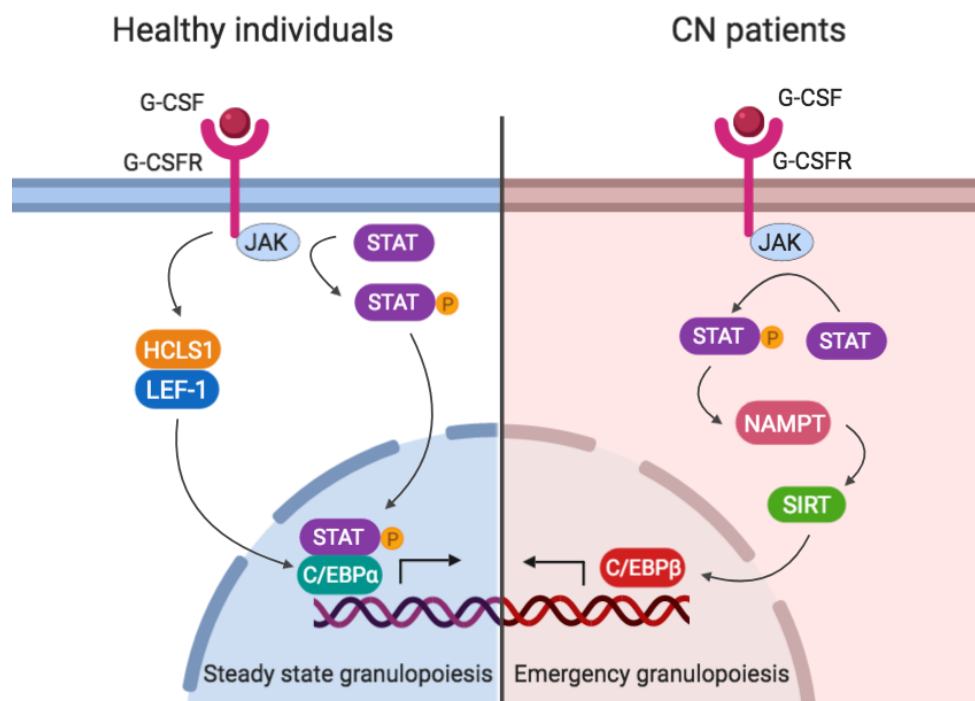


Figure 1: Transcriptional regulation of granulopoiesis in healthy individuals vs. CN patients. In healthy individuals, G-CSF triggers a signaling cascade including JAK/STAT and HCLS1-LEF-1 activation leading to the expression of C/EBP α which in turn mediates steady-state granulopoiesis. In CN patients, however, the HCLS1-LEF-1-C/EBP α axis is markedly diminished. Thus, emergency granulopoiesis relies on the NAMPT/SIRT axis leading to the activation of C/EBP β . The scheme was created with BioRender.

GADD45 stress sensor proteins

The growth arrest and DNA damage inducible 45 (GADD45) proteins family consists of three members: GADD45 α (also known as GADD45 or DNA damage-inducible

transcript 1, DDIT1), GADD45 β (also known as myeloid differentiation primary response 118, MyD118) and GADD45 γ (also known as cytokine response gene 6, CR6). GADD45 proteins are small (18 kDa), highly acidic and rapidly inducible upon physiological (e.g. cytokines) and environmental (e.g. IR/UV irradiation, DNA damaging agents) stress stimulation⁸². The genes encoding for GADD45 α , GADD45 β and GADD45 γ are located on chromosomes 1p31.3, 19p13.3 and 9q22.2, respectively. GADD45 proteins are highly conserved among metazoa and are very similar to each other, with around 55 % of amino acid sequence homology⁸². *GADD45* genes have independent regulatory elements and their expression is different in various tissues suggesting different content-dependent functions. GADD45 α is directly regulated by p53 and is induced by UV irradiation⁸³. GADD45 β is the only family member of which the expression is regulated by TGF β ⁸⁴ and TNF α ⁸⁵, while IL-3, IL-6, G-CSF, and GM-CSF induce both GADD45 β and GADD45 γ ⁸⁶. Although similar stimuli activate GADD45 genes, their roles in stress response are specific to stimulus and tissue type⁸⁷.

GADD45 proteins are adapter proteins without catalytic activity and are implicated in many intracellular pathways such as cell cycle arrest, DNA repair, apoptosis, or cell survival by direct interaction with other proteins. For proper functions, GADD45 proteins form homo- or heterodimers⁸⁸.

Apoptosis and cell survival

In response to genotoxic stress, GADD45 proteins may induce cell cycle arrest by interacting with the CDC2/CyclinB1 complex to inhibit CDC2 kinase activating the G2/M checkpoint^{89, 90}. They can also interact with the cyclin-dependent kinase inhibitor p21 that is implicated in G1/S and G2/M cell cycle arrest^{91, 92}. Cell cycle arrest allows the cell to repair damaged DNA, thus protecting from apoptosis. GADD45 proteins are involved in the nucleotide excision repair (NER) by interacting with proliferating cell nuclear antigen (PCNA). They recruit PCNA and the repair machinery to the lesion site and modulate DNA accessibility⁹¹⁻⁹³. In the absence of GADD45 proteins, PCNA presence at DNA damage sites is abolished⁹³. Besides, Gadd45 α was implicated in base excision repair (BER), a repair pathway mainly responsible for small base lesions caused either by endogenous metabolic byproducts or exogenous damaging agents. Gadd45 α and PCNA recruit BER proteins and mediate DNA repair as one complex⁹⁴. Another postulated mechanism

Introduction

suggests that GADD45 α interacts with histones, causing relaxation of DNA at damage sites to facilitate the accessibility to the DNA repair machinery⁹⁵. Importantly, Gadd45 α null mice showed enhanced genomic instability, chromosome abnormalities, sensitivity to radiation carcinogenesis and aberrant mitosis⁹⁶. Furthermore, these mice displayed impaired NER and thus increased mutation levels as well as susceptibility to cancer development⁹⁷.

Hematopoietic cells from Gadd45 α and Gadd45 β null mice were reported to undergo apoptosis, when exposed to genotoxic stress compared to wildtype counterparts⁹⁸. In detail, pro-survival functions of GADD45 α and GADD45 β in hematopoietic cells were mediated by the activation of the pro-survival p38/NF κ B pathway and by Gadd45 β -mediated JNK inhibition⁹⁸. Controversially, previous studies reported that Gadd45-mediated activation of p38 has been implicated in apoptosis. GADD45 proteins interact with MTK1 (also known as MEKK4) in response to environmental stress inducing apoptosis through p38/JNK pathway⁹⁹ and repressing autophagy through p38/Atg5¹⁰⁰. However, Gadd45 can also directly interact with p38 to induce apoptosis¹⁰¹. In addition, TGF β -induced apoptosis requires GADD45 β -mediated p38 activation¹⁰². In contrast to its pro-apoptotic function, in response to TNF α /NF κ B, GADD45 β possesses a pro-survival function by inhibiting the catalytic activity of MKK7 downstream of MTK1^{103, 104}. Of note, NF κ B-mediated cell survival in tumor cells requires suppression of GADD45 α and GADD45 γ ¹⁰⁵. UV irradiation-induced GADD45 β was shown to modulate MKK4 activity, thus inhibiting JNK-mediated apoptosis¹⁰⁶.

Many studies suggest that the type of stimulus, its magnitude, affected cell type and intracellular GADD45 interaction partners ultimately define whether the cell directs towards survival or apoptosis¹⁰⁶.

Epigenetic role of GADD45 proteins

Recently, GADD45 α was identified as a top hit in a screen for active DNA demethylases¹⁰⁷. Since the DNA repair machinery was reported to participate in active DNA demethylation and GADD45 proteins recruit DNA repair proteins to genomic sites, this was an attractive link to explain GADD45 function in DNA demethylation¹⁰⁷.

Active DNA demethylation is a DNA replication-independent process with two mechanisms: repair-based or oxidative DNA demethylation. Repair-based removal of 5-methylcytosine (5mC) is mediated by DNA repair enzymes from base excision repair (BER), NER or mismatch repair (MMR). Three repair-mediated pathways via removal of 5mC have been described: i) replacement of 5mC or its oxidized derivatives with unmethylated cytosine by BER¹⁰⁸, ii) deamination of 5mC by AID/APOBEC proteins followed by its removal by BER¹⁰⁹ and iii) removal of 5mC by NER¹¹⁰. The oxidative removal of 5mC involves the oxidation of 5mC by ten-eleven-translocation (TET) proteins to 5-hydroxymethylcytosine (5hmC)^{111, 112}. 5hmC can either be further oxidized to 5-formylcytosine (5fC) and 5-carboxylcytosine (5caC)¹¹³, or directly deaminated by AID/APOBEC enzymes to 5-hydroxymethyluracil (5hmU)¹¹⁴. Finally, the thymine DNA glycosylase (TDG) mediates the exchange of 5hmU¹¹⁴ as well as 5fC/5caC¹¹⁵ by the BER machinery with unmethylated cytosine.

GADD45-mediated DNA demethylation is prominently induced by differentiation signals or cellular stress. Thus, upon differentiation of mesenchymal stem cells, Gadd45 α mediates demethylation of osteogenic genes¹¹⁶. Both Gadd45 α and Gadd45 β were shown to antagonize DNMT1 functions in promoting epidermal progenitor maintenance by inhibiting progenitor growth and initiating demethylation of differentiation genes¹¹⁷. Furthermore, Gadd45 β was reported to be essential in adult neurogenesis by demethylation-mediated activation of neurogenic gene promoters *e.g.* *Bdnf IX*¹¹⁸, which is hypermethylated in psychotic disorders due to reduced Gadd45 β expression^{119, 120}. The role of GADD45 family members in DNA demethylation is controversially discussed among many groups. Although the role of GADD45 protein in DNA demethylation was questioned by some studies^{121, 122}, the majority of studies underline their importance in gene-specific DNA demethylation^{107, 109, 114, 116-119, 123}.

Importantly, the question was raised about the mechanism by which GADD45 proteins mediate DNA demethylation while lacking enzymatic activity. Their key role was found to underlie in the close interaction with the DNA repair machinery. Indeed, in zebrafish embryos, Gadd45 α was shown to induce AID and Apobec2b levels while Gadd45 β induced Apobec2a, suggesting that the interactions of Gadd45 members and distinct AID/Apobec enzymes are coordinated transcriptionally¹⁰⁹. Moreover, Gadd45 proteins were shown to physically cooperate with the deaminases

Introduction

AID/Apobec and the glycosylase Mbd4 to mediate the exchange of a 5mC against unmethylated cytosine¹⁰⁹. Additionally, Gadd45 and AID were also shown to interact with TDG¹¹⁴. TDG seems to create a link between 5mC deaminases, Gadd45 α and BER-mediated demethylation of deaminated or oxidized 5mC. Furthermore, Gadd45 also plays a role in DNA demethylation which is mediated by NER. Gadd45 α is targeted to specific genomic sites and recruits NER enzymes, specifically the endonuclease XPG (also known as ERCC5), to mediate DNA demethylation^{107, 110, 124}.

Notably, Gadd45 proteins interact with nuclear hormone receptors including RXR α , RAR α , ER α , PPAR $\alpha/\beta/\gamma$ ¹²⁵, hyperacetylated histones⁹⁵, and inhibitor of growth 1 (ING1)¹²⁶, suggesting that Gadd45 together with these interactors might target promoters for gene demethylation. In this model, Gadd45 promotes AID/MBD4 or AID/TDG complex formation and recruits these complexes or XPG to certain genomic sites.

Recent studies demonstrated that GADD45 proteins also play a role in oxidative DNA demethylation by physical and functional interaction with TET proteins to oxidize 5mC by positively regulating their activity^{127, 128}. Gadd45 α interacts with both, TET1 and TDG, to promote the removal of 5fC and 5caC¹²⁷. In mouse embryonic stem cells, Gadd45 α/β deficiency resulted in hypermethylation at genomic loci known for TDG-mediated demethylation¹²⁹. Moreover, GADD45 α was shown to possess the capability to bind¹³⁰ and read promoter-associated regulatory R-loops, which are DNA-(Inc)RNA hybrids, guiding DNA demethylating factors such as TET1 and TDG to these sites^{128, 131}.

The importance of GADD45 proteins in DNA demethylation was demonstrated by different studies^{107, 109, 114, 116-119, 123}. Most of which mainly focused on the well-characterized isoform, GADD45 α . As a consequence of GADD45 members' similarity, the described mechanisms of GADD45 α -mediated DNA demethylation are likely applicable to GADD45 β and GADD45 γ proteins.

Role of GADD45 β in hematopoiesis

The expression of all three GADD45 genes is induced in myeloid cells upon treatment with myelopoietic cytokines, like IL-3, IL-6, GM-CSF, M-CSF, and G-CSF⁸⁷. The expression levels of the GADD45 isoforms were dependent on the cytokine that

was used for stimulation^{86, 87}. Since GADD45 proteins are stress sensors, their deletion did not have an effect on steady-state, but on stress-induced hematopoiesis. Indeed, hematopoietic cells deficient for Gadd45 α and Gadd45 β reacted more sensitive to genotoxic stress induced by UV irradiation⁹⁸. Moreover, Gadd45 α - and Gadd45 β - deficient BM mononuclear cells showed reduced differentiation capacity towards granulocytes and monocytes as well as increased apoptosis, compared to wildtype cells⁸⁷. The deletion of Gadd45 α increased HSC regeneration capacity and led to resistance to DNA damage-induced apoptosis¹³². Both proteins seem to play a crucial role in physiological stress-induced hematopoiesis⁸⁷ and their deregulation might lead to malignant transformation¹³². In addition to terminal differentiation, Gadd45 α and Gadd45 β were implicated in granulocyte and macrophage functions in mice. Thus, Gadd45 α and Gadd45 β deficient mice showed impaired recruitment of myeloid cells to lipopolysaccharide (LPS)-injected sites. *In vitro*, Gadd45 α and Gadd45 β deficient mouse cells showed dysfunctional migration in chemotactic assays and phagocytosis, produced less reactive oxygen species (ROS) and pro-inflammatory cytokines upon LPS stimulation¹³³.

In addition to the above-mentioned cytokines, Gadd45 β is the only member which was reported to be induced by TGF β ⁸⁴ and TNF α ⁸⁵. TNF α or LPS induce Gadd45 β via the NF κ B pathway¹³⁴. The p65 (RelA) subunit of NF κ B binds directly to three κ B sites in the Gadd45 β promoter activating its expression¹³⁵.

Although it is referred to as 'myeloid differentiation primary response' gene, Gadd45 β plays a role in the adaptive immune system. In B cells, Gadd45 β expression was induced along with anti-apoptotic proteins to protect the cells from activation-induced apoptosis¹³⁶. In CD4⁺ T_h cells, Gadd45 β was expressed upon stimulation with the IL-1 family members, IL-18 and IL-12, resulting in increased INF γ secretion driving T_h1 differentiation^{137, 138}. In CD8⁺ cytotoxic T cells, another IL-1 member, IL-33, induced Gadd45 β transcription¹³⁹. Stimulation of the T cell receptor (TCR) itself also activated Gadd45 β expression suggesting its essential role in inflammation¹³⁸.

Role of GADD45 proteins in cancer

In some studies, GADD45 proteins are referred to as "tumor suppressor" proteins. Their deficiency might promote malignant transformation through the accumulation of

Introduction

DNA damage and induction of differentiation block¹³². In fact, the promoters of GADD45 proteins are frequently hypermethylated and their expression downregulated in many cancer types¹⁴⁰⁻¹⁴⁴. Ectopic expression of GADD45 proteins in tumor cells induced growth arrest, terminal differentiation or apoptosis^{86, 145, 146}.

Gadd45 α expression was found to be diminished in FLT3-ITD and AML-ETO AMLs^{147, 148}. In breast cancer, Gadd45 α expression is hormone receptor dependent¹⁴⁹ and was reported to suppress Ras-driven breast cancer by activating apoptosis/senescence pathways. In contrast, Gadd45 α acted as a tumor promoter in Myc-driven breast cancer by negatively regulating β -Catenin signaling, thereby promoting tumor vascularization¹⁵⁰. Gadd45 β expression was shown to induce apoptosis or cell cycle arrest in AML⁸⁴. Gadd45 β deficiency was demonstrated to accelerate BCR-ABL driven CML¹⁵¹. In fact, Gadd45 β seems to play an important role in tumor immunosurveillance. Gadd45 β -deficient CD8⁺ T cells displayed less IFN γ production upon tumor detection, TCR and IL-12/IL-18 stimulation. Remarkably, tumor vaccination failed in mice in the absence of Gadd45 β and Gadd45 γ ¹⁵². Moreover, low Gadd45 β expression was associated with hepatitis C virus (HCV) and HCV-associated hepatocellular carcinoma¹⁵³. Gadd45 γ expression is also downregulated in many cancers including anaplastic thyroid cancer, hepatocellular carcinomas¹⁵⁴, non-Hodgkin's lymphoma, Hodgkin's lymphoma, nasopharyngeal, cervical, esophageal and lung carcinoma¹⁴¹. GADD45 β and GADD45 γ were reported to act as tumor suppressors in pituitary tumors and were shown to be frequently downregulated^{155, 156}. Contrary to the reports about its immunosurveillance-promoting and tumor-suppressing functions, GADD45 β overexpression was shown to correlate with poor overall survival in several human cancers^{157, 158}.

Finally, the role of GADD45 proteins was discussed controversially by many studies. Depending on their expression level, tumor type and oncogenic signals, GADD45 proteins act either tumor-suppressing or promoting. Thus in some cancers targeting GADD45 proteins became attractive in anti-tumor therapy. Several drugs, e.g. Genistein¹⁵⁹, Trichostatin A¹⁶⁰, or Decitabine¹⁶¹, required GADD45 for their function and either induce GADD45 protein expression or stabilize its transcript. How and why GADD45 proteins play controversial roles in tumors still needs to be elucidated.

CRISPR/Cas9 technology as a tool to study hematopoiesis

Clustered regularly interspaced short palindromic repeats (CRISPR) sequences are recognized and cleaved by CRISPR-associated proteins (Cas). The CRISPR/Cas system represents the immune system in prokaryotes to protect themselves against foreign DNA. The CRISPR/Cas9 system is built of three components consisting of the Cas9 endonuclease, target-specific CRISPR RNA (crRNA) and transactivating crRNA (tracrRNA)¹⁶². CRISPR/Cas9 RNP binds specifically to its target region by base complementarity leading to DNA cleavage. Gene knockout is obtained by the non-homologous end-joining repair (NHEJ) pathway in the cell by insertions or deletions (indels) leading to a frameshift. Gene knock-in is achieved by homology-directed repair (HDR) pathway either using the second allele or a simultaneously delivered repair template¹⁶³.

The potential of CRISPR/Cas9 is enormous since it allows targeting of any genomic region. This feature allowed genome engineering and genome editing in any cell, opening the way for clinical applications. Shortly after the discovery of CRISPR/Cas9, a report was published on its use in gene-editing of human cells¹⁶⁴. Since then, the CRISPR/Cas9 system has been highly evolving to adapt it to the multiple demands in research and clinics. Nowadays, gene knockout, gene knock-in, gene interference, gene activation or repression, gene tagging and many other applications using CRISPR/Cas9 are possible. Most interestingly, CRISPR/Cas9 became a promising tool for regenerative medicine to cure many diseases. Indeed, efforts are made to correct mutations in human stem cells using CRISPR/Cas9 to cure β -hemoglobinopathies^{165, 166}, Duchenne muscular dystrophy¹⁶⁷, HIV¹⁶⁸, brain disorders¹⁶⁹ and many others.

Ex vivo approaches are probably the first that will pave the way of CRISPR/Cas9-gene editing to the clinic, since the CRISPR/Cas9 gene-edited cells can be handled easily in (good manufacturing practice) laboratory settings and can be returned to the patients by autologous transplantation. There are more than 260 hereditary monogenic disorders impairing the hematopoietic system¹⁷⁰. Hematopoietic stem cells are relatively easy to obtain and culture while providing potential cure for a bunch of hematologic disorders. Thus, patients who were dependent on allogenic hematopoietic stem cell transplantations could be cured independently of suitable transplant donors. Moreover, by autologous approaches graft versus host disease

Introduction

(GvHD) could be avoided. In fact, several studies reported successful gene editing of sickle cell disease and restoration of erythropoiesis using CRISPR/Cas9^{165, 166}. Also, X-linked chronic granulomatous disease and X-linked severe combined immunodeficiency phenotypes were corrected using CRISPR/Cas9 genome editing^{171, 172}. Moreover, according to the ClinicalTrials.gov database, there are diverse CRISPR/Cas9 based gene and cellular therapies for several cancers, HIV infection, neurofibromatosis type I, gastrointestinal infection and sickle cell disease that are already in phase I or II clinical trials¹⁷³.

Furthermore, CRISPR/Cas9 is a valuable experimental tool for researchers worldwide since it allows extremely fast, relatively cheap and very efficient gene modifications. CRISPR/Cas9 applications like gene deletion, gene insertion, translocations, gene editing, gene interference, gene activation and epigenome editing provide researchers novel tools to study gene functions, disease models and their potential treatments¹⁷⁴. Inserting disease-associated mutations into healthy donor adult stem cells or iPSCs allows studying diseases *in vitro* and exploiting the disease mechanisms, or identifying potential drugs rescuing the disease phenotype. Taken together, CRISPR/Cas9 became an indispensable tool in science and is highly developing according to research demands.

II. OBJECTIVES OF THE STUDY

Our research aims were to understand the pathomechanism underlying severe congenital neutropenia, a pre-leukemic bone marrow failure syndrome characterized by a maturation arrest of granulopoiesis at the level of promyelocytes. CN patients suffer from severe infections and have a high risk (22 % after 10 years) to develop MDS or AML. The current study focuses on two main aspects of our research.

Mechanism of maturation arrest of granulopoiesis in congenital neutropenia

Maturation arrest at the level of promyelocytes is a hallmark of CN. Through the accumulation of immature progenitors in the bone marrow, CN patients have very low levels of mature neutrophils in peripheral blood and a high risk of developing AML. The pathomechanism of maturation arrest of granulopoiesis in CN patients is largely unknown.

GADD45 β was identified by our group as a G-CSF-responsive protein in healthy individuals, which was not activated by G-CSF in CN promyelocytes. Since GADD45 β was reported to play a role in stress-induced hematopoiesis in mice, its function in granulocytic differentiation should be elucidated by loss-of-function in human HSPCs and iPSCs. Additionally, the effect of the ectopic GADD45 β expression on granulocytic differentiation of CN HSPCs should be investigated. Understanding the role of key players downstream of G-CSF/GADD45 β signaling would enable targeted activation of pathways that are essential in granulopoiesis. That would offer therapy options additionally to daily G-CSF treatment.

Disease modeling and gene therapy for congenital neutropenia

Research on CN HSPCs is challenging since pediatric bone marrow cells are a restricted source. Thus, disease modeling using patient-derived iPSCs allows the investigation of dysregulated signaling pathways on an unlimited cell source. CN

patient-derived iPSCs should be established to study molecular pathomechanism of defective granulocytic differentiation caused by inherited mutations. The internal stress due to *ELANE* mutations should be reconstituted in the iPSC system and contribute to the understanding of deregulated signaling in CN. On top of that, the development of a CN disease model would allow the development and testing of novel therapies that may correct the disease phenotype.

Strategies to target *ELANE* gene or protein might offer a promising treatment for CN patients. In fact, *Elane*^{-/-} mice show unaffected granulopoiesis. Thus, deleting *ELANE* in CN HSPCs by CRISPR/Cas9 might cure the disease phenotype. This should be assessed by *in vitro* granulocytic differentiation and neutrophil functional assays in CN iPSCs and HSPCs.

III. RESULTS & DISCUSSION

Mechanism of maturation arrest of granulopoiesis in congenital neutropenia

Covered in published manuscript A and submitted manuscript B:

- A. M. Nasri*, **P. Mir***, B. Dannenmann, D. Amend, T. Skroblyn, Y. Xu, K. Schulze-Osthoff, M. Klimiankou, K. Welte and J. Skokowa, '*Fluorescent labeling of CRISPR/Cas9 RNP for gene knockout in HSPCs and iPSCs reveals an essential role for GADD45 β in stress response*', *Blood Advances*, vol. 3, no. 1, p. 63-71, January 2019. (*equal contribution)
- B. **P. Mir**, M. Klimiankou, B. Dannenmann, N. Aghaallaei, M. Nasri, S. Wingert, F. Thalheimer, B. Findik, L. Doll, M. Ritter, T. Thumberger, S. Kandabarau, C. Zeidler, M. Rieger, B. Bajoghli, K. Welte and J. Skokowa, '*GADD45 β -mediated active gene demethylation is essential for G-CSF-triggered granulocytic differentiation*', manuscript in revision.

To understand the maturation arrest of granulopoiesis in CN and to be able to target dysregulated pathways, we investigated CN HSPCs. CN HSPCs are not capable of giving rise to a sufficient number of neutrophils, often leading to life-threatening bacterial infections. This defective granulopoiesis is caused by different gene mutations leading, however, to the same phenotype suggesting that similar downstream molecular pathways are affected⁷⁰. In the case of *ELANE*- and *HAX1*-CN, this might be the result of internal stress caused by the mutations inducing ER stress or mitochondrial dysfunctions. HSPCs undergo apoptosis upon sustained stress to maintain HSPC pool integrity and avoid malignant transformation⁷¹⁻⁷³.

In fact, we could show that early HSCs of both *ELANE*- and *HAX1*-CN have enhanced levels of the genotoxic stress marker γ H2AX compared to healthy control HSCs treated with G-CSF while later progenitors remain unaffected. This finding is in line with the report of van Galen et al. showing that early HSCs undergo apoptosis upon ER stress while later progenitors are directed towards terminal differentiation⁷¹.

Results & Discussion

By removing stressed HSCs, the integrity of the bone marrow is ensured and malignant transformation prevented⁷¹.

Resulting from this measurable internal stress, we detected a differentiation bias of CN HSPCs from myeloid towards lymphoid lineage, despite G-CSF treatment: while G-CSF treatment of healthy control HSPCs resulted in an increase of CMP and GMP and a decrease of MLP cells compared to untreated healthy control HSPCs, the opposite is the case in CN HSPCs, independently from the genetic background. Wang et *al.* demonstrated that DNA damage in HSPCs induced lymphoid over myeloid differentiation in a G-CSF/STAT3-dependent manner by activating BATF¹⁷⁵. In line with these findings, our study confirms that internal stress might change the differentiation output of HSPCs. Despite G-CSF treatment, in CN patients we observed low percentages of CMP and GMP and high amounts of MLP compared to healthy donors.

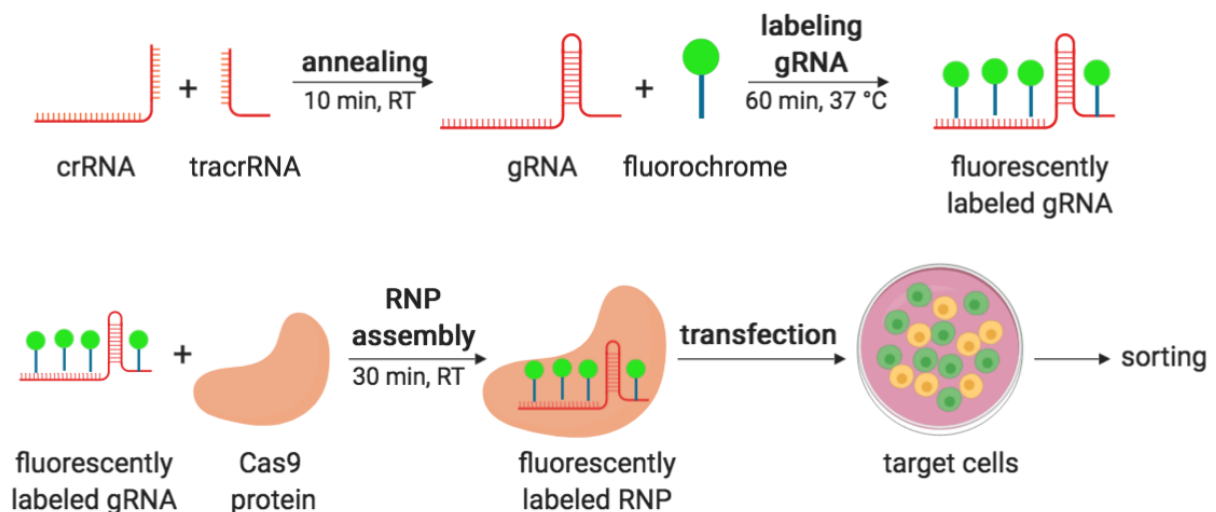
Furthermore, we identified a stress sensor gene that plays a role in myeloid differentiation and is abrogated in CN HSPCs, GADD45 β . GADD45 β (also called MyD118) is a member of the myeloid differentiation primary response genes that belongs to the growth arrest and DNA damage inducible protein family. GADD45 β expression is induced by various pro-myeloid and inflammatory stimuli, including G-CSF^{86, 87}. We found that in healthy control promyelocytes, G-CSF induces GADD45 β expression by 10-fold. GADD45 β protein is located predominantly in the nucleus. GADD45 proteins were reported to bind nuclear hormone receptors and act as transcriptional coactivators suggesting their main function within the nucleus¹²⁵. In CN promyelocytes, however, G-CSF is not capable of inducing GADD45 β expression leading to low protein levels mainly located to the cytosol. Thus, in CN promyelocytes, nuclear interactors of GADD45 β might not accomplish their full functions in the absence of nuclear GADD45 β .

We hypothesized that the ectopic GADD45 β expression might rescue CN phenotype and, therefore, overexpressed GADD45 β in CN HSPCs and differentiated these cells into granulocytes *in vitro*. In fact, we detected restored granulocytic differentiation in CN HSPCs transduced with GADD45 β cDNA compared to control transduced cells. In line with this, *in vitro* differentiation of mouse LT-HSCs transduced with Gadd45 β show increased granulocyte numbers. Flow cytometric analysis of LT-HSCs revealed that Gadd45 β transduced cells contained less immature HSPCs compared to control transduced cells while the number of GMP and mature granulocytes was dramatically

increased over time. Our results are supported by Gupta *et al.*, who demonstrated the crucial role of Gadd45 β in myeloid differentiation in mice⁸⁷. They showed that Gadd45 α - and Gadd45 β -deficient mice displayed disrupted myeloid differentiation upon stimulation with myeloid-specific cytokines⁸⁷.

To further unveil the function of GADD45 β in granulocytic differentiation, we performed CRISPR/Cas9-mediated GADD45 β knockout (KO) in healthy control iPSCs and primary bone marrow HSPCs.

CRISPR/Cas9 technology is the key tool to study genes that play a role in hematopoiesis and hematopoietic malignancies. It is relatively cheap, easy-to-handle and highly efficient. Using CRISPR/Cas9 ribonucleoprotein (RNP) is the most efficient and safe way for gene modifications. It is virus- and DNA-free, thus, avoiding the continuous expression of the active Cas9 endonuclease, DNA integration into the host genome and undesirable immune response. However, the major disadvantage of CRISPR/Cas9 RNP-based gene editing is the lack of a selection marker that enables the enrichment of gene modified cells. To overcome these hurdles, we established a method to chemically label guide RNA with a fluorescent dye allowing the tracking of CRISPR/Cas9 RNP transfected cells (**Figure 2**). We investigated the fluorescent labeling of CRISPR/Cas9 RNP using a guide RNA against *GADD45B*. By fluorescent labeling of CRISPR/Cas9 RNP, we could separate gene modified from unmodified cells and increase gene modification efficiency in human iPSCs and primary human HSPCs, among others.



Results & Discussion

Figure 2: CRISPR/Cas9 RNP fluorescent labeling scheme (adapted from Nasri M & Mir P., et al., 2019¹⁷⁶). CRISPR/Cas9 gRNA is labeled with a fluorescent dye for 60 min at 37 °C prior to assembly with Cas9 protein. After assembly with Cas9 protein, target cells are transfected with labeled CRISPR/Cas9 RNP. Transfected cells might be enriched by flow cytometry 24 h post transfection. The scheme was created with BioRender.

Differentiation of GADD45 β KO HSPCs towards neutrophils was investigated by liquid culture method. GADD45 β KO HSPCs produced significantly less neutrophils. Also, homozygous GADD45 β KO iPSC clones did not produce CFU-G colonies at all. Moreover, in embryoid body (EB)-based neutrophilic differentiation culture of iPSCs, we found that the numbers of CD11b⁺CD15⁺ and CD15⁺CD16⁺ granulocytes were severely diminished in GADD45 β KO iPSCs compared to control cells. Interestingly, the number of CD14⁺ monocytes was slightly increased, which is similar to the hemogram of CN patients showing low neutrophil but elevated monocyte counts⁷⁰.

To validate the role of GADD45 β in granulopoiesis *in vivo*, we first evaluated its expression in zebrafish embryos. GADD45 proteins are evolutionarily highly conserved. We found two zebrafish orthologs of human GADD45 β : *gadd45ba* and *gadd45bb*. Only *gadd45bb* was expressed in the hematopoietic tissue of zebrafish embryos, thus we focused on this paralog. We performed knockout of *gadd45bb* using CRISPR/Cas9 in the one-cell stage embryo of a transgenic zebrafish line, Tg(mpo:gfp), in which the expression of the green fluorescent protein (GFP) is driven by the neutrophil-specific myeloperoxidase (mpo) promoter¹⁷⁷. We determined the number of neutrophils in the caudal hematopoietic tissue (CHT, akin to mammalian fetal liver) 3 days post fertilization (dpf). Intriguingly, *gadd45bb* deficiency resulted in drastically decreased numbers of mpo⁺ cells in the CHT. G-CSF treatment of wildtype embryos leads to increased numbers of mpo⁺ cells compared to untreated embryos. Upon G-CSF injection, *gadd45bb* knockout embryos restored mpo⁺ cell numbers comparable to untreated wildtype embryos. However, this increase was much lower, than in G-CSF-stimulated wildtype embryos. These *in vitro* and *in vivo* findings indicate a crucial evolutionarily conserved role for GADD45 β in neutrophil development and maturation. In zebrafish, GADD45 β was reported to mediate podocyte injury by activating the ROS-GADD45 β -p38 pathway¹⁷⁸. Moreover, Rai et al. showed that active DNA demethylation takes place in zebrafish regulating gene expression. This process involves Gadd45 proteins, which induce the expression of

the deaminase *Aid* and the glycosylase *Mbd4*¹⁰⁹. These studies indicate an essential and conserved role for GADD45 proteins in signal transduction and gene demethylation regulation.

Up to date, there is no *in vivo* experimental model of CN. Mice with *Elane* mutations, or *Hax1*^{-/-} animals do not develop neutropenia^{179, 180}. Thus, we have established *gadd45bb*^{-/-} zebrafish as a suitable model to study neutropenia that could be used to develop novel therapeutic options for CN patients in the future.

We further aimed to understand how G-CSF regulates GADD45 β expression. We performed *in silico* analysis of the GADD45 β promoter and found that it possesses four C/EBP transcription factor binding sites. We identified C/EBP α as a transcriptional activator of GADD45 β expression using luciferase reporter gene and chromatin immunoprecipitation (ChIP) assay. Of note, the expression of C/EBP α is abrogated in CN HSPCs⁴⁰ and thus it cannot activate the expression of GADD45 β upon G-CSF stimulation.

GADD45 proteins do not possess catalytic activity, so we sought to understand by which mechanism GADD45 β mediates granulocytic differentiation. GADD45 proteins are known as significant players in DNA demethylation^{107, 109, 114, 116-119, 123}. Thus, we decided to test whether gene demethylation is a possible mechanism by which GADD45 β could mediate differentiation downstream of G-CSFR. We performed EPIC methylation array and RNA sequencing of wildtype and GADD45 β KO HSPCs of three healthy donors treated or not with 50 ng/ml of G-CSF. Interestingly, we found that most of the genes that were upregulated in the G-CSF-treated wildtype group, but not in the GADD45 β KO group, were myeloid lineage-related genes. Some of which are myeloid differentiation regulating genes, for instance, *RXRA*, *FGR*, *TFPI* and *HK3*, some play a role in neutrophil adhesion, and migration (*e.g.*, *ITGAM*, *SIGLEC5*, *CX3CR1*, *CXCR1*, *FPR1*, *FPR2*, and *CORO1A*) and some are important in neutrophil activation (*NCF2*, *MYL6*, and *NLRP12*). Strikingly, similar gene sets were detected to be upregulated in healthy donor promyelocytes upon G-CSF treatment but not in CN patient promyelocytes in microarray analysis, that was performed previously. We identified GADD45 β -dependent biological processes as myeloid leukocyte activation, neutrophil degranulation, neutrophil migration, response to stimulus and response to stress. Various diseases were associated with the expression signature caused by GADD45 β deficiency including leukocyte disorders, agranulocytosis, and MDS/AML. Our results are supported by other studies

Results & Discussion

confirming the role of GADD45 proteins in terminal differentiation¹⁴⁰⁻¹⁴⁴. Thus, the downregulation of these proteins might also promote malignant transformation¹³².

To identify master regulators upstream of identified gene sets, we performed motif enrichment analysis using iRegulon¹⁸¹. We found that several myeloid transcription factors were predicted to bind enriched motifs in the differentially expressed genes in WT but not KO group. Among these transcription factors are RXRA/RARA, SPI1 (PU.1), and C/EBP β . PU.1, and C/EBP β are well-known transcription factors regulating myeloid differentiation¹⁸². Notably, RXRA, which we identified downstream of GADD45 β , is activated in mouse hematopoietic stem/progenitor cells upon G-CSF treatment¹⁸³. RXRA was shown to play an important role in myeloid differentiation¹⁸⁴. Tsai et al. demonstrated that dominant negative retinoic acid receptors block neutrophil differentiation at promyelocytic level¹⁸⁵. Moreover, GADD45 proteins were reported to interact with nuclear hormone receptors (NHRs), including RXR α . GADD45 β possesses two LXXLL signature motifs which is typically present in nuclear coactivators. The binding of GADD45 proteins to NHRs and their function as transcriptional coactivators was proven *in vitro* by Yi et al.¹²⁵.

In the analysis of methylation arrays, we found that G-CSF induced the hypomethylation of 13.516 and the hypermethylation of 6.236 CpG sites in wildtype HSPCs. However, in GADD45 β KO HSPCs G-CSF was only able to induce hypomethylation of 8.440 and hypermethylation of 4.674 CpG sites (χ^2 test: $p = 0.0001$). Similar to differentially expressed genes, gene ontology analysis of differentially methylated sites (adjusted p value < 0.05) revealed that GADD45 β , downstream of G-CSF, regulated biological processes linked to myeloid leukocyte differentiation, neutrophil activation, cell migration, and chemotaxis and signaling pathways as hematopoietic cell kinase, SRC, CXCR1, G-CSFR and RARA signaling. Again, leukopenia/neutropenia, leukocyte disorders, AML, and immunologic deficiency syndromes are among associated diseases.

We identified *RXRA*, *MEFV*, *FPR2*, *CSF3R*, and several genes encoding neutrophil granule proteins (e.g., *ELANE*, *MPO*, and *AZU1*) among the top genes with differentially methylated regions (DMRs, ≥ 5 DMPs). DMRs were associated with datasets representing regions occupied by H3K9K14ac in ATRA-treated NB4 cells, RARA binding sites in the PML-RAR α zinc-inducible cell line and SPI-associated regions as assessed by genomic locus overlap enrichment analysis¹⁸⁶. Recently, Schäfer et al. showed that GADD45 α , together with ING1 mediated local DNA

demethylation at C/EBP β - and C/EBP δ -dependent super-enhancers via long-range chromatin loops facilitating their target gene binding¹⁸⁷. Similar mechanisms of epigenetic regulation might also apply to GADD45 β during differentiation.

Combined analysis of RNA sequencing and methylation array data disclosed 16 genes, including *RXRA*, *MEFV*, *CXCR1*, *FPR2*, and *SERPINA1* that were epigenetically regulated by GADD45 β downstream of G-CSF. Gene ontology analysis again confirmed the importance of these genes in neutrophil-related biological processes, signaling pathways and diseases. With the help of the RNA sequencing and methylation array data, we identified the retinoic acid signaling pathway to be inactive in the absence of GADD45 β . In fact, we could successfully bypass the activation of GADD45 β by treating CN HSPCs with all-trans retinoic acid (ATRA) and thereby rescue the diminished granulopoiesis. ATRA is an FDA-approved drug for the treatment of human promyelocytic leukemia and MDS^{188, 189}. Thus, it could also serve as a therapy option for CN patients to overcome promyelocytic maturation arrest.

We did not identify high numbers of GADD45 β -responsive genes which might result from assay limitations of whole genome arrays covering only very few CpG sites of the genome. Moreover, our experiments were a 'snapshot' at one time point, allowing analysis of static instead of dynamic changes. Although we found that not many genes are regulated by GADD45 β downstream of G-CSF, our findings are in line with previous studies showing that the GADD45-mediated DNA demethylation is a highly selective process. It is not only gene-specific but, in some cases, even CpG-specific^{107, 126, 190}.

Overall, our study is the first to connect the neutrophil maturation arrest in congenital neutropenia patients to the deficiency of the stress sensor gene GADD45 β . We demonstrated that GADD45 β is a target gene of C/EBP α and plays an essential role in the G-CSF triggered granulopoiesis by mediating specific DNA demethylation of neutrophil-related genes. Moreover, we could show that activating the retinoic acid signaling pathway by ATRA could rescue the diminished granulopoiesis in CN patients (**Figure 3**).

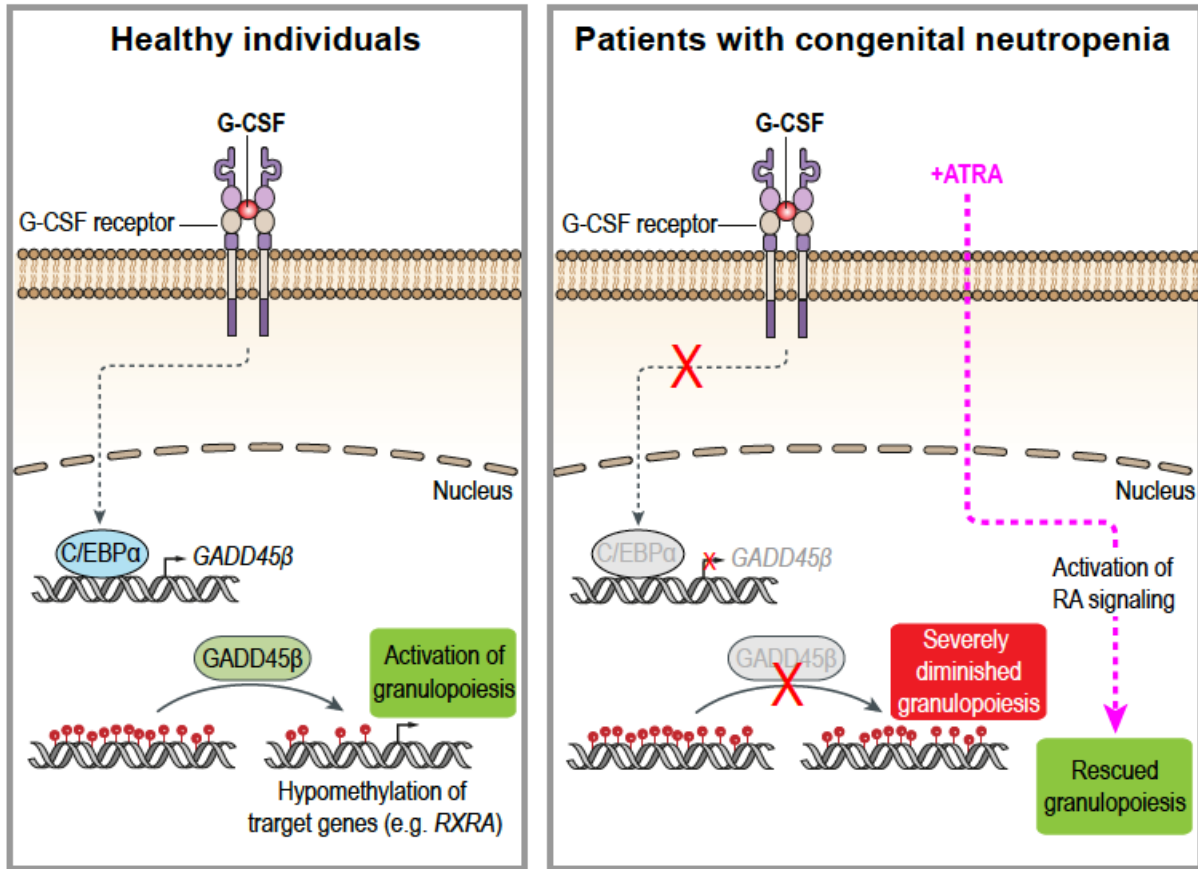


Figure 3: Mechanism of GADD45 β -mediated regulation of granulopoiesis in HSPCs via active DNA demethylation upon G-CSF stimulation in healthy individuals and CN patients. Treatment of CN HSPCs with ATRA rescues granulopoiesis. The scheme was created using Adobe Illustrator.

Disease modeling and gene therapy for congenital neutropenia

Covered in published manuscripts C, D and E:

- C. **P. Mir**, M. Ritter, K. Welte, J. Skokowa and M. Klimiankou, '*Gene Knockout in Hematopoietic Stem and Progenitor Cells Followed by Granulocytic Differentiation*', RNA Interference and CRISPR Technologies, *Methods in Molecular Biology*, vol. 2115, p. 455-469, February 2020
- D. M. Nasri, M. Ritter*, **P. Mir***, B. Dannenmann*, N. Aghaallaei, D. Amend, V. Makaryan, Y. Xu, B. Fletcher, R. Bernhard, I. Steiert, K. Hähnel, J. Berger, I. Koch, B. Sailer, K. Hipp C. Zeidler, M. Klimiankou, B. Bajoghli, D. C. Dale, K. Welte and J. Skokowa, '*CRISPR/Cas9 mediated ELANE knockout enables neutrophilic maturation of primary hematopoietic stem and progenitor cells and induced pluripotent stem cells of severe congenital neutropenia patients*', *Haematologica*, vol. 105, no. 3, p. 1-12, June 2019. (*equal contribution)
- E. B. Dannenmann, A. Zahabi, **P. Mir**, B. Oswald, R. Bernhard, M. Klimiankou, T. Morishima, K. Schulze-Osthoff, C. Zeidler, L. Kanz, N. Lachmann, T. Moritz, K. Welte and J. Skokowa, '*Human iPSC-based model of severe congenital neutropenia reveals elevated UPR and DNA damage in CD34⁺ cells preceding leukemic transformation*', *Experimental Hematology*, vol. 71, p. 51-60, January 2019.

To investigate granulopoiesis in CN patients, we established a protocol for efficient gene editing of HSPCs followed by granulocytic differentiation. However, primary bone marrow material from pediatric patients is a restricted source, thus we established a CN disease model using iPSCs. Patient-derived iPSCs offer the opportunity to understand the molecular mechanisms behind disease phenotypes and develop therapeutic approaches. These iPSCs might be used for drug screenings targeting deregulated pathways or other novel therapy options (**Figure 4**). We were able to establish CN and CN/AML disease models using patient-derived iPSCs to study: (1) mechanisms of neutrophil maturation arrest; (2) stepwise leukemogenic progression of CN iPSC-derived HSPCs and (3) gene therapy approaches.

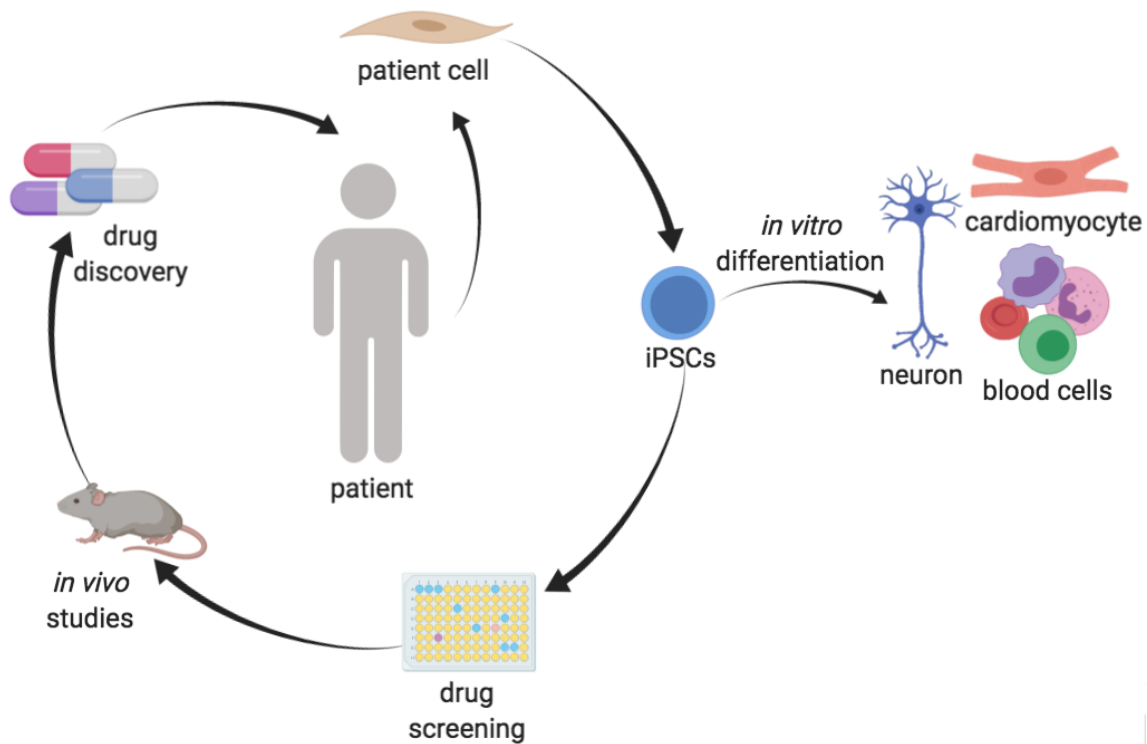


Figure 4: Disease modeling using patient-derived iPSCs (adapted from Sternecker et al., 2014¹⁹¹). Somatic cells can be reprogrammed using pluripotency factors to induced pluripotent stem cells. These cells can be either used to investigate the differentiation process or to screen for new drugs *in vitro* and *in vivo*. Implementation of iPSCs as a disease model allows identification of patient-specific disease pathogenesis and adapted therapy. The scheme was created with BioRender.

Using our embryoid body (EB)-based differentiation of iPSCs derived from two CN patients, we observed diminished granulocytic and elevated monocytic differentiation. In fact, monocytosis is a common finding in the peripheral blood of neutropenia patients⁷⁰. Thus, we were able to recapitulate *in vitro* the neutrophil maturation arrest observed in CN patients *in vivo*. We further could reconstitute the enhanced UPR in our iPSC model, which is known from primary CN cells.

Furthermore, we used our CN iPSC disease model to investigate CRISPR/Cas9-mediated gene modifications as a gene therapy option for CN patients. Mutated *ELANE* causes ER stress^{54, 57, 192}, thus we aimed to investigate if the knockout of both, mutated and wildtype *ELANE* had beneficial effects on the myeloid differentiation of CN HSPCs. Since *Elane*-deficient mice did not show neutropenia, we expected *ELANE* to be insignificant for neutrophil differentiation and functions¹⁹³. Moreover, patients with Papillon-Lefevre Syndrome exhibit NE deficiency, nonetheless, their neutrophils show no defects in bactericidal functions¹⁹⁴. We did

CRISPR/Cas9 RNP-mediated knockout of *ELANE* in CN iPSCs and examined granulocytic differentiation. We found that *ELANE* KO in CN iPSCs was sufficient to restore granulocytic differentiation as assessed by EB-based differentiation and CFU assay. Importantly, *ELANE* knockout in healthy donor iPSCs had no damaging effects on the *in vitro* granulopoiesis, indicating that *ELANE* is dispensable for this process. Encouraged by these findings, we performed CRISPR/Cas9 RNP-mediated *ELANE* knockout in primary HSPCs of five CN patients harboring *ELANE* mutations. Granulocytic differentiation was investigated in liquid culture and neutrophils discriminated using flow cytometric and morphologic analysis. We could successfully reconstitute granulocytic differentiation in *ELANE* KO CN HSPCs compared to unmodified CN HSPCs. Since NE is a part of host defense against bacterial infections, we further examined functions of neutrophils generated from CN *ELANE* KO HSPCs. Neutrophils generated from CN *ELANE* KO HSPCs exhibit proper ROS production, phagocytosis, and chemotaxis *in vitro*. *In vivo* phagocytic activity of neutrophils generated from CN *ELANE* KO HSPCs was comparable to healthy control neutrophils, as assessed by transplantation of cells in zebrafish embryos.

Taken together, we report a safe, DNA- and virus-free CRISPR/Cas9 RNP-mediated knockout of *ELANE* as potential gene therapy for CN. *ELANE* KO in CN HSPCs dramatically increased neutrophil counts and did not negatively affect neutrophil functions. NE and proteinase 3 are very similar in their functions suggesting its potentially redundant action to overcome *ELANE* KO. *ELANE* KO as a therapeutic approach is very promising since it is a generic application compatible with all CN patients with *ELANE* mutations independently of the mutation position, whereas correction of *ELANE* mutations would require patient-specific settings and the introduction of donor repair templates consisting of DNA. Regenerative therapy using *ELANE* KO in CN HSPCs would help patients to overcome the requirement of G-CSF treatment and, importantly, offer a therapy option to G-CSF-nonresponding patients. Gene deletions using CRISPR/Cas9 RNP should be considered as a well-tolerable alternative to gene correction approaches depending on the mutated genes. Recently, CRISPR/Cas9-mediated gene deletion was published by two groups as a promising therapeutic approach for sickle cell anemia and β -thalassemia^{195, 196}. A clinical trial (03745287) to treat sickle cell disease and β -thalassemia with autologous

Results & Discussion

CRISPR/Cas9 modified HSPCs was already initiated by November 2018. First results are expected by February 2021.

Further molecular and *in vivo* studies are required before CRISPR/Cas9-mediated *ELANE* KO will be able to pave the way into clinics in the future.

OUTLOOK

In this work, congenital neutropenia (CN) was examined to address different research aims: 1) molecular mechanism of maturation arrest of granulopoiesis in CN; 2) CN disease modeling; 3) gene therapy options for CN.

We could show that the inability of G-CSF to activate GADD45 β expression is a major factor in the pathogenesis of granulocytic maturation arrest of HSPCs of CN patients. Since it is not easy to activate the expression of GADD45 β , we thought about targeting GADD45 β downstream pathways as a therapeutic option for CN patients in the future. Indeed, RNA-seq and methylation array analyses revealed that retinoic acid and calcifediol signaling pathways were activated in G-CSF-treated HSPCs downstream of GADD45 β . Thus, it would be interesting to validate *in vitro* and *in vivo* if activation of retinoic acid and calcifediol can be used for the treatment of CN patients. To this end, our preliminary experiments showed a rescue of granulopoiesis in CN HSPCs treated with all-trans retinoic acid.

To further understand the molecular pathways of defective granulopoiesis in CN, we established a patient-derived iPSCs-based experimental model of granulopoiesis. Using iPSCs, we were able to reconstitute the CN phenotype *in vitro* and develop a potential gene therapy approach by knockout of mutated *ELANE* using CRISPR/Cas9. This model can also be used for testing novel therapies for CN, or to unveil the mechanisms of leukemogenic transformation of CN HSPCs. However, to realistically bring gene therapy approaches for CN into clinics, we need to establish safe and efficient strategies to knockout or correct mutated CN-causing genes.

Modeling CN, unveiling the pathomechanisms behind defective granulopoiesis and establishing new therapy options are challenges assessed by our group within several projects. In the future, we might offer alternatives to daily G-CSF treatment, provide long-term therapy solutions (especially to G-CSF non-responders), reduce risk of leukemogenic transformation and thus improve the quality of life of CN patients.

DANKSAGUNG

Ich bedanke mich herzlich bei Prof. Dr. Julia Skokowa für das interessante Promotionsprojekt, für die Betreuung und Begutachtung meiner Arbeit. Über die professionelle Beziehung hinaus, bedanke ich mich bei Julia und Karl für die stets offenen Ohren bei unseren Problemen, egal welcher Natur und für ihren Einsatz bei der Lösungsfindung.

Ich danke Prof. Dr. Klaus Schulze-Osthoff für die Begutachtung meiner Dissertation.

Ich danke all meinen Laborkollegen, die mich während meiner Doktorarbeit professionell und persönlich unterstützt haben. Regine, Karin, Ursel, Inge und Ilona danke ich für die hervorragende technische Assistenz und Unterstützung. Ich danke Masoud, Benni, Yun, Malte, Jeremy, Maksim, Narges, Baubak, Advaita, Larissa, Christine, Brigitte und Daniela für die schöne Arbeitsatmosphäre, die gute Zusammenarbeit und die gegenseitige Unterstützung. Natalia und Anne danke ich für die Freundschaft, die lustigen Gespräche und für das Teilen der schönen und nicht so schönen Momente im Labor.

Natalia, danke, dass du in sehr schwierigen Zeiten für mich da warst und bist. Du bist eine wahre Freundin.

Meiner Familie und meinem Mann danke ich von Herzen für ihre Unterstützung, ihren Rückhalt und ihre Liebe.

REFERENCES

1. Silva, A., Anderson, A.R. & Gatenby, R. A multiscale model of the bone marrow and hematopoiesis. *Math Biosci Eng* **8**, 643-658 (2011).
2. Morrison, S.J. & Weissman, I.L. The long-term repopulating subset of hematopoietic stem cells is deterministic and isolatable by phenotype. *Immunity* **1**, 661-673 (1994).
3. Morrison, S.J., Wandycz, A.M., Hemmati, H.D., Wright, D.E. & Weissman, I.L. Identification of a lineage of multipotent hematopoietic progenitors. *Development* **124**, 1929-1939 (1997).
4. Till, J.E. & McCulloch, E.A. Hemopoietic stem cell differentiation. *Biochim Biophys Acta* **605**, 431-459 (1980).
5. Spangrude, G.J. et al. Mouse hematopoietic stem cells. *Blood* **78**, 1395-1402 (1991).
6. Kondo, M., Weissman, I.L. & Akashi, K. Identification of clonogenic common lymphoid progenitors in mouse bone marrow. *Cell* **91**, 661-672 (1997).
7. Akashi, K., Traver, D., Miyamoto, T. & Weissman, I.L. A clonogenic common myeloid progenitor that gives rise to all myeloid lineages. *Nature* **404**, 193-197 (2000).
8. Galy, A., Travis, M., Cen, D. & Chen, B. Human T, B, natural killer, and dendritic cells arise from a common bone marrow progenitor cell subset. *Immunity* **3**, 459-473 (1995).
9. Shortman, K. & Liu, Y.J. Mouse and human dendritic cell subtypes. *Nat Rev Immunol* **2**, 151-161 (2002).
10. Manz, M.G., Miyamoto, T., Akashi, K. & Weissman, I.L. Prospective isolation of human clonogenic common myeloid progenitors. *Proc Natl Acad Sci U S A* **99**, 11872-11877 (2002).
11. Adolfsson, J. et al. Identification of Flt3+ lympho-myeloid stem cells lacking erythromegakaryocytic potential a revised road map for adult blood lineage commitment. *Cell* **121**, 295-306 (2005).
12. Mansson, R. et al. Molecular evidence for hierarchical transcriptional lineage priming in fetal and adult stem cells and multipotent progenitors. *Immunity* **26**, 407-419 (2007).
13. Yamamoto, R. et al. Clonal analysis unveils self-renewing lineage-restricted progenitors generated directly from hematopoietic stem cells. *Cell* **154**, 1112-1126 (2013).
14. Bruns, I. et al. Megakaryocytes regulate hematopoietic stem cell quiescence through CXCL4 secretion. *Nat Med* **20**, 1315-1320 (2014).
15. Heazlewood, S.Y. et al. Megakaryocytes co-localise with hemopoietic stem cells and release cytokines that up-regulate stem cell proliferation. *Stem Cell Res* **11**, 782-792 (2013).
16. Zhao, M. et al. Megakaryocytes maintain homeostatic quiescence and promote post-injury regeneration of hematopoietic stem cells. *Nat Med* **20**, 1321-1326 (2014).
17. Notta, F. et al. Distinct routes of lineage development reshape the human blood hierarchy across ontogeny. *Science* **351**, aab2116 (2016).
18. Doulatov, S. et al. Revised map of the human progenitor hierarchy shows the origin of macrophages and dendritic cells in early lymphoid development. *Nat Immunol* **11**, 585-593 (2010).
19. Laurenti, E. et al. The transcriptional architecture of early human hematopoiesis identifies multilevel control of lymphoid commitment. *Nat Immunol* **14**, 756-763 (2013).
20. Gorgens, A. et al. Revision of the human hematopoietic tree: granulocyte subtypes derive from distinct hematopoietic lineages. *Cell Rep* **3**, 1539-1552 (2013).

References

21. Katakura, F. et al. Paralogs of Common Carp Granulocyte Colony-Stimulating Factor (G-CSF) Have Different Functions Regarding Development, Trafficking and Activation of Neutrophils. *Front Immunol* **10**, 255 (2019).
22. Watari, K. et al. Serum granulocyte colony-stimulating factor levels in healthy volunteers and patients with various disorders as estimated by enzyme immunoassay. *Blood* **73**, 117-122 (1989).
23. Kawakami, M. et al. Levels of serum granulocyte colony-stimulating factor in patients with infections. *Blood* **76**, 1962-1964 (1990).
24. Lieschke, G.J. et al. Mice lacking granulocyte colony-stimulating factor have chronic neutropenia, granulocyte and macrophage progenitor cell deficiency, and impaired neutrophil mobilization. *Blood* **84**, 1737-1746 (1994).
25. Duhrsen, U. et al. Effects of recombinant human granulocyte colony-stimulating factor on hematopoietic progenitor cells in cancer patients. *Blood* **72**, 2074-2081 (1988).
26. Welte, K. et al. Purification and biochemical characterization of human pluripotent hematopoietic colony-stimulating factor. *Proc Natl Acad Sci U S A* **82**, 1526-1530 (1985).
27. Welte, K., Gabrilove, J., Bronchud, M.H., Platzer, E. & Morstyn, G. Filgrastim (r-metHuG-CSF): the first 10 years. *Blood* **88**, 1907-1929 (1996).
28. Bonilla, M.A. et al. Effects of recombinant human granulocyte colony-stimulating factor on neutropenia in patients with congenital agranulocytosis. *N Engl J Med* **320**, 1574-1580 (1989).
29. Fukunaga, R., Ishizaka-Ikeda, E. & Nagata, S. Growth and differentiation signals mediated by different regions in the cytoplasmic domain of granulocyte colony-stimulating factor receptor. *Cell* **74**, 1079-1087 (1993).
30. Hermans, M.H. et al. Signaling mechanisms coupled to tyrosines in the granulocyte colony-stimulating factor receptor orchestrate G-CSF-induced expansion of myeloid progenitor cells. *Blood* **101**, 2584-2590 (2003).
31. Kindwall-Keller, T.L. et al. Role of the proteasome in modulating native G-CSFR expression. *Cytokine* **43**, 114-123 (2008).
32. Barge, R.M. et al. Tryptophan 650 of human granulocyte colony-stimulating factor (G-CSF) receptor, implicated in the activation of JAK2, is also required for G-CSF-mediated activation of signaling complexes of the p21ras route. *Blood* **87**, 2148-2153 (1996).
33. Zhu, Q.S. et al. G-CSF induced reactive oxygen species involves Lyn-PI3-kinase-Akt and contributes to myeloid cell growth. *Blood* **107**, 1847-1856 (2006).
34. Dong, F. & Larner, A.C. Activation of Akt kinase by granulocyte colony-stimulating factor (G-CSF): evidence for the role of a tyrosine kinase activity distinct from the Janus kinases. *Blood* **95**, 1656-1662 (2000).
35. Baumann, M.A., Paul, C.C., Lemley-Gillespie, S., Oyster, M. & Gomez-Cambronero, J. Modulation of MEK activity during G-CSF signaling alters proliferative versus differentiative balancing. *Am J Hematol* **68**, 99-105 (2001).
36. Rausch, O. & Marshall, C.J. Cooperation of p38 and extracellular signal-regulated kinase mitogen-activated protein kinase pathways during granulocyte colony-stimulating factor-induced hemopoietic cell proliferation. *J Biol Chem* **274**, 4096-4105 (1999).
37. Futami, M. et al. G-CSF receptor activation of the Src kinase Lyn is mediated by Gab2 recruitment of the Shp2 phosphatase. *Blood* **118**, 1077-1086 (2011).
38. Yamanashi, Y. et al. Identification of HS1 protein as a major substrate of protein-tyrosine kinase(s) upon B-cell antigen receptor-mediated signaling. *Proc Natl Acad Sci U S A* **90**, 3631-3635 (1993).
39. Skokowa, J. et al. Interactions among HCLS1, HAX1 and LEF-1 proteins are essential for G-CSF-triggered granulopoiesis. *Nat Med* **18**, 1550-1559 (2012).
40. Skokowa, J. et al. LEF-1 is crucial for neutrophil granulocytogenesis and its expression is severely reduced in congenital neutropenia. *Nat Med* **12**, 1191-1197 (2006).

41. Smith, L.T., Hohaus, S., Gonzalez, D.A., Dziennis, S.E. & Tenen, D.G. PU.1 (Spi-1) and C/EBP alpha regulate the granulocyte colony-stimulating factor receptor promoter in myeloid cells. *Blood* **88**, 1234-1247 (1996).
42. Skokowa, J. et al. NAMPT is essential for the G-CSF-induced myeloid differentiation via a NAD(+)-sirtuin-1-dependent pathway. *Nat Med* **15**, 151-158 (2009).
43. Ai, J., Druhan, L.J., Loveland, M.J. & Avalos, B.R. G-CSFR ubiquitination critically regulates myeloid cell survival and proliferation. *PLoS One* **3**, e3422 (2008).
44. Hortner, M. et al. Suppressor of cytokine signaling-3 is recruited to the activated granulocyte-colony stimulating factor receptor and modulates its signal transduction. *J Immunol* **169**, 1219-1227 (2002).
45. Dong, F. et al. Mutations in the gene for the granulocyte colony-stimulating-factor receptor in patients with acute myeloid leukemia preceded by severe congenital neutropenia. *N Engl J Med* **333**, 487-493 (1995).
46. Forbes, L.V. et al. An activating mutation in the transmembrane domain of the granulocyte colony-stimulating factor receptor in patients with acute myeloid leukemia. *Oncogene* **21**, 5981-5989 (2002).
47. Maxson, J.E. et al. Oncogenic CSF3R mutations in chronic neutrophilic leukemia and atypical CML. *N Engl J Med* **368**, 1781-1790 (2013).
48. Skokowa, J. et al. Cooperativity of RUNX1 and CSF3R mutations in severe congenital neutropenia: a unique pathway in myeloid leukemogenesis. *Blood* **123**, 2229-2237 (2014).
49. Kostmann, R. Infantile genetic agranulocytosis; agranulocytosis infantilis hereditaria. *Acta Paediatr Suppl* **45**, 1-78 (1956).
50. Kostman, R. Infantile genetic agranulocytosis. A review with presentation of ten new cases. *Acta Paediatr Scand* **64**, 362-368 (1975).
51. Welte, K. et al. Differential effects of granulocyte-macrophage colony-stimulating factor and granulocyte colony-stimulating factor in children with severe congenital neutropenia. *Blood* **75**, 1056-1063 (1990).
52. Rosenberg, P.S. et al. Stable long-term risk of leukaemia in patients with severe congenital neutropenia maintained on G-CSF therapy. *Br J Haematol* **150**, 196-199 (2010).
53. Rosenberg, P.S. et al. The incidence of leukemia and mortality from sepsis in patients with severe congenital neutropenia receiving long-term G-CSF therapy. *Blood* **107**, 4628-4635 (2006).
54. Tidwell, T. et al. Neutropenia-associated ELANE mutations disrupting translation initiation produce novel neutrophil elastase isoforms. *Blood* **123**, 562-569 (2014).
55. Grenda, D.S. et al. Mutations of the ELA2 gene found in patients with severe congenital neutropenia induce the unfolded protein response and cellular apoptosis. *Blood* **110**, 4179-4187 (2007).
56. Nanua, S. et al. Activation of the unfolded protein response is associated with impaired granulopoiesis in transgenic mice expressing mutant Elane. *Blood* **117**, 3539-3547 (2011).
57. Nustede, R. et al. ELANE mutant-specific activation of different UPR pathways in congenital neutropenia. *Br J Haematol* **172**, 219-227 (2016).
58. Kollner, I. et al. Mutations in neutrophil elastase causing congenital neutropenia lead to cytoplasmic protein accumulation and induction of the unfolded protein response. *Blood* **108**, 493-500 (2006).
59. Dale, D.C. et al. Mutations in the gene encoding neutrophil elastase in congenital and cyclic neutropenia. *Blood* **96**, 2317-2322 (2000).
60. Dale, D.C. & Hammond, W.P.t. Cyclic neutropenia: a clinical review. *Blood Rev* **2**, 178-185 (1988).
61. Hammond, W.P.t., Price, T.H., Souza, L.M. & Dale, D.C. Treatment of cyclic neutropenia with granulocyte colony-stimulating factor. *N Engl J Med* **320**, 1306-1311 (1989).
62. Makaryan, V. et al. The diversity of mutations and clinical outcomes for ELANE-associated neutropenia. *Curr Opin Hematol* **22**, 3-11 (2015).

References

63. Klimenkova, O. et al. A lack of secretory leukocyte protease inhibitor (SLPI) causes defects in granulocytic differentiation. *Blood* **123**, 1239-1249 (2014).
64. Klein, C. et al. HAX1 deficiency causes autosomal recessive severe congenital neutropenia (Kostmann disease). *Nat Genet* **39**, 86-92 (2007).
65. Suzuki, Y. et al. HAX-1, a novel intracellular protein, localized on mitochondria, directly associates with HS1, a substrate of Src family tyrosine kinases. *J Immunol* **158**, 2736-2744 (1997).
66. Vafiadaki, E. et al. The anti-apoptotic protein HAX-1 interacts with SERCA2 and regulates its protein levels to promote cell survival. *Mol Biol Cell* **20**, 306-318 (2009).
67. Liu, H. et al. Regulation of Focal Adhesion Dynamics and Cell Motility by the EB2 and Hax1 Protein Complex. *J Biol Chem* **290**, 30771-30782 (2015).
68. Ortiz, D.F. et al. Identification of HAX-1 as a protein that binds bile salt export protein and regulates its abundance in the apical membrane of Madin-Darby canine kidney cells. *J Biol Chem* **279**, 32761-32770 (2004).
69. Zhao, W. et al. The anti-apoptotic protein HAX-1 is a regulator of cardiac function. *Proc Natl Acad Sci U S A* **106**, 20776-20781 (2009).
70. Skokowa, J. & Welte, K. Dysregulation of myeloid-specific transcription factors in congenital neutropenia. *Ann N Y Acad Sci* **1176**, 94-100 (2009).
71. van Galen, P. et al. The unfolded protein response governs integrity of the haematopoietic stem-cell pool during stress. *Nature* **510**, 268-272 (2014).
72. Ito, K. et al. Reactive oxygen species act through p38 MAPK to limit the lifespan of hematopoietic stem cells. *Nat Med* **12**, 446-451 (2006).
73. Maryanovich, M. et al. The ATM-BID pathway regulates quiescence and survival of haematopoietic stem cells. *Nat Cell Biol* **14**, 535-541 (2012).
74. Dahl, R. et al. Regulation of macrophage and neutrophil cell fates by the PU.1:C/EBPalpha ratio and granulocyte colony-stimulating factor. *Nat Immunol* **4**, 1029-1036 (2003).
75. McKercher, S.R. et al. Targeted disruption of the PU.1 gene results in multiple hematopoietic abnormalities. *EMBO J* **15**, 5647-5658 (1996).
76. Hromas, R. et al. Hematopoietic lineage- and stage-restricted expression of the ETS oncogene family member PU.1. *Blood* **82**, 2998-3004 (1993).
77. Rosenbauer, F. et al. Lymphoid cell growth and transformation are suppressed by a key regulatory element of the gene encoding PU.1. *Nat Genet* **38**, 27-37 (2006).
78. Belenky, P., Bogan, K.L. & Brenner, C. NAD⁺ metabolism in health and disease. *Trends Biochem Sci* **32**, 12-19 (2007).
79. Revollo, J.R., Grimm, A.A. & Imai, S. The NAD biosynthesis pathway mediated by nicotinamide phosphoribosyltransferase regulates Sir2 activity in mammalian cells. *J Biol Chem* **279**, 50754-50763 (2004).
80. Bitterman, K.J., Anderson, R.M., Cohen, H.Y., Latorre-Esteves, M. & Sinclair, D.A. Inhibition of silencing and accelerated aging by nicotinamide, a putative negative regulator of yeast sir2 and human SIRT1. *J Biol Chem* **277**, 45099-45107 (2002).
81. Hirai, H. et al. C/EBPbeta is required for 'emergency' granulopoiesis. *Nat Immunol* **7**, 732-739 (2006).
82. Liebermann, D.A. & Hoffman, B. Gadd45 in stress signaling. *J Mol Signal* **3**, 15 (2008).
83. Carrier, F. et al. Characterization of human Gadd45, a p53-regulated protein. *J Biol Chem* **269**, 32672-32677 (1994).
84. Selvakumaran, M. et al. The novel primary response gene MyD118 and the proto-oncogenes myb, myc, and bcl-2 modulate transforming growth factor beta 1-induced apoptosis of myeloid leukemia cells. *Mol Cell Biol* **14**, 2352-2360 (1994).
85. De Smaele, E. et al. Induction of gadd45beta by NF-kappaB downregulates pro-apoptotic JNK signalling. *Nature* **414**, 308-313 (2001).
86. Zhang, W. et al. CR6: A third member in the MyD118 and Gadd45 gene family which functions in negative growth control. *Oncogene* **18**, 4899-4907 (1999).
87. Gupta, S.K., Gupta, M., Hoffman, B. & Liebermann, D.A. Hematopoietic cells from gadd45a-deficient and gadd45b-deficient mice exhibit impaired stress responses to

- acute stimulation with cytokines, myeloablation and inflammation. *Oncogene* **25**, 5537-5546 (2006).
88. Kovalsky, O., Lung, F.D., Roller, P.P. & Fornace, A.J., Jr. Oligomerization of human Gadd45a protein. *J Biol Chem* **276**, 39330-39339 (2001).
 89. Wang, X.W. et al. GADD45 induction of a G2/M cell cycle checkpoint. *Proc Natl Acad Sci U S A* **96**, 3706-3711 (1999).
 90. Vairapandi, M., Balliet, A.G., Hoffman, B. & Liebermann, D.A. GADD45b and GADD45g are cdc2/cyclinB1 kinase inhibitors with a role in S and G2/M cell cycle checkpoints induced by genotoxic stress. *J Cell Physiol* **192**, 327-338 (2002).
 91. Vairapandi, M., Balliet, A.G., Fornace, A.J., Jr., Hoffman, B. & Liebermann, D.A. The differentiation primary response gene MyD118, related to GADD45, encodes for a nuclear protein which interacts with PCNA and p21WAF1/CIP1. *Oncogene* **12**, 2579-2594 (1996).
 92. Azam, N., Vairapandi, M., Zhang, W., Hoffman, B. & Liebermann, D.A. Interaction of CR6 (GADD45gamma) with proliferating cell nuclear antigen impedes negative growth control. *J Biol Chem* **276**, 2766-2774 (2001).
 93. Smith, M.L. et al. p53-mediated DNA repair responses to UV radiation: studies of mouse cells lacking p53, p21, and/or gadd45 genes. *Mol Cell Biol* **20**, 3705-3714 (2000).
 94. Jung, H.J. et al. Base excision DNA repair defect in Gadd45a-deficient cells. *Oncogene* **26**, 7517-7525 (2007).
 95. Carrier, F. et al. Gadd45, a p53-responsive stress protein, modifies DNA accessibility on damaged chromatin. *Mol Cell Biol* **19**, 1673-1685 (1999).
 96. Hollander, M.C. et al. Genomic instability in Gadd45a-deficient mice. *Nat Genet* **23**, 176-184 (1999).
 97. Hollander, M.C. et al. Dimethylbenzanthracene carcinogenesis in Gadd45a-null mice is associated with decreased DNA repair and increased mutation frequency. *Cancer Res* **61**, 2487-2491 (2001).
 98. Gupta, M. et al. Hematopoietic cells from Gadd45a- and Gadd45b-deficient mice are sensitized to genotoxic-stress-induced apoptosis. *Oncogene* **24**, 7170-7179 (2005).
 99. Takekawa, M. & Saito, H. A family of stress-inducible GADD45-like proteins mediate activation of the stress-responsive MTK1/MEKK4 MAPKKK. *Cell* **95**, 521-530 (1998).
 100. Keil, E. et al. Phosphorylation of Atg5 by the Gadd45beta-MEKK4-p38 pathway inhibits autophagy. *Cell Death Differ* **20**, 321-332 (2013).
 101. Bulavin, D.V., Kovalsky, O., Hollander, M.C. & Fornace, A.J., Jr. Loss of oncogenic H-ras-induced cell cycle arrest and p38 mitogen-activated protein kinase activation by disruption of Gadd45a. *Mol Cell Biol* **23**, 3859-3871 (2003).
 102. Yoo, J. et al. Transforming growth factor-beta-induced apoptosis is mediated by Smad-dependent expression of GADD45b through p38 activation. *J Biol Chem* **278**, 43001-43007 (2003).
 103. Papa, S. et al. Insights into the structural basis of the GADD45beta-mediated inactivation of the JNK kinase, MKK7/JNKK2. *J Biol Chem* **282**, 19029-19041 (2007).
 104. Papa, S. et al. Gadd45 beta mediates the NF-kappa B suppression of JNK signalling by targeting MKK7/JNKK2. *Nat Cell Biol* **6**, 146-153 (2004).
 105. Zerbini, L.F. et al. NF-kappa B-mediated repression of growth arrest- and DNA-damage-inducible proteins 45alpha and gamma is essential for cancer cell survival. *Oncogene* **23**, 13618-13623 (2004).
 106. Gupta, M., Gupta, S.K., Hoffman, B. & Liebermann, D.A. Gadd45a and Gadd45b protect hematopoietic cells from UV-induced apoptosis via distinct signaling pathways, including p38 activation and JNK inhibition. *J Biol Chem* **281**, 17552-17558 (2006).
 107. Barreto, G. et al. Gadd45a promotes epigenetic gene activation by repair-mediated DNA demethylation. *Nature* **445**, 671-675 (2007).
 108. He, Y.F. et al. Tet-mediated formation of 5-carboxylcytosine and its excision by TDG in mammalian DNA. *Science* **333**, 1303-1307 (2011).

References

109. Rai, K. et al. DNA demethylation in zebrafish involves the coupling of a deaminase, a glycosylase, and gadd45. *Cell* **135**, 1201-1212 (2008).
110. Le May, N. et al. NER factors are recruited to active promoters and facilitate chromatin modification for transcription in the absence of exogenous genotoxic attack. *Mol Cell* **38**, 54-66 (2010).
111. Tahiliani, M. et al. Conversion of 5-methylcytosine to 5-hydroxymethylcytosine in mammalian DNA by MLL partner TET1. *Science* **324**, 930-935 (2009).
112. Ito, S. et al. Role of Tet proteins in 5mC to 5hmC conversion, ES-cell self-renewal and inner cell mass specification. *Nature* **466**, 1129-1133 (2010).
113. Ito, S. et al. Tet proteins can convert 5-methylcytosine to 5-formylcytosine and 5-carboxylcytosine. *Science* **333**, 1300-1303 (2011).
114. Cortellino, S. et al. Thymine DNA glycosylase is essential for active DNA demethylation by linked deamination-base excision repair. *Cell* **146**, 67-79 (2011).
115. Maiti, A. & Drohat, A.C. Thymine DNA glycosylase can rapidly excise 5-formylcytosine and 5-carboxylcytosine: potential implications for active demethylation of CpG sites. *J Biol Chem* **286**, 35334-35338 (2011).
116. Zhang, R.P., Shao, J.Z. & Xiang, L.X. GADD45A protein plays an essential role in active DNA demethylation during terminal osteogenic differentiation of adipose-derived mesenchymal stem cells. *J Biol Chem* **286**, 41083-41094 (2011).
117. Sen, G.L., Reuter, J.A., Webster, D.E., Zhu, L. & Khavari, P.A. DNMT1 maintains progenitor function in self-renewing somatic tissue. *Nature* **463**, 563-567 (2010).
118. Ma, D.K. et al. Neuronal activity-induced Gadd45b promotes epigenetic DNA demethylation and adult neurogenesis. *Science* **323**, 1074-1077 (2009).
119. Gavin, D.P. et al. Growth arrest and DNA-damage-inducible, beta (GADD45b)-mediated DNA demethylation in major psychosis. *Neuropsychopharmacology* **37**, 531-542 (2012).
120. Matrisciano, F., Dong, E., Gavin, D.P., Nicoletti, F. & Guidotti, A. Activation of group II metabotropic glutamate receptors promotes DNA demethylation in the mouse brain. *Mol Pharmacol* **80**, 174-182 (2011).
121. Jin, S.G., Guo, C. & Pfeifer, G.P. GADD45A does not promote DNA demethylation. *PLoS Genet* **4**, e1000013 (2008).
122. Engel, N. et al. Conserved DNA methylation in Gadd45a(-/-) mice. *Epigenetics* **4**, 98-99 (2009).
123. Li, Y. et al. Overexpression of the growth arrest and DNA damage-induced 45alpha gene contributes to autoimmunity by promoting DNA demethylation in lupus T cells. *Arthritis Rheum* **62**, 1438-1447 (2010).
124. Schafer, A., Schomacher, L., Barreto, G., Doderlein, G. & Niehrs, C. Gemcitabine functions epigenetically by inhibiting repair mediated DNA demethylation. *PLoS One* **5**, e14060 (2010).
125. Yi, Y.W. et al. Gadd45 family proteins are coactivators of nuclear hormone receptors. *Biochem Biophys Res Commun* **272**, 193-198 (2000).
126. Schafer, A., Karaulanov, E., Stapf, U., Doderlein, G. & Niehrs, C. Ing1 functions in DNA demethylation by directing Gadd45a to H3K4me3. *Genes Dev* **27**, 261-273 (2013).
127. Kienhofer, S. et al. GADD45a physically and functionally interacts with TET1. *Differentiation* **90**, 59-68 (2015).
128. Arab, K. et al. GADD45A binds R-loops and recruits TET1 to CpG island promoters. *Nat Genet* **51**, 217-223 (2019).
129. Li, Z. et al. Gadd45a promotes DNA demethylation through TDG. *Nucleic Acids Res* **43**, 3986-3997 (2015).
130. Sytnikova, Y.A., Kubarenko, A.V., Schafer, A., Weber, A.N. & Niehrs, C. Gadd45a is an RNA binding protein and is localized in nuclear speckles. *PLoS One* **6**, e14500 (2011).
131. Arab, K. et al. Long noncoding RNA TARID directs demethylation and activation of the tumor suppressor TCF21 via GADD45A. *Mol Cell* **55**, 604-614 (2014).

132. Chen, Y. et al. Gadd45a regulates hematopoietic stem cell stress responses in mice. *Blood* **123**, 851-862 (2014).
133. Salerno, D.M., Tront, J.S., Hoffman, B. & Liebermann, D.A. Gadd45a and Gadd45b modulate innate immune functions of granulocytes and macrophages by differential regulation of p38 and JNK signaling. *J Cell Physiol* **227**, 3613-3620 (2012).
134. Zhang, N. et al. NF-kappaB and not the MAPK signaling pathway regulates GADD45beta expression during acute inflammation. *J Biol Chem* **280**, 21400-21408 (2005).
135. Yang, Z., Song, L. & Huang, C. Gadd45 proteins as critical signal transducers linking NF-kappaB to MAPK cascades. *Curr Cancer Drug Targets* **9**, 915-930 (2009).
136. Zazzeroni, F. et al. Gadd45 beta mediates the protective effects of CD40 costimulation against Fas-induced apoptosis. *Blood* **102**, 3270-3279 (2003).
137. Yang, J., Zhu, H., Murphy, T.L., Ouyang, W. & Murphy, K.M. IL-18-stimulated GADD45 beta required in cytokine-induced, but not TCR-induced, IFN-gamma production. *Nat Immunol* **2**, 157-164 (2001).
138. Lu, B., Ferrandino, A.F. & Flavell, R.A. Gadd45beta is important for perpetuating cognate and inflammatory signals in T cells. *Nat Immunol* **5**, 38-44 (2004).
139. Yang, Q. et al. IL-33 synergizes with TCR and IL-12 signaling to promote the effector function of CD8+ T cells. *Eur J Immunol* **41**, 3351-3360 (2011).
140. Wang, W. et al. Analysis of methylation-sensitive transcriptome identifies GADD45a as a frequently methylated gene in breast cancer. *Oncogene* **24**, 2705-2714 (2005).
141. Ying, J. et al. The stress-responsive gene GADD45G is a functional tumor suppressor, with its response to environmental stresses frequently disrupted epigenetically in multiple tumors. *Clin Cancer Res* **11**, 6442-6449 (2005).
142. Ramachandran, K. et al. Methylation-mediated repression of GADD45alpha in prostate cancer and its role as a potential therapeutic target. *Cancer Res* **69**, 1527-1535 (2009).
143. Na, Y.K. et al. Hypermethylation of growth arrest DNA-damage-inducible gene 45 in non-small cell lung cancer and its relationship with clinicopathologic features. *Mol Cells* **30**, 89-92 (2010).
144. Zerbini, L.F. et al. JunD-mediated repression of GADD45alpha and gamma regulates escape from cell death in prostate cancer. *Cell Cycle* **10**, 2583-2591 (2011).
145. Zhan, Q. et al. The gadd and MyD genes define a novel set of mammalian genes encoding acidic proteins that synergistically suppress cell growth. *Mol Cell Biol* **14**, 2361-2371 (1994).
146. Li, Y. et al. Adenoviral-mediated gene transfer of Gadd45a results in suppression by inducing apoptosis and cell cycle arrest in pancreatic cancer cell. *J Gene Med* **11**, 3-13 (2009).
147. Perugini, M. et al. Repression of Gadd45alpha by activated FLT3 and GM-CSF receptor mutants contributes to growth, survival and blocked differentiation. *Leukemia* **23**, 729-738 (2009).
148. Perugini, M. et al. GADD45A methylation predicts poor overall survival in acute myeloid leukemia and is associated with IDH1/2 and DNMT3A mutations. *Leukemia* **27**, 1588-1592 (2013).
149. Tront, J.S., Willis, A., Huang, Y., Hoffman, B. & Liebermann, D.A. Gadd45a levels in human breast cancer are hormone receptor dependent. *J Transl Med* **11**, 131 (2013).
150. Tront, J.S., Huang, Y., Fornace, A.J., Jr., Hoffman, B. & Liebermann, D.A. Gadd45a functions as a promoter or suppressor of breast cancer dependent on the oncogenic stress. *Cancer Res* **70**, 9671-9681 (2010).
151. Sha, X., Hoffman, B. & Liebermann, D.A. Loss of Gadd45b accelerates BCR-ABL-driven CML. *Oncotarget* **9**, 33360-33367 (2018).
152. Ju, S. et al. Gadd45b and Gadd45g are important for anti-tumor immune responses. *Eur J Immunol* **39**, 3010-3018 (2009).
153. Higgs, M.R., Lerat, H. & Pawlotsky, J.M. Downregulation of Gadd45beta expression by hepatitis C virus leads to defective cell cycle arrest. *Cancer Res* **70**, 4901-4911 (2010).

References

154. Sun, L. et al. GADD45gamma, down-regulated in 65% hepatocellular carcinoma (HCC) from 23 chinese patients, inhibits cell growth and induces cell cycle G2/M arrest for hepatoma Hep-G2 cell lines. *Mol Biol Rep* **30**, 249-253 (2003).
155. Michaelis, K.A. et al. Identification of growth arrest and DNA-damage-inducible gene beta (GADD45beta) as a novel tumor suppressor in pituitary gonadotrope tumors. *Endocrinology* **152**, 3603-3613 (2011).
156. Bahar, A., Bicknell, J.E., Simpson, D.J., Clayton, R.N. & Farrell, W.E. Loss of expression of the growth inhibitory gene GADD45gamma, in human pituitary adenomas, is associated with CpG island methylation. *Oncogene* **23**, 936-944 (2004).
157. Verzella, D. et al. GADD45beta Loss Ablates Innate Immunosuppression in Cancer. *Cancer Res* **78**, 1275-1292 (2018).
158. Zhao, Z. et al. GADD45B as a Prognostic and Predictive Biomarker in Stage II Colorectal Cancer. *Genes (Basel)* **9** (2018).
159. Oki, T. et al. Genistein induces Gadd45 gene and G2/M cell cycle arrest in the DU145 human prostate cancer cell line. *FEBS Lett* **577**, 55-59 (2004).
160. Hirose, T. et al. p53-independent induction of Gadd45 by histone deacetylase inhibitor: coordinate regulation by transcription factors Oct-1 and NF-Y. *Oncogene* **22**, 7762-7773 (2003).
161. Al-Romaih, K. et al. Decitabine-induced demethylation of 5' CpG island in GADD45A leads to apoptosis in osteosarcoma cells. *Neoplasia* **10**, 471-480 (2008).
162. Jinek, M. et al. A programmable dual-RNA-guided DNA endonuclease in adaptive bacterial immunity. *Science* **337**, 816-821 (2012).
163. Capecchi, M.R. Altering the genome by homologous recombination. *Science* **244**, 1288-1292 (1989).
164. Cong, L. et al. Multiplex genome engineering using CRISPR/Cas systems. *Science* **339**, 819-823 (2013).
165. Dever, D.P. et al. CRISPR/Cas9 beta-globin gene targeting in human haematopoietic stem cells. *Nature* **539**, 384-389 (2016).
166. DeWitt, M.A. et al. Selection-free genome editing of the sickle mutation in human adult hematopoietic stem/progenitor cells. *Sci Transl Med* **8**, 360ra134 (2016).
167. Amoasii, L. et al. Gene editing restores dystrophin expression in a canine model of Duchenne muscular dystrophy. **362**, 86-91 (2018).
168. Ophinni, Y., Inoue, M., Kotaki, T. & Kameoka, M. CRISPR/Cas9 system targeting regulatory genes of HIV-1 inhibits viral replication in infected T-cell cultures. *Sci Rep* **8**, 7784 (2018).
169. Lee, B. et al. Nanoparticle delivery of CRISPR into the brain rescues a mouse model of fragile X syndrome from exaggerated repetitive behaviours. *Nat Biomed Eng* **2**, 497-507 (2018).
170. Picard, C. et al. Primary Immunodeficiency Diseases: an Update on the Classification from the International Union of Immunological Societies Expert Committee for Primary Immunodeficiency 2015. *J Clin Immunol* **35**, 696-726 (2015).
171. De Ravin, S.S. et al. CRISPR-Cas9 gene repair of hematopoietic stem cells from patients with X-linked chronic granulomatous disease. *Sci Transl Med* **9** (2017).
172. Schirolli, G. et al. Preclinical modeling highlights the therapeutic potential of hematopoietic stem cell gene editing for correction of SCID-X1. *Sci Transl Med* **9** (2017).
173. Lau, C.H. & Suh, Y. In vivo genome editing in animals using AAV-CRISPR system: applications to translational research of human disease. *F1000Res* **6**, 2153 (2017).
174. Pickar-Oliver, A. & Gersbach, C.A. The next generation of CRISPR-Cas technologies and applications. *Nat Rev Mol Cell Biol* (2019).
175. Wang, J. et al. A Differentiation Checkpoint Limits Hematopoietic Stem Cell Self-Renewal in Response to DNA Damage. *Cell* **158**, 1444 (2014).
176. Nasri, M. et al. Fluorescent labeling of CRISPR/Cas9 RNP for gene knockout in HSPCs and iPSCs reveals an essential role for GADD45b in stress response. *Blood Adv* **3**, 63-71 (2019).

177. Renshaw, S.A. et al. A transgenic zebrafish model of neutrophilic inflammation. *Blood* **108**, 3976-3978 (2006).
178. Chen, Z. et al. GADD45B mediates podocyte injury in zebrafish by activating the ROS-GADD45B-p38 pathway. *Cell Death Dis* **7**, e2068 (2016).
179. Grenda, D.S. et al. Mice expressing a neutrophil elastase mutation derived from patients with severe congenital neutropenia have normal granulopoiesis. *Blood* **100**, 3221-3228 (2002).
180. Chao, J.R. et al. Hax1-mediated processing of HtrA2 by Parl allows survival of lymphocytes and neurons. *Nature* **452**, 98-102 (2008).
181. Janky, R. et al. iRegulon: from a gene list to a gene regulatory network using large motif and track collections. *PLoS Comput Biol* **10**, e1003731 (2014).
182. Rosenbauer, F. & Tenen, D.G. Transcription factors in myeloid development: balancing differentiation with transformation. *Nat Rev Immunol* **7**, 105-117 (2007).
183. Niu, H. et al. Endogenous retinoid X receptor ligands in mouse hematopoietic cells. *Sci Signal* **10** (2017).
184. Johnson, B.S. et al. Retinoid X receptor (RXR) agonist-induced activation of dominant-negative RXR-retinoic acid receptor alpha403 heterodimers is developmentally regulated during myeloid differentiation. *Mol Cell Biol* **19**, 3372-3382 (1999).
185. Tsai, S. & Collins, S.J. A dominant negative retinoic acid receptor blocks neutrophil differentiation at the promyelocyte stage. *Proc Natl Acad Sci U S A* **90**, 7153-7157 (1993).
186. Sheffield, N.C. & Bock, C. LOLA: enrichment analysis for genomic region sets and regulatory elements in R and Bioconductor. *Bioinformatics* **32**, 587-589 (2016).
187. Schafer, A. et al. Impaired DNA demethylation of C/EBP sites causes premature aging. *Genes Dev* **32**, 742-762 (2018).
188. Huang, M.E. et al. Use of all-trans retinoic acid in the treatment of acute promyelocytic leukemia. *Blood* **72**, 567-572 (1988).
189. Baldus, M., Walter, H., Moller, M., Schurfeld, C. & Brass, H. All-Trans-Retinoic Acid (Atra) in the Treatment of Myelodysplastic-Syndromes - Results in 5 Cases. *Onkologie* **17**, 515-520 (1994).
190. Schmitz, K.M. et al. TAF12 recruits Gadd45a and the nucleotide excision repair complex to the promoter of rRNA genes leading to active DNA demethylation. *Mol Cell* **33**, 344-353 (2009).
191. Sternecker, J.L., Reinhardt, P. & Scholer, H.R. Investigating human disease using stem cell models. *Nat Rev Genet* **15**, 625-639 (2014).
192. Nayak, R.C. et al. Pathogenesis of ELANE-mutant severe neutropenia revealed by induced pluripotent stem cells. *J Clin Invest* **125**, 3103-3116 (2015).
193. Hirche, T.O., Atkinson, J.J., Bahr, S. & Belaaouaj, A. Deficiency in neutrophil elastase does not impair neutrophil recruitment to inflamed sites. *Am J Respir Cell Mol Biol* **30**, 576-584 (2004).
194. Pham, C.T., Ivanovich, J.L., Raptis, S.Z., Zehnauer, B. & Ley, T.J. Papillon-Lefevre syndrome: correlating the molecular, cellular, and clinical consequences of cathepsin C/dipeptidyl peptidase I deficiency in humans. *J Immunol* **173**, 7277-7281 (2004).
195. Ye, L. et al. Genome editing using CRISPR-Cas9 to create the HPFH genotype in HSPCs: An approach for treating sickle cell disease and beta-thalassemia. *Proc Natl Acad Sci U S A* **113**, 10661-10665 (2016).
196. Traxler, E.A. et al. A genome-editing strategy to treat beta-hemoglobinopathies that recapitulates a mutation associated with a benign genetic condition. *Nat Med* **22**, 987-990 (2016).

APPENDIX I: LIST OF ACCEPTED PUBLICATIONS

Nasri M. & Mir P. et al., 2019, *Blood Advances*

Mir P. et al., 2020, *Methods in Molecular Biology*

Nasri M. et al., 2019, *Haematologica*

Dannenmann B. et al., 2019, *Experimental Hematology*

Nasri M. & Mir P. et al., 2019, *Blood Advances*

Fluorescent labeling of CRISPR/Cas9 RNP for gene knockout in HSPCs and iPSCs reveals an essential role for GADD45b in stress response

Masoud Nasri,^{1,*} Perihan Mir,^{1,2,*} Benjamin Dannenmann,¹ Diana Amend,¹ Tessa Skroblyn,^{1,3} Yun Xu,¹ Klaus Schulze-Osthoff,^{2,4} Maksim Klimiankou,¹ Karl Welte,^{1,5} and Julia Skokowa^{1,2}

¹Department of Oncology, Hematology, Immunology, Rheumatology, and Pulmonology, University Hospital Tübingen, Tübingen, Germany; ²German Cancer Research Center, Heidelberg, Germany; ³Max Delbrück Center for Molecular Medicine in the Helmholtz Association, Berlin, Germany; ⁴Interfaculty Institute of Biochemistry, Tübingen University, Tübingen, Germany; and ⁵University Children's Hospital Tübingen, Tübingen, Germany

Key Points

- Fluorescent labeling of CRISPR/Cas9–gRNA RNP enables sorting of edited HSPCs and iPSCs for further applications.
- GADD45B plays a crucial role in UV stress-induced response of HSPCs and iPSCs.

CRISPR/Cas9-mediated gene editing of stem cells and primary cell types has several limitations for clinical applications. The direct delivery of ribonucleoprotein (RNP) complexes consisting of Cas9 nuclease and guide RNA (gRNA) has improved DNA- and virus-free gene modifications, but it does not enable the essential enrichment of the gene-edited cells. Here, we established a protocol for the fluorescent labeling and delivery of CRISPR/Cas9–gRNA RNP in primary human hematopoietic stem and progenitor cells (HSPCs) and induced pluripotent stem cells (iPSCs). As a proof of principle for genes with low-abundance transcripts and context-dependent inducible expression, we successfully deleted growth arrest and DNA-damage-inducible β (*GADD45B*). We found that GADD45B is indispensable for DNA damage protection and survival in stem cells. Thus, we describe an easy and efficient protocol of DNA-free gene editing of hard-to-target transcripts and enrichment of gene-modified cells that are generally difficult to transfect.

Introduction

CRISPR/Cas9-mediated gene editing^{1,2} has a tremendous potential for clinical applications, such as gene therapy of inherited disorders or boosting of immune cells for cancer immunotherapies.^{3–9} Several monogenic disorders, including life-threatening bone marrow failure syndromes, might be treated by CRISPR/Cas9-mediated gene correction in autologous hematopoietic stem and progenitor cells (HSPCs) *ex vivo*. This procedure could then be followed by transplantation of the corrected HSPCs without exposing the patient to harsh immunosuppression regimens (ie, chemotherapy, irradiation).

Two groups recently published successful gene therapy approaches to cure sickle cell disease, a common inherited blood disorder. They generated deletions in the β -globin gene locus using CRISPR/Cas9 technology to mimic the hereditary persistence of fetal hemoglobin mutations.^{10,11} First attempts at gene editing using CRISPR/Cas9 for cancer therapy have also been launched recently. CRISPR/Cas9-generated chimeric antigen receptor–modified T cells targeting the checkpoint receptor programmed cell death 1 have been injected in a patient with metastatic non-small cell lung cancer.^{12,13} In addition to HSPCs, CRISPR/Cas9-mediated gene editing was successfully applied in neurons, hepatocytes, and cardiomyocytes.^{14–20}

To further advance clinical applications of the CRISPR/Cas9 technology, unspecific integrations of viral or plasmid CRISPR/Cas9 DNA in the host genome and undesirable immune responses must be prevented. This may be achieved by transient virus- and DNA-free delivery approaches using CRISPR/Cas9–guide RNA (gRNA) ribonucleoprotein (RNP) complexes. Compared with DNA-based approaches, the direct delivery of CRISPR/Cas9–gRNA RNP complexes might have several advantages. Due to the

Submitted 24 December 2017; accepted 28 November 2018. DOI 10.1182/bloodadvances.2017015511.

*M.N. and P.M. contributed equally to this work.

The full-text version of this article contains a data supplement.

© 2019 by The American Society of Hematology

cellular degradation of the RNP complex, exposure of cells to Cas9 is generally only transient and restricted, thereby limiting potential off-target effects of endonuclease overexpression.

Gundry et al recently described the efficient delivery of CRISPR/Cas9-gRNA RNP in HSPCs²¹; however, the method used in that study did not allow the enrichment of gene-edited cells. Purification of gene-edited HSPCs early in the manufacturing process is desirable, especially for clinical applications, because HSPCs differentiate and progressively lose their long-term repopulating capacity during culture. This is especially true for genes with low-abundance messenger RNA (mRNA) transcripts or inducible mRNA expression. These genes may be difficult to target, also due to epigenetic modifications, leading to tightly packed chromatin at the time of gRNA delivery. In these cases, the selection of gene-edited cells is indispensable. Nonmodified cells may retain a proliferative advantage over gene-edited cells, especially in mixed populations.

Introduction of a fluorescent tag to the CRISPR/Cas9-gRNA RNP enables enrichment of gene-edited cells for further experimental and clinical applications. Tagging of Cas9 protein could be achieved by fusion of Cas9 with fluorescent proteins or by chemical labeling of the CRISPR/Cas9-gRNA RNP with a fluorescent dye. However, Cas9-GFP fusion proteins might affect the intracellular localization, activity, or on- and off-target specificity of the endonuclease. Therefore, in the present study, we established a safe, simple, and efficient method for CRISPR/Cas9 gene knockout using transfection of stem cells with fluorescently labeled CRISPR/Cas9-gRNA RNP complexes.

Materials and methods

Cell culture

Human embryonic kidney 293FT (HEK293FT) and Jurkat cells were cultured under standard conditions (37°C, 5% CO₂) using Dulbecco's modified Eagle medium high glucose (HEK293FT cells) or RPMI 1640 GlutaMAX (Jurkat cells) medium supplemented with 10% fetal calf serum (Sigma-Aldrich) and 1% penicillin/streptomycin (Biochrome). HEK293FT cells were detached using 0.05% Trypsin-EDTA (Gibco) and seeded at a density of 1×10^5 cells per milliliter of medium. Jurkat cells were seeded at a density of 1 to 2×10^5 cells per milliliter of medium.

Human CD34⁺ HSPCs were isolated from the bone marrow or leukapheresis mononuclear cell fraction by magnetic bead separation (Human CD34 Progenitor Cell Isolation kit; Miltenyi Biotech). CD34⁺ cells were cultured in a density of 2×10^5 cells/mL of Stemline II medium (Sigma Aldrich) supplemented with 10% fetal calf serum, 1% penicillin/streptomycin, 1% L-glutamine, and a cytokine cocktail consisting of 20 ng/mL IL-3, 20 ng/mL IL-6, 20 ng/mL thrombopoietin, 50 ng/mL SCF, and 50 ng/mL Flt-3L. Human induced pluripotent stem cells (iPSCs) were cultured on plates coated with Geltrex lactate dehydrogenase elevating virus-free reduced growth factor basement membrane matrix (cat. no. A1413201; Thermo Fisher Scientific) at a density of 2×10^5 cells/mL in StemFlex medium (cat. no. A3349401; Thermo Fisher Scientific) supplemented with 1% penicillin/streptomycin.

Generation and testing of the *GADD45B* gRNA

Specific CRISPR RNA (crRNA) for the first exon of the *GADD45B* gene (GCTCGTGGCGTGCGACAACGCGG, cut site: chr19

[+2,476,389: -2,476,389], NM_015675.3 Exon 1, 31bp; NP_056490.2 position N11) was designed using an online tool from the University of Heidelberg (<http://crispr.cos.uni-heidelberg.de>). The crRNA for *GADD45B* was first tested in transfected HEK293FT cells showing a gene modification efficiency of 67% in the total population of transfected cells.

Labeling of gRNA and plasmid DNA

Trans-activating CRISPR RNA (tracrRNA) and crRNA, obtained from IDT, were annealed at a ratio of 1:1 by incubating for 15 minutes at room temperature to generate gRNA. gRNA was fluorescently labeled using LabellIT CX-Rhodamine (cat. no. MIR7022; Mirus) or LabellIT Fluorescein (cat. no. MIR7025; Mirus) kits according to the manufacturer's instructions. Labeling reagent and nucleic acid ratio were used at a ratio of 1:1 leading to 1 label per 20 to 60 bases, which is suitable for most applications.

Generation of crRNA-tracrRNA duplexes (gRNA) was conducted by adding 800 pmol of *GADD45B*-targeting crRNA and 800 pmol tracrRNA into 40 μ L nuclease-free duplex buffer (IDT) at room temperature for 15 minutes. Labeling of the gRNA was performed by mixing gRNA, DNase- and RNase-free water, 10 \times labeling buffer A and 1:10 of LabellIT Reagent (CX-rhodamine or fluorescein). The reaction was incubated at 37°C for 1 hour while centrifuging briefly after 30 minutes to minimize evaporation and maintain the appropriate concentration of the reaction components.

Purification of labeled gRNA was conducted using the ethanol precipitation method. To this end, 5 M sodium chloride (0.1 volume) and ice-cold ethanol (2.5 volume) were added to the reaction, mixed well, and placed at -20°C for 30 minutes. Afterwards, the sample was centrifuged at 14 000g at 4°C for 30 minutes to pellet the labeled gRNA. Once pelleted, the supernatant was discarded gently without disturbing the pellet. The pellet was washed using 70% ethanol at room temperature and centrifuged at 14 000g for 30 minutes. After centrifugation, the pellet was air dried for 5 minutes and resolved in IDT nuclease-free duplex buffer. The labeled gRNA stock was stored at -20°C for up to 2 months.

Labeling of the pMAX GFP plasmid (Lonza) was carried out using LabellIT Tracker Intracellular Nucleic Acid Localization Kit (cat. no. MIR7022; Mirus) following the manufacturer's protocol.

Assessment of the RNA integrity using Agilent Bioanalyzer

Labeled and unlabeled gRNA were analyzed using the Agilent RNA 6000 Pico Kit according to the manufacturer's instructions on the Agilent 2100 Bioanalyzer using the total RNA program.

Transfection of cells with CRISPR/Cas9-gRNA RNP complexes

Transfection was carried out either using TransIT-X2 (cat. no. MIR6003; Mirus) dynamic delivery system or the Amaxa nucleofection system (P3 primary kit, cat. no. V4XP-3024) according to the manufacturers' instructions. For 0.5×10^5 HEK293FT cells, 100 pmol of labeled duplexed gRNA was mixed with 100 pmol of Cas9 protein (Alt-R S.p. Cas9 Nuclease 3NLS, cat. no. 1074182; IDT) in IDT nuclease-free duplex buffer and assembled for 30 minutes at room temperature. Afterwards, the CRISPR/Cas9-gRNA RNP was mixed with either Opti-MEM I reduced-serum medium and TransIT-X2 transfection reagent (HEK293FT) or with electroporation mix for the

Amaya nucleofection system according to the manufacturer's protocol (Jurkat, and human iPSCs and CD34⁺ HSPCs, respectively). Jurkat cells (1.0×10^6) were electroporated with 300 pmol labeled duplexed gRNA mixed with 300 pmol Cas9 protein. Human iPSCs and CD34⁺ HSPCs (1.0×10^6) were electroporated with 400 pmol labeled duplexed gRNA and 400 pmol Cas9 protein. Transfection of HEK293FT cells with CX-rhodamine-labeled pMAX GFP plasmid was performed using TransIT-LT1 transfection reagent (cat. no. MIR2304; Mirus).

Genomic DNA isolation, PCR, Sanger sequencing and TIDE assay

Genomic DNA (gDNA) was isolated using the QIAamp DNA Mini Kit (cat. no. 51306; Qiagen) according to the manufacturer's instructions. Polymerase chain reaction (PCR) with isolated gDNA and *GADD45B*-specific primers (forward: 5'-GACTACCGTTGGTTCCGCAAC-3', reverse: 5'-ATACATCAGGATACGGCAGCCC-3') was carried out using the GoTaq Hot Start Polymerase Kit (cat. no. M5006; Promega) using 50 ng of gDNA template for each PCR reaction. PCR product purification was conducted with ExoSAP (ratio 3:1), a master mix of 1 part Exonuclease I 20 U/ μ L (cat. no. EN0581; Thermo Fisher Scientific) and 2 parts of FastAP thermosensitive alkaline phosphatase 1U/ μ L (cat. no. EF0651; Thermo Fisher Scientific). Sanger sequencing of purified PCR product was performed by Eurofins Genomics and analyzed using the TIDE (Tracking of Indels by Decomposition) webtool developed by Brinkman et al.²²

Establishment of gene-edited cell lines and human iPSCs from single-cell clones using limiting dilution

Cells were serially diluted to 0.5 cells per 100 μ L by adding of 60 cells in 12 mL Dulbecco's modified Eagle medium or RPMI medium and pipetting of 100 μ L of cell suspension per well of the 96-well plate. The 96-well plate was incubated for 2 to 3 weeks until appearance of growing cells.

Human iPSCs (15 000) were plated on a Geltrex-coated 10-cm dish in StemFlex medium (cat. no. A3349401; Thermo Fisher Scientific) and RevitaCell supplement (cat. no. A2644501; Thermo Fisher Scientific). Medium was changed every 24 hours without RevitaCell supplement. After 9 to 12 days, each colony was picked and transferred on the Geltrex-coated 96-well plate.

Cloning of the PCR products for the evaluation of the gene modification mode in *GADD45B*-edited clones

gDNA was isolated from gene-edited *GADD45B*^{+/-} and *GADD45B*^{-/-} iPSCs. The Cas9 RNP-targeted region of the *GADD45B* gene was amplified from gDNA using PCR with followed primers: forward 5'-GACTACCGTTGGTTCCGCAAC-3', reverse 5'-ATACATCAGGATACGGCAGCCC-3'. PCR product was purified from the agarose gel using QIAquick Gel Extraction kit (cat no./ID: 28706; Qiagen) and cloned into the linearized pMiniT 2.0 vector using the NEB PCR Cloning Kit (cat. no. E1202S; New England Biolabs) followed by transformation of competent *Escherichia coli* and subsequent colony PCR of *E coli* colonies, according to the manufacturer's instructions (cat. no. M5006; Promega). PCR products were analyzed using Sanger sequencing.

UV exposure and cell viability assay

Cells were irradiated with UV light (7 mJ/cm²) for 5 minutes and subsequently incubated for 2 hours under standard culture conditions before measuring the percentage of live *GADD45B*-targeting

CRISPR/Cas9-gRNA RNP-transfected cells by quantitation of CX-rhodamine- or fluorescein-positive cells using a BD FACS-Canto II flow cytometer.

Intracellular staining and fluorescence-activated cell sorter analysis of γ H2AX (pSer139) protein

Intracellular γ H2AX (pSer139) protein levels were measured in UV-irradiated cells. Briefly, cells were washed with phosphate-buffered saline and stained using the IntraSure kit (cat. no. 641778; BD) according to the manufacturer's instructions and incubated with Alexa-Fluor 488 mouse anti-H2AX pSer139 antibody (1:100; cat. no. 560445; BD) for 15 minutes at room temperature, washed twice, fixed with 0.5% paraformaldehyde and analyzed using a FACSCanto II flow cytometer.

LORD-Q-DNA damage quantification

gDNA was isolated using a QIAamp DNA Mini Kit according to the manufacturer's instructions. Long-run real-time PCR-based DNA-damage quantification (LORD-Q) was performed and analyzed according to the protocol of Lehle et al.²³

Results

Design of the CRISPR/Cas9-gRNA RNP fluorescent labeling

We generated gRNA by annealing crRNA with tracrRNA. gRNA was covalently labeled with CX-rhodamine or fluorescein and incubated with recombinant Cas9 protein to generate CRISPR/Cas9-gRNA RNP complexes (Figure 1A). To assess the efficiency of fluorescent labeling, we transfected HEK293FT cells with a CX-rhodamine-labeled plasmid encoding GFP protein. GFP signals were colocalized with CX-rhodamine signals, thus proving efficient labeling of the GFP plasmid with CX-rhodamine (supplemental Figure 1A). An Agilent Bioanalyzer was used to further confirm that fluorescent labeling does not affect gRNA integrity (Figure 1B).

Specific knockout of *GADD45B* using labeled CRISPR/Cas9-gRNA RNP

To functionally validate the knockout of weakly expressed genes with inducible mRNA expression using labeled CRISPR/Cas9-gRNA RNP, we chose to disrupt the human growth arrest and DNA-damage-inducible 45 β (*GADD45B*) gene.²⁴ We designed crRNA for exon 1 of *GADD45B* (Figure 1C), generated labeled *GADD45B* CRISPR/Cas9-gRNA RNP, and transfected HEK293FT cells, the Jurkat T-ALL cell line, bone marrow CD34⁺ HSPCs, and iPSCs. We detected CX-rhodamine or fluorescein signals 6 hours (HEK293FT cells) or 12 hours (Jurkat cells, CD34⁺ HSPCs, and iPSCs) after transfection. Transfection efficiency varied between 40% and 80%, depending on the cell type (Figure 2A-B). The intracellular fluorescent signal disappeared ~48 hours after transfection. Labeling did not affect the gene-editing efficiency of CRISPR/Cas9-gRNA RNP, as assessed by Sanger sequencing and tracking of indels by decomposition (TIDE) assay analysis of HEK293FT cells, Jurkat cells, CD34⁺ HSPCs, and human iPSCs transfected with labeled or unlabeled *GADD45B*-targeting CRISPR/Cas9-gRNA RNP (Figure 2C). Using fluorescein or rhodamine signals of labeled CRISPR/Cas9-gRNA RNP, we sorted and enriched gene-edited fluorescent cells by flow cytometry. Gene-modification efficiency in sorted cells was approximately 40% in iPSCs, 60% in HSPCs, and 70% in Jurkat cells (Figure 2D).

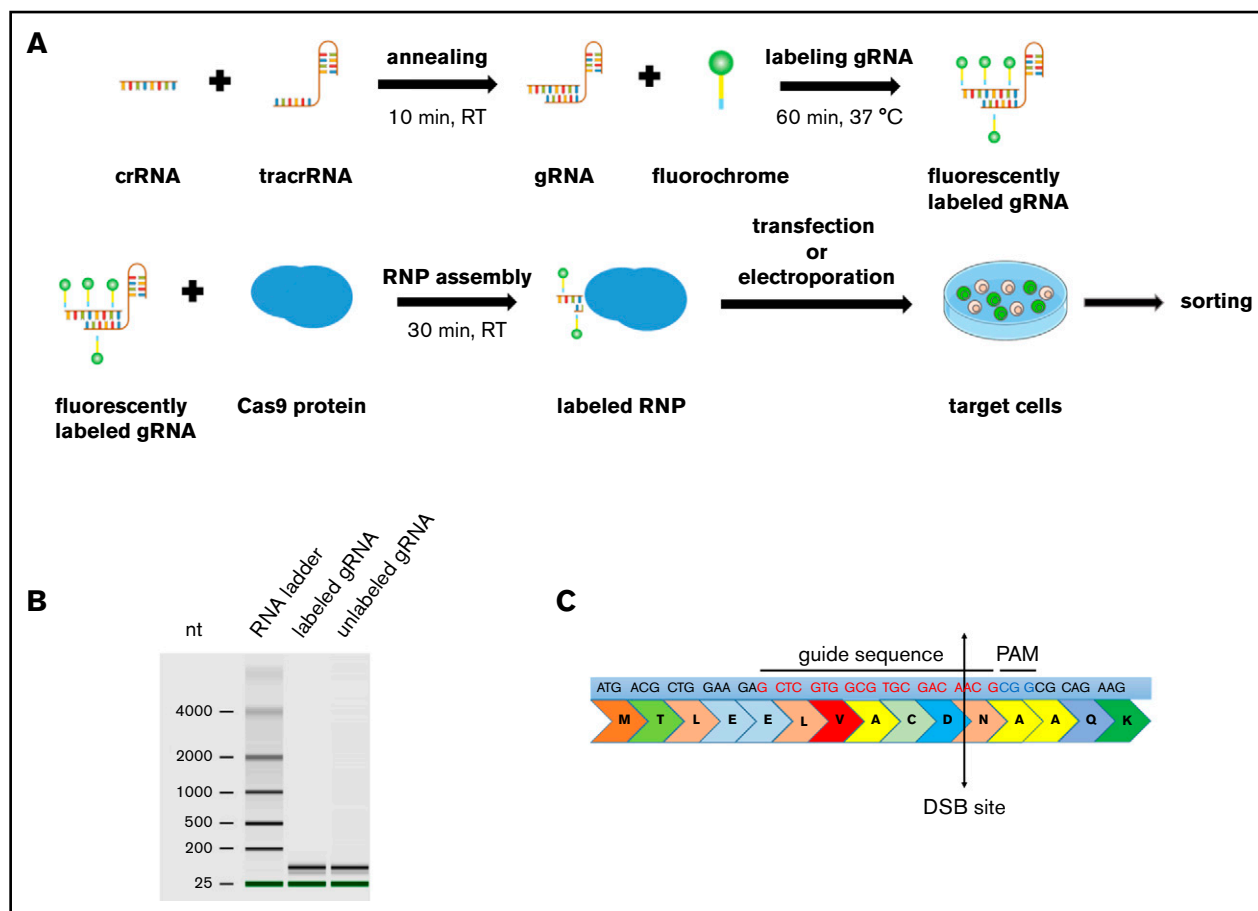


Figure 1. Scheme of CRISPR/Cas9-gRNA RNP labeling and cell transfection. (A) crRNA and tracrRNA were annealed at room temperature for 10 minutes. The resulting gRNA was labeled with fluorescein- or CX-rhodamine-coupled Label IT Tracker labeling reagent. The fluorescent *GADD45B*-targeting gRNA was assembled with recombinant Cas9 protein prior to transfection to assemble an active CRISPR/Cas9-gRNA RNP complex targeting human *GADD45B*. Cells were transfected with TransIT-X2 Transfection Reagent or by using the Amaxa Nucleofector System and were incubated for 24 hours before sorting the CX-rhodamine⁺ or fluorescein⁺ cells using a BD FACSARIA II. After sorting, some of the cells were used for a single-cell culture, and the rest were used for DNA isolation or cell-based assays. (B) Virtual gel of an Agilent Bioanalyzer analysis revealing no difference in the size or quality of labeled gRNA compared with unlabeled gRNA. (C) *GADD45B* was targeted using gRNA (highlighted in red), which inserts a double-strand break at NM_015675.3 exon 1, 31 bp after ATG; NP_056490.2, p.N11.

Transfection of cells with a nontargeting RNP, consisting of tracrRNA and Casp9 alone, did not affect genome integrity (supplemental Figure 1B). We also compared fluorescent labeling of crRNA with the expression of Cas9-EGFP fusion protein. We detected much lower editing efficiency of the fused Cas9-EGFP protein assembled with *GADD45B*-targeting gRNA compared with CRISPR/Cas9-gRNA RNP (supplemental Figure 2A).

Cloning of the PCR products from genomic DNA of single-cell clones of the gene-edited Jurkat cells and iPSCs revealed compound heterozygous *GADD45B* frameshift mutations in Jurkat cells (supplemental Figure 3A), and heterozygous, as well as homozygous, *GADD45B* deletions in iPSC clones (supplemental Figure 3B). We found no off-target activities of the *GADD45B*-specific crRNA, with the possibility of 3 bp mismatches. We also detected only a small number of potential off-target sites in other genes that could be targeted (<3 mismatches) with low probability (0.2%-0.9%) by the *GADD45B*-specific crRNA (supplemental Table 1). However, we did not detect any mutations in the selected gene regions in the edited cell types used in our study (supplemental Figure 4A).

GADD45B is essential for the induction of DNA damage response in human hematopoietic cells and iPSCs

We further performed functional studies of the effect of *GADD45B* knockout on cell growth and sensitivity to UV-induced DNA damage. Remarkably, we detected a strongly diminished viability of *GADD45B*-deficient HEK293FT cells, Jurkat cells, iPSCs, and CD34⁺ HSPCs compared with control transfected cells (Figure 3A). We also found markedly elevated susceptibility of *GADD45B*-deficient Jurkat cells and CD34⁺ HSPCs to UV-induced DNA damage, as documented by increased expression of the DNA damage marker γ H2AX (phospho-Ser139). Basal levels of γ H2AX (phospho-Ser139) were also elevated in *GADD45B*-modified HSPCs and Jurkat cells (Figure 3B-C). In addition, we detected an accumulation of DNA lesions in *GADD45B*-deficient cells compared with wild-type Jurkat cells (Figure 3D). As revealed by LORD-Q DNA damage-quantification analysis,²³ *GADD45B*-deficient cells exhibited increased DNA damage rates in the mitochondrial DNA (mtDNA), as well as in 2 analyzed genomic loci

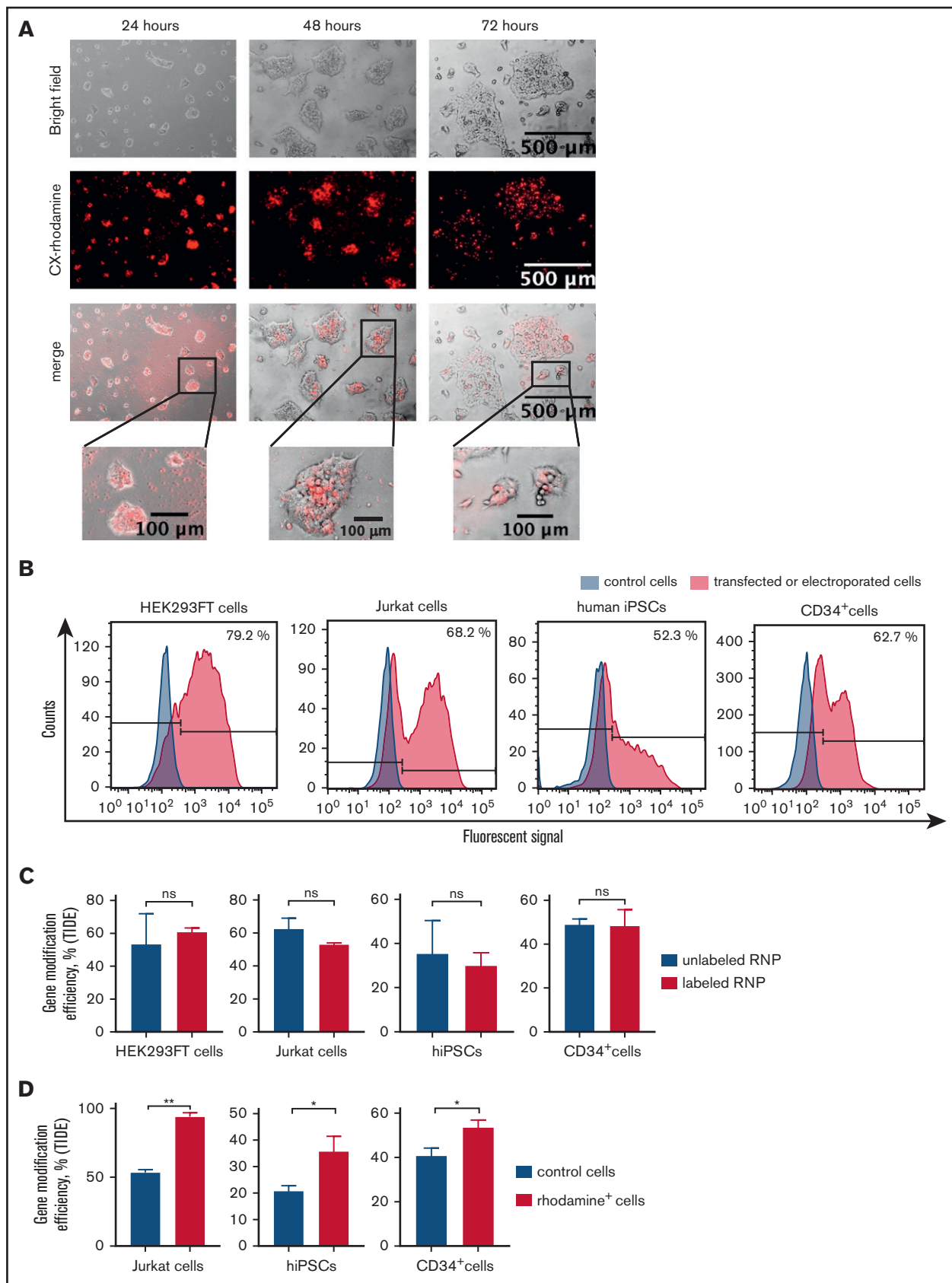


Figure 2.

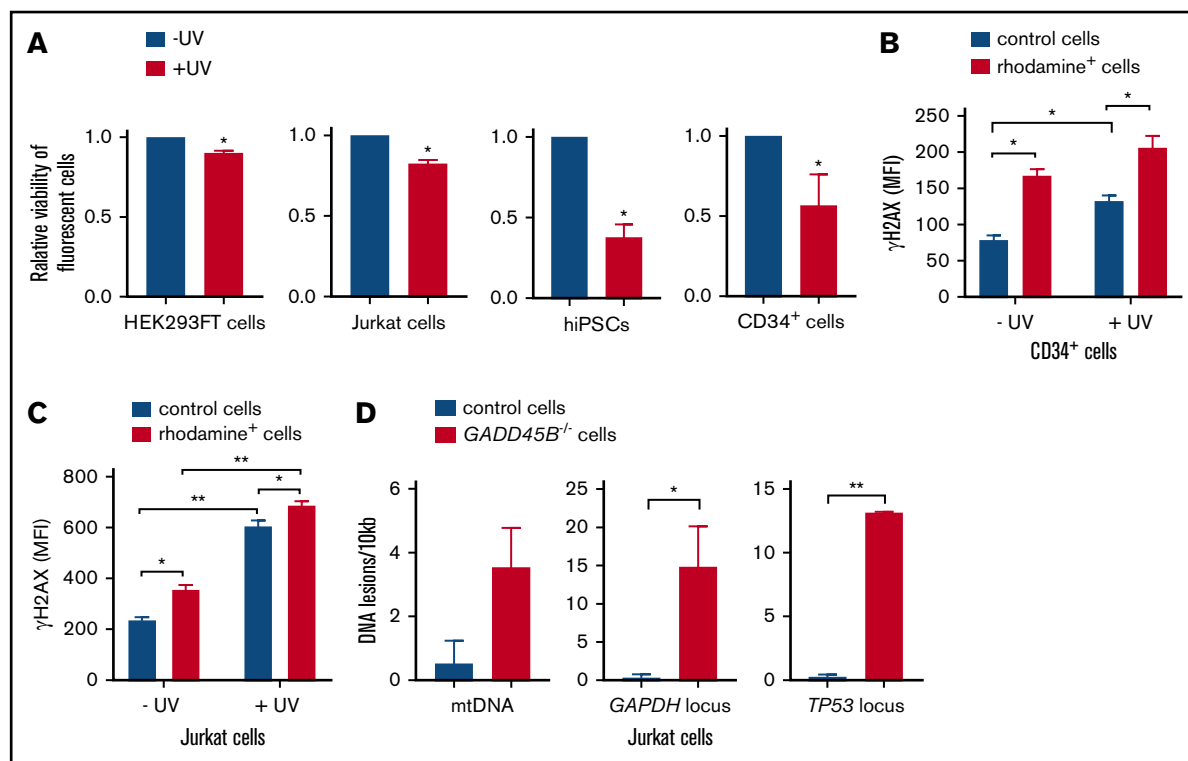


Figure 3. *GADD45B* knockout leads to reduced cell viability and increased UV-induced cellular stress. (A) Cell viability of HEK293FT cells, Jurkat cells, iPSCs, and CD34⁺ HSPCs, transfected with labeled tracr-Cas9 RNP (nontarget RNP) or with labeled *GADD45B*-targeting CRISPR/Cas9-gRNA RNP, was measured after exposing the cells to UV for 5 minutes, followed by 2 hours of additional incubation. Relative viability of nonirradiated control cells was set as 1.0. (B) CD34⁺ HSPCs were transfected with fluorescein-labeled *GADD45B*-targeting CRISPR/Cas9-gRNA RNP. After 48 hours, the cells were exposed to UV irradiation for 5 minutes. Following 2 hours of further incubation, intracellular γ H2AX (phospho-Ser139) levels were measured by flow cytometry. (C) Jurkat cells were transfected with CX-rhodamine-labeled *GADD45B*-targeting CRISPR/Cas9-gRNA RNP. After 48 hours, the total population was exposed to UV irradiation for 5 minutes, followed by 2 hours of incubation before performing intracellular staining and FACS analysis for the DNA damage marker γ H2AX (phospho-Ser139). (D) mtDNA damage (left panel) and nuclear DNA damage in the *GAPDH* locus (middle panel) and *TP53* locus (right panel) were quantified in Jurkat control cells and a *GADD45B*^{-/-} Jurkat clone using the LORD-Q method. Data are mean \pm standard deviation from 3 (A-B) or 2 (C-D) independent experiments, each performed in duplicates. * $P \leq .05$, ** $P \leq .01$, Student *t* test.

of nuclear DNA. Based on these observations, we conclude that *GADD45B* knockout in cells transfected with labeled *GADD45B*-targeting CRISPR/Cas9-gRNA RNP led to increased susceptibility to DNA damage.

***GADD45B* protects iPSCs from UV stress in a dose-dependent manner**

Interestingly, *GADD45B*^{+/-} and *GADD45B*^{-/-} iPSCs retained pluripotency (Figure 4A), but we detected markedly elevated

phospho-Ser139 γ H2AX levels in *GADD45B*-haploinsufficient and *GADD45B*-homozygous-knockout iPSCs. Elevated DNA damage was observed under steady-state conditions and, more profoundly, upon genotoxic UV exposure compared with wild-type iPSCs (Figure 4B). In line with upregulated γ H2AX (phospho-Ser139) levels, we measured elevated DNA damage in *GADD45B*^{+/-} and *GADD45B*^{-/-} iPSCs, as determined by the LORD-Q DNA damage-quantification assay (Figure 4C-D). These data are in accordance with our observations in *GADD45B*-deficient Jurkat cells and HSPCs.

Figure 2. Transfection- and genome-editing efficiency in different cell types using CX-rhodamine-labeled CRISPR/Cas9-gRNA RNP targeting *GADD45B*.

(A) HEK293FT cells were transfected with CX-rhodamine-labeled *GADD45B*-targeting CRISPR/Cas9-gRNA RNP. Fluorescence signal could be detected for up to 72 hours posttransfection. Representative images of 3 experiments are shown. (B) HEK293FT cells, Jurkat cells, human iPSCs, and CD34⁺ cells were transfected with labeled *GADD45B*-targeting CRISPR/Cas9-gRNA RNP. At 24 hours posttransfection, cells were harvested and measured for transfection efficiency using a BD FACSCanto II flow cytometer. Representative line graphs of 3 independent experiments are shown. (C) HEK293FT cells, Jurkat cells, human iPSCs, and CD34⁺ HSPCs were transfected with unlabeled or labeled *GADD45B*-targeting CRISPR/Cas9-gRNA RNP and analyzed for gene-modification efficiency using a TIDE assay. (D) Jurkat cells, human iPSCs, and CD34⁺ HSPCs were transfected with CX-rhodamine-labeled *GADD45B*-targeting CRISPR/Cas9-gRNA RNP and sorted 24 hours posttransfection using a flow cytometer. Genomic DNA was isolated 48 hours posttransfection from the total population of transfected cells and from sorted CX-rhodamine⁺ or fluorescein⁺ cells. TIDE assay analysis showed significantly higher gene modification efficiency in CX-rhodamine⁺ cells. Data in panels C and D are mean \pm standard deviations derived from 3 (HEK293FT cells, Jurkat cells, CD34⁺ HSPCs) or 4 (iPSCs) independent experiments. * $P \leq .05$, ** $P \leq .01$, Student *t* test. ns, not significant.

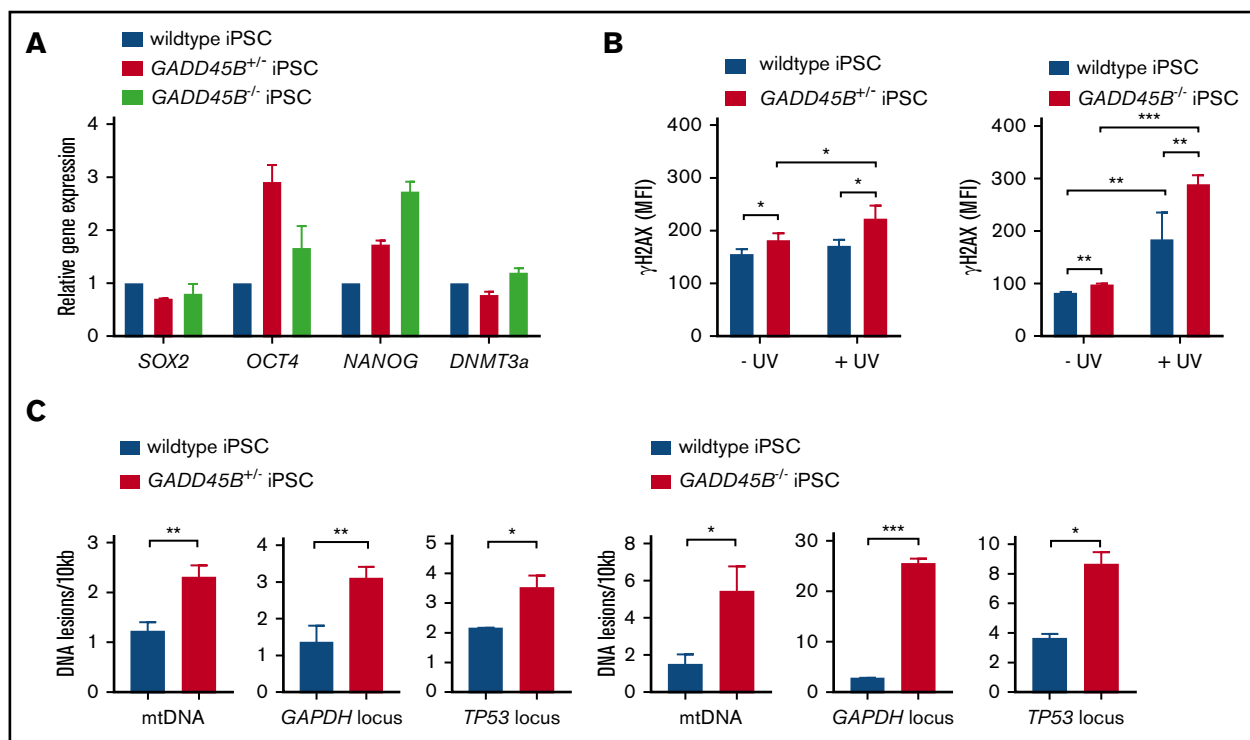


Figure 4. Heterozygous and homozygous *GADD45B* knockout in human iPSCs results in high levels of DNA damage. (A) Pluripotency state of *GADD45B*^{+/+} and *GADD45B*^{-/-} iPSCs was assessed by real-time quantitative PCR and compared with validated healthy donor-derived human iPSCs expressing wild-type *GADD45B*. (B) *GADD45B* wild-type, *GADD45B*^{+/+}, and *GADD45B*^{-/-} iPSCs were irradiated with UV light for 5 minutes, incubated under cell culture conditions for 2 hours, and stained for intracellular γ H2AX (phospho-Ser139). DNA damage in *GADD45B* wild-type and *GADD45B* heterozygous-knockout (C) or homozygous-knockout (D) iPSCs was quantified by the LORD-Q method. Cells were analyzed for mtDNA damage and nuclear DNA damage in the *GAPDH* and *TP53* gene loci. All data are mean \pm standard deviation derived from 3 independent experiments. * $P \leq .05$, ** $P \leq .01$, *** $P \leq .001$, Student *t* test.

Discussion

In the present study, we have developed a new method of CRISPR/Cas9-mediated gene editing in primary HSPCs and iPSCs using fluorescent labeling of CRISPR/Cas9-gRNA RNP complexes. Using fluorescein or CX-rhodamine signals from labeled CRISPR/Cas9-gRNA RNP, we were able to enrich gene-edited cells by fluorescent cell sorting. For clinical settings, it is essential to select and enrich gene-edited HSPCs because of the limited capacity of these cells to divide, to retain their engraftment capability, and to generate unlimited numbers of progeny cells. Sorting of the labeled cells also allows removal of untargeted HSPCs that may compete with gene-edited cells. In addition, application of CRISPR/Cas9 RNP decreases the probability and frequency of off-target effects, because CRISPR/Cas9 RNP activity is preserved in cells for only ~48 hours.

Dever et al recently reported the CRISPR/Cas9 RNP-based modification and enrichment of human HSPCs by introduction of a repair template targeting the human β -globin gene through a GFP-expressing adeno-associated virus-based vector.³ Although considered safer than retroviral constructs, adeno-associated virus-based expression constructs may induce antiviral host immune responses and may integrate into the host genome nonspecifically. Because RNP-mediated gene knockout allows the efficient virus- and DNA-free transfection and selection of edited cells, future studies should further investigate our method of fluorescent labeling of

CRISPR/Cas9 RNP in a gene-correction approach mediated by homology-directed repair, which additionally requires a donor template DNA. Again, the short exposure of cells to CRISPR/Cas9 RNP activity makes it superior to virus-based delivery techniques.

We also tested EGFP-conjugated CRISPR Cas9 RNP but found that EGFP tagging resulted in reduced editing efficiency compared with unlabeled CRISPR Cas9 RNP. At the same time, labeling of CRISPR/Cas9 RNP using our method described here does not affect editing.

Although we studied gene editing in primary hematopoietic stem cells and iPSCs, the method described here may be extended to other primary cell types. Gene-modification efficiency is dependent on the cell type, cell cycle stage, activation of DNA-repair pathways, chromatin dynamics at the gRNA-targeted gene locus, and the delivery method.²⁵⁻²⁷ Delivery and editing protocols may be further improved (eg, by synchronizing of the targeted cells), which could increase nuclear uptake of the RNP components and chromatin relaxation.

For a proof of principle, we chose to target the *GADD45B* gene and found that homo- and even heterozygous deficiency in *GADD45B* led to increased susceptibility to DNA damage. *GADD45B* belongs to a family of evolutionarily conserved *GADD45* proteins²⁸ that functions as stress sensors regulating cell cycle, survival, and apoptosis in response to various stress stimuli.²⁹ With some degree of redundancy, *GADD45* proteins exhibit specific functions, depending on the stimulus and cell type. *Gadd45b*-knockout mice

are viable, but *Gadd45b*^{-/-} primary mouse embryonic fibroblasts proliferate slowly and accumulate increased levels of DNA damage and features of premature senescence.³⁰⁻³³ It has also been shown that myeloid differentiation is compromised in *Gadd45b*^{-/-} mice.³³ Nothing was known about GADD45b functions in the DNA damage response of human HSPCs and iPSCs. Our study demonstrates an essential role for GADD45B in the survival and protection from DNA damage in human leukemia cells and CD34⁺ HSPCs that are not compensated for by other GADD45 proteins.

Our study is the first report describing transfection of iPSCs with labeled CRISPR/Cas9-gRNA RNP with high transfection and knockout efficiency. In future studies, gene correction using labeled RNP complexes for ex vivo gene therapy and transplantation could be tested in CD34⁺ cells. There are also reports describing in vivo gene correction in neurons, hepatocytes, and cardiomyocytes.^{3,14-20} Currently, there are many challenges associated with using CRISPR/Cas9 approaches. Efficient gene editing is reliant on the successful delivery of the Cas9 nuclease and the gRNA, which is especially cumbersome in primary cell types resistant to DNA transfection. Moreover, plasmid and viral delivery lead to persistent over-expression of Cas9, which can potentially result in off-targets. In contrast, direct delivery of RNP complexes, which are gradually cleared by intracellular degradation over time, does not result in Cas9 persistence and, therefore, reduces potential off-target effects. Furthermore, we did not detect toxic or inhibitory effects of the labeling on the gene-editing efficiency or on cell growth. As a result of their short exposure, it is also unlikely that the fluorochrome dyes used in our study are immunogenic in vivo. However, further optimizations are required for the in vivo application of our method. For instance, different dyes should be tested for their immunogenicity.

Taken together, chemical labeling of the gRNA and the direct transfection of RNP complexes provide a simple, safe, and efficient method that could considerably expand future therapeutic avenues for CRISPR/Cas9-mediated gene editing.

References

- Jinek M, Chylinski K, Fonfara I, Hauer M, Doudna JA, Charpentier E. A programmable dual-RNA-guided DNA endonuclease in adaptive bacterial immunity. *Science*. 2012;337(6096):816-821.
- Ran FA, Hsu PD, Wright J, Agarwala V, Scott DA, Zhang F. Genome engineering using the CRISPR-Cas9 system. *Nat Protoc*. 2013;8(11):2281-2308.
- Dever DP, Bak RO, Reinisch A, et al. CRISPR/Cas9 β -globin gene targeting in human haematopoietic stem cells. *Nature*. 2016;539(7629):384-389.
- Huai C, Jia C, Sun R, et al. CRISPR/Cas9-mediated somatic and germline gene correction to restore hemostasis in hemophilia B mice. *Hum Genet*. 2017;136(7):875-883.
- Ren J, Liu X, Fang C, Jiang S, June CH, Zhao Y. Multiplex genome editing to generate universal CAR T cells resistant to PD1 inhibition. *Clin Cancer Res*. 2017;23(9):2255-2266.
- Liu X, Zhang Y, Cheng C, et al. CRISPR-Cas9-mediated multiplex gene editing in CAR-T cells. *Cell Res*. 2017;27(1):154-157.
- Ren J, Zhang X, Liu X, et al. A versatile system for rapid multiplex genome-edited CAR T cell generation. *Oncotarget*. 2017;8(10):17002-17011.
- Eyquem J, Mansilla-Soto J, Giavridis T, et al. Targeting a CAR to the TRAC locus with CRISPR/Cas9 enhances tumour rejection. *Nature*. 2017;543(7643):113-117.
- Rupp LJ, Schumann K, Roybal KT, et al. CRISPR/Cas9-mediated PD-1 disruption enhances anti-tumor efficacy of human chimeric antigen receptor T cells. *Sci Rep*. 2017;7(1):737.
- Ye L, Wang J, Tan Y, et al. Genome editing using CRISPR-Cas9 to create the HPFH genotype in HSPCs: an approach for treating sickle cell disease and β -thalassemia. *Proc Natl Acad Sci USA*. 2016;113(38):10661-10665.

Acknowledgments

The authors thank Regine Bernhardt, Ingeborg Steiert, Karin Haehnel, and Ursula Hermanutz-Klein for the excellent technical assistance. The authors thank the FACS Core Facility of the University Hospital Tübingen, especially Kristin Bieber, Cornelia Gimmel, and Stella Autenrieth, for assistance with cell sorting. They also thank Kai Witte and D. Campana for providing 8E permeabilization reagent.

This work was supported by the Excellence Initiative of the Faculty of Medicine, University of Tübingen (J.S.), Madeleine Schickedanz Kinderkrebsstiftung (M.N.), German Cancer Consortium (P.M. and J.S.), DFG (M.K.), the Fresenius Foundation (M.K.), the Fritz Thyssen Foundation (B.D.), and the Jose Carreras Leukemia Foundation (J.S. and B.D.).

Authorship

Contribution: M.N., P.M., and J.S. made initial observations, designed the experiments, analyzed the data, and wrote the manuscript; M.N. and P.M. performed labeling of CRISPR/Cas9-gRNA RNP complexes, electroporation or transfection of cells, cell culture, treatment with UV light, FACS analysis, cell counts, cell sorting, Sanger sequencing, and LORD-Q experiments; B.D. and M.N. conducted experiments with iPSCs; M.N. and T.S. established transfection of iPSCs; Y.X. performed real-time quantitative PCR for pluripotency markers; D.A. performed image analysis of HEK293FT cells; K.S.-O. assisted with LORD-Q experiments and provided insightful comments; and M.K. and K.W. assisted with the interpretation of data and provided insightful comments.

Conflict-of-interest disclosure: The authors declare no competing financial interests.

Correspondence: Julia Skokowa, Division of Translational Oncology, Department of Hematology, Oncology, Clinical Immunology, Rheumatology and Pulmonology, University Hospital Tübingen, Otfried-Müller-Str 10, 72076 Tübingen, Germany; e-mail: julia.skokowa@med.uni-tuebingen.de.

11. Traxler EA, Yao Y, Wang YD, et al. A genome-editing strategy to treat β -hemoglobinopathies that recapitulates a mutation associated with a benign genetic condition. *Nat Med*. 2016;22(9):987-990.
12. Cyranoski D. CRISPR gene-editing tested in a person for the first time. *Nature*. 2016;539(7630):479.
13. Zhan T, Rindtorff N, Betge J, Ebert MP, Boutros M. CRISPR/Cas9 for cancer research and therapy. *Semin Cancer Biol*. 2018;S1044-579X(17)30274-2.
14. Staahl BT, Benekareddy M, Coulon-Bainier C, et al. Efficient genome editing in the mouse brain by local delivery of engineered Cas9 ribonucleoprotein complexes. *Nat Biotechnol*. 2017;35(5):431-434.
15. Xue W, Chen S, Yin H, et al. CRISPR-mediated direct mutation of cancer genes in the mouse liver. *Nature*. 2014;514(7522):380-384.
16. Yin H, Song CO, Dorkin JR, et al. Therapeutic genome editing by combined viral and non-viral delivery of CRISPR system components in vivo. *Nat Biotechnol*. 2016;34(3):328-333.
17. Wang X, Raghavan A, Chen T, et al. CRISPR-Cas9 targeting of PCSK9 in human hepatocytes in vivo—brief report. *Arterioscler Thromb Vasc Biol*. 2016;36(5):783-786.
18. Pankowicz FP, Barzi M, Legras X, et al. Reprogramming metabolic pathways in vivo with CRISPR/Cas9 genome editing to treat hereditary tyrosinaemia. *Nat Commun*. 2016;7(1):12642.
19. Liang WC, Liang PP, Wong CW, et al. CRISPR/Cas9 technology targeting Fas gene protects mice from concanavalin-A induced fulminant hepatic failure. *J Cell Biochem*. 2017;118(3):530-536.
20. Xie C, Zhang YP, Song L, et al. Genome editing with CRISPR/Cas9 in postnatal mice corrects PRKAG2 cardiac syndrome. *Cell Res*. 2016;26(10):1099-1111.
21. Gundry MC, Brunetti L, Lin A, et al. Highly efficient genome editing of murine and human hematopoietic progenitor cells by CRISPR/Cas9. *Cell Reports*. 2016;17(5):1453-1461.
22. Brinkman EK, Chen T, Amendola M, van Steensel B. Easy quantitative assessment of genome editing by sequence trace decomposition. *Nucleic Acids Res*. 2014;42(22):e168.
23. Lehle S, Hildebrand DG, Merz B, et al. LORD-Q: a long-run real-time PCR-based DNA-damage quantification method for nuclear and mitochondrial genome analysis. *Nucleic Acids Res*. 2014;42(6):e41.
24. Selvakumaran M, Lin HK, Sjin RT, Reed JC, Liebermann DA, Hoffman B. The novel primary response gene MyD118 and the proto-oncogenes myb, myc, and bcl-2 modulate transforming growth factor beta 1-induced apoptosis of myeloid leukemia cells. *Mol Cell Biol*. 1994;14(4):2352-2360.
25. Lin S, Staahl BT, Alla RK, Doudna JA. Enhanced homology-directed human genome engineering by controlled timing of CRISPR/Cas9 delivery. *eLife*. 2014;3:e04766.
26. Yang D, Scavuzzo MA, Chmielowiec J, Sharp R, Bajic A, Borowiak M. Enrichment of G2/M cell cycle phase in human pluripotent stem cells enhances HDR-mediated gene repair with customizable endonucleases. *Sci Rep*. 2016;6(1):21264.
27. Chen X, Rinsma M, Janssen JM, Liu J, Maggio I, Gonçalves MA. Probing the impact of chromatin conformation on genome editing tools. *Nucleic Acids Res*. 2016;44(13):6482-6492.
28. Zhan Q, Lord KA, Alamo I Jr, et al. The gadd and MyD genes define a novel set of mammalian genes encoding acidic proteins that synergistically suppress cell growth. *Mol Cell Biol*. 1994;14(4):2361-2371.
29. Liebermann DA, Hoffman B. Gadd45 in stress signaling. *J Mol Signal*. 2008;3:15.
30. Magimaidas A, Madireddi P, Maifrede S, Mukherjee K, Hoffman B, Liebermann DA. Gadd45b deficiency promotes premature senescence and skin aging. *Oncotarget*. 2016;7(19):26935-26948.
31. Gupta M, Gupta SK, Balliet AG, et al. Hematopoietic cells from Gadd45a- and Gadd45b-deficient mice are sensitized to genotoxic-stress-induced apoptosis. *Oncogene*. 2005;24(48):7170-7179.
32. Gupta M, Gupta SK, Hoffman B, Liebermann DA. Gadd45a and Gadd45b protect hematopoietic cells from UV-induced apoptosis via distinct signaling pathways, including p38 activation and JNK inhibition. *J Biol Chem*. 2006;281(26):17552-17558.
33. Gupta SK, Gupta M, Hoffman B, Liebermann DA. Hematopoietic cells from gadd45a-deficient and gadd45b-deficient mice exhibit impaired stress responses to acute stimulation with cytokines, myeloablation and inflammation. *Oncogene*. 2006;25(40):5537-5546.

Mir P. et al., 2020, *Methods in Molecular Biology*



Gene Knockout in Hematopoietic Stem and Progenitor Cells Followed by Granulocytic Differentiation

Perihan Mir, Malte Ritter, Karl Welte, Julia Skokowa, and Maksim Klimiankou

Abstract

In this chapter, we present an optimized CRISPR/Cas9 RNP nucleofection approach for gene knockout (KO) in hematopoietic stem and progenitor cells (HSPCs). With experimentally proved active locus-specific sgRNAs, we routinely reach over 80% gene KO in HSPCs, thus avoiding the need for cell sorting or enrichment of targeted cell population. Additionally, we provide a protocol for in vitro granulocytic differentiation of HSPCs after gene KO and detailed description of granulocyte function tests which can be applied to study the effects of a particular gene KO.

Key words Hematopoietic stem and progenitor cells, Gene knockout, CRISPR/Cas9, Single-guide RNA, Ribonucleoprotein, Nucleofection, Granulocytic differentiation

1 Introduction

CRISPR (clustered regularly interspaced short palindromic repeat) DNA editing technology is becoming a revolutionary tool in biotechnology, medical, and biological research. In less than a decade after publishing the critical discovery that CRISPR/Cas9 can be reprogrammed to target a desired DNA locus in bacteria [1], RNA-programmable gene editing has transformed biological research, thanks to its extreme flexibility, efficiency, and ease of use (*see* Chapters 1 and 19). Currently, the most popular choice for genome editing is CRISPR/Cas9 system from *Streptococcus pyogenes*. Briefly, the complex of Cas9 protein and a guide RNA bind to DNA through base complementarity. This binding induces DNA cleavage [2]. Gene KO can be achieved by error-prone DNA repair mechanism called nonhomologous end joining pathway which induces insertions or deletions (indels) at position of the DNA cut site. Precise nucleotide sequence integration in desired

DNA locus can be achieved by exploiting the homology-directed repair pathway.

CRISPR/Cas9 system is widely used because of the short and simple NGG protospacer-adjacent motif (PAM) sequence, the best characterized on- and off-target profiles, availability of online tools to assist in performing CRISPR/Cas9 experiments, and its existence in different formats (plasmid, RNA, protein) from an expanding number of companies. Over the past few years, many engineered Cas9 variants have been developed. Different Cas9 variants have been generated (e.g., high-fidelity Cas9 variants including eSpCas9 [3], SpCas9-HF1 [4], and HypaCas9 [5], catalytically dead Cas9 (dCas9) [6], Cas9 nickase [7], and Cas9 variant with expanded PAM recognition site [8]). This discovery enables targeted genome modification with unprecedented flexibility and efficiency (*see* Chapter 21).

Another critical part of CRISPR/Cas9 system is a guide RNA. Guide RNA can be used as single-guide RNA (sgRNA) or as a two-component system which includes CRISPR RNA (crRNA) and trans-activating CRISPR RNA (tracrRNA). Additionally, chemical modifications of sgRNA can substantially increase genome editing efficiency in human primary cells ([9], *see* Chapter 2). Availability of highly purified Cas9 protein and chemically modified guide RNA with enhanced stability and low immune-stimulatory properties from commercial vendors makes nucleofection of CRISPR/Cas9 RNP complex the cost-effective and efficient way of generating targeted gene KOs (*see* Chapter 26).

The advantages of CRISPR/Cas9 RNP complex nucleofection over transfection with Cas9 and sgRNA DNA (plasmid) or RNA or virus-assisted delivery are as follows: it is a nontoxic, well-tolerable genome editing approach with short but high activity window, short persistence of RNP complex in the nuclei reduces probability of cuts at off-target DNA loci, CRISPR/Cas9 RNP complex does not require cellular transcription or translation machinery, no/low induction of inflammatory or cell response against foreign DNA and RNA after RNP complex nucleofection, and visualization of RNP by labeling of Cas9 protein [10].

CRISPR/Cas9 gene KO efficiency depends on multiple factors. Among the most important is the on-target score of sgRNA. Although, a broad range of prediction algorithms and methods for on-target sgRNA activity estimation are available online [11–13], the functional sgRNA validation after *in silico* on-target activity analysis remains the most comprehensive way to identify a highly active locus-specific sgRNA. Usually, 3–5 sgRNAs are tested per gene or gene locus. In our hands, sgRNA efficiencies have varied from 10% to 99% of edited allele. The second most important factor for successful gene KO is the usage of a sufficient number of viable HSPCs (too less or too many cells per nucleofection reaction may lead to suboptimal results). Preliminary tests may help to determine

the optimal amount of CRISPR/Cas9 RNP complex and the number of HSPCs used for nucleofection.

After successful induction of gene KO, HSPCs can be further differentiated *in vitro* to cells of the myeloid lineage using appropriate culture conditions. If myeloid differentiation is not disturbed by gene KO, then these cells are expected to demonstrate upregulation of myeloid specific surface markers, morphological maturation, and recapitulation of granulocyte functions. Thus, the coupling of targeted gene KO approach via CRISPR/Cas9 RNP nucleofection with a protocol of granulocytic differentiation of HSPCs and granulocyte function tests allows investigation of the role of certain genes in hematopoiesis in a fast and robust way. It should be noted that the entire protocol can be completed in 3 weeks (Fig. 1).

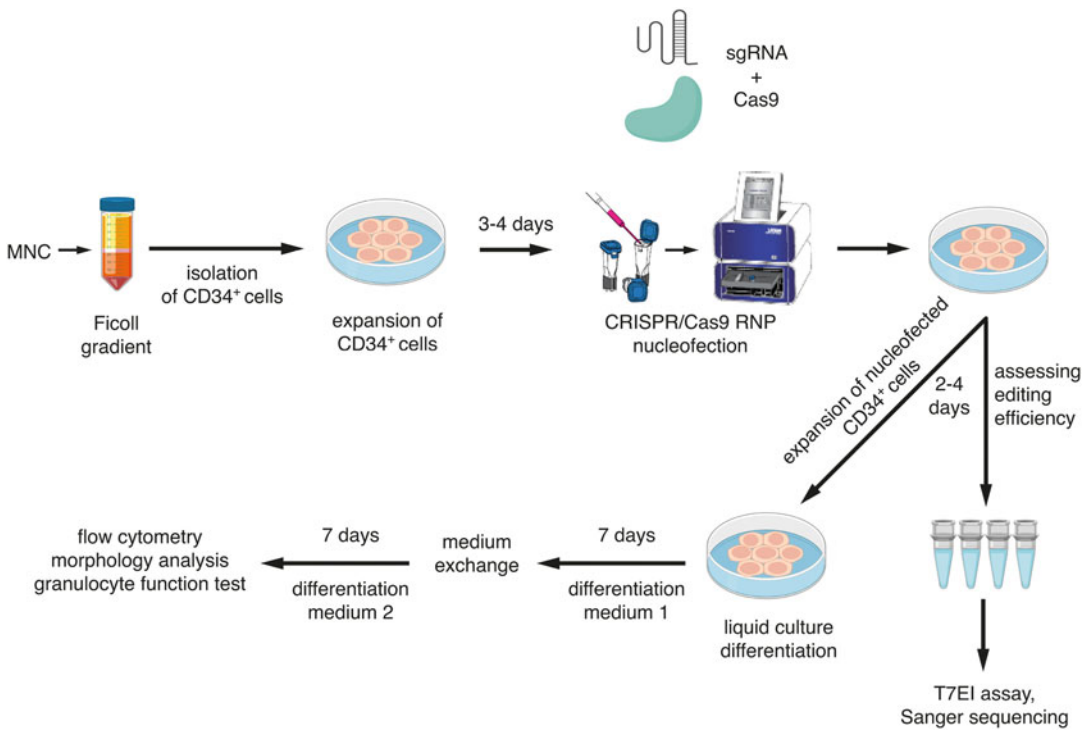


Fig. 1 Scheme of gene KO in HSPCs followed by *in vitro* granulocytic differentiation. CD34⁺ cells are isolated from BM or mobilized blood MNCs and expanded *in vitro* for 3–4 days. After expansion CD34⁺ cells are nucleofected with CRISPR/Cas9 RNP using the Lonza 4D nucleofection system. Knockout HSPCs are differentiated *in vitro* toward granulocyte lineage for 14 days and then analyzed by flow cytometry, morphologic analysis, and granulocyte function tests. Gene editing efficiency is assessed 2–4 days after nucleofection by T7EI assay and/or Sanger sequencing. Indel efficiency is determined by TIDE or ICE analysis web tools

2 Materials

All reagents, lab equipment, and web tools described in this section have been successfully tested by us, but other commercially available equivalents can be alternatively used after some optimization steps.

2.1 CD34⁺ Isolation and Expansion

1. Bone marrow (BM) or mobilized blood from healthy individuals or patients as source for CD34⁺ cells.
2. Ficoll-Paque density gradient media (density: 1.077 g/mL) for isolation of BM or peripheral blood mononuclear cell (BMMNCs or PBMNCs, respectively).
3. Human CD34 MicroBead Kit for magnetic beads-based isolation of CD34⁺ cells from BMMNCs or PBMNCs.
4. Cell freezing medium: PSC cryopreservation medium or 90% FCS supplemented with 10% DMSO.
5. CD34⁺ expansion medium: Stemline II Hematopoietic Stem Cell Expansion medium supplemented with 10% FCS, 1% L-glutamine, 1% penicillin/streptomycin, and a human recombinant cytokine cocktail consisting of 20 ng/mL IL-3, 20 ng/mL IL-6, 20 ng/mL TPO, 50 ng/mL SCF, and 50 ng/mL FLT-3L.
6. 24- or 48-well cell culture plates.

2.2 CRISPR/Cas9 RNP Nucleofection

1. Chemically synthesized CRISPR/Cas9 single-guide RNA with 2'-O-methyl 3'phosphorothioate modifications at the 3' and 5' termini produced at small scale 15–20 nmol. For selection of the most efficient sgRNA, it is recommended to order and test 3–5 sgRNAs per locus.
2. Alt-R[®] S.p. Cas9 Nuclease V3 or Alt-R[®] S.p. HiFi Cas9 Nuclease V3 (IDT).
3. Amaxa 4D-Nucleofector[™] System.
4. P3 Primary Cell 4D-Nucleofector Kit.
5. RNase-free aerosol-resistant pipette tips.
6. RNase-free SafeSeal microcentrifuge tubes.
7. 1x TE Buffer pH 7.5.

2.3 Estimation of Gene-Editing Efficiency

1. DNA extraction kit.
2. Nanodrop or Qubit device and Qubit dsDNA High Sensitivity Assay Kit.
3. PCR: GoTaq Hot Start DNA Polymerase Kit, PCR primers for amplification of genome locus of interest.
4. PCR Nucleotide Mix.

5. T7 Endonuclease I Assay (T7EI) is a quick and cheap method of gene editing efficiency estimation which requires T7 Endonuclease I and NEB buffer 2.
6. PCR product purification kit or enzymatic cleanup using ExoSAP [14].
7. Sanger sequencing by commercial service provider or in-house Sanger sequencing facility.

2.4 Analysis of Granulocytic Differentiation

1. Colony-forming unit (CFU) assay: MethoCult™ Enriched (STEMCELL Technologies), IMDM with 2% FCS (STEMCELL Technologies), Antibiotic-Antimycotic Solution (Sigma Aldrich), 35 mm culture dishes, sterile 16 gauge needles, 1.5 in. long with a metal Luer Lock hub (STEMCELL Technologies).
2. Liquid culture differentiation: Differentiation medium 1 for day 0–7 consists of RPMI 1640 supplemented with 10% FCS, 1% penicillin/streptomycin, and human recombinant cytokines: 5 ng/mL SCF, 5 ng/mL IL-3, 5 ng/mL GM-CSF, and 10 ng/mL G-CSF. Differentiation medium 2 for day 7–14 consists of RPMI 1640 supplemented with 10% FCS, 1% penicillin/streptomycin, and 10 ng/mL G-CSF.
3. Morphology analysis: Shandon Cytospin centrifuge, Cytospin microscope slides, May–Grünwald, and Wright–Giemsa staining solutions.
4. FACS staining: antihuman CD45, antihuman CD34, antihuman CD33, antihuman CD11b, antihuman CD14, antihuman CD15, antihuman CD16 antibodies, PBS supplemented with 2% FCS and 0.02% sodium azide.

2.5 Analysis of Granulocyte Functions

1. Chemotaxis: 24-well Transwell reaction plates, inserts with 5 μm pore size, *N*-formyl-Met-Leu-Phe (fMLP), RPMI 1640 medium, bovine serum albumin (BSA), 5 mL FACS tubes, flow cytometer.
2. Phagocytosis: fluorescein-conjugated *Staphylococcus aureus* BioParticles, RPMI 1640 without Phenol red, 5 mL FACS tubes, flow cytometer capable of measuring FITC signal.
3. Netosis: IncuCyte® Live Cell Imaging system, Phorbol 12-myristate 13-acetate (PMA), RPMI 1640 without Phenol red, BSA, 96-well plate flat bottom, Sytox green dye, 0.001% Poly-L-Lysine Solution.
4. ROS production: ROS-Glo H₂O₂ Assay, bioluminescence reader, and 96-well plates.

3 Methods

3.1 sgRNA Design

1. Usually, the design of sgRNAs is performed with the assistance of online web tools. We routinely use the DESKGEN cloud platform (www.deskgen.com) or Benchling (www.benchling.com). Both online resources require a free registration.
2. For gene KO, make sure to target all possible isoforms of the gene of interest or design multiple sgRNAs (*see Note 1*).
3. Select all sgRNA target sites around the ideal position, and evaluate on-target and off-target prediction scores (*see Note 2*).
4. Choose from 3 to 5 sgRNAs per locus with the lowest off-target and highest on-target prediction score.
5. Test sgRNAs, as described in the following sections.

3.2 PCR Primers for Assessing CRISPR/Cas9 Gene-Editing Efficiency

1. Primer-BLAST (<http://www.ncbi.nlm.nih.gov/tools/primer-blast>) is a suitable online tool to design PCR primers [15] for assessing CRISPR/Cas9 gene editing efficiency by sequence trace decomposition.
2. Design PCR primers to ideally have a PCR product length of 700 bp.
3. To allow correct estimation of gene editing efficiency by sequence trace decomposition, the projected Cas9 cut site should be located around 200 bp away from reverse and forward primers used for sequencing.

3.3 CD34⁺ Isolation and Expansion

1. Pipet 15 mL Ficoll-Paque medium into a 50 mL tube.
2. Dilute BM or mobilized PB sample 1:2 with PBS and carefully layer it onto the Ficoll-Paque medium (*see Note 3*).
3. Centrifuge at $500 \times g$ for 25 min at room temperature (RT) with the centrifuge brake set off.
4. The mononuclear cell fraction is located in the interphase. Transfer the complete interphase layer to a sterile tube and wash the cells twice with 30 mL ice-cold PBS by centrifuging at $300 \times g$ for 8 min at 8 °C.
5. Resuspend cells in ice-cold PBS and determine cell count of BMMNCs or PBMNCs (*see Note 4*).
6. Resuspend cells in 300 μ L MACS buffer. Use 200 μ L FcR blocking and 100 μ L CD34 microbeads for up to 10^8 cells (*see Note 5*).
7. Mix gently and incubate for 30 min at 4 °C in the refrigerator.
8. Wash cells with 5–10 mL MACS buffer by centrifugation at $300 \times g$ for 10 min. Remove supernatant.

9. Resuspend cells in 500 μ L MACS buffer.
10. Place the separation column in the magnetic field.
11. Rinse the column with 3 mL MACS buffer if you use a LS column, and if you use MS column, rinse with 500 mL prior to use (*see Note 6*).
12. Apply cell suspension onto the column (*see Note 7*). If desired, collect the CD34-negative cells in the flow-through fraction.
13. Wash LS column three times with 3 mL MACS buffer (if you use MS column, wash with 500 μ L three times).
14. Remove column from magnetic field and put it onto a 15 mL tube.
15. Pipet 3 mL of MACS buffer on the column (1 mL for MS column) and flush out the cells by pushing the plunger into the column.
16. Determine number of CD34⁺ HSPCs (*see Note 8*).
17. Either use cells freshly for gene editing experiment or freeze them for long-term preservation.
18. Perform cryopreservation in either 0.5 mL PSC cryopreservation medium or in 1 mL 90% FCS supplemented with 10% DMSO.
19. Defreeze CD34⁺ HSPCs in a pre-warmed standard medium for suspension cells (e.g., RPMI 1640 with 10% FCS and 1% penicillin/streptomycin) (*see Note 9*). After centrifugation, resuspend the cells in hematopoietic stem cell expansion medium.
20. Culture CD34⁺ HSPCs in CD34⁺ expansion medium at a density of 2×10^5 /mL (*see Note 10*) at 37 °C and 5% CO₂.
21. Determine cell count at day 3 or day 4 after culturing. If cells proliferate and cell viability is higher than 80% (e.g., by trypan blue), perform CRISPR/Cas9 RNP nucleofection.

3.4 CRISPR/Cas9 RNP Nucleofection

1. Assemble Cas9 protein with sgRNA for 30 min at RT. Use 136 pmol Cas9 protein and 330 pmol sgRNA for 1×10^6 cells.
2. For a single Nucleocuvette™ vessel, mix 18 μ L of Supplement 1 and 82 μ L P3 Primary Cell Nucleofector™ Solution from P3 Primary Cell Nucleofection Kit (Lonza) (*see Note 11*).
3. We recommend to use “mock” nucleofected cells to control the effect of nucleofection itself.
4. Add CRISPR/Cas9 RNP complex to the nucleofection buffer mix (*see Note 12*).
5. Wash cells once with PBS. Gently remove as much of the supernatant as possible.

6. Resuspend the cell pellet in the RNP-nucleofection buffer mix and transfer the mixture into the Nucleocuvette™ vessel, avoiding bubbles.
7. Place the Nucleocuvette™ vessel in the retainer of the 4D-Nucleofector X Unit.
8. Select and start the Nucleofector™ program CA-137 (*see Note 13*).
9. Carefully transfer the nucleofected cells into CD34⁺ expansion medium, avoiding repeated aspiration of the sample (*see Note 14*). Culture CD34⁺ cells, as described in Subheading 3.3.
10. After 2–4 days, harvest 1×10^5 cells for DNA isolation to determine the gene editing efficiency.

3.5 Estimation of CRISPR/Cas9 Gene-Editing Efficiency

1. Isolate DNA from harvested cells using the column-based QIAamp DNA Mini Kit according to the manufacturer's protocol and determine the DNA concentration using a Nanodrop or Qubit.
2. Alternatively, for quick estimation of KO efficiency, lyse $0.5\text{--}1 \times 10^5$ cells in 25–50 μL of QuickExtract DNA Extraction Solution (Lucigen) and then incubate at 65 °C for 6 min and at 98 °C for 2 min (*see Note 15*).
3. Run PCR for target genome locus of interest using the GoTaq Hot Start Polymerase Kit. Per reaction, pipet a master mix consisting of 4 μL of 5x Flexi buffer, 0.5 μL dNTP mix (10 mM each), 1 μL 25 mM MgCl₂, 1 μL forward and reverse primer (10 μM each), and 0.125 μL Go-Taq polymerase (5 U/ μL). Add 100 ng DNA (or 2–4 μL of QuickExtract DNA Extraction Solution) to the PCR master mix and PCR-grade H₂O to a final volume of 20 μL . The PCR program is as follows: denaturation 1 min at 95 °C, annealing for 1 min at the temperature that is optimal for selected primer pair (usually, it is 5 °C below the T_m of the primers used), and extension 1 min at 72 °C. Repeat PCR cycles for 35 times. A final extension for 5 min at 72 °C is recommended.
4. To quickly estimate gene-editing efficiency, T7EI assay may be performed. T7EI recognizes and cleaves hetero-duplexed DNA (*see Note 16*). First, mix 11 μL of PCR product and 2 μL of NEB buffer 2. Anneal PCR sample in thermal cycler using the following hybridization conditions: denaturation at 95 °C for 10 min, annealing at 95–85 °C with ramp rate –2 °C/s followed by second annealing at 85–25 °C with ramp rate –0.3 °C/s. Add 2 μL of T7EI (20 U) to the sample

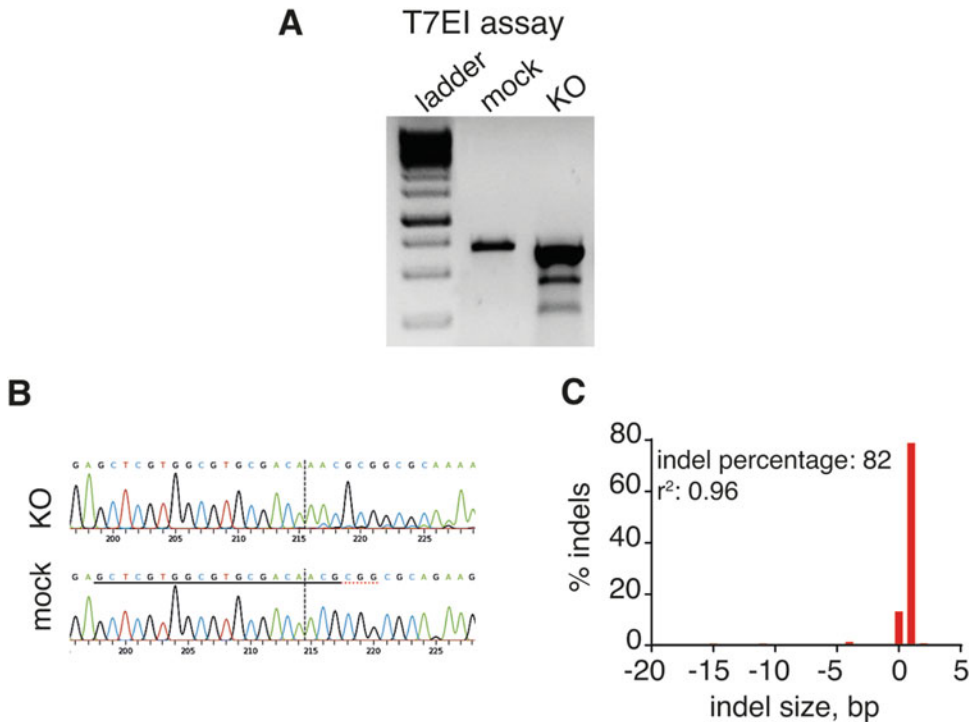


Fig. 2 (a) Agarose gel electrophoresis of PCR products after T7EI assay showing two extra bands in KO cells revealed the presence of heteroduplexed DNA resulting from gene editing. (b) Representative result of CRISPR/Cas9 RNP-mediated knockout in HSPCs showing Sanger sequencing of total population aligned to sequence track of mock cells. The position of DNA cut is depicted by dashed line. Target DNA sequence for guide RNA is underlined. (c) Representative ICE graph reconstructs the spectrum of indels in gene-edited HSPCs. Total editing efficiency is estimated approximately 82% with $r^2 = 0.96$ and one base insertion in the majority of cells. (b and c) were generated using ICE web tool from Synthego

and incubate at 37 °C for 1 h. Load sample into a 1.5% agarose gel and run it at 85 V for 1 h. Detect PCR products using a gel documentation system. In samples with successful gene editing, two low size extra bands are visible (Fig. 2a). The gene-editing efficiency can be calculated using density profile of the DNA bands by the following formula [16]:

$$\% \text{ gene modification} = 100 \times (1 - (1 - \text{fraction cleaved})^{1/2})$$

- For analysis of gene KO efficiency by sequence trace decomposition, PCR products from mock and CRISPR/Cas9 RNP nucleofected cells should be purified by column-based QIAquick PCR Purification Kit or enzymatic PCR clean-up using ExoSAP. Sanger sequencing traces have to be clean and have sufficient length to allow confident decomposition. Assess the gene modification efficiency using web tools such as TIDE assay [17] (<https://tide.deskgen.com>) or ICE analysis

(<https://ice.synthego.com>). For that, upload sgRNA sequence, sequencing traces (.ab1 file) of the mock sample, and the sample after gene editing (Fig. 2b, c).

6. Detailed analysis of mutation composition in the edited cells can be performed by cloning of PCR product into *E. coli* followed by sequencing of single bacteria clones. The most precise method of estimation of mutant allele frequency after gene editing/gene knockout is deep sequencing of PCR product generated from edited DNA locus.
7. Additionally, the analysis of off-target sites may be performed (*see Note 17*).

3.6 Characterization of Granulocytic Differentiation of HSPCs

3.6.1 Colony-Forming Unit Assay

1. Resuspend $3\text{--}10 \times 10^3$ cells (*see Note 18*) in 300 μL IMDM with 2% FCS, and then add 30 μL Antibiotic–Antimycotic Solution.
2. Add the cell suspension to 3 mL MethoCult™ Enriched medium. Vortex thoroughly, and wait until air bubbles disappear.
3. Seed the cell suspension into two 3.5 cm culture dishes (1.1 mL per dish) using sterile gauge needle.
4. Keep the plates in CO₂ cell culture incubator for 14 days and determine colony numbers and types at day 14 (*see Note 19*).

3.6.2 Liquid Culture Granulocytic Differentiation

1. After CRISPR/Cas9 RNP nucleofection, seed the cells at a density of $2 \times 10^5/\text{mL}$. During the first 7 days of differentiation, the cells are kept in differentiation medium 1 with medium exchange every second day (*see Note 20*).
2. At day 7, replace medium 1 with differentiation medium 2. The medium has to be changed every second day until day 14.
3. At day 14, perform flow cytometric analysis using antibodies specific for the following hematopoietic/myeloid markers: CD45 (leukocyte marker), CD34 (HSPC marker), CD33 (promyelocyte marker), CD11b (myeloid cell marker), CD14 (monocyte marker), and CD15 and CD16 (neutrophil markers). You may determine neutrophil percentage by gating on neutrophils as follows: CD45⁺CD11b⁺CD15⁺, or CD45⁺CD11b⁺CD16⁺, or CD45⁺CD15⁺CD16⁺ cells.

3.6.3 Evaluation of Cell Morphology

1. Load the Cytoclip™ slide clips by fitting the filter card, the sample chamber, and the glass slide. Place an assemble Cytoclip™ slide clips in the slide clip support plate of the cytospin centrifuge ensuring that the centrifuge is balanced.
2. Pipette 2×10^4 cells from liquid culture differentiation (100 μL) into Cytofunnel™.
3. Centrifuge for 3 min at $200 \times g$.

4. Stain cytospin slides for 5 min in May–Grünwald stain, rinse shortly with ddH₂O, and then stain for 10 min in Wright–Giemsa stain. Afterwards rinse shortly with ddH₂O.
5. Determine cell morphology using a microscope.

3.7 Granulocyte Function Tests

3.7.1 Chemotaxis Assay

1. Resuspend the cells at 1×10^6 cells/mL in RPMI with 0.5% BSA and seed 200 μ L of the cell suspension on top of the polycarbonate membrane with 5 μ m pore size.
2. Fill the bottom well with RPMI 1640 medium supplemented with 0.5% BSA with or without 1 nM fMLP (*see* **Note 21**).
3. Incubate the plate for 2 h at 37 °C, 5% CO₂.
4. Add 70 μ L of 50 mM EDTA to the lower chamber and transfer the plate to 4 °C for 30 min.
5. After incubation, remove the inserts, resuspend the cells vigorously, and transfer the cell suspension from the lower chamber into FACS tubes.
6. Count cells on flow cytometer.

3.7.2 Phagocytosis Assay

1. Resuspend 3–10 $\times 10^4$ cells in 100 μ L RPMI 1640 medium supplemented with 2% BSA.
2. Add fluorescent-labeled *Staphylococcus aureus* bioparticles in a ratio of 1:100 per cell and incubate at 37 °C for 2 h. Make sure to have untreated controls to determine background fluorescence.
3. After incubation, wash the cells twice with PBS supplemented with 2% BSA, resuspend cells in PBS with 2% BSA, and then measure the number of FITC-positive cells using flow cytometer.

3.7.3 Netosis Assay

1. Coat the wells of a flat bottom 96-well plate for 30 min at RT with 50 μ L/well 0.0001% Poly-L-Lysin solution.
2. Remove the solution after coating and wash twice with PBS.
3. Seed 2×10^4 cells in 100 μ L per well, add Sytox Green reagent to a final concentration of 250 nM, and let cells to adhere for 20 min at RT.
4. Carefully add stimulant of choice to induce net release. We used PMA at 100 nM.
5. Place the plates in the InCuCyte[®] live cell analysis system and perform phase-contrast and GFP imaging every 10 min at 20 \times magnifications overnight.
6. Analyzed the data on integrated software.

3.7.4 ROS Production

1. Seed the cells at a density of 1×10^5 /mL, and then add fMLP at a final concentration of 10 nM to activate ROS production.
2. Incubate for 30 min at 37 °C, 5% CO₂.
3. Measure the level of hydrogen peroxide (H₂O₂) ROS by the ROS-Glo H₂O₂ Assay Kit according to manufacturer's protocol.

4 Notes

1. The preferred localization of guide RNA binding site for introduction of KO by CRISPR/Cas9 system is the first exon, which is present in all coding RNA transcripts. It is important to make sure that the selected DNA sequence is unique, thus reducing the probability of multiple binding of guide RNA to human genome.
2. Benchling and DESKGEN web sites provide on-target and off-target scores for every designed protospacer sequence. For comprehensive analysis of potential off-target sites, a bioinformatics-based tool, COSMID (CRISPR Off-target Sites with Mismatches, Insertions, and Deletions, <https://crispr.bme.gatech.edu>) [18], may be used. Additionally, calculation of microhomology-associated score can be helpful for the estimation of frequency of undesired in-frame deletion and selection of the gene locus with high out-of-frame score. Microhomology-Predictor tool [19] is available under <http://www.rgenome.net/mich-calculator>.
3. When layering the PB or BM sample onto Ficoll-Paque medium, pipet it gently to avoid mixing of medium and diluted BM/mobilized blood sample.
4. In case of cells clumps, use a nylon mesh (pre-separation filter with 30 μm, Miltenyi) to remove cell clumps prior to microbead labeling, to avoid a clogged column.
5. You may scale up or down the amount of beads and FcR blocking reagent, according to the cell number.
6. For 1×10^8 PBMNCs or BMMNCs, use either MS or LS columns.
7. For each step, wait until the column reservoir is empty before proceeding to the next step. At the same time, do not let the column to dry out.
8. We recommend to check the isolated CD34⁺ cell fraction for its purity by staining the cells with an anti-CD34 antibody and flow cytometric analysis before proceeding with gene editing experiments.

9. Hematopoietic stem cell medium and cytokines are expensive cell culture reagents. RPMI 1640 cell medium or other equivalents may be used for the defreezing of CD34⁺ cells with no adverse effects for the cells.
10. CD34⁺ HSPCs proliferate better in a dense cell culture with close cell-to-cell contact. Do not seed them with a density lower than 2×10^5 /mL.
11. For testing several sgRNAs, you may use the Lonza 16-well Nucleocuvette™ strip to nucleofect $1\text{--}10 \times 10^5$ cells in a total volume of 20 μ L. This way is cost-effective for saving CRISPR/Cas9 RNP and valuable primary cells.
12. The total volume of RNP-nucleofection buffer mix should not exceed 110 μ L for nucleofection in the Nucleocuvette™ vessel.
13. Optional: we recommend to let the cells stay for 10 min after nucleofection at RT or in cell culture incubator before transferring them into the cell culture plate.
14. Lonza Nucleocuvette™ vessel may be reused for up to three times. Rinse the cuvettes three times with ddH₂O and once with EtOH. Then expose Nucleocuvette™ vessel with open lid to UV light for at least 30 min.
15. Cell lysis in the QuickExtract DNA Extraction Solution does not allow DNA concentration measurements. Usually, 2–5 μ L of the lysate is sufficient for PCR. If PCR yields no product while the positive control shows specific PCR band, then dilute the quicklyzed DNA 1:3–1:5 with the QuickExtract DNA Extraction Solution and repeat PCR.
16. T7EI assay might not give an exact estimation of gene modification efficiency.
17. CRISPR/Cas9 RNP off-targets site analysis may be performed as follows:
 - (a) In silico prediction of off-target DNA loci followed by Sanger sequencing of the top predicted off-target sites (low sensitivity, time consuming, low output).
 - (b) Custom NGS panel designed for predicted off-target DNA regions (high sensitivity, long turnover time).
 - (c) Whole genome or exome DNA sequencing with high depth (can be expensive, especially at the genome level, high quality, and amount of DNA is necessary).
18. CD34⁺ cells lose stemness during in vitro culture. The number of cells plated for CFU experiment depends on how long cells were kept in culture. If CD34⁺ cells are cultured more than 1 week, then use 10×10^3 cells per CFU experiment.

19. Place two 3.5 cm CFU dishes and an extra dish with 2 mL of PBS and without a lid in a 10 cm dish to avoid the 3.5 dishes from drying out.
20. It is not recommended to disturb the cells every second day by collecting the whole medium volume. Instead, without disturbing or soaking up the cells, gently remove as much medium as possible and add the same amount of fresh medium to the cells.
21. Each sample needs to be tested with and without chemoattractant (fMLP) to control for spontaneous migration. Additionally, each condition should be conducted at least in technical duplicates.

Acknowledgments

This work was supported by German Cancer Consortium (P.M. and J.S.), DFG (J.S., M.K.), the Fresenius Foundation (M.K.), and the Jose Carreras Leukemia Foundation (M. R.).

References

1. Jinek M, Chylinski K, Fonfara I, Hauer M, Doudna JA, Charpentier E (2012) A programmable dual-RNA-guided DNA endonuclease in adaptive bacterial immunity. *Science* 337 (6096):816–821
2. Jinek M, East A, Cheng A, Lin S, Ma E, Doudna J (2013) RNA-programmed genome editing in human cells. *Elife* 2:e00471
3. Slaymaker IM, Gao L, Zetsche B, Scott DA, Yan WX, Zhang F (2016) Rationally engineered Cas9 nucleases with improved specificity. *Science* 351(6268):84–88
4. Kleinstiver BP, Pattanayak V, Prew MS, Tsai SQ, Nguyen NT, Zheng Z, Joung JK (2016) High-fidelity CRISPR-Cas9 nucleases with no detectable genome-wide off-target effects. *Nature* 529(7587):490–495
5. Chen JS, Dagdas YS, Kleinstiver BP, Welch MM, Sousa AA, Harrington LB, Sternberg SH, Joung JK, Yildiz A, Doudna JA (2017) Enhanced proofreading governs CRISPR-Cas9 targeting accuracy. *Nature* 550 (7676):407–410
6. Qi LS, Larson MH, Gilbert LA, Doudna JA, Weissman JS, Arkin AP, Lim WA (2013) Repurposing CRISPR as an RNA-guided platform for sequence-specific control of gene expression. *Cell* 152(5):1173–1183
7. Mali P, Aach J, Stranges PB, Esvelt KM, Moosburner M, Kosuri S, Yang L, Church GM (2013) CAS9 transcriptional activators for target specificity screening and paired nickases for cooperative genome engineering. *Nat Biotechnol* 31(9):833–838
8. Hu JH, Miller SM, Geurts MH, Tang W, Chen L, Sun N, Zeina CM, Gao X, Rees HA, Lin Z, Liu DR (2018) Evolved Cas9 variants with broad PAM compatibility and high DNA specificity. *Nature* 556(7699):57–63
9. Hendel A, Bak RO, Clark JT, Kennedy AB, Ryan DE, Roy S, Steinfeld I, Lunstad BD, Kaiser RJ, Wilkens AB, Bacchetta R, Tsalenko A, Dellinger D, Bruhn L, Porteus MH (2015) Chemically modified guide RNAs enhance CRISPR-Cas genome editing in human primary cells. *Nat Biotechnol* 33 (9):985–989
10. Nasri M, Mir P, Dannenmann B, Amend D, Skroblyn T, Xu Y, Schulze-Osthoff K, Klimiankou M, Welte K, Skokowa J (2019) Fluorescent labeling of CRISPR/Cas9 RNP for gene knockout in HSPCs and iPSCs reveals an essential role for GADD45b in stress response. *Blood Adv* 3(1):63–71
11. Doench JG, Fusi N, Sullender M, Hegde M, Vaimberg EW, Donovan KF, Smith I, Tothova Z, Wilen C, Orchard R, Virgin HW, Listgarten J, Root DE (2016) Optimized sgRNA design to maximize activity and

- minimize off-target effects of CRISPR-Cas9. *Nat Biotechnol* 34(2):184–191
12. Chari R, Mali P, Moosburner M, Church GM (2015) Unraveling CRISPR-Cas9 genome engineering parameters via a library-on-library approach. *Nat Methods* 12(9):823–826
 13. Doench JG, Hartenian E, Graham DB, Tothova Z, Hegde M, Smith I, Sullender M, Ebert BL, Xavier RJ, Root DE (2014) Rational design of highly active sgRNAs for CRISPR-Cas9-mediated gene inactivation. *Nat Biotechnol* 32(12):1262–1267
 14. Kim JB, Blackshaw S (2001) One-step enzymatic purification of PCR products for direct sequencing. *Curr Protoc Hum Genet*. Chapter 11:Unit 11 16. <https://doi.org/10.1002/0471142905.hg1106s30>
 15. Ye J, Coulouris G, Zaretskaya I, Cutcutache I, Rozen S, Madden TL (2012) Primer-BLAST: a tool to design target-specific primers for polymerase chain reaction. *BMC Bioinformatics* 13:134
 16. Guschin DY, Waite AJ, Katibah GE, Miller JC, Holmes MC, Rebar EJ (2010) A rapid and general assay for monitoring endogenous gene modification. *Methods Mol Biol* 649:247–256
 17. Brinkman EK, Chen T, Amendola M, van Steensel B (2014) Easy quantitative assessment of genome editing by sequence trace decomposition. *Nucleic Acids Res* 42(22):e168
 18. Cradick TJ, Qiu P, Lee CM, Fine EJ, Bao G (2014) COSMID: a web-based tool for identifying and validating CRISPR/Cas off-target sites. *Mol Ther Nucleic Acids* 3:e214
 19. Bae S, Kweon J, Kim HS, Kim JS (2014) Microhomology-based choice of Cas9 nuclease target sites. *Nat Methods* 11(7):705–706

Nasri M. et al., 2019, *Haematologica*



Ferrata Storti Foundation

Haematologica 2020
Volume 105(3):598-609

CRISPR/Cas9-mediated *ELANE* knockout enables neutrophilic maturation of primary hematopoietic stem and progenitor cells and induced pluripotent stem cells of severe congenital neutropenia patients

Masoud Nasri,¹ Malte Ritter,^{1*} Perihan Mir,^{1*} Benjamin Dannenmann,^{1*} Narges Aghaallaei,¹ Diana Amend,¹ Vahagn Makaryan,² Yun Xu,¹ Breanna Fletcher,² Regine Bernhard,¹ Ingeborg Steiert,¹ Karin Hähnel,¹ Jürgen Berger,³ Iris Koch,³ Brigitte Sailer,³ Katharina Hipp,³ Cornelia Zeidler,⁴ Maksim Klimiankou,¹ Baubak Bajoghli,¹ David C. Dale,² Karl Welte^{1,5,§} and Julia Skokowa^{1,§}

¹Department of Oncology, Hematology, Immunology, Rheumatology and Clinical Immunology, University Hospital Tübingen, Tübingen, Germany; ²Department of Medicine, University of Washington, Seattle, WA, USA; ³Max Planck Institute for Developmental Biology, Tübingen, Germany; ⁴Department of Oncology, Hematology, Immunology and Bone Marrow Transplantation, Hannover Medical School, Hannover, Germany and ⁵University Children's Hospital Tübingen, Tübingen, Germany

*MR, PM and BD are co-second authors.

§KW and JS are co-senior authors.

ABSTRACT

Autosomal-dominant *ELANE* mutations are the most common cause of severe congenital neutropenia. Although the majority of congenital neutropenia patients respond to daily granulocyte colony stimulating factor, approximately 15 % do not respond to this cytokine at doses up to 50 µg/kg/day and approximately 15 % of patients will develop myelodysplasia or acute myeloid leukemia. “Maturation arrest,” the failure of the marrow myeloid progenitors to form mature neutrophils, is a consistent feature of *ELANE* associated congenital neutropenia. As mutant neutrophil elastase is the cause of this abnormality, we hypothesized that *ELANE* associated neutropenia could be treated and “maturation arrest” corrected by a CRISPR/Cas9-sgRNA ribonucleoprotein mediated *ELANE* knockout. To examine this hypothesis, we used induced pluripotent stem cells from two congenital neutropenia patients and primary hematopoietic stem and progenitor cells from four congenital neutropenia patients harboring *ELANE* mutations as well as HL60 cells expressing mutant *ELANE*. We observed that granulocytic differentiation of *ELANE* knockout induced pluripotent stem cells and primary hematopoietic stem and progenitor cells were comparable to healthy individuals. Phagocytic functions, ROS production, and chemotaxis of the *ELANE* KO (knockout) neutrophils were also normal. Knockdown of *ELANE* in the mutant *ELANE* expressing HL60 cells also allowed full maturation and formation of abundant neutrophils. These observations suggest that *ex vivo* CRISPR/Cas9 RNP based *ELANE* knockout of patients' primary hematopoietic stem and progenitor cells followed by autologous transplantation may be an alternative therapy for congenital neutropenia.

Introduction

Autosomal dominant *ELANE* mutations encoding neutrophil elastase (NE) are the most common cause of severe congenital neutropenia (CN), an inherited bone marrow failure syndrome.¹⁻³ Patients with CN suffer from severe life-threatening bacterial infections starting early after birth due to the absence or very low numbers of neutrophils in the peripheral blood (usually less than 500 cells per µL³).

Correspondence:

JULIA SKOKOWA
Julia.Skokowa@med.uni-tuebingen.de

Received: March 14, 2019.

Accepted: June 21, 2019.

Pre-published: June 27, 2019.

doi:10.3324/haematol.2019.221804

Check the online version for the most updated information on this article, online supplements, and information on authorship & disclosures: www.haematologica.org/content/105/3/598

©2020 Ferrata Storti Foundation

Material published in *Haematologica* is covered by copyright. All rights are reserved to the Ferrata Storti Foundation. Use of published material is allowed under the following terms and conditions:

<https://creativecommons.org/licenses/by-nc/4.0/legalcode>.

Copies of published material are allowed for personal or internal use. Sharing published material for non-commercial purposes is subject to the following conditions:

<https://creativecommons.org/licenses/by-nc/4.0/legalcode>,

sect. 3. Reproducing and sharing published material for commercial purposes is not allowed without permission in writing from the publisher.



Hematopoietic stem and progenitor cells (HSPC) of CN patients fail to differentiate into mature neutrophils. This differentiation defect can be partially restored with daily or alternate-day subcutaneous injections of recombinant human granulocyte colony stimulating factor (rhG-CSF) in supra-physiological concentrations.⁴ Although rhG-CSF therapy improves the life expectancy and quality of life of CN patients, a subgroup does not respond to rhG-CSF. Additionally, about 15 % of CN patients developed myelodysplastic syndrome (MDS) or acute myeloid leukemia (AML) till now.³ There is a positive correlation between a rhG-CSF dose required to achieve acceptable neutrophil counts and a cumulative incidence to develop MDS or AML in CN patients.⁵ Therefore, CN patients, especially patients who either require high rhG-CSF dosages (above 50 µg/kg/day) and those who do not respond at all, need alternative therapeutic options. Hematopoietic stem cell transplantation (HSCT) would be a treatment of choice in CN patients, but it is associated with many adverse events, *e.g.* acute or chronic graft-versus-host-disease (GvHD), life-threatening infections, graft failure or graft rejection. Indeed, the overall survival of CN patients after HSCT is approximately 80 % only.

Recently established new technologies of CRISPR/Cas9-mediated gene editing in mammalian cells^{6,7} offer novel therapeutic options, especially for inherited monogenic disorders, including *ELANE* mutations associated CN. In this case, CRISPR/Cas9-mediated gene correction or knockout of the mutant gene in patient's HSPC *ex vivo* followed by autologous transplantation of the corrected HSPC might be a better treatment than high dose rhG-CSF or allogeneic stem cell transplantation.

ELANE mutations induce unfolded protein response (UPR) and endoplasmic reticulum (ER) stress in HSPC of CN patients that leads to increased apoptosis and defective granulocytic differentiation.⁸⁻¹¹ Therefore, inactivation of *ELANE* using CRISPR/Cas9-mediated knockout may abrogate UPR and ER stress caused by mutated *ELANE* with subsequent restoration of granulocytic differentiation. In support of this hypothesis, we recently identified a β-lactam-based inhibitor of human neutrophil elastase (NE), MK0339, which restored defective granulocytic differentiation of induced pluripotent stem cells (iPSC) and HL60 cells expressing mutated NE.¹² In addition, a recent report by Nayak *et al.* demonstrated the restoration of the *in vitro* granulopoiesis of *ELANE*-CN patient-derived iPSC upon treatment with Sivelestat, another NE-specific small-molecule inhibitor.^{12,13} Moreover, the fact that individuals showing mosaicism of inherited *ELANE* mutations have a higher proportion of *ELANE* mutated mature neutrophils hematopoietic cells in the bone marrow than in the blood^{14,15} supports the hypothesis that inactivation of *ELANE* mutations will improve neutrophil differentiation.

Another possibility to correct the disease phenotype is the direct correction of the specific gene mutation by the activation of homology-directed repair (HDR) of the mutated gene allele after cutting by CRISPR/Cas9 and co-transfection with a repair template. Most CN patients harbor inherited autosomal dominant missense or frameshift *ELANE* mutations that are distributed throughout all five exons and two introns.¹⁶ Therefore, CRISPR/Cas9-mediated correction of *ELANE* mutations would need to be patient/mutation specific. Since mutated *ELANE* may induce UPR and ER stress in edited cells, the introduction of new indels in the *ELANE* gene during the process of

CRISPR/Cas9 based editing may be not beneficial for the integrity of the hematopoietic stem cell (HSC) pool.

The first pre-clinical CRISPR/Cas9-based gene therapy study of common inherited blood disorders, sickle cell disease, and β-thalassemia, was reported.^{17,18} In these settings, the β-globin gene locus was inactivated by the introduction of deletions in autologous HSPC by CRISPR/Cas9-mediated gene editing. This was done to mimic the hereditary persistence of fetal hemoglobin mutations in HSC.^{17,18}

Here, we describe a CRISPR/Cas9 mediated *ELANE* KO by electroporation of HSPC and iPSC with *ELANE* specific CRISPR/Cas9-sgRNA ribonucleoprotein (RNP) complexes. *ELANE* KO induces granulocytic differentiation of HSPC and iPSC of CN patients harboring *ELANE* mutations without affecting their phagocytic functions. These results suggest that it may be possible to use CRISPR/Cas9 based *ELANE* KO in autologous HSCT as a therapy for *ELANE* associated neutropenia.

Methods

Patients

Three healthy donors and five severe congenital neutropenia patients harboring *ELANE* mutations (*ELANE*-CN) were used in the study. Bone marrow and peripheral blood samples from patients were collected in association with an annual follow-up recommended by the Severe Chronic Neutropenia International Registry. Study approval was obtained from the Ethical Review Board of the Medical Faculty, University of Tübingen. Informed written consent was obtained from all participants of this study.

Cell culture

Human CD34⁺ HSPC were isolated from bone marrow mononuclear cell fraction using Ficoll gradient centrifugation followed by magnetic bead separation using Human CD34 Progenitor Cell Isolation Kit, (Miltenyi Biotech, #130-046-703). CD34⁺ cells were cultured in a density of 2 × 10⁵ cells/mL in Stemline II Hematopoietic Stem Cell Expansion medium (Sigma Aldrich, #50192) supplemented with 10 % FBS, 1 % penicillin/streptomycin, 1 % L-Glutamine and a cytokine cocktail consisting of 20 ng/mL IL-3, 20 ng/mL IL-6, 20 ng/mL TPO, 50 ng/ml SCF and 50 ng/mL FLT-3L (all cytokines were purchased from R&D Systems). Human induced pluripotent stem cells (iPSC) were cultured on Geltrex LDEV-free reduced growth factor basement membrane matrix (Thermo Fisher Scientific, #A1413201) coated plates in a density of 2 × 10⁵ cells/mL in StemFlex medium (Thermo Fisher Scientific, #A3349401) supplemented with 1 % penicillin/streptomycin. HL60 cells were maintained in RPMI-1640 supplemented with 10 % fetal bovine serum (FBS) (Gemini Bio Products, West Sacramento, CA, USA), 2 mM L-glutamine, and 1 % penicillin/streptomycin (Thermo Fisher Scientific) at 37°C and 5 % CO₂.

Design of the *ELANE*-specific guide RNA (gRNA)

Specific CRISPR-RNA (crRNA) for the knockout of the *ELANE* gene (cut site: chr19 [CTGCGCGGAGGC-CACTTCTG, +852,969 : -852,969], NM_001972.3 Exon 2, 161 bp; NP_001963.1 p.F54) was designed using the CCTop website.¹⁹

CRISPR/Cas9-gRNA RNP mediated *ELANE* KO in iPSC and HSPC

Electroporation was carried out using the Amaxa nucleofection system (P3 primary kit, #V4XP-3024) according to the manufacturer's instructions. 1×10^6 human iPSC or CD34⁺ HSPC were electroporated with assembled gRNA (8 μ g) and Cas9 (15 μ g) protein (Integrated DNA Technologies).

Isolation of single cell iPSC clones

8×10^3 human iPSC were plated on Geltrex-coated 10-cm dish in StemFlex medium (Thermo Fisher Scientific, #A3349401) and RevitaCell supplement (Thermo Fisher Scientific, #A2644501). The medium was changed every 24 hours without RevitaCell supplement. On day 7, single iPSC colonies were picked and transferred to the Geltrex-coated 96-well plates (one clone/well).

Colony Forming Unit (CFU) assay

CD34⁺ cells were resuspended in IMDM supplemented with 2 % FBS (Stemcell Technologies, #07700) and enriched Methocult (Stemcell Technologies, #H4435). The cell suspension was plated on 3.5 cm dishes (3×10^3 cells/dish) for 14 days.

In vitro phagocytosis assay

Cells were incubated with or without fluorescein-conjugated *Staphylococcus aureus* BioParticles (Invitrogen, #S2851) at a ratio of 100 particles per cell for two hours at 37°C, washed twice with PBS/ 2 % BSA, resuspended in 300 μ L FACS buffer and analyzed by flow cytometry.

Statistical analysis

Differences in mean values between groups were analyzed using two-sided, unpaired Student's *t*-tests using GraphPad Prism software.

Additional Material and Methods are available in the *Online Supplementary Material and Methods*.

Results

Inhibition of *ELANE* expression restored defective granulocytic differentiation of HL60 cell lines expressing endogenous *ELANE* mutations

We created CRISPR/Cas9 edited mutant *ELANE* knock-in HL60 human promyelocytic cell lines expressing either p.P139L or p.C151Y *ELANE* mutations. All-trans retinoic acid (ATRA) induced differentiation of wild-type and

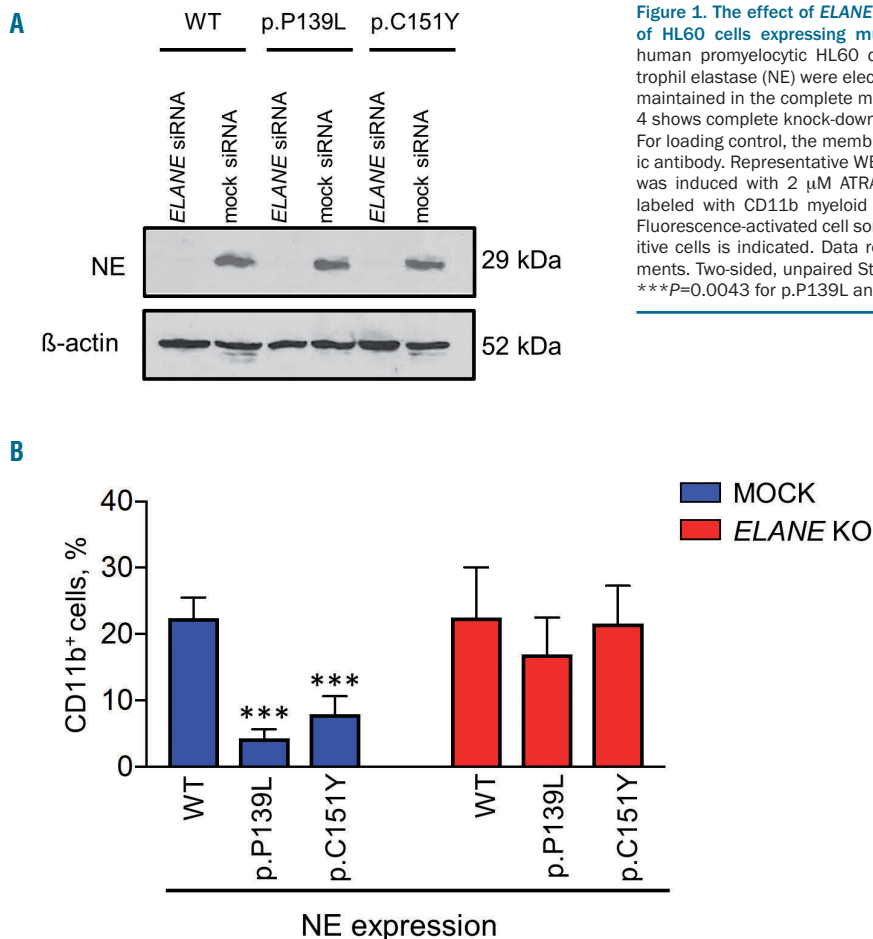


Figure 1. The effect of *ELANE* knock-down on the impaired myeloid differentiation of HL60 cells expressing mutant neutrophil elastase. (A) CRISPR/Cas9 edited human promyelocytic HL60 cells expressing p.P139L and p.C151Y mutant neutrophil elastase (NE) were electroporated with scrambled and anti-*ELANE* siRNA and maintained in the complete medium for five days. Western blot (WB) analysis at day 4 shows complete knock-down of NE detected with an anti-NE monoclonal antibody. For loading control, the membrane was stripped and re-probed with a β -actin-specific antibody. Representative WB membranes are depicted. (B) Myeloid differentiation was induced with 2 μ M ATRA (all-trans retinoic acid). After five days, cells were labeled with CD11b myeloid differentiation surface marker and examined using Fluorescence-activated cell sorting (FACS) analysis. The proportion of CD11b-PE positive cells is indicated. Data represent means \pm SD from four independent experiments. Two-sided, unpaired Student's *t*-test *P*-values are shown, ****P*<0.0001 and ****P*=0.0043 for p.P139L and p.C151Y respectively compared to wild-type (WT).

mutant HL60 clones revealed a typical impairment of granulocytic differentiation capacities in both mutant cell lines, as assessed by the significantly lower proportion of cells expressing CD11b granulocytic differentiation marker in p.P139L and p.C151Y mutant cell lines compared to the wild-type ($P < 0.0001$ and $P = 0.00043$, respectively) on day 5 of differentiation (Figure 1A-B and *Online Supplementary Figure S1A-C*). These findings are consistent with *ELANE* associated neutropenia patients phenotype.

As a proof-of-principle experiment, we have used RNA interference (RNAi) technology to knock down the expression of the *ELANE* gene in these cell lines. Thereby, we investigated the biological effects of inhibition of mutant NE on the granulocytic differentiation. Indeed, transfection of commercially available siRNA against the exon 4 of *ELANE*, completely knocked down the expression of NE in all cell lines. Production of CD11b positive cells was significantly restored in both mutant cell lines ($P = 0.00041$ for p.P139L and $P = 0.00048$ for p.C151Y), but

not in wild-type cells (Figure 1A-B and *Online Supplementary Figure S1A-C*).

Design and validation of sgRNA targeting *ELANE*

We further generated guide RNA (gRNA) specifically targeting exon 2 of *ELANE* by annealing CRISPR-RNA (crRNA) with trans-activating crRNA (tracrRNA). gRNA was incubated with recombinant Cas9 protein to generate CRISPR/Cas9-gRNA RNP complexes. The gRNA targeting exon 2 of *ELANE* (cut site: chr19[+852.969:-852.969], Figure 2A) was selected to introduce stop-codon mutations and to induce nonsense-mediated mRNA decay (NMD) of *ELANE* mRNA, which is caused by stop-codon or frameshift mutations at the beginning of *ELANE* mRNA. Based on our experimental analysis, the selected gRNA has high on-target activity with low off-target score (*data not shown*). To evaluate inhibition of NE expression by CRISPR/Cas9 RNP mediated targeting of exon 2 of *ELANE*, we generated an *ELANE* KO myeloid cell line

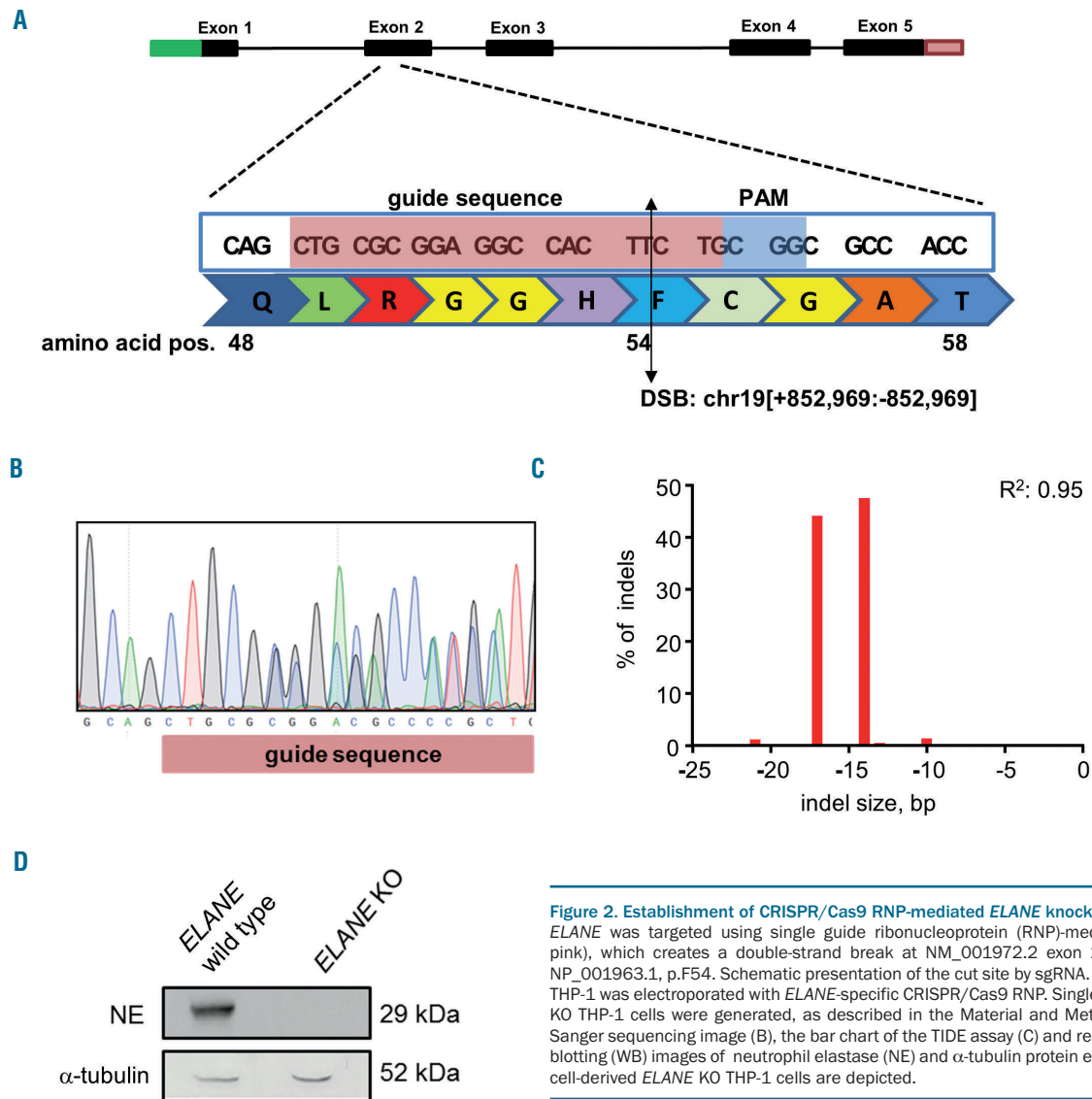


Figure 2. Establishment of CRISPR/Cas9 RNP-mediated *ELANE* knockout in THP-1 cells. (A) *ELANE* was targeted using single guide ribonucleoprotein (RNP)-mediated (highlighted in pink), which creates a double-strand break at NM_001972.2 exon 2, 161 bp after ATG; NP_001963.1, p.F54. Schematic presentation of the cut site by sgRNA. (B-D) Myeloid cell line THP-1 was electroporated with *ELANE*-specific CRISPR/Cas9 RNP. Single cell clones of *ELANE* KO THP-1 cells were generated, as described in the Material and Methods. Representative Sanger sequencing image (B), the bar chart of the TIDE assay (C) and representative Western blotting (WB) images of neutrophil elastase (NE) and α -tubulin protein expression (D) in single cell-derived *ELANE* KO THP-1 cells are depicted.

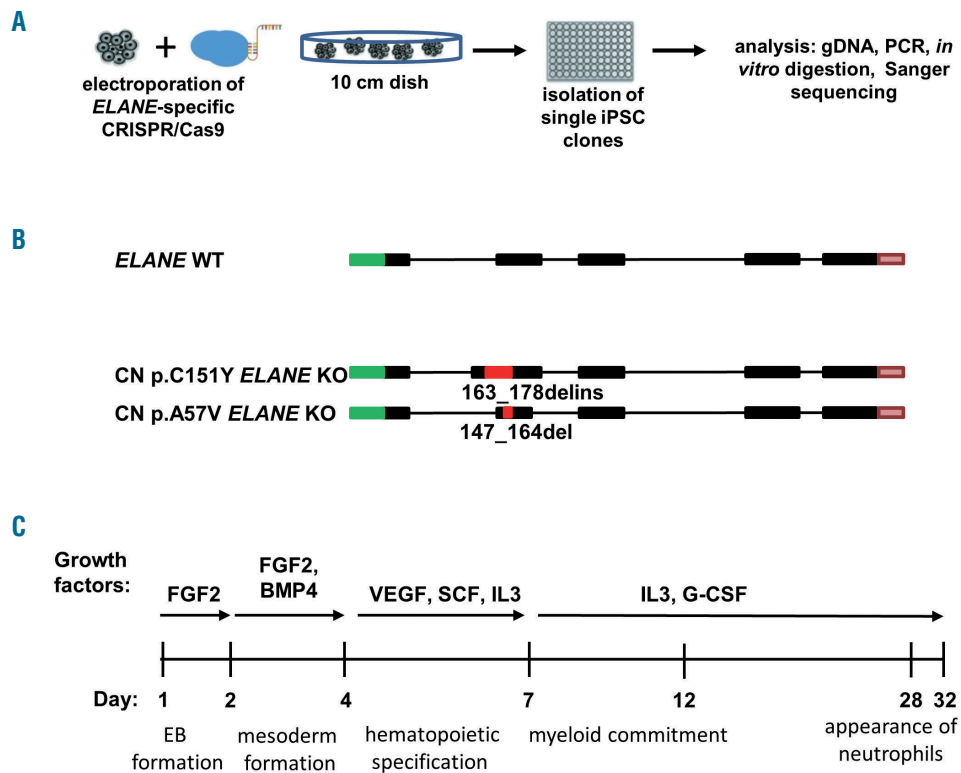


Figure 3. Generation of *ELANE* KO CN iPSC clones. (A) Scheme of the *ELANE*-specific CRISPR/Cas9-ribonucleoprotein electroporation of induced pluripotent stem cells (iPSC) and generation of *ELANE* KO iPSC clones. Generation of single *ELANE* knockout iPSC clones was made by seeding single iPSC, subsequent picking of each clone and transferring them into 96 well plates. Screening of each iPSC clone was done by Cas9 *in vitro* digestion and Sanger sequencing. (B) Scheme of CRISPR/Cas9 introduced modifications in the *ELANE* gene in iPSC clones of congenital neutropenia (CN) patients. Red inserts show positions of indels in *ELANE* mRNA (NM_001972.2) and numbers refer to bp position after ATG. (C) Scheme of the EB-based hematopoietic/neutrophilic differentiation of iPSC.

THP-1, which has high basal expression levels of *ELANE* and NE. The efficiency of *ELANE* knockout in the total population of edited THP-1 cells was 77 %, as assessed by Sanger sequencing and tracking of indels by decomposition (TIDE) analysis (*data not shown*). The pure *ELANE* KO THP-1 cell clone has compound heterozygosity of 14 and 17 bp deletions on each allele (Figure 2B-C). The NE expression was completely absent in the pure *ELANE* KO THP-1 cell clone, as determined by Western blotting (WB) using anti-NE antibody against the C-terminus of NE protein (Figure 2D, *Online Supplementary Figure S2A-B*). These data suggest that sgRNA targeting *ELANE* that we designed led to a complete loss of NE protein.

Restoration of the *in vitro* granulocytic differentiation in *ELANE*-CN iPSC clones after *ELANE* knockout

We generated iPSC from peripheral blood mononuclear cells (PB MNC) of two *ELANE*-CN patients, harboring *ELANE* mutations p.C151Y or p.A57V (CN p.C151Y iPSC and CN p.A57V iPSC, respectively). Additionally, iPSC of one healthy control (healthy ctrl iPSC) were evaluated. All three iPSC lines expressed elevated mRNA and protein levels of pluripotent stem cell-specific factors, displayed alkaline phosphatase activity and expression of pluripotent embryonic stem cell surface markers (*Online Supplementary Figure 3A-C*).

Next, we used electroporation of iPSC clones with *ELANE*-specific CRISPR/Cas9-sgRNA RNP to generate pure *ELANE* KO CN iPSC clones. For this, electroporated iPSC were seeded on a geltrex coated culture dish and single-cell derived iPSC clones were isolated transferred to geltrex coated 96 well-plates for the subsequent selection of *ELANE* knockout clones (Figure 3A). Confirmed *ELANE* knockout iPSC clones have followed *ELANE* modifica-

tions: 274 bp del/ins in CN p.C151Y *ELANE* KO iPSC, and 17 bp del in CN p.A57V *ELANE* KO iPSC (Figure 3B). The editing efficiency of healthy ctrl iPSC was 97 % (*Online Supplementary Figure S4A*), therefore, we used the total population of gene-edited healthy control (ctrl) iPSC for further analysis. We did not detect any off-target activity of the gRNA for the selected cDNA sites in all studied iPSC, as assessed using Sanger sequencing (*Online Supplementary Figure S4B* and *Tables S1, S2*).

Applying a slightly modified *in vitro* embryoid body (EB)-based iPSC differentiation method that allows generation of hematopoietic cells and mature myeloid cells for approximately 30 days,^{22,23} we found an increase in the percentage of CD15⁺CD16⁺CD45⁺ granulocytes in *ELANE* KO CN-iPSC cell culture, as compared to CN-iPSC. The generation of granulocytes from *ELANE* KO CN-iPSC was comparable to iPSC generated from a healthy donor (Figure 3C, 4A, and *Online Supplementary Figure S5A*). Generation of immature hematopoietic cells (CD34⁺KDR⁺, CD34⁺CD43⁺, CD45⁺CD235⁺CD41a⁺ and CD45⁺CD34⁺ cells) and CD45⁺CD33⁺ myeloid progenitor cells in *ELANE* KO CN- and CN-iPSC lines were similar or increased, in comparison to corresponding MOCK treated iPSC lines (*Online Supplementary Figure S6A*).

A CFU assay was performed with *ELANE*⁺ iPSC-derived CD34⁺ cells from CN patients and showed elevated levels of CFU-G but reduced CFU-M colony numbers, as compared to CD34⁺ cells derived from MOCK treated CN iPSC clones (Figure 4C). These data suggest that *ELANE* knockout restores granulocytic differentiation in CN.

We did not observe any significant defects in *in vitro* granulocytic differentiation of *ELANE* KO iPSC generated from a healthy donor, as compared to MOCK treated cells (Figure 4A-C, *Online Supplementary Figures S5* and *S6*).

ELANE knockout in HSPC of ELANE-CN patients restores diminished granulocytic differentiation

To further evaluate the clinical applicability of *ELANE* KO as a treatment option of *ELANE*-associated CN, we performed CRISPR/Cas9 RNP-mediated gene editing in primary bone marrow CD34⁺ HSPC of four *ELANE*-CN patients (Table 1) and three healthy donors and differentiated the cells towards neutrophils. *ELANE* knockout in CD34⁺ HSPC was performed by electroporation of human CD34⁺ HSPC with assembled *ELANE* specific sgRNA and Cas9 protein (Figure 5A). The editing efficiency varied between 27 % and 94 % (Figure 5B, *Online Supplementary Figure S7*). As expected, NE levels in neutrophils differentiated from the total population of edited cells were markedly reduced (Figure 5C-D, *Online Supplementary Figure S8A-B*). Moreover, *ELANE* KO leads to elevated granulocytic differentiation, as assessed by the percentage of CD15⁺CD11b⁺CD45⁺ cells (Figure 6A, *Online Supplementary Figure S9A-B*) and morphological examination of cytospin preparations of mature granulocytes generated on day 14 of the *in vitro* granulocytic differentiation using liquid culture (Figure 6B). At the same time, the ratio of *ELANE* KO cells increased from day 7 to day 14 of differentiation (Figure 5B). Simultaneously, the percentage of CD34⁺CD45⁺ cells was reduced in *ELANE* KO cells of CN patients, but not in healthy donor cells (*Online Supplementary Figure S10A*). In one patient (CN I120F), no difference in the percentage of CD15⁺CD11b⁺CD45⁺ cells between MOCK and *ELANE* KO samples was observed, but a clear improvement of granulocytic differentiation was detected in cytospin slides. This finding may be explained by relative mild neutropenia (*Online Supplementary Table 3*) and possible expression of CD15 in not fully mature myeloid cells in this patient.

Scanning and transmission electron microscopy revealed that *ELANE* KO cells of both healthy control and one CN patient showed no significant differences in morphology or intracellular structures, compared with MOCK cells of a healthy donor (Figure 6C-D).

Altogether, these data suggest that *ELANE* KO cells have a differentiation advantage over the HSPC carrying mutated *ELANE*.

Neutrophils generated from *ELANE* KO HSPC exhibited unaffected ROS production, phagocytosis and chemotaxis upon activation *in vitro*

We further evaluated *in vitro* activation of neutrophils generated from *ELANE* KO HSPCs in liquid culture for 14 days. We first performed an assessment of H₂O₂ levels (ROS) in fMLP-activated *ELANE* KO neutrophils generated from a healthy donor. We detected no differences between *ELANE* WT and *ELANE* KO neutrophils (Figure 7A).

Phagocytosis was evaluated by incubation of cells with fluorescein-conjugated *Staphylococcus aureus* BioParticles for two hours. Percentage of GFP⁺ granulocytes that engulfed bacteria were assessed by FACS using gating on granulocyte population in the dot plot of forward-scatter light (FSC) versus side-scatter light (SSC) channels. We did not detect any significant differences in phagocytosis of *ELANE* KO neutrophilic granulocytes, as compared to control MOCK cells (Figure 7B). As an independent evaluation of phagocytosis kinetics, we performed live cell imaging of neutrophils incubated with pHrodo Green *E. coli* Bioparticles Conjugate using IncuCyte ZOOM system and observed similar phagocytosis behavior of

MOCK and *ELANE* KO neutrophils generated from a healthy donor or one CN patient (Figure 7C).

Chemotactic activity of fMLP-treated neutrophils was also comparable between MOCK and *ELANE* KO groups (Figure 7D).

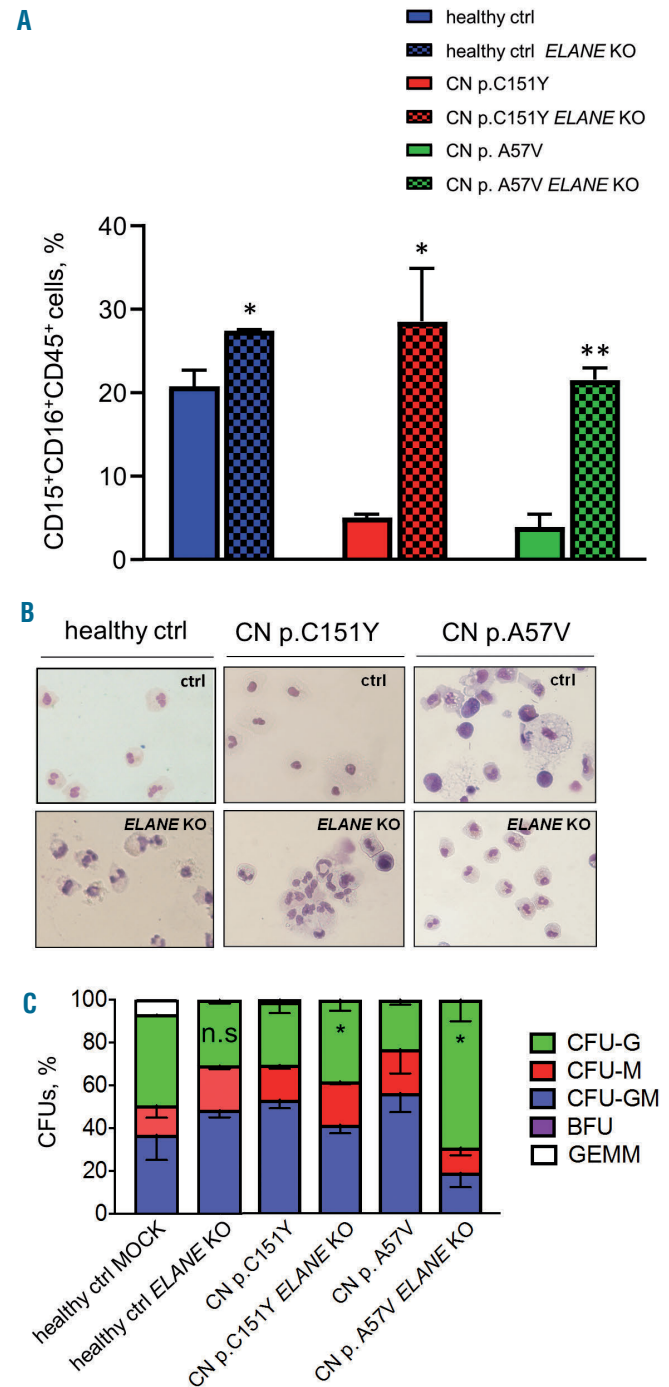


Figure 4. *ELANE* knockout restored granulocytic differentiation of *ELANE*-CN iPSC. (A) Flow cytometry analysis of suspension cells harvested from embryoid body (EB)-based granulocytic cell culture of respective iPSC clones on day 28 or 32 of differentiation. Data represent means \pm standard deviation (SD) from two independent experiments. * $P < 0.05$, ** $P < 0.01$. (B) Wright-Giemsa staining of cytospin preparations of suspension myeloid cells harvested from iPSC culture at day 28 or 32 of differentiation. Representative images are depicted. (C) Colony-forming unit (CFU) assay of CD34⁺ cells harvested from EB-based iPSC culture on day 14 of differentiation. Data represent means \pm SD from two independent experiments. * $P < 0.05$.

Unaffected phagocytic activity of *ELANE* KO PMN in zebrafish embryos

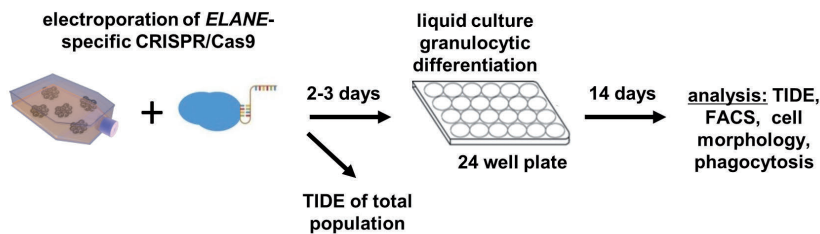
To evaluate the phagocytic activity of *ELANE* KO PMN *in vivo*, we transplanted fluorescently labeled polymorphonuclear leukocytes (PMN) generated from *ELANE* KO HD into zebrafish embryos (Figure 8A). PMN were injected into the duct of Cuvier, a wide circulation channel on the yolk sac connecting the heart to the trunk vasculature. Subsequently, Alexa-594-conjugated *Staphylococcus aureus* BioParticles were injected locally in the tail fin close to the caudal vein. Live imaging showed that human neutrophils migrated into the caudal hematopoietic tissue (CHT), which is equivalent to the fetal liver in mammals and provides a human-compatible environment.^{24,25} Confocal imaging of this region revealed that most of the *ELANE* KO neutrophils were found inside the perivascular pocket (Figure 8B) and many of them have engulfed bacteria (white arrows in Figure 8B and 8C, *Online Supplementary Movie S1*). Time-lapse *in vivo* imaging of the xenotrans-

planted embryos also revealed that human *ELANE* KO PMN have the capability to form surface protrusion within the perivascular region (Figure 8D, *Online Supplementary Movie S2*). We could not detect a difference between transplanted human *ELANE* KO and control MOCK PMN in zebrafish embryos (*data not shown*). These observations indicate that human *ELANE* KO PMN are able to migrate and phagocyte *in vivo*.

ELANE KO restores deregulated expression of UPR gene BiP and anti-apoptotic factor Bcl-x1 in *ELANE* KO iPSC derived cells of CN patients

We further evaluated the effects of *ELANE* KO on the expression of UPR gene BiP and anti-apoptotic factor Bcl-x1 (*Online Supplementary Figure S11*). We analyzed pure *ELANE* KO HSPC (for Bcl-x1) or neutrophils (for BiP) generated from iPSC of two CN patients. We found that *ELANE* KO HSPC express elevated mRNA levels of Bcl-x1 and BiP expression was markedly reduced in *ELANE* KO

A



B

Sample, <i>ELANE</i> mutation position	Exon	Indel Efficiency, %	
		day 7	day 14
healthy ctrl 1	-	71	69
healthy ctrl 2	-	57	46
healthy ctrl 3	-	86	94
CN p.A57V	Exon 2	52	63
CN p.I120F	Exon 3	81	90
CN p.S126L	Exon 4	45	57
CN p.C223AfsX17	Exon 5	27	37

C



D

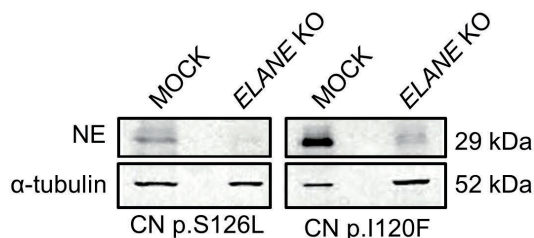


Figure 5. Efficient CRISPR/Cas9 RNP-based *ELANE* knockout in HSPC. (A) Scheme of the generation of *ELANE* KO HSPC using electroporation with *ELANE*-specific CRISPR/Cas9-gRNA ribonucleoprotein (RNP). (B) TIDE results of edited CD34⁺ HSPC at day 7 and 14 of liquid culture differentiation. (C and D) Hematopoietic stem and progenitor cells (HSPC) of healthy controls (C), or two CN patients (D) were electroporated with *ELANE*-specific CRISPR/Cas9 RNP, on day 14 of culture, cells were lysed in Laemmli buffer and Western blotting (WB) analysis using anti-neutrophil elastase (NE) antibody against C-terminus of NE was performed, staining with α -tubulin antibody was used as loading control. Representative WB images of cells from two independent experiments are depicted.

PMN, compared to cells carrying mutated *ELANE*. As expected, *ELANE* mRNA levels were severely diminished in *ELANE* KO cells (Online Supplementary Figure S11).

Discussion

The majority of patients suffering from congenital neutropenia respond well to daily treatment with rhG-CSF leading to a normal quality of life. However, in the last 25 years, we learned that CN is a preleukemic syndrome and that approximately 15 % of patients do not respond to

even ultra-high dosages (>50 µg/kg/d) of rhG-CSF. Therefore, we are searching for other treatment modalities for CN patients that may prevent leukemic transformation and may be useful for those who are requiring high dosages of rhG-CSF or not responding at all to rhG-CSF. For these patients, the only available treatment is stem cell transplantation with the risk of transplant-associated adverse events such as acute or chronic GvHD.

In the present study, we described for the first time the establishment of an *in vitro* cellular model of CRISPR/Cas9 mediated gene therapy of CN associated with autosomal dominant *ELANE* mutations, the most frequent cause of

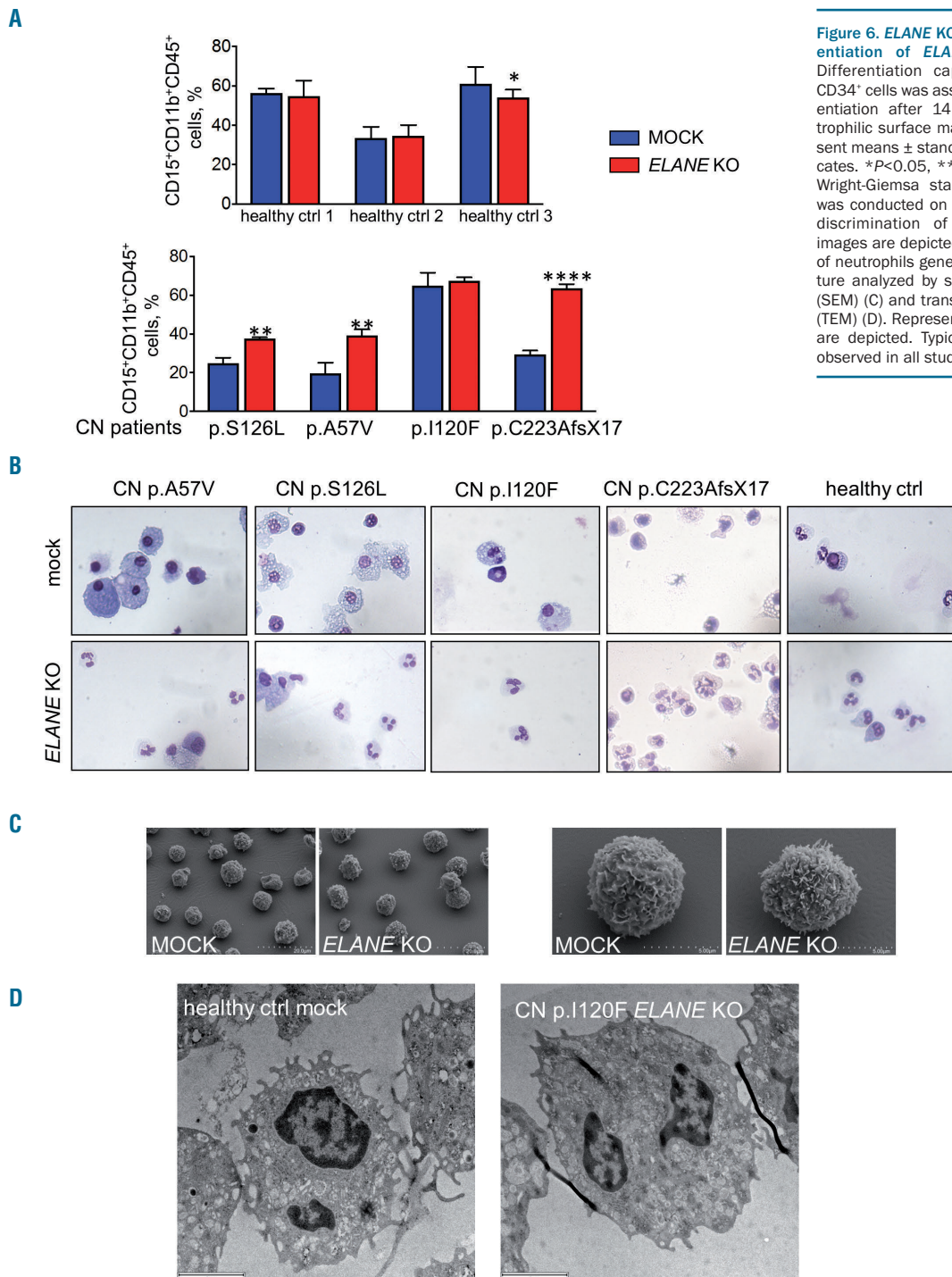


Figure 6. *ELANE* KO restored granulocytic differentiation of *ELANE*-CN primary HSPC. (A) Differentiation capacity of *ELANE* knockout CD34⁺ cells was assessed by liquid culture differentiation after 14 days by investigating neutrophilic surface marker expression. Data represent means ± standard deviation (SD) from triplicates. **P*<0.05, ***P*<0.01, *****P*<0.0001. (B) Wright-Giemsa staining of differentiated cells was conducted on day 14 allowing morphologic discrimination of the cells. Representative images are depicted. (C-D) Electron micrographs of neutrophils generated on day 14 of liquid culture analyzed by scanning electron microscopy (SEM) (C) and transmission electron microscopy (TEM) (D). Representative SEM and TEM images are depicted. Typical neutrophil morphology is observed in all studied samples.

CN. We tested *ex vivo* CRISPR/Cas9 RNP-based *ELANE* knockout in HSPC of CN patients that may be used for autologous transplantation as a therapeutic approach for *ELANE*-CN patients. Virus- and DNA-free application of CRISPR/Cas9 RNP markedly increases gene editing efficiency and simultaneously decreases the probability and frequency of off-target effects, because CRISPR/Cas9 RNP activity is preserved in cells for only approximately 48 hours. We recently reported the establishment of the fluorescent labeling of CRISPR/Cas9 RNP complexes for gene editing of primary hematopoietic stem cells and subsequent sorting of gene-modified cells for further applications.²⁶ Implementation of this method will improve the efficiency of gene knockout or gene correction in HSPC, including *ELANE* knockout or correction of *ELANE* mutations.

In case of *ELANE* KO, different combinations of the *ELANE* gene editing are expected: we may generate unedited, monoallelic edited (of mutated or WT allele), or bi-allelic edited HSPC. Since we did not use any selection marker for edited HSPC, we were not able to estimate the proportion of HSPC with inactivation of the mutated *ELANE* allele. The fact that the proportion of *ELANE* KO cells was elevated upon granulocytic differentiation strongly argues for the differentiation advantage of the edited cells lacking *ELANE* (including loss of the mutated allele).

There are several potential unforeseen consequences of the *ELANE* gene knockout strategy. For example, Tidwell *et al.* reported the presence of two in-frame ATG codons in exon 2 and exon 4 of *ELANE*.²⁷ They showed that the internal translation of NE can be initiated when the canon-

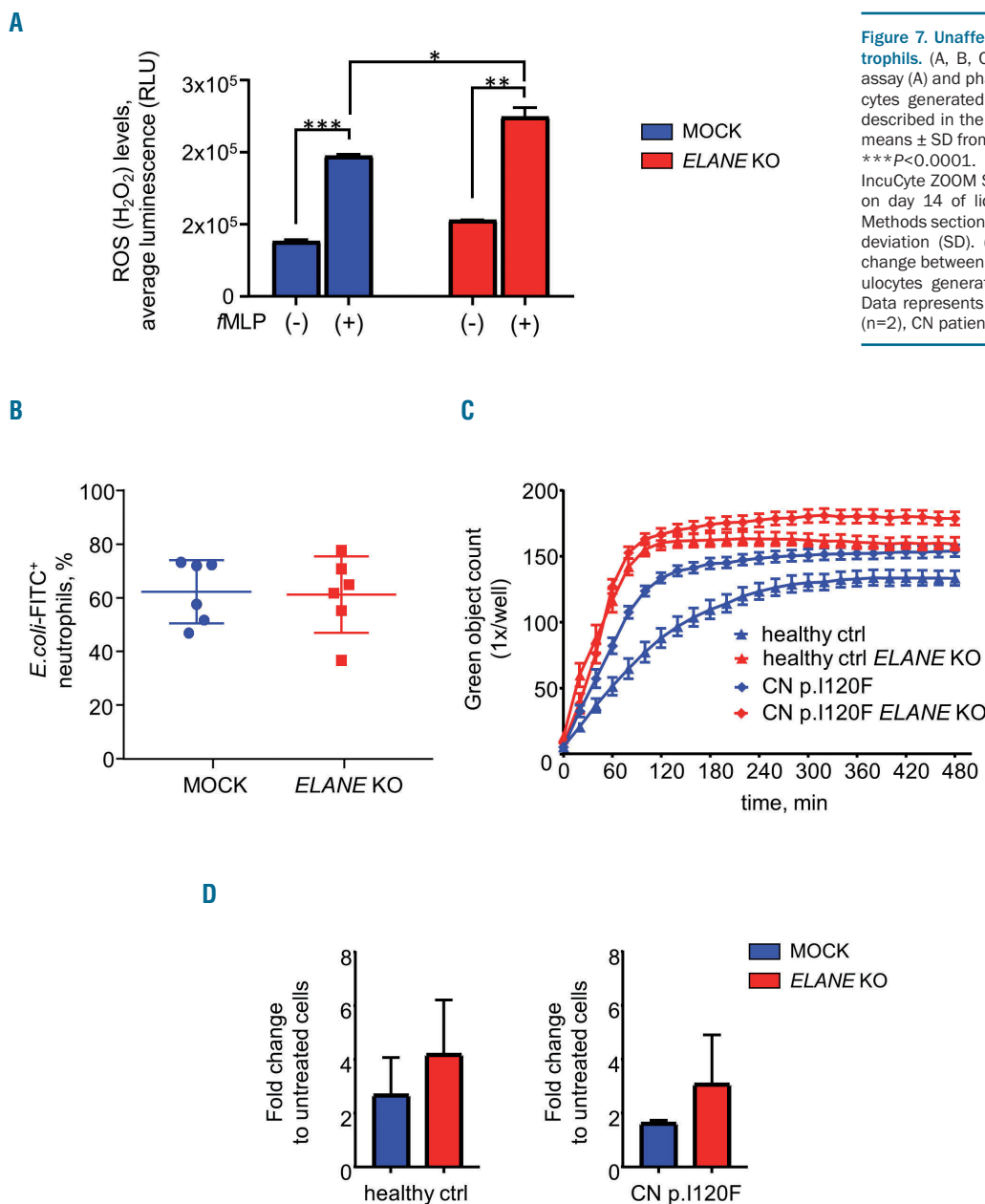


Figure 7. Unaffected functions of *ELANE* KO neutrophils. (A, B, C) Reactive oxygen species (ROS) assay (A) and phagocytosis assay (B, C) of granulocytes generated on day 14 of liquid culture, as described in the *Methods* section. Data represent means ± SD from duplicates. **P*<0.05, ***P*<0.01, ****P*<0.0001. (C) Phagocytosis Kinetic using InCuCyte ZOOM System of granulocytes generated on day 14 of liquid culture as described in the *Methods* section. Data represent mean ± standard deviation (SD). (D) Chemotaxis depicted as fold change between fMLP-treated and untreated granulocytes generated on day 14 of liquid culture. Data represents mean ± SD, healthy control (ctrl) (n=2), CN patient (n=1).

ical translational start site and/or internal start sites in exon 2 are disrupted and that expression of internally-initiated *ELANE* is pathogenic. We found a marked reduction of *ELANE* mRNA, most probably due to the induction of nonsense-mediated mRNA decay (NMD) of *ELANE* mRNA after exposure of cells to *ELANE*-specific CRISPR/Cas9 sgRNA RNP. We also did not detect any additional NE protein bands on WB analysis of edited cells using antibody recognizing C-terminus of NE. Based on these observations, we concluded that our sgRNA is inducing loss of NE protein without activation of the pathogenic *ELANE* forms from the internal ATG.

We did not detect off-target activity in edited cells, but recent results from Alan Bradley have suggested that the introduction of CRISPR/Cas9 editing can cause multiple genomic changes far beyond the actual target.²⁸ Therefore,

for clinical applications, evaluation of the off-target activity of CRISPR/Cas9 on whole genome level using next-generation sequencing should be performed. In addition, it would be important to evaluate that the editing of *ELANE* occurred in the repopulating hematopoietic stem cell population and that these cells maintained their ability to engraft immunodeficient mice *in vivo*. Since most probably HSC are not expressing NE, we will not expect any damaging effects of the *ELANE* KO on the functions and integrity of HSC.

We demonstrated here, that CRISPR/Cas9 mediated *ELANE* KO in HSPC and iPSC of CN patients induces granulocytic differentiation and *in vitro* generated *ELANE* KO neutrophils have no defects in the phagocytic activity, ROS production, and chemotaxis. NE is a proteolytic enzyme of the neutrophil serine protease (NSP) family,

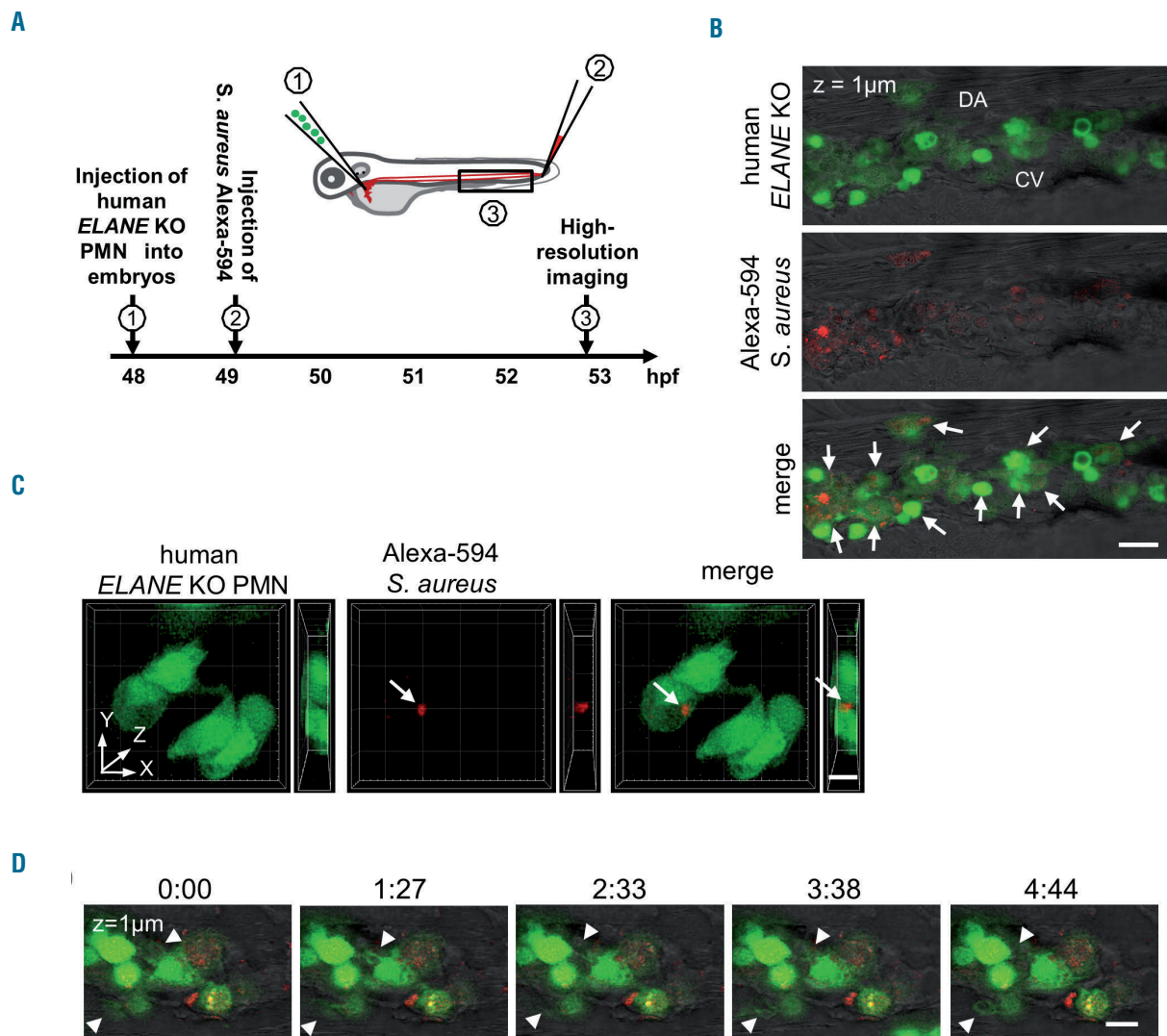


Figure 8. Human *ELANE* KO PMN are capable to migrate and to phagocytose *S. aureus* BioParticles in zebrafish embryos *in vivo*. (A) The scheme of *in vivo* phagocytosis assay in zebrafish embryos xenotransplanted with human fluorescently labeled polymorphonuclear leukocytes (PMN). (B) A representative confocal image highlighting the presence of transplanted human *ELANE* KO PMN in the caudal hematopoietic site of a zebrafish embryo at 53 hpf. White arrows indicate *S. aureus* BioParticles phagocytosed by human *ELANE* KO PMN. CV: caudal vein; DA: dorsal aorta. Scale bar: 20 μm. (C) Three-dimensional rendering of a z-stacks of 12 μm illustrating human *ELANE* KO PMN, one of them has engulfed *S. aureus* BioParticles (white arrow). Scale bar: 10 μm. (D) Still photographs from a time-lapse recording illustrating the phagocytic activity of transplanted human *ELANE* KO PMN in the zebrafish embryo. Arrowheads indicate the formation of neutrophil protrusions. Numbers indicate time in minutes. Scale bar: 10 μm.

including also cathepsin G (CG), proteinase 3 (PR3) and azurocidin (AZU1). NSP are stored in cytoplasmic granules, can be secreted into the extra- and peri-cellular space upon cellular activation and considered to be crucially involved in bacterial defense. NE and PR3 are very similar in their substrate specificity supporting a potentially redundant function for these two enzymes. *Elane*^{-/-} mice have normal neutrophil counts, but there are conflicting results regarding the effect of NE-deficiency on neutrophil extravasation to sites of inflammation, phagocytosis, and neutrophil extracellular traps in mice. NE may or may not be essential for these processes.²⁹⁻³³ Papillon-Lefevre Syndrome (PLS) is the only human disorder known to cause NE deficiency. This rare autosomal recessive disease is due to loss-of-function mutations in the DPPI gene locus with the loss of the lysosomal cysteine protease cathepsin C/dipeptidyl peptidase I (DPPI). The activation of NSP, including NE, depends on the N-terminal processing activity of DPPI. Therefore, PLS patients exhibit a severe reduction in the activity and stability of all three NSP including NE. Intriguingly, patients with PLS have no defects in their ability to kill bacteria e.g. *Staphylococcus aureus* or *E.coli*, suggesting that redundancies in the neutrophil's bactericidal mechanisms negate the necessity for serine proteases for killing common bacteria.³⁴ Moreover, since the other serine proteases including CG, PR3 and neutrophil serine protease 4 remain intact, we do not expect for the resultant cells to develop any neutrophil-specific functional anti-bacterial or immunodeficiency phenotype in *ELANE* KO cells. Based on these observations, at this juncture, we believe that CRISPR/Cas9 based knockout of *ELANE* in HSPC of CN patients may restore defective granulopoiesis in CN patients without seriously impairing neutrophil functions. Further studies, including gene expression analysis to understand which pathways are affected by *ELANE* mutations and verifying that these pathways are indeed restored by *ELANE* KO, are essential to justify the therapeutic applications of *ELANE* KO technology in the future. It will also contribute to the understanding of the pathophysiology of the CN caused by *ELANE* mutations. Our first attempts to investigate intracellular signaling pathways affected by mutated *ELANE* revealed the restoration of mRNA expression of anti-apoptotic Bcl-xl factor that is downregulated in CN myeloid progenitor cells.³⁵ Moreover, we found downregulation of mRNA levels of the key UPR player BiP, normally upregulated in HSPC of CN patients harboring *ELANE* mutations.⁸⁻¹⁰

CRISPR/Cas9 technology also allowed correction of the specific gene mutations. We selected the *ELANE* knockout approach since *ELANE* mutations are heterozygous gain-of-function gene defects that are distributed throughout all five exons and two introns of *ELANE* and specific *ELANE* mutations correction would require specific settings for each patient based on the mutation position. In addition, the requirement of the introduction of the donor repair template DNA in a gene correction approach

requires the activation of HDR making it difficult to achieve efficient correction in primary HSPC. We and other investigators have reported that *ELANE* mutations induce UPR and ER stress.⁸⁻¹¹ We also described deregulated signaling pathways in HSPC of CN patients downstream of *ELANE* mutations, such as diminished expression of transcription factors LEF-1, and C/EBP α ,³⁶⁻³⁹ abrogated expression and phosphorylation of the adaptor protein HCLS1,⁴⁰ elevated apoptosis³⁵ and hyperactivated NAMPT/sirtuins.⁴¹ These intracellular defects may lead to the elevated fragility of HSPC during *ex vivo* gene manipulations and may affect gene correction efficiency. Moreover, gene editing strategy directed to the correction of *ELANE* mutations may lead to the creation of novel missense or frameshift mutations that may result in the novel mutant NE protein with damaging functions and potential generation of the pre-leukemic HSPC clones with proliferative advantage and possible leukemic transformation. Adeno-associated virus (AAV)-based vector may be used for the delivery of the donor repair template and is considered safer than retroviral constructs. Two groups recently published successful gene deletions as a gene therapy approach to cure sickle cell disease, a common inherited blood disorder.^{17,18} It should be noted that AAV-based expression constructs may induce anti-viral host immune responses and may non-specifically integrate into the host genome.

In summary, we report here for the first time a method of CRISPR/Cas9 mediated *ELANE* gene deletion in hematopoietic stem cells and iPSC from CN patients harboring *ELANE* mutations. The *ELANE* gene deletion resulted in the increase of granulocytic differentiation to functional normal mature neutrophils in these patients *in vitro*. Therefore, CRISPR/Cas9 based gene knockout of *ELANE* in CN patients harboring *ELANE* mutation might be a useful treatment option especially in patients requiring high G-CSF dosages or do not responding to G-CSF at all. In addition, it remains to be investigated in subsequent clinical studies whether, in CN patients harboring *ELANE* mutations, the *ELANE* gene knockout would also abrogate the leukemogenesis.

Acknowledgments

We would like to thank the FACS core facility of the UKT especially Stella Autenrieth for the assistance in flow cytometry; Michael Schindler and Esther Lehmann for their support in confocal microscopy. This work was supported by the Excellence Initiative of the Faculty of Medicine, University of Tübingen (JS), Jose Carreras Leukemia Foundation (JS, PM, MR), Madeleine Schickedanz Kinderkrebsstiftung (JS, MK, MN), DFG (JS, MK), intramural Fortüne program of the Medical Faculty of the Tübingen University (MK, DA, YX), German-Israeli Foundation for Scientific Research and Development (GIF) (KW, BD), German Cancer Consortium (PM), Else Kröner-Fresenius Stiftung (MK, BD), Fritz Thyssen Foundation (MR and BD), NIH R24 AI 049393 (VM, BF, CZ, DCD).

References

- Dale DC, Person RE, Bolyard AA, et al. Mutations in the gene encoding neutrophil elastase in congenital and cyclic neutropenia. *Blood*. 2000; 96(7):2317-2322.
- Skokowa J, Germeshausen M, Zeidler C, Welte K. Severe congenital neutropenia: inheritance and pathophysiology. *Curr Opin Hematol*. 2007; 14(1):22-28.
- Skokowa J, Dale DC, Touw IP, Zeidler C, Welte K. Severe congenital neutropenias. *Nat Rev Dis Primers*. 2017;3:17032.
- Welte K, Gabrilove J, Bronchud MH, Platzer E, Morstyn G. Filgrastim (r-metHuG-CSF): the first 10 years. *Blood*. 1996;88(6):1907-1929.
- Rosenberg PS, Zeidler C, Bolyard AA, et al.

- Stable long-term risk of leukaemia in patients with severe congenital neutropenia maintained on G-CSF therapy. *Br J Haematol.* 2010;150(2):196-199.
6. Jinek M, Chylinski K, Fonfara I, Hauer M, Doudna JA, Charpentier E. A programmable dual-RNA-guided DNA endonuclease in adaptive bacterial immunity. *Science.* 2012;337(6096):816-821.
 7. Ran EA, Hsu PD, Wright J, Agarwala V, Scott DA, Zhang F. Genome engineering using the CRISPR-Cas9 system. *Nat Protoc.* 2013;8(11):2281-2308.
 8. Grenda DS, Murakami M, Ghatak J, et al. Mutations of the ELA2 gene found in patients with severe congenital neutropenia induce the unfolded protein response and cellular apoptosis. *Blood.* 2007;110(13):4179-4187.
 9. Nanea S, Murakami M, Xia J, et al. Activation of the unfolded protein response is associated with impaired granulopoiesis in transgenic mice expressing mutant Elane. *Blood.* 2011;117(13):3539-3547.
 10. Nustede R, Klimiankou M, Klimenkova O, et al. ELANE mutant-specific activation of different UPR pathways in congenital neutropenia. *Br J Haematol.* 2016;172(2):219-227.
 11. Kollner I, Sodeik I, Schreek S, et al. Mutations in neutrophil elastase causing congenital neutropenia lead to cytoplasmic protein accumulation and induction of the unfolded protein response. *Blood.* 2006;108(2):493-500.
 12. Makaryan V, Kelley ML, Fletcher B, Bolyard AA, Aprikyan AA, Dale DC. Elastase inhibitors as potential therapies for ELANE-associated neutropenia. *J Leukoc Biol.* 2017;102(4):1143-1151.
 13. Nayak RC, Trump LR, Aronow BJ, et al. Pathogenesis of ELANE-mutant severe neutropenia revealed by induced pluripotent stem cells. *J Clin Invest.* 2015;125(8):3103-3116.
 14. Ancliff PJ, Gale RE, Watts MJ, et al. Paternal mosaicism proves the pathogenic nature of mutations in neutrophil elastase in severe congenital neutropenia. *Blood.* 2002;100(2):707-709.
 15. Benson KF, Horwitz M. Possibility of somatic mosaicism of ELA2 mutation overlooked in an asymptomatic father transmitting severe congenital neutropenia to two offspring. *Br J Haematol.* 2002;118(3):923; author reply 924.
 16. Makaryan V, Zeidler C, Bolyard AA, et al. The diversity of mutations and clinical outcomes for ELANE-associated neutropenia. *Curr Opin Hematol.* 2015;22(1):3-11.
 17. Ye L, Wang J, Tan Y, et al. Genome editing using CRISPR-Cas9 to create the HPFH genotype in HSPCs: An approach for treating sickle cell disease and beta-thalassemia. *Proc Natl Acad Sci U S A.* 2016;113(38):10661-10665.
 18. Traxler EA, Yao Y, Wang YD, et al. A genome-editing strategy to treat beta-hemoglobinopathies that recapitulates a mutation associated with a benign genetic condition. *Nat Med.* 2016;22(9):987-990.
 19. Stemmer M, Thumberger T, Del Sol Keyer M, Wittbrodt J, Mateo JL. CCTop: an intuitive, flexible and reliable CRISPR/Cas9 target prediction tool. *PLoS One.* 2015;10(4):e0124633.
 20. Brinkman EK, Chen T, Amendola M, van Steensel B. Easy quantitative assessment of genome editing by sequence trace decomposition. *Nucleic Acids Res.* 2014;42(22):e168.
 21. Bajoghli B, Kuri P, Inoue D, et al. Noninvasive in toto imaging of the thymus reveals heterogeneous migratory behavior of developing T cells. *J Immunol.* 2015;195(5):2177-2186.
 22. Lachmann N, Ackermann M, Frenzel E, et al. Large-scale hematopoietic differentiation of human induced pluripotent stem cells provides granulocytes or macrophages for cell replacement therapies. *Stem Cell Reports.* 2015;4(2):282-296.
 23. Dannenmann B, Zahabi A, Mir P, et al. Human iPSC-based model of severe congenital neutropenia reveals elevated UPR and DNA damage in CD34(+) cells preceding leukemic transformation. *Exp Hematol.* 2019;71:51-60.
 24. Hamilton N, Sabroe I, Renshaw SA. A method for transplantation of human HSCs into zebrafish, to replace humanised murine transplantation models. *F1000Res.* 2018;7:594.
 25. Staal FJ, Spaik HP, Fibbe WE. Visualizing human hematopoietic stem cell trafficking in vivo using a zebrafish xenograft model. *Stem Cells Dev.* 2016;25(4):360-365.
 26. Nasri M, Mir P, Dannenmann B, et al. Fluorescent labeling of CRISPR/Cas9 RNP for gene knockout in HSPCs and iPSCs reveals an essential role for GADD45b in stress response. *Blood Adv.* 2019;3(1):63-71.
 27. Tidwell T, Wechsler J, Nayak RC, et al. Neutropenia-associated ELANE mutations disrupting translation initiation produce novel neutrophil elastase isoforms. *Blood.* 2014;123(4):562-569.
 28. Kosicki M, Tomberg K, Bradley A. Repair of double-strand breaks induced by CRISPR-Cas9 leads to large deletions and complex rearrangements. *Nat Biotechnol.* 2018;36(8):765-771.
 29. Allport JR, Lim YC, Shipley JM, et al. Neutrophils from MMP-9- or neutrophil elastase-deficient mice show no defect in transendothelial migration under flow in vitro. *J Leukoc Biol.* 2002;71(5):821-828.
 30. Martinod K, Witsch T, Farley K, Gallant M, Remold-O'Donnell E, Wagner DD. Neutrophil elastase-deficient mice form neutrophil extracellular traps in an experimental model of deep vein thrombosis. *J Thromb Haemost.* 2016;14(3):551-558.
 31. Hirche TO, Atkinson JJ, Bahr S, Belaouaj A. Deficiency in neutrophil elastase does not impair neutrophil recruitment to inflamed sites. *Am J Resp Cell Mol Biol.* 2004;30(4):576-584.
 32. Young RE, Thompson RD, Larbi KY, et al. Neutrophil elastase (NE)-deficient mice demonstrate a nonredundant role for NE in neutrophil migration, generation of proinflammatory mediators, and phagocytosis in response to zymosan particles in vivo. *J Immunol.* 2004;172(7):4493-4502.
 33. Belaouaj A, McCarthy R, Baumann M, et al. Mice lacking neutrophil elastase reveal impaired host defense against gram negative bacterial sepsis. *Nat Med.* 1998;4(5):615-618.
 34. Pham CT, Ivanovich JL, Raptis SZ, Zehnbauser B, Ley TJ. Papillon-Lefevre syndrome: correlating the molecular, cellular, and clinical consequences of cathepsin C/dipeptidyl peptidase I deficiency in humans. *J Immunol.* 2004;173(12):7277-7281.
 35. Cario G, Skokowa J, Wang Z, et al. Heterogeneous expression pattern of pro- and anti-apoptotic factors in myeloid progenitor cells of patients with severe congenital neutropenia treated with granulocyte colony-stimulating factor. *Br J Haematol.* 2005;129(2):275-278.
 36. Skokowa J, Cario G, Uenalan M, et al. LEF-1 is crucial for neutrophil granulocytopenia and its expression is severely reduced in congenital neutropenia. *Nat Med.* 2006;12(10):1191-1197.
 37. Skokowa J, Welte K. LEF-1 is a decisive transcription factor in neutrophil granulopoiesis. *Ann N Y Acad Sci.* 2007;1106:143-151.
 38. Skokowa J, Welte K. Dysregulation of myeloid-specific transcription factors in congenital neutropenia. *Ann N Y Acad Sci.* 2009;1176:94-100.
 39. Skokowa J, Welte K. Defective G-CSFR signaling pathways in congenital neutropenia. *Hematol Oncol Clin North Am.* 2013;27(1):75-88, viii.
 40. Skokowa J, Klimiankou M, Klimenkova O, et al. Interactions among HCLS1, HAX1 and LEF-1 proteins are essential for G-CSF-triggered granulopoiesis. *Nat Med.* 2012;18(10):1550-1559.
 41. Skokowa J, Lan D, Thakur BK, et al. NAMPT is essential for the G-CSF-induced myeloid differentiation via a NAD(+)-sirtuin-1-dependent pathway. *Nat Med.* 2009;15(2):151-158.

Dannenmann B. et al., 2019, *Experimental Hematology*



ELSEVIER



Experimental Hematology 2019;71:51–60

**Experimental
Hematology**

Human iPSC-based model of severe congenital neutropenia reveals elevated UPR and DNA damage in CD34⁺ cells preceding leukemic transformation

Benjamin Dannenmann^a, Azadeh Zahabi^a, Perihan Mir^{a,b}, Benedikt Oswald^a, Regine Bernhard^a, Maksim Klimiankou^a, Tatsuya Morishima^a, Klaus Schulze-Osthoff^{b,c}, Cornelia Zeidler^d, Lothar Kanz^a, Nico Lachmann^e, Thomas Moritz^e, Karl Welte^f, and Julia Skokowa^a

^aDepartment of Oncology, Hematology, Immunology, Rheumatology, and Pulmonology, University Hospital Tuebingen, Tuebingen, Germany;

^bGerman Cancer Research Center (DKFZ), Heidelberg, Germany; ^cInterfaculty Institute of Biochemistry, Tübingen University, Germany;

^dDepartment of Hematology, Oncology, and Bone Marrow Transplantation, Hannover Medical School, Hannover, Germany; ^eInstitute of Experimental Hematology, Hannover Medical School, Hannover, Germany; ^fUniversity Children's Hospital Tuebingen, Tuebingen, Germany

(Received 10 October 2018; revised 23 December 2018; accepted 30 December 2018)

We describe the establishment of an embryoid-body-based protocol for hematopoietic/myeloid differentiation of human induced pluripotent stem cells that allows the generation of CD34⁺ cells or mature myeloid cells in vitro. Using this model, we were able to recapitulate the defective granulocytic differentiation in patients with severe congenital neutropenia (CN), an inherited preleukemia bone marrow failure syndrome. Importantly, in vitro maturation arrest of granulopoiesis was associated with an elevated unfolded protein response (UPR) and enhanced expression of the cell cycle inhibitor p21. Consistent with this, we found that CD34⁺ cells of CN patients were highly susceptible to DNA damage and showed diminished DNA repair. These observations suggest that targeting the UPR pathway or inhibiting DNA damage might protect hematopoietic cells of CN patients from leukemogenic transformation, at least to some extent. © 2019 ISEH – Society for Hematology and Stem Cells. Published by Elsevier Inc. All rights reserved.

Severe congenital neutropenia (CN) is a monolineage preleukemia bone marrow failure syndrome characterized by early onset of neutropenia and severe infections due to promyelocytic maturational arrest in the bone marrow [1,2]. CN is a heterogeneous disease caused by mutations in a number of genes, including *ELANE* [3] (the most common [1]), *HAXI* [4], *CSF3R* [5,6], *JAGN1* [7], *G6PC3* [8], *TCIRG1* [9], and others. In most cases, *ELANE* mutations are missense mutations that are distributed throughout all five exons of the *ELANE* gene, although a majority of mutations are found in exons 4 and 5 [10]. Hematopoietic stem and progenitor cells (HSPCs) of CN patients (CN-HSPCs) fail to differentiate into neutrophilic granulocytes, but show no severe maturation defects in other blood

lineages [1,2,11,12]. Exposure of CN-HSPCs to high concentrations of granulocyte colony-stimulating factor (G-CSF) partially reverses granulocytic maturation defects [1,12], but approximately 10% of CN patients do not respond to G-CSF doses up to 50 $\mu\text{g}/\text{kg}/\text{d}$. The mechanism underlying the granulocytic differentiation defects in bone marrow HSPCs of CN patients has only been partially elucidated. Among the relevant factors, we have identified deregulated levels of LEF-1 [13,14], C/EBP α [13], and PU.1 [15,16] transcription factors; hyperactivated JAK2 [17] and phospho-STAT5a [18]; elevated NAMPT/SIRT1 signaling [19]; abrogated expression of the anti-apoptotic genes Bcl2 and Bcl-xl [20], and markedly diminished expression of the natural inhibitor of neutrophil proteases SLPI (secretory leukocyte protease inhibitor) [21]. In addition, we and others have shown that mutant neutrophil elastase (NE) triggers activation of the unfolded protein response (UPR) and induction of endoplasmic reticulum (ER) stress caused by accumulation of altered (incompletely

Offprint requests to: Prof. Julia Skokowa, Department of Oncology, Hematology, Immunology, Rheumatology and Pulmonology, University Hospital Tuebingen, Otfried-Müller-Str. 10, Tübingen D-72076, Germany; E-mail: julia.skokowa@med.uni-tuebingen.de

folded or misfolded) NE protein within the ER or by disturbed intracellular trafficking of NE [22–24].

Despite these insights, we are still far from a clear understanding of the ultimate origin of the defective granulopoiesis and leukemic transformation in CN. There are no animal models of CN, except for rare neutropenia cases caused by inherited mutations in *GFII* (growth factor independent 1). *Elane*^{-/-} and *Hax1*^{-/-} mice, as well as transgenic mice with a knock-in of a human *ELANE* mutation [23], exhibit normal hematopoietic phenotypes and are not neutropenic. Reprogramming somatic cells of CN patients into induced pluripotent stem cells (iPSCs), followed by hematopoietic differentiation of iPSCs, provides a means for establishing an in vitro model of neutropenia and leukemic transformation in CN. iPSC hematopoietic differentiation models have limitations and cannot fully replace in vivo mouse disease models, but they represent an excellent source of immature hematopoietic cells and mature myeloid cells for further experimentation. Generation of CN-patient-specific iPSCs that recapitulate the maturation arrest of granulopoiesis has been described previously [25–28].

In the present study, we describe the establishment of an experimental in vitro model for studying CN using patient-derived iPSCs. Using this model, we were able to identify upregulation of key components of the UPR pathway and enhanced DNA damage and increased p21 protein levels in CD34⁺ cells and CD45⁺ cells of CN patients.

Methods

iPSC cell culture

iPSCs were maintained on mitomycin-C-treated SNL-feeder cells (Public Health England, GB) in iPSC medium consisting of DMEM F12 (Sigma-Aldrich, Germany) supplemented with 20% Knockout Serum Replacement (Invitrogen, USA), 30 ng/mL basic fibroblast growth factor (bFGF; Peprotech, USA), 1% nonessential amino acid solution (Invitrogen, USA), 100 μmol/L 2-mercapto-ethanol, and 2 mmol/L L-glutamine. iPSC medium was replaced every day. hiPSCs were subcultured by manual colony picking on new SNL feeder cells every 10 days.

Reprogramming of peripheral blood mononuclear cells

A total of 1.5×10^6 peripheral blood mononuclear cells were cultured after thawing for 6 days in CD34⁺ cell expansion medium (Stemline II Medium, Sigma-Aldrich, Germany) supplemented with 10% fetal calf serum, 1% penicillin/streptomycin, 1% glutamine, and the following cytokines: interleukin-3 (IL-3; 20 ng/μL), IL-6 (20 ng/μL), thrombopoietin (20 ng/μL), stem cell factor (SCF; 50 ng/μL), and FLT3L (50 ng/μL). All cytokines were purchased from R&D Systems (USA). After 1 week, cells were added to Retronectin (Clontech, USA)-coated 12-well plates together with OSKM lentiviral supernatant (pRRL.PPT.SF.hOct34.hKlf4.

hSox2.i2dTomato.pre.FRT, provided by A. Schambach) with multiplicity of infection of 2. Four days later, cells were transferred to SNL feeders and cultured in an 1:1 mixture of iPSC medium and CD34⁺ cell expansion medium supplemented with 2 mmol/L valproic acid and 50 μg/mL vitamin C. Medium was gradually changed to iPSC medium only. The first iPSC colonies appeared approximately 3 weeks after initiation of reprogramming.

Quantitative reverse transcription polymerase chain reaction

For quantitative reverse transcription polymerase chain reaction (qRT-PCR), RNA was isolated using RNeasy Micro Kit (Qiagen, Germany). cDNA was prepared from 1 μg of total RNA using the Omniscript RT Kit (Qiagen, Germany). qRT-PCR was performed using SYBR Green qPCR Master Mix (Roche, Switzerland) on Light Cycler 480 (Roche). Data were analyzed using the ddCT method. Target genes were normalized to *GAPDH* and *ACTB* as housekeeper genes. qRT-PCR primer sequences are listed in Supplementary Table E1 (online only, available at www.exphem.org).

Western blotting

A total of 1×10^6 cells were lysed in 200 μL of 3 × Laemmli buffer. Protein was denatured for 10 min at 95°C. Then, 5 μL of cell lysate in Laemmli buffer was loaded per lane. Proteins were separated on a 12% polyacrylamide gel and transferred on a nitrocellulose membrane (GE Healthcare, USA) for 1 hour at 100 V and 4°C. Membrane was blocked for 1 hour in 5% bovine serum albumin (BSA)/Tris-buffered saline + Tween 20 and incubated in primary antibody overnight at 4°C. The following primary antibodies were used: anti-p21 (Cell Signaling Technology, #2947S), anti-CHOP (Cell Signaling Technology, #2895S), and anti-NE (Santa Cruz Biotechnology, sc-55549) and anti-β-actin (Cell Signaling Technology, #13E5). Next, membranes were washed and incubated with secondary horseradish peroxidase-coupled (Santa Cruz Biotechnology) antibody for 1 hour at room temperature. Enhanced chemoluminescence solution (Thermo Fisher Scientific, USA) and Amersham Hyperfilm were used to detect chemiluminescence signal of proteins.

Embryoid-body-based hematopoietic differentiation of iPSCs

iPSCs were dissociated from SNL feeders or Matrigel (Corning, USA)-coated plates using phosphate-buffered saline (PBS)/ethylenediaminetetraacetic acid (0.02%) for 5 min. Embryoid body (EB) generation was done via centrifugation of 20,000 cells per EB in 96-well plates using APEL serum-free differentiation medium (StemCell Technologies, Canada) supplemented with bFGF (20 ng/μL) and Rho kinase (ROCK) inhibitor (10 μmol/L) (R&D Systems). The next day, bone morphogenetic protein 4 (BMP4; 20 ng/μL) was added to the culture to induce mesodermal differentiation. On day four, EBs were plated on Matrigel-coated six-well plates (10 EBs/well) in APEL medium supplemented with vascular endothelial growth factor (VEGF; 40 ng/μL), SCF (50 ng/μL), and IL-3 (50 ng/μL). For neutrophilic differentiation, medium was changed 3 days later to fresh APEL medium supplemented with IL-3 (50 ng/μL) and G-CSF (50 ng/μL). The first hematopoietic suspension cells appeared on day 12 to day 14.

Suspension cells were harvested every 3–4 days and analyzed starting from day 14 to day 32. All cytokines were purchased from R&D Systems if not otherwise indicated.

Flow cytometry

A total of 30,000 suspension cells collected from an EB-based hematopoietic differentiation system were used for flow cytometry. For cell surface staining, cells were prepared in PBS/1% BSA containing 0.05% sodium azide and stained with the mouse monoclonal antihuman antibody. For detection of mature myeloid cells, a multicolor fluorescence-activated cell-sorting (FACS) antibody panel for “late-stage” hematopoietic differentiation using the following antibodies was applied: CD15-PE, CD16-FITC, CD14-APC-H7, CD45-BV510, CD33-BV421, CD11b-PE-Cy7, and 7-AAD. Samples were analyzed using a FACSCanto II (BD Biosciences, Germany) and FlowJo version 10 software. Antibodies for flow cytometry were purchased from BD Biosciences if not otherwise indicated.

Morphological analysis

Wright–Giemsa-stained cytospin slides were prepared using Hema-Tek slide stainer (LabX, Canada). Hematopoietic cells were classified into four groups according to the differentiation state: myeloblast and promyelocyte (MB/ProM), myelocyte and metamyelocyte (Myelo/Meta), band and segmented neutrophils (Band/Seg), and monocytes/macrophages (Mo/MΦ).

DNA damage quantification

A total of 2.5×10^4 iPSC-derived CD34⁺/CD45⁺ cells were resuspended in PBS and treated with the indicated concentrations of bleomycin for 5 min at room temperature. Genomic DNA was isolated using the QIAamp DNA Mini Kit (Qiagen, Germany). Long-run real-time PCR-based DNA-damage quantification (LORD-Q) was performed and analyzed according to Lehle et al. [29].

Statistical analysis

Differences in mean values between groups were analyzed using two-sided, unpaired Student *t* tests using the SPSS (IBM, USA) version 9.0 statistical package.

Results

In vitro EB-based iPSC differentiation model reveals severely impaired myelopoiesis of CN and CN/acute myeloid leukemia patient-derived iPSCs

We generated iPSCs from two *ELANE*-CN patients, one patient with p.C151Y (CN1), and another patient with p.G214R (CN2) *ELANE* mutations. From one CN patient, we were able to generate iPSC clones harboring either an *ELANE* p.C151Y mutation only (CN-iPSC clone) or additional *CSF3R* and *RUNX1* mutations and trisomy 21 (CN/acute myeloid leukemia [AML]-iPSC clone). All iPSC lines expressed elevated protein and mRNA levels of pluripotent stem-cell-specific factors and showed inactivation of the lentiviral plasmid used for reprogramming.

To evaluate myeloid differentiation of *ELANE*-CN patients iPSCs, we slightly modified an in vitro EB-based iPSC differentiation method developed by Lachmann et al. [30] that allows generation of hematopoietic cells and mature myeloid cells for more than 30 days. EB formation was performed by first centrifuging dissociated iPSCs (20,000 cells/EB) in 96-well conical-bottomed plates in APEL serum-free differentiation medium containing bFGF and ROCK inhibitors, followed by induction of mesodermal differentiation by the addition of BMP4 on day 1 of culture. To induce hematopoietic differentiation, we plated EBs on Matrigel-coated six-well plates (10 EBs/well) in APEL medium supplemented with VEGF, SCF, and IL-3 on day 4 of culture. Neutrophilic differentiation was initiated 3 days later by replacement of cytokines with IL-3 and G-CSF (Figure 1A). In EBs cultured from healthy donor (HD)-derived iPSCs, hematopoietic cells appeared in the supernatants on day 14 and the number of cells was markedly increased at day 28 of culture (Figure 1B). In contrast, the number of hematopoietic cells in culture supernatants of EBs from CN patient-derived iPSCs was markedly diminished and almost no myeloid cells were produced from cultured CN/AML iPSCs (Figure 1B). Consistent with these observations, granulocytic differentiation into mature polymorphonuclear neutrophils (CD15⁺CD16⁺CD45⁺ cell population) was markedly reduced in iPSC lines of both *ELANE*-CN patients compared with HD-derived iPSCs and was abolished in CN/AML-iPSCs (Figure 1C). However, the number of monocytes (CD14⁺ CD11b⁺CD45⁺ cells) produced by CN patient-derived iPSCs was strongly increased compared with that produced by HD-derived iPSCs (Figure 1C). This pattern recapitulates the situation in CN patients, in whom monocyte numbers in the peripheral blood are elevated [31]. Morphological examinations of Giemsa-stained cytospin slides confirmed these results (Figure 1D). Therefore these observations demonstrate the successful establishment of an in vitro model to evaluate mechanisms of diminished granulocytic differentiation of hematopoietic cells in CN patients.

Elevated ER stress and UPR in CD34⁺ and CD45⁺ cells from CN patient- and CN1/AML patient-derived iPSCs

We next investigated whether intracellular signaling pathways operating during induction of the UPR, which is known to be hyperactivated in primary HSPCs and granulocytes of CN patients [21–24], are also affected in iPSC-derived hematopoietic cells. We found that *ELANE* mRNA and NE protein levels were highly upregulated in CD34⁺ cells generated from CN1/AML-iPSCs compared with those generated from CN-iPSCs and HD-iPSCs (Figures 2A and 2C). We detected deregulation of mRNA expression of the UPR downstream targets in CN1 and CN2 iPSC-derived CD34⁺ cells. Therefore DDIT3 (DNA-

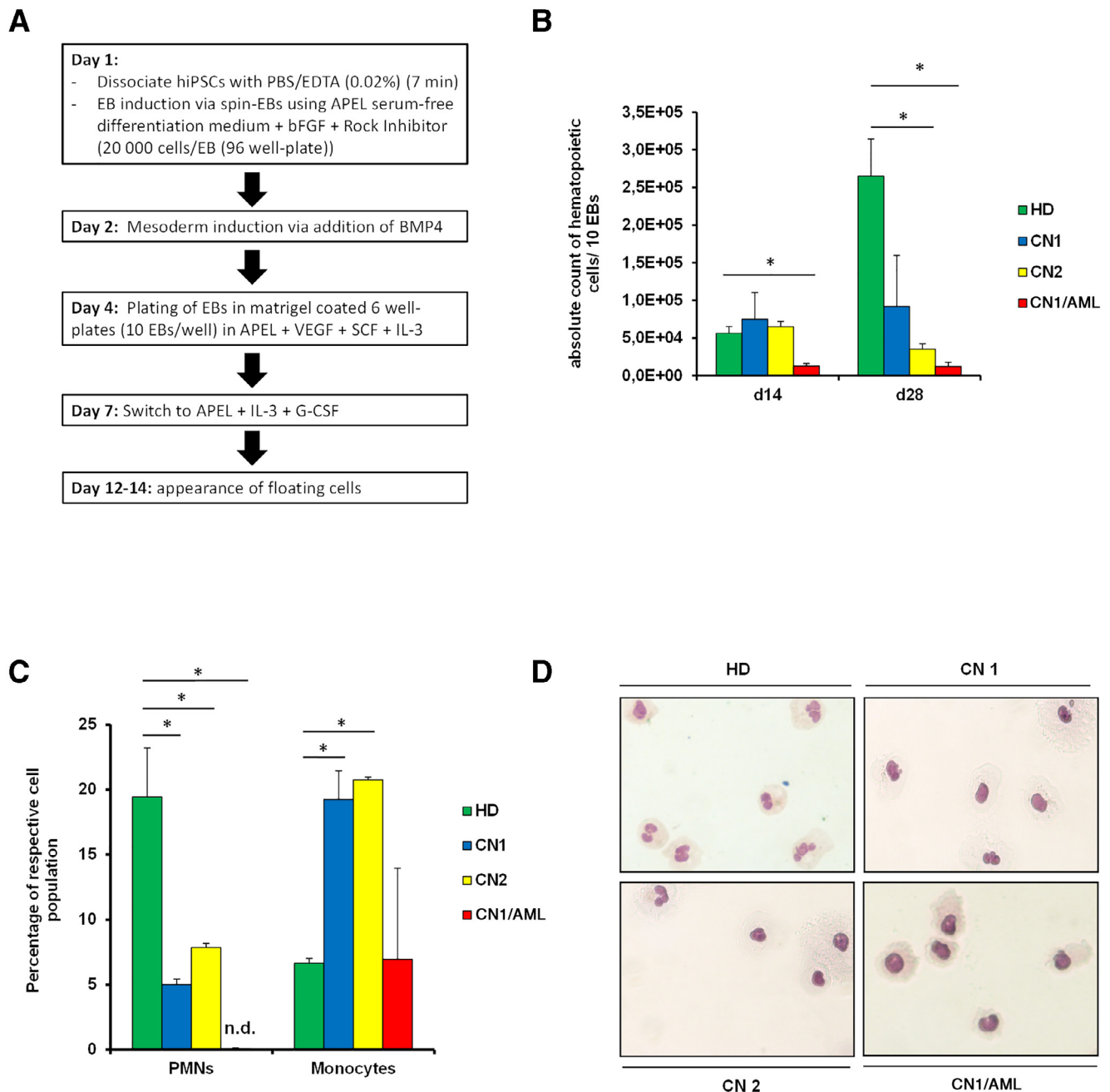


Figure 1. In vitro model of CN and CN/AML using EB-based myeloid differentiation method of patients iPSCs. **(A)** Scheme of the protocol for EB-based hematopoietic and neutrophilic differentiation of iPSCs. **(B)** Production of hematopoietic cells from iPSCs over time in the EB-based differentiation system. Hematopoietic cells were harvested from EB culture supernatants starting from day 14 to day 28 and counted using trypan blue dye exclusion. Data represent means \pm SD from two independent experiments. Two-sided, unpaired Student *t* test *p* values to HD are shown. $*p < 0.05$. **(C)** Flow cytometry analysis of suspension cells harvested from EBs culture on day 28 of differentiation. Data represent means \pm SD from two independent experiments. $*p < 0.05$. **(D)** Morphological analysis of suspension cells harvested from iPSCs at day 28 of differentiation (Wright-Giemsa Stain). Representative cytopsin slide pictures are shown. HD, healthy donor.

damage inducible transcript 3, also called CHOP) was increased in CD34⁺ cells generated from CN1-iPSCs, CN2-iPSCs, and CN1/AML-iPSCs compared with those from HD-iPSCs (Figure 2B). In contrast, expression of mRNA for BiP (binding immunoglobulin protein) was upregulated in CN2, but not CN1-iPSC- or CN1/AML-iPSC-derived

CD34⁺ cells. ATF6 (activating transcription factor 6) mRNA was highly expressed in CD34⁺ cells derived from CN1-iPSCs, but not in CN2-iPSC- or CN1/AML-iPSC-derived cells. In contrast, maximum ATF4 (activating transcription factor 4) mRNA expression was detected in CD34⁺ cells from CN2-iPSCs and CN1/AML-iPSCs, but

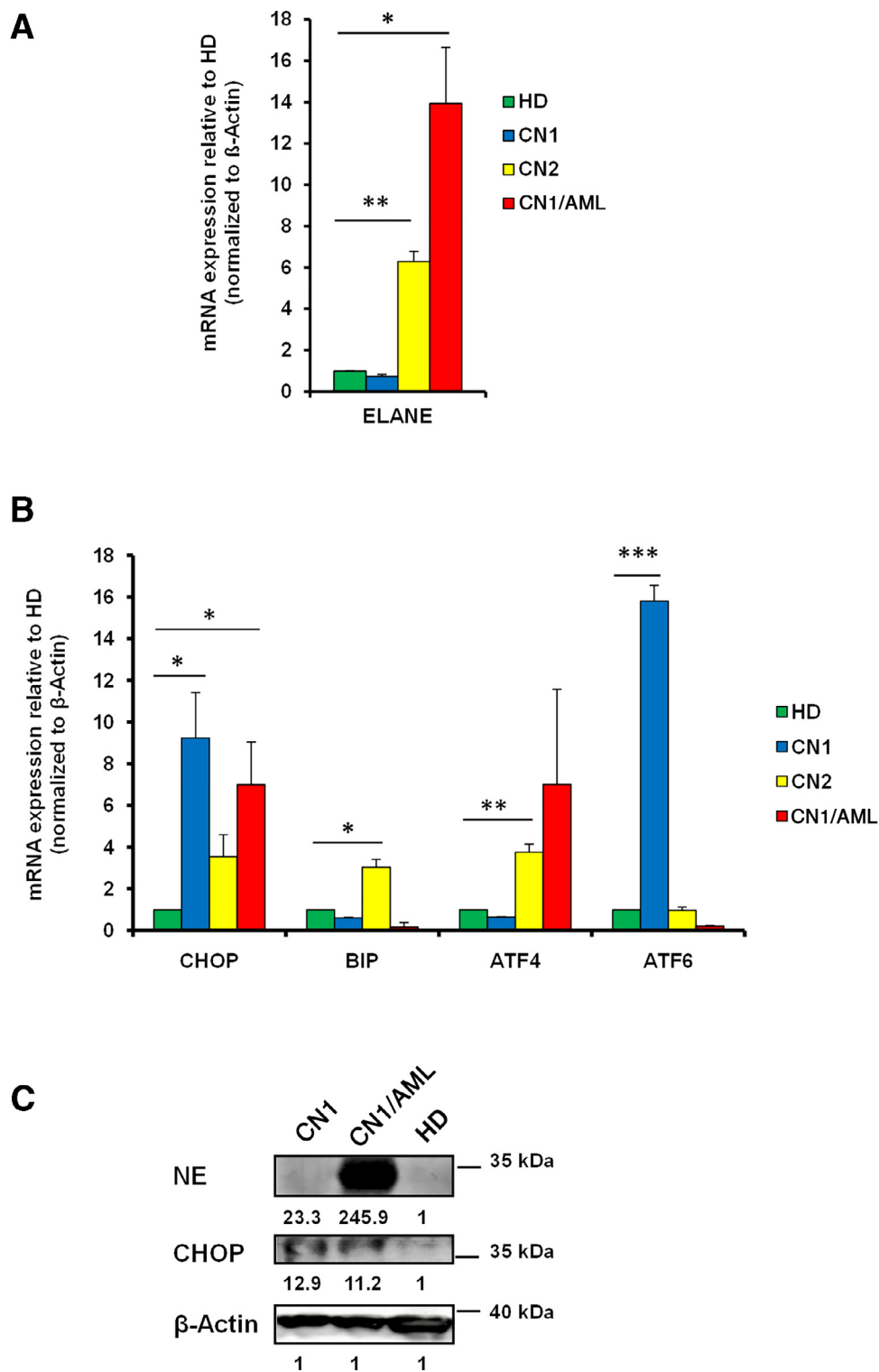


Figure 2. Analysis of ER stress and unfolded protein response (UPR) in CD34⁺ and CD45⁺ cells derived from CN- and CN/AML-iPSCs. **(A)** qRT-PCR analysis of ELANE mRNA expression in CD45⁺CD34⁺ cells at day 14 of iPSC differentiation. Data represent means \pm SD from two independent experiments. * p < 0.05, ** p < 0.001. **(B)** qRT-PCR analysis of mRNA expression of UPR-related genes in CD45⁺CD34⁺ cells at day 14 of iPSC differentiation, as indicated. Data represent means \pm SD from two independent experiments. * p < 0.05, ** p < 0.01, *** p < 0.001. **(C)** Representative Western blot images of NE and CHOP protein expression in CD45⁺ cells at day 28 of iPSC differentiation, as indicated. Numbers below Western blot images indicate protein expression levels normalized to β -Actin.

not in those from CN1-iPSCs or HD-iPSCs (Figure 2B). CHOP protein levels were also elevated in CD45⁺ cells derived on day 28 of EB differentiation of CN and CN/AML iPSCs (Figure 2C).

DNA damage and DNA-repair responses in CD34⁺ cells from CN-iPSCs

We further assessed whether elevated ER stress resulting from UPR sensitizes CN-iPSC-derived CD34⁺ cells to DNA damage. DNA damage was induced by treating cells with bleomycin for 5 min, after which bleomycin was removed and DNA damage and DNA repair were assessed immediately and after 2 hours of incubation (Figure 3A). Long-run, real-time PCR-based DNA-damage quantification (LORD-Q [29]) of genomic DNA loci (*GAPDH* and *TP53*) and mitochondrial DNA (mtDNA) revealed a robust increase in mtDNA and nuclear DNA lesions in CN-iPSC-derived CD34⁺ cells compared with HD-iPSC-derived cells (Figure 3B). Damaged mtDNA and *GAPDH* DNA loci, but not *TP53* DNA loci, were also more frequent in CD34⁺ cells from CN-iPSCs 2 hours after bleomycin treatment compared with that in HD-iPSC-derived CD34⁺ cells. These data suggest delayed DNA repair and increased susceptibility to DNA damage in CD34⁺ cells from CN-iPSC lines (Figure 3C).

p21 upregulation in CD34⁺ and CD45⁺ cells from CN-iPSCs and CN/AML-iPSCs

We next sought to determine whether DNA damage pathways are differentially regulated in CD34⁺ and CD45⁺ cells generated from iPSCs of CN or CN/AML patients compared with HD-generated cells. Our assessment of the role of the p53-p21 pathway, which is typically activated upon DNA damage, showed no differences in *TP53* mRNA expression, but revealed an approximately threefold increase in p21 mRNA expression in CN-iPSC-derived blood cells compared with those derived from HD cells and a fivefold to sixfold increase in CN/AML-iPSC-derived cells (Figure 3D). p21 protein levels were also elevated in CN/AML cells (Figure 3E). The expression of *MDM2* mRNA was markedly diminished in CN/AML cells, and *GADD45a* mRNA expression was slightly induced in both CN-iPSC- and CN/AML-iPSC-derived cells compared with those derived from HD-iPSCs (Figure 3D). Interestingly, p21 mRNA expression was also upregulated in primary bone marrow CD33⁺ cells of CN patients compared with those of G-CSF-treated healthy individuals, in which p21 levels were even suppressed by G-CSF (data not shown).

Discussion

In the present study, we established an in vitro model of CN using patient-derived iPSCs. We also

successfully reprogrammed AML blasts from one CN/AML patient and were able to compare hematopoietic and myeloid differentiation of iPSCs derived from CN/AML cells, CN patients, and a healthy donor. Our data provide strong evidence that, despite some limitations, iPSCs represent a valuable resource for disease modeling, especially for investigations on inherited bone marrow failure syndromes. Primary bone marrow material from pediatric patients with bone marrow failure is extremely limited and mouse models are not available for many of these syndromes. In this latter context, *elane*^{-/-} mice, *hax1*^{-/-} mice, and transgenic mice carrying mutated *elane* do not exhibit neutropenia. In addition, transgenic mice carrying a truncated G-CSF receptor (*csf3r*) mutant never develop leukemia. These acquired *CSF3R* mutations are observed in leukemic blasts of more than 80% of CN patients with overt AML or MDS [32].

Using our iPSC model, we were able to recapitulate the hematopoietic and myeloid differentiation defects of HSPCs observed in CN patients in vivo. Specifically, we detected diminished granulocytic differentiation of CN-iPSCs, an observation consistent with the induction of UPR. iPSC lines from two CN patients showed different behavior during first 2 weeks of hematopoietic differentiation, when differentiation of EBs into CD34⁺ CD45⁺ cells occurs, but both CN patients' iPSC lines demonstrated similar markedly diminished granulocytic differentiation at later stages. These early differentiation stage differences may be explained by the varying effects of the mutated NE protein on blood cell formation, which is dependent on the mutated amino acid residues. Interestingly, different *ELANE* mutations resulted in abolished granulocytic differentiation of CN patient-derived iPSCs, an observation consistent with insights gained from CN patients [1]. Monocytic differentiation was elevated in CN-iPSC lines, an observation that parallels the common finding of peripheral blood monocytosis in CN patients [1,31]. One possible explanation for this monocytosis is a compensatory reaction of the bone marrow to diminished neutrophil counts and function that serves to induce an immune response to bacterial pathogens. An alternative explanation is deregulated expression of lineage-specific (granulocyte-specific vs. monocyte-specific) transcription factors in myeloid progenitor cells of CN patients. Deregulated expression of relevant transcription factors (e.g., diminished expression of LEF-1 and C/EBP α , but elevated PU.1 expression) has been described by us previously [15]. Elevated monocytic maturation of CN patients' iPSC lines in vitro further supports the theory that deregulation of a transcriptional program in HSPCs is a cause of neutropenia and monocytosis.

UPR hyperactivation in primary HSPCs of CN patients has been described previously [22–24]. It is presumed that

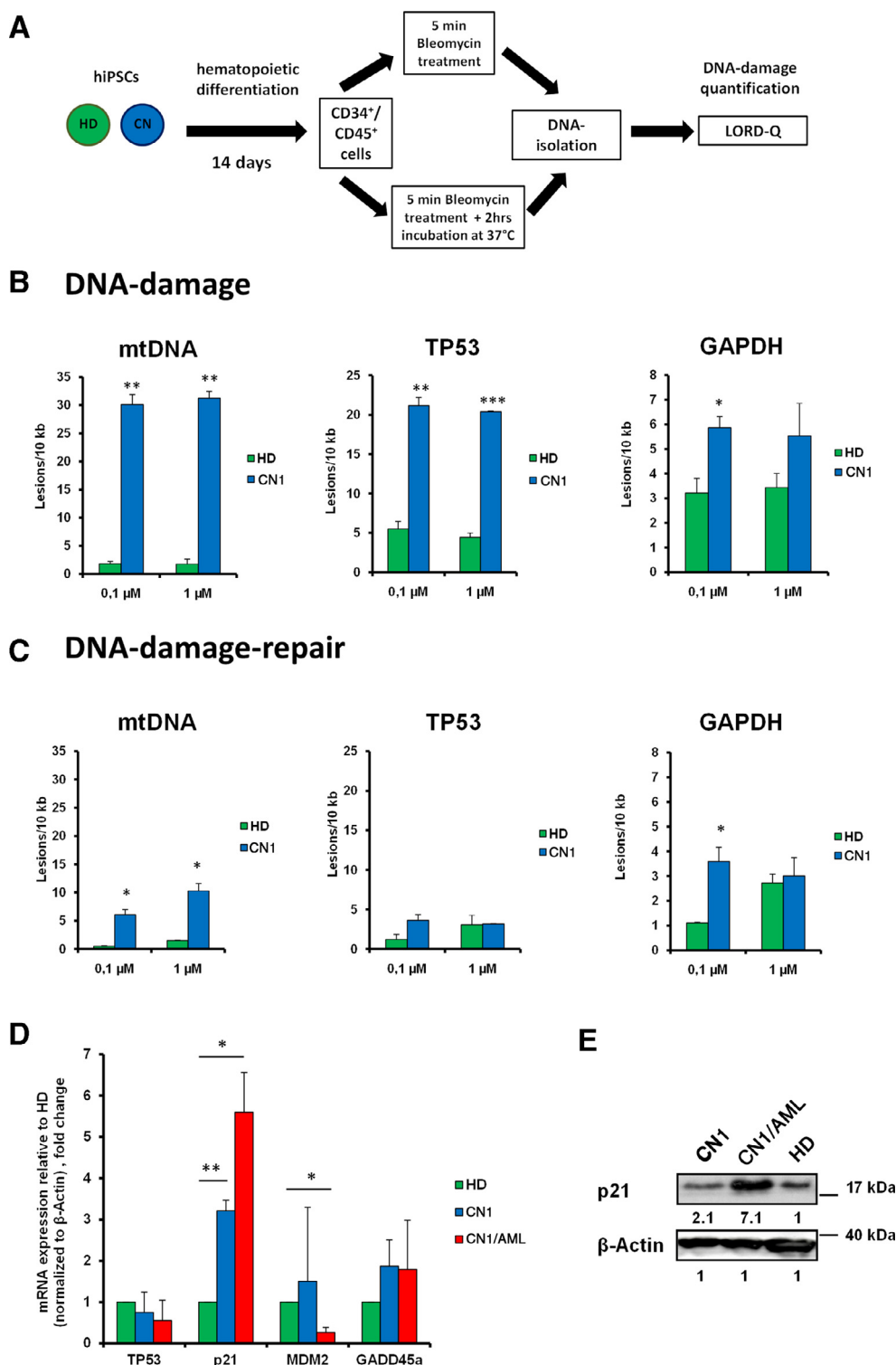


Figure 3. Quantification of DNA damage and p21 expression in CD34⁺ and CD45⁺ cells derived from patient-specific iPSCs. **(A)** Scheme for DNA damage measurements in HD- and CN-iPSCs derived CD34⁺CD45⁺ cells. **(B,C)** Measurement of DNA damage loci for mitochondrial DNA (mtDNA) and DNA of *TP53* or *GAPDH* gene loci of CN-iPSC-derived CD45⁺CD34⁺ cells upon 5-min treatment with 0.1 and 1 μmol/L bleomycin. DNA lesions were assessed directly 5 min (DNA damage **(B)**) and 2 hours (DNA repair **(C)**) after bleomycin treatment. Data are shown as means ± SD from two independent experiments. **p* < 0.05, ***p* < 0.01, ****p* < 0.001. **(D)** qRT-PCR analysis of selected genes in CD45⁺CD34⁺ cells generated from different iPSCs clones on day 14 of iPSC differentiation. mRNA expression of target genes was normalized to β-actin and shown relative to HD. Data represent means ± SD from two independent experiments. **p* < 0.05, ***p* < 0.01, ****p* < 0.001. **(E)** Representative Western blot images of p21 protein and β-actin expression in CD45⁺ cells at day 28 of iPSC differentiation. Numbers below the Western blot images indicate protein expression levels normalized to β-actin.

proper folding and intracellular localization of mutated NE is severely affected in myeloid cells of *ELANE*-CN patients. These defects ultimately lead to activation of the UPR and ER stress. We detected no activation of ATF6 and BiP in CN/AML cells compared with CN cells. These differences may be attributable to a dosage effect of mutated NE or additional coregulation of ATF4, but not ATF6, by mutated *RUNX1* and trisomy 21. Interestingly, elevated expression of ATF4 is associated with resistance to current chemotherapeutic drugs [33] and we detected hyperactivation of ATF4 in CN/AML cells. We have recently reported activation of different UPR pathways depending on the type of *ELANE* mutation [22]. Consistent with this, we demonstrate here that *ELANE* mutant p.C151Y induces expression of ATF4, ATF6, and CHOP, but not BiP. At the same time, p.G214R *ELANE* mutation caused upregulation of BiP, ATF4, and CHOP, but not ATF6. The impact of inherited CN-associated mutations (e.g., in *ELANE*) and UPR activation on leukemic progression is still unclear. It has been shown that induction of ER stress protects gastric cancer cells against apoptosis [34]. It is also known that activation of the UPR remodels the sensitivity of tumor cells to chemotherapeutic agents, making them more sensitive in some cases and more resistant in others [35]. Interestingly, upon ER stress, ATF4 is activated in mouse HSPCs, but not in more committed progenitors, leading to apoptosis of HSPCs [36]. Elevated levels of mutated NE, which we detected in CD45⁺ cells derived from CN-iPSCs and CN/AML-iPSCs, may further amplify the UPR, and additional signaling pathways (e.g., hyperactivated STAT5a [18] or mutated *RUNX1* [37]) may protect these cells from apoptosis, resulting in leukemogenic transformation of these cells. Because *ELANE* expression is regulated by *RUNX1* [38], it will be interesting to determine how missense *RUNX1* mutations affect *ELANE* expression. Cai et al. demonstrated an attenuated UPR in HSPCs from *Runx1*^{-/-} mice [39] and another study showed induction of UPR by trisomy 21 in immortalized lymphocytes and fibroblasts of Down syndrome patients [40]. The induction of UPR and ER stress in HSPCs of these patients has not yet been studied, but it is known that individuals with Down syndrome often develop AML.

We identified an increased susceptibility of CN CD34⁺ CD45⁺ cells to DNA damage, a finding consistent with the observed prolongation in DNA repair. Interestingly, ER stress suppresses DNA double-strand break repair in tumor cells [41]. Moreover, Nagelkerle et al. demonstrated that the UPR increases the resistance of tumor cells to therapeutic agents by regulating the DNA damage response [42]. In CN patients with inherited *ELANE* mutations, a permanent stress response caused by a chronically elevated UPR may cause genotoxic stress, increasing the susceptibility of HSPCs to secondary leukemia-causing events, although the

complete pathomechanism remains to be investigated. An evaluation of the expression levels of the main players in p53 signaling, a classical DNA damage response pathway, revealed strong upregulation of p21 mRNA levels, but not p53 mRNA expression, in CN and CN/AML CD34⁺ cells. p21 protein expression was also elevated in CD45⁺ cells of CN/AML patients compared with CN and HD-derived cells. The mechanism of p21 upregulation in CN and CN/AML cells remains to be investigated, but may be explained by increased p53 protein stability or diminished levels of the p53 ubiquitin E3 ligase MDM2. Another possibility is p53-independent activation of p21 expression. In this context, Galanos et al. reported p53-independent upregulation of p21 selectively in more aggressive tumor cells, which featured increased genomic instability, aggressiveness, and chemoresistance [43]. Unaffected expression of GADD45a, another p53 target, also argues for possibly inactive p53 and thus a p53-independent mechanism of p21 activation in CD34⁺ cells of CN patients. Less is known about UPR-mediated regulation of p21 expression. One study described inhibition of p21 expression by CHOP [44], but we found that both CHOP and p21 levels were elevated in CN and CN/AML CD34⁺ and CD45⁺ cells. It is known that accumulated cytoplasmic p21 exerts anti-apoptotic functions in AML cells [45,46] and high p21 levels are associated with chemoresistance in AML [47]. Elevated expression of p21 in preleukemic cells of CN patients may make these cells resistant to apoptosis, leading to an increase in their survival and an increased probability of their leukemogenic transformation. AML blasts of CN patients are resistant to conventional chemotherapy, so bone marrow transplantation is the only treatment option in these patients [1].

Taken together, our findings demonstrate that the iPSC-based model established here is a reliable in vitro model for studying defective signaling systems underlying impaired hematopoietic differentiation in patients with bone marrow failure syndromes (in our case, CN). This model may also be used for drug development or generation of isogenic iPSC lines using CRISPR/Cas9-mediated correction of inherited disease-causing mutations.

Acknowledgments

This work was supported by the Excellence Initiative of the Faculty of Medicine, University of Tuebingen (JS), the Jose Carreras Leukemia Foundation (JS, BD), Madeleine Schickedanz Kinderkrebsstiftung (JS, MK), the Deutsche Forschungsgemeinschaft (JS, MK), the Medical Faculty of the Tübingen University (intramural Fortüne funding to M.K.), the German–Israeli Foundation for Scientific Research and Development (KW, AZ, BD), the German Cancer Consortium (KS-O, JS, PM), and the Fritz Thyssen Foundation (B.D.).

Author contributions

JS and BD made initial observations, designed the experiments, and analyzed the data; BD performed the main experiments, generated, characterized, cultured, and differentiated human iPSCs, and performed FACS, qRT-PCRs, and WBs; BO differentiated iPSCs and performed FACS; PM conducted LORD-Q experiments; AZ with the help of NL and TM established iPSC generation and EB-based hematopoietic differentiation in the laboratory; RB assisted in iPSC culture and qRT-PCR; KS-O assisted with LORD-Q experiments and provided insightful comments; CZ and KW provided patient material; LK provided insightful comments; and KW and JS supervised and supported the study and wrote the manuscript (with the help of BD).

References

- Skokowa J, Dale DC, Touw IP, Zeidler C, Welte K. Severe congenital neutropenias. *Nat Rev Dis Primers*. 2017;3:17032.
- Skokowa J, Germeshausen M, Zeidler C, Welte K. Severe congenital neutropenia: inheritance and pathophysiology. *Curr Opin Hematol*. 2007;14:22–28.
- Dale DC, Person RE, Bolyard AA, et al. Mutations in the gene encoding neutrophil elastase in congenital and cyclic neutropenia. *Blood*. 2000;96:2317–2322.
- Klein C, Grudzien M, Appaswamy G, et al. HAX1 deficiency causes autosomal recessive severe congenital neutropenia (Kostmann disease). *Nat Genet*. 2007;39:86–92.
- Triot A, Järvinen PM, Arostegui JI, et al. Inherited biallelic CSF3R mutations in severe congenital neutropenia. *Blood*. 2014;123:3811–3817.
- Klimiankou M, Klimenkova O, Uenal M, et al. GM-CSF stimulates granulopoiesis in a congenital neutropenia patient with loss-of-function biallelic heterozygous CSF3R mutations. *Blood*. 2015;126:1865–1867.
- Boztug K, Järvinen PM, Salzer E, et al. JAGN1 deficiency causes aberrant myeloid cell homeostasis and congenital neutropenia. *Nat Genet*. 2014;46:1021–1027.
- Boztug K, Appaswamy G, Ashikov A, et al. A syndrome with congenital neutropenia and mutations in G6PC3. *N Engl J Med*. 2009;360:32–43.
- Makaryan V, Rosenthal EA, Bolyard AA, et al. UW Center for Mendelian Genomics. TCIRG1-associated congenital neutropenia. *Hum Mutat*. 2014;35:824–827.
- Makaryan V, Zeidler C, Bolyard AA, et al. The diversity of mutations and clinical outcomes for ELANE-associated neutropenia. *Curr Opin Hematol*. 2015;22:3–11.
- Welte K, Dale D. Pathophysiology and treatment of severe chronic neutropenia. *Ann Hematol*. 1996;72:158–165.
- Welte K, Zeidler C, Dale DC. Severe congenital neutropenia. *Semin Hematol*. 2006;43:189–195.
- Skokowa J, Cario G, Uenal M, et al. LEF-1 is crucial for neutrophil granulopoiesis and its expression is severely reduced in congenital neutropenia. *Nat Med*. 2006;12:1191–1197.
- Skokowa J, Welte K. LEF-1 is a decisive transcription factor in neutrophil granulopoiesis. *Ann N Y Acad Sci*. 2007;1106:143–151.
- Skokowa J, Welte K. Dysregulation of myeloid-specific transcription factors in congenital neutropenia. *Ann N Y Acad Sci*. 2009;1176:94–100.
- Skokowa J, Welte K. Defective G-CSFR signaling pathways in congenital neutropenia. *Hematol Oncol Clin North Am*. 2013;27:75–88. viii.
- Rauprich P, Kasper B, Tidow N, Welte K. The protein tyrosine kinase JAK2 is activated in neutrophils from patients with severe congenital neutropenia. *Blood*. 1995;86:4500–4505.
- Gupta K, Kuznetsova I, Klimenkova O, et al. Bortezomib inhibits STAT5-dependent degradation of LEF-1, inducing granulocytic differentiation in congenital neutropenia CD34(+) cells. *Blood*. 2014;123:2550–2561.
- Skokowa J, Lan D, Thakur BK, et al. NAMPT is essential for the G-CSF-induced myeloid differentiation via a NAD(+)-sirtuin-1-dependent pathway. *Nat Med*. 2009;15:151–158.
- Cario G, Skokowa J, Wang Z, et al. Heterogeneous expression pattern of pro- and anti-apoptotic factors in myeloid progenitor cells of patients with severe congenital neutropenia treated with granulocyte colony-stimulating factor. *Br J Haematol*. 2005;129:275–278.
- Klimenkova O, Ellerbeck W, Klimiankou M, et al. A lack of secretory leukocyte protease inhibitor (SLPI) causes defects in granulocytic differentiation. *Blood*. 2014;123(8):1239–1249.
- Nustede R, Klimiankou M, Klimenkova O, et al. ELANE mutant-specific activation of different UPR pathways in congenital neutropenia. *Br J Haematol*. 2016;172:219–227.
- Nanua S, Murakami M, Xia J, et al. Activation of the unfolded protein response is associated with impaired granulopoiesis in transgenic mice expressing mutant Elane. *Blood*. 2011;117:3539–3547.
- Grenda DS, Murakami M, Ghatak J, et al. Mutations of the ELA2 gene found in patients with severe congenital neutropenia induce the unfolded protein response and cellular apoptosis. *Blood*. 2007;110:4179–4187.
- Morishima T, Watanabe K, Niwa A, et al. Genetic correction of HAX1 in induced pluripotent stem cells from a patient with severe congenital neutropenia improves defective granulopoiesis. *Haematologica*. 2014;99:19–27.
- Nayak RC, Trump LR, Aronow BJ, et al. Pathogenesis of ELANE-mutant severe neutropenia revealed by induced pluripotent stem cells. *J Clin Invest*. 2015;125:3103–3116.
- Hiramoto T, Ebihara Y, Mizoguchi Y, et al. Wnt3a stimulates maturation of impaired neutrophils developed from severe congenital neutropenia patient-derived pluripotent stem cells. *Proc Natl Acad Sci U S A*. 2013;110:3023–3028.
- Pittermann E, Lachmann N, MacLean G, et al. Gene correction of HAX1 reversed Kostmann disease phenotype in patient-specific induced pluripotent stem cells. *Blood Adv*. 2017;1:903–914.
- Lehle S, Hildebrand DG, Merz B, et al. LORD-Q: a long-run real-time PCR-based DNA-damage quantification method for nuclear and mitochondrial genome analysis. *Nucleic Acids Res*. 2014;42:e41.
- Lachmann N, Ackermann M, Frenzel E, et al. Large-scale hematopoietic differentiation of human induced pluripotent stem cells provides granulocytes or macrophages for cell replacement therapies. *Stem Cell Reports*. 2015;4:282–296.
- Bonilla MA, Dale D, Zeidler C, et al. Long-term safety of treatment with recombinant human granulocyte colony-stimulating factor (r-metHuG-CSF) in patients with severe congenital neutropenias. *Br J Haematol*. 1994;88:723–730.
- Germeshausen M, Skokowa J, Ballmaier M, Zeidler C, Welte K. G-CSF receptor mutations in patients with congenital neutropenia. *Curr Opin Hematol*. 2008;15:332–337.
- Ye J, Koumenis C. ATF4, an ER stress and hypoxia-inducible transcription factor and its potential role in hypoxia tolerance and tumorigenesis. *Curr Mol Med*. 2009;9:411–416.
- Feng R, Zhai WL, Yang HY, Jin H, Zhang QX. Induction of ER stress protects gastric cancer cells against apoptosis induced by cisplatin and doxorubicin through activation of p38 MAPK. *Biochem Biophys Res Commun*. 2011;406:299–304.
- Mann MJ, Hendershot LM. UPR activation alters chemosensitivity of tumor cells. *Cancer Biol Ther*. 2006;5:736–740.

36. van Galen P, Kreso A, Mbong N, et al. The unfolded protein response governs integrity of the haematopoietic stem-cell pool during stress. *Nature*. 2014;510:268–272.
37. Skokowa J, Steinemann D, Katsman-Kuipers JE, et al. Cooperativity of RUNX1 and CSF3R mutations in severe congenital neutropenia: a unique pathway in myeloid leukemogenesis. *Blood*. 2014;123:2229–2237.
38. Lausen J, Liu S, Fliegauf M, Lübbert M, Werner MH. ELA2 is regulated by hematopoietic transcription factors, but not repressed by AML1-ETO. *Oncogene*. 2006;25:1349–1357.
39. Cai X, Gao L, Teng L, et al. Runx1 deficiency decreases ribosome biogenesis and confers stress resistance to hematopoietic stem and progenitor cells. *Cell Stem Cell*. 2015;17:165–177.
40. Aivazidis S, Coughlan CM, Rauniyar AK, et al. The burden of trisomy 21 disrupts the proteostasis network in Down syndrome. *PLoS One*. 2017;12:e0176307.
41. Yamamori T, Meike S, Nagane M, Yasui H, Inanami O. ER stress suppresses DNA double-strand break repair and sensitizes tumor cells to ionizing radiation by stimulating proteasomal degradation of Rad51. *FEBS Lett*. 2013;587:3348–3353.
42. Nagelkerke A, Bussink J, van der Kogel AJ, Sweep FC, Span PN. The PERK/ATF4/LAMP3-arm of the unfolded protein response affects radioresistance by interfering with the DNA damage response. *Radiother Oncol*. 2013;108:415–421.
43. Galanos P, Vougas K, Walter D, et al. Chronic p53-independent p21 expression causes genomic instability by deregulating replication licensing. *Nat Cell Biol*. 2016;18:777–789.
44. Mihailidou C, Papazian I, Papavassiliou AG, Kiaris H. CHOP-dependent regulation of p21/waf1 during ER stress. *Cell Physiol Biochem*. 2010;25:761–766.
45. Schepers H, Geugien M, Eggen BJ, Vellenga E. Constitutive cytoplasmic localization of p21(Waf1/Cip1) affects the apoptotic process in monocytic leukaemia. *Leukemia*. 2003;17:2113–2121.
46. Abbas T, Dutta A. p21 in cancer: intricate networks and multiple activities. *Nat Rev Cancer*. 2009;9:400–414.
47. Zhang W, Kornblau SM, Kobayashi T, Gambel A, Claxton D, Deisseroth AB. High levels of constitutive WAF1/Cip1 protein are associated with chemoresistance in acute myelogenous leukemia. *Clin Cancer Res*. 1995;1:1051–1057.

APPENDIX II: LIST OF SUBMITTED MANUSCRIPTS

Mir P. et *al.*, manuscript in revision.

Retinoic acid restores granulocytic differentiation in severe congenital neutropenia:

Role of GADD45 β -dependent gene demethylation

Running title: Reduced GADD45 β levels in congenital neutropenia

Perihan Mir^{1,2}, Maksim Klimiankou¹, Benjamin Dannenmann¹, Narges Aghaallaei¹, Masoud Nasri¹, Susanne Wingert³, Frederic B. Thalheimer³, Betuel Findik¹, Larissa Doll¹, Malte U. Ritter¹, Thomas Thumberger⁴, Sergei Kandabarau¹, Cornelia Zeidler⁶, Michael A. Rieger^{2,3,5}, Baubak Bajoghli¹, Karl Welte⁷, Julia Skokowa^{1,2*}

¹Department of Oncology, Hematology, Immunology, Rheumatology, University Hospital Tübingen, Tübingen, Germany; ²German Cancer Research Center (DKFZ), Heidelberg, Germany; ³Department of Medicine, Hematology/Oncology, Goethe University Frankfurt, Frankfurt am Main, Germany; ⁴Centre for Organismal Studies (COS), Heidelberg University, Heidelberg, Germany; ⁵Frankfurt Cancer Institute, Frankfurt am Main, Germany; ⁶Hematology / Oncology, SCNIR, Hannover Medical School, Hannover, Germany; ⁷The University Children's Hospital Tübingen, Tübingen, Germany

*Correspondence: Julia Skokowa, Division of Translational Oncology, Dept. of Hematology, Oncology, Clinical Immunology, Rheumatology and Pulmonology, University Hospital Tübingen, Otfried-Müller-Straße 10, Tübingen, 72076, Germany, e-mail: Julia.skokowa@med.uni-tuebingen.de

Abstract

In severe congenital neutropenia (CN) patients, elevated DNA damage in hematopoietic stem and progenitor cells (HSPCs) induces maturation arrest of granulopoiesis in the bone marrow. Here, we explored the mechanisms underlying the hypersensitivity of CN HSPCs to stress conditions. We detected markedly reduced expression of growth arrest and DNA-damage-inducible 45, beta (GADD45 β) in myeloid progenitors of G-CSF-treated CN patients compared to G-CSF-treated healthy individuals. Rescue of GADD45 β expression in CN HSPCs induced granulocytic differentiation. At the same time, CRISPR/Cas9-mediated GADD45 β knockout in HSPCs and iPSCs from healthy individuals, as well as in zebrafish embryos led to diminished granulocytic differentiation. GADD45 β is known to regulate active DNA demethylation, and we found that GADD45 β -dependent hypomethylation is essential for granulopoiesis and regulation of neutrophil functions via activation of retinoic acid signaling. Importantly, the treatment of CN HSPCs with retinoic acid receptor agonist, all-trans-retinoic acid (ATRA) restored diminished G-CSF-triggered granulocytic differentiation. Therefore, ATRA may be used for the treatment of patients with CN.

Introduction

Inherited mutations in *ELANE* (which encodes neutrophil elastase) or *HAXI* (which encodes HCLS1-associated protein X-1) cause intracellular stress responses in hematopoietic stem and progenitor cells (HSPCs) of patients with severe congenital neutropenia (CN)¹. Inappropriate activation and regulation of intrinsic stress due to inherited mutations may be a cause of the defective granulocytic differentiation of HSPCs in CN patients. Granulocyte colony-stimulating factor (G-CSF) normally induces granulocytic differentiation of HSPCs by triggering G-CSFR to activate intracellular signal transduction pathways. In CN patients, G-CSF fails to activate granulopoiesis at physiological concentrations; such patients require life-long daily treatment with very high pharmacological doses of G-CSF to maintain neutrophil numbers at a level sufficient to prevent severe infections¹. We have reported various deregulated G-CSFR signaling pathways in the HSPCs of CN patients, and propose that they may cause maturation arrest of granulopoiesis in the bone marrow²⁻¹². These alterations include the almost complete loss of LEF-1 and C/EBP α expression, diminished levels of HCLS1 and SLPI, and constitutive activation of phospho-STAT5A^{2,5,11,13}. Conversely, the G-CSF-induced activation of NAMPT/SIRT1-mediated granulopoiesis may be involved in the granulocytic maturation of CN HSPCs¹⁰. These observations suggest that the HSPCs of CN patients are continuously exposed to endo- and exogenous stress stimuli. The endogenous stress is caused by the inherited mutations and underlying signal transduction defects mentioned above, while the exogenous stress is due to life-long treatment with non-physiological doses of G-CSF. HSPCs of CN patients exhibit elevated endoplasmic reticulum (ER) stress and unfolded protein response (UPR), dysregulation of the inner mitochondrial membrane potential, and/or increased sensitivity to apoptosis due to inherited mutations in *ELANE* or *HAXI*^{6,11,14-19}. UPR and ER stress may induce DNA damage and genetic instability in HSPCs. It is known that HSPCs react to the abnormal stress activation by shifting of the differentiation program. For example, exposure of HSPCs to γ -irradiation is associated with

induction of lymphoid differentiation and inhibition of myeloid differentiation²⁰. Moreover, UPR governs the integrity of the HSC pool by depleting HSCs but not progenitors upon stress^{21,22}. An abnormal response of CN HSPCs to stress conditions, such as the persistent activation of DNA damage response pathways¹², may block granulocytic differentiation. One potential explanation for the abnormal response of CN HSPCs to stress and G-CSF is defective regulation of stress-induced factors.

Growth arrest and DNA damage-inducible 45, beta (GADD45 β), also called myeloid differentiation primary response 118 (MyD118), functions as a stress sensor in regulating the cell cycle, cell survival, and apoptosis in response to ER stress or DNA damage²³⁻²⁷. GADD45 β belongs to the evolutionarily conserved and highly homologous GADD45 protein family, along with GADD45 α and GADD45 γ ²⁸⁻³¹. The GADD45 proteins show some degree of redundancy, but also exhibit specific functions depending on the stimulus and cell type^{32,33}. Gadd45 β -deficient primary mouse embryonic fibroblasts (MEFs) proliferate slowly, accumulate increased levels of DNA damage, and exhibit signs of premature senescence^{27,34}. Gadd45 β is essential for stress-induced murine hematopoiesis, and myeloid differentiation is severely compromised in *Gadd45b* knockout mice^{27,34}. Upon TNF α activation, GADD45 β expression is induced via NF κ B³⁵. GADD45 β protects hematopoietic cells from UV-induced apoptosis by suppressing JNK signaling²⁷. We recently demonstrated that CRISPR/Cas9-mediated *GADD45B* knockout (KO) elevated the DNA damage induced by UV exposure of human HSPCs and iPSCs³⁶. GADD45 proteins have been shown to coordinate active DNA demethylation by recruiting deaminases and glycosylases to the promoter regions of target genes³⁷⁻⁴⁰. GADD45 proteins bind to a methylated promoter region proximal to an acetylated histone to recruit deaminases, which convert 5-methylcytosine to thymine to create a T:G mismatch. After that, a GADD45-recruited DNA glycosylase removes thymine from the T:G mismatch, and the thymine is replaced by an unmethylated cytosine⁴¹. Very little is known about the transcriptional programs that are regulated by the G-CSF-induced DNA

demethylation of HSPCs and during the granulocytic differentiation of HSPCs. Moreover, the regulation of hematopoiesis and granulopoiesis by GADD45 β -mediated active DNA demethylation has not yet been explored in detail.

In the present study, we examined the HSPC pool of CN patients and how stress-response regulation by GADD45 β -mediated active DNA demethylation contributes to the G-CSF-triggered granulocytic differentiation. We found that retinoic acid signaling is regulated by GADD45 β and stimulation of HSPCs with all-trans-retinoic acid (ATRA) restores defective granulocytic differentiation in CN patients.

Material and methods

Patients

Twenty-nine severe congenital neutropenia patients (19 *ELANE*-CN and 13 *HAXI*-CN patients) were used in the study. All studied CN patients were on G-CSF therapy and received G-CSF (daily dose ranged between 1.4 and 9.4 $\mu\text{g}/\text{kg}/\text{day}$) within the last 3-5 days before sampling. Bone marrow samples from patients were collected in association with an annual follow-up recommended by the Severe Chronic Neutropenia International Registry. Healthy control cells were obtained from healthy bone marrow donors. Study approval was obtained from the Ethical Review Board of the Medical Faculty, University of Tübingen. Informed written consent was obtained from all participants of this study.

CRISPR/Cas9-gRNA ribonucleoprotein (RNP) mediated *GADD45B* knockout

150 pmol of *GADD45B* CRISPR/Cas9 RNP (crRNA: GCTCGTGGCGTGCGACAACGCGG, cut site: chr19 [+2,476,389: -2,476,389], NM_015675.3:r.266, NP_056490.2:p.N11) was used for the nucleofection of 1×10^6 CD34⁺ cells or iPSCs. Nucleofection was performed with the Lonza 4D Nucleofector X using the P3 Primary Cell 4D-Nucleofector X kit (Lonza, #V4XP-3012) and program CA-137, according to the manufacturer's instructions. After nucleofection, cells were resuspended in pre-warmed culture medium. Tracking of Indels by Decomposition (TIDE) webtool⁴² and ICE webtool (Synthego) were used to estimate CRISPR/Cas9 editing efficiency.

Liquid culture differentiation of CD34⁺ cells

CD34⁺ cells (2×10^5 cells/ml) were incubated for 7 days in RPMI 1640 GlutaMAX supplemented with 10 % FBS, 1 % penicillin/streptomycin, 5 ng/ml SCF, 5 ng/ml IL-3, 5 ng/ml GM-CSF and 10 or 1 ng/ml G-CSF as previously described in Skokowa et al.¹⁰. Medium was exchanged every second day. On day 7, medium was changed to RPMI 1640 GlutaMAX supplemented with 10 % FBS, 1 % penicillin/streptomycin and 10 ng/ml or 1 ng/ml G-CSF. Medium was exchanged every second day until day 14. On day 14, cells were

analyzed by flow cytometry using following antibodies: mouse anti-human CD45 (Biolegend, #304036), mouse anti-human CD11b (BD, #557754), mouse anti-human CD15 (BD, #555402), mouse anti-human CD16 (BD, #561248) on FACSCanto II. ATRA was added to the differentiation medium in a concentration of 1 μ M and was refreshed during the medium exchange every second day.

Statistics

Statistical analysis was performed using a two-sided unpaired Student's t-test for the analysis of differences in mean values between groups. Statistical analysis of patient groups was performed using an unpaired nonparametric t-test (Mann-Whitney *U*).

Results

Elevated DNA damage levels and lymphopoiesis-biased hematopoietic differentiation of CN HSPCs

We first evaluated intrinsic stress levels in primary bone marrow hematopoietic cells of CN patients. We found that CD49f⁺ HSCs²¹ obtained from eight *ELANE*-CN and seven *HAXI*-CN patients exhibited elevated DNA damage, as assessed by γH2AX protein staining (**Figure 1A**). γH2AX may also mark proliferating cells, but since CN patients hematopoietic cells have cell cycle arrest at the G0-G1 stage, we assume, that using γH2AX staining, we measured DNA damage response.

Intrinsic stress and DNA damage may affect the hematopoietic differentiation of HSPCs, and failure of the control mechanisms may change the fate of HSPCs (e.g., via inappropriately biased differentiation)^{20,21}. We further compared the composition of bone marrow HSPCs obtained from G-CSF-treated CN patients (*ELANE*-CN n = 12, *HAXI*-CN n = 10) and healthy individuals treated (n = 5) or not (n = 7) with G-CSF. As expected, treatment of healthy individuals with G-CSF resulted in a shift towards myeloid differentiation; we observed a 5-fold increase of common myeloid progenitors (CMPs), a 3-fold increase of granulocyte-monocyte progenitors (GMPs), and a 10-fold decrease of multi-lymphoid progenitors (MLPs). In contrast, the hematopoietic differentiation of CN patients was substantially shifted from myeloid (5- and 10-fold decreases of CMPs for *ELANE*-CN and *HAXI*-CN, respectively) to lymphoid (more than 100-fold increases of MLPs for *ELANE*-CN and *HAXI*-CN) differentiation, and we detected reductions in the numbers of GMPs (3-fold for both *ELANE*-CN and *HAXI*-CN) (**Figure 1B**). These data suggest that the integrity control of HSPCs from CN patients has defects that may alter the response to G-CSF and ultimately lead to severe neutropenia.

Markedly diminished expression of the stress response protein, GADD45 β , in myeloid progenitor cells of CN patients

The DNA damage and stress response protein, Gadd45 β , is known to regulate stress-induced granulopoiesis in mice⁴³. GADD45 β is also expressed in human HSPCs with increasing levels during myeloid commitment and maximum expression in mature neutrophilic granulocytes, as judged by *Bloodspot* database⁴⁴ (**Supplemental Figure 1A**). We compared GADD45 β mRNA expression levels in bone marrow promyelocytes obtained from G-CSF-treated CN patients (n = 7), healthy controls treated (n = 2) or not (n = 3) with G-CSF for 3 days, and patients with metabolic neutropenia (n = 3) chronically treated with G-CSF. Interestingly, we found that G-CSF induced GADD45 β mRNA expression in CD33⁺ cells of healthy controls and patients with metabolic neutropenia, but not in those of CN patients (**Figure 1C**). Moreover, a DUOLINK assay revealed that nuclear GADD45 β protein was highly expressed in CD33⁺ cells of G-CSF-treated healthy controls, but it was almost entirely absent from the nuclei of promyelocytes from CN patients (**Figure 1D**). We did not detect any correlation between GADD45 β expression levels and response to G-CSF therapy in CN patients (data not shown).

Ectopic expression of GADD45 β in CD34⁺ cells of *ELANE*-CN patients restores diminished granulocytic differentiation

We tested whether restoration of the diminished GADD45 β expression in primary CD34⁺ HSPCs of CN patients would affect their granulocytic differentiation *in vitro*. We used a Venus⁺-lentiviral vector to overexpress the GADD45 β cDNA in CD34⁺ HSPCs obtained from two *ELANE*-CN patients, and differentiated the transduced cells towards neutrophils in liquid culture (**Figure 2A**). Transduction efficiency of control virus was around 60 % and of GADD45 β cDNA-containing virus around 10 %. Indeed, we detected dramatically elevated

amounts of CD11b⁺CD15⁺, CD11b⁺CD16⁺, and CD15⁺CD16⁺ cells within the Venus⁺CD45⁺ cell population of GADD45 β -transduced *ELANE*-CN CD34⁺ HSPCs, compared to control samples (**Figure 2B**). These data suggest that GADD45 β induces and supports granulocytic differentiation in CN CD34⁺ cells.

Gadd45 β promotes differentiation of mouse LT-HSCs

To evaluate the effects of GADD45 β overexpression on the *in vitro* myeloid differentiation of primary HSPCs, we transduced mouse long-term repopulating HSCs (LT-HSCs) with ectopic *Gadd45b* and differentiated the cells into myeloid lineage in liquid culture *in vitro* and analyzed differentiated cells at different time points by FACS. We found that HSCs transduced with Gadd45 β displayed accelerated and enhanced myeloid differentiation, as assessed by FACS: percentage of immature HSPCs rapidly decreased, while the number of granulocyte-monocyte progenitors (GMPs) and mature myeloid cells increased over time, as compared to control transduced cells (**Figure 2C,D**). Colony forming unit (CFU) assay and CFU re-plating assay revealed that HSCs expressing ectopic *Gadd45 β* have myeloid-biased colony forming potential and generate more mature cells with lower re-plating capacity in comparison to control virus expressing cells (**Figure 2E**).

GADD45 β KO inhibits the granulocytic differentiation of human hematopoietic cells

To study the impact of GADD45 β deficiency on the granulocytic differentiation of human HSPCs, we knocked out GADD45 β in human iPSCs and CD34⁺ HSPCs of healthy individuals using GADD45 β -specific CRISPR/Cas9-gRNA RNPs, and differentiated the gene-edited cells towards neutrophils *in vitro*. The editing efficiency of gene-modified CD34⁺ HSPCs was around 44-85% (**Supplemental Figure 2A-C and data not shown**). We found that GADD45 β knockout abrogated granulocytic differentiation in liquid culture, as assessed

by diminished percentages of CD11b⁺CD15⁺, CD11b⁺CD16⁺, and CD15⁺CD16⁺ cells in the CD45⁺ cell populations of GADD45 β -KO cells compared to wild type control cells (**Figure 3A**).

To study the role of complete GADD45 β knockout on granulocytic differentiation of human HSPCs *in vitro*, we tested granulocytic differentiation of pure GADD45 β knockout iPSC clones³⁶. In line with the observations from primary HSPCs, no CFU-G colonies were generated from GADD45 β ^{-/-} iPSC-derived CD34⁺ HSPCs, compared to healthy control iPSCs (**Figure 3B**). Moreover, during embryoid body (EB)-based hematopoietic differentiation, we observed increased amounts of immature cells on day 14 in culture and strongly diminished amounts of mature neutrophils on day 28 in culture for GADD45 β ^{-/-} iPSCs compared to healthy control iPSCs (**Figure 3C, Supplemental Figure 3A**). This was confirmed by morphological analysis of Wright-Giemsa-stained cytospin preparations of differentiated cells collected on days 21 and 28 of culture. We detected dramatically increased amounts of immature hematopoietic cells and far fewer mature neutrophils in the GADD45 β -deficient samples compared to healthy control iPSCs (**Figure 3D, E and Supplemental Figure 3B**). The presented data suggest an essential role for GADD45 β in granulopoiesis.

Zebrafish *gadd45bb* is required for neutrophil development

We next examined whether GADD45 β is required for *in vivo* granulopoiesis. We used zebrafish as an *in vivo* model system, because the mechanisms underlying hematopoiesis are evolutionarily conserved in vertebrates^{45,46}. Two orthologs of human GADD45 β , *gadd45ba* and *gadd45bb*, are present in the genome of zebrafish, but only the *gadd45bb* paralog is expressed in the embryonic hematopoietic site at 1 day post-fertilization (dpf, data not shown)⁴⁷. To test whether *gadd45bb* is required for granulopoiesis, we performed transient CRISPR/Cas9 targeting of the *gadd45bb* gene in the transgenic line, Tg(*mpo:gfp*), in which

expression of green fluorescent protein (GFP) is driven by the neutrophil-specific myeloperoxidase (*mpo*) promoter⁴⁸. Compared with non-injected siblings, *gadd45bb* crispants showed significantly fewer GFP⁺ cells in the caudal hematopoietic tissue (akin to the mammalian fetal liver) at 3 dpf (**Figure 4A**). In another set of experiment, injection of Cas9 alone did not change the neutrophil count in embryos (**Supplemental Figure 4A**). We next asked whether the reduced number of neutrophils caused by mutation of *gadd45bb* could be rescued by *csf3a* mis-expression. To test this, we used a heat-inducible system⁴⁹ to ectopically express *csf3a* in zebrafish embryos at 1 dpf. Consistent with a previous report⁵⁰, we found that ectopic expression of *csf3a* increased the number of *mpo*-expressing cells at the hematopoietic site of wild-type embryos (**Figure 4B**). When *csf3a* was induced in *gadd45bb* crispants, the number of *mpo*-expressing cells increased to a level comparable with that seen in the uninjected group (**Figure 4B**). Together, these results suggest that *gadd45bb* plays a crucial role in zebrafish granulopoiesis and *csf3a* compensates for the lack of *gadd45bb* in this process.

GADD45 β expression is directly regulated by C/EBP α

To investigate the mechanism underlying the G-CSF-mediated activation of GADD45 β expression, we performed *in silico* analysis of the GADD45 β gene promoter using Genomatix software. This analysis identified four putative binding sites for C/EBP transcription factors (**Figure 4C**). We previously reported that C/EBP α levels were markedly reduced in myeloid progenitor cells of CN patients^{2,7-9}. Therefore, we tested for possible C/EBP α -mediated regulation of GADD45 β expression that might be abolished in C/EBP α -deficient CN progenitors. We performed ChIP assays with an anti-C/EBP α antibody in lysates of THP1 cells expressing both C/EBP α and GADD45 β , and identified three C/EBP α binding sites on the GADD45 β gene promoter, located -655 bp, -214 bp, and -77 bp from the

ATG (**Figure 4C and Supplemental Figure 5A**). We further generated a reporter gene construct by cloning a GADD45 β promoter fragment (1.2 kb from the ATG) into the pGL4.10 [*luc2*] vector, and performed dual luciferase reporter gene assays in HEK293T cells co-transfected with the *C/EBPA* cDNA and a GADD45 β reporter construct. Indeed, we found that C/EBP α specifically and dose-dependently activated the GADD45 β promoter (**Figure 4D**).

In HSPCs, GADD45 β regulates mRNA expression programs that are essential for granulopoiesis and responsible for neutrophil activation

To identify intracellular signaling pathways regulated by GADD45 β in G-CSF treated human primary bone marrow HSPCs, we cultured WT or GADD45 β -KO CD34⁺ HSPCs obtained from three healthy donors for 72 hours with or without 50 ng/ml G-CSF, and performed RNA sequencing (**Figure 5A**). For GADD45 β KO, we electroporated cells with GADD45 β -specific CRISPR/Cas9-gRNA RNP complexes. The efficiency of GADD45 β KO was up to 84%, as assessed by Sanger sequencing and ICE assay (**Supplemental Figure 2A-C**). We found that 94 genes were differentially expressed between G-CSF-treated control and G-CSF-treated GADD45 β -KO cells (adjusted *p*-value < 0.05) (**Figure 5B, Supplemental Table 1**). Strikingly, most of the differentially expressed genes regulate myeloid differentiation (e.g., *RXRA*, *FGR*, *TFPI*, *HK3*, and *NLRP12*), are induced by DNA damage in G-CSF-treated cells (e.g., *BATF*), or are essential players in neutrophil adhesion, migration (*ITGAM*, *SIGLEC5*, *CX3CR1*, *CXCR1*, *FPR1*, *FPR2*, and *CORO1A*), and activation (*NCF2*, *MYL6*, and *NLRP12*). Previously published microarray data² indicate that GADD45 β -regulated genes were also up-regulated in bone marrow CD33⁺ myeloid progenitor cells of G-CSF-treated healthy individuals, but not in the same cell population of CN patients chronically treated with G-CSF (**Figure 5C**).

Using Genomatix pathway analysis of significantly upregulated genes in GADD45 β -WT and GADD45 β -KO groups treated with G-CSF, we identified response to cytokines, response to stress, regulation of intracellular signal transduction, regulation of ERK1/2 signaling, neutrophil activation, degranulation, and migration as being among the top significant biological processes differentially regulated by G-CSF via GADD45 β (**Figure 5D**). Analysis of associated signaling pathways revealed that integrin-, inflammatory-, CXCR1-, FPR1-, and SRC kinase signaling were upregulated by G-CSF via GADD45 β (**Figure 5E**). We also identified associations with various disease phenotypes, including leukocyte disorders, leukopenia, agranulocytosis, neutropenia, phagocyte bactericidal dysfunctions, and (importantly) AML/MDS (**Figure 5F**).

iRegulon analysis of the significantly enriched transcription factor binding motifs within significantly upregulated genes^{51,52} revealed that genes with hematopoietic- or myeloid-specific transcription factor binding motifs were strongly enriched in G-CSF-treated control CD34⁺ HSPCs compared to GADD45 β -deficient G-CSF-exposed samples. In particular, we identified enrichment of the binding motifs for RXRA/RARA, SPI1, and C/EBP β in G-CSF-treated control cells but not in the corresponding GADD45 β -KO samples (**Figure 5G, Supplemental Figure 6A**).

Together, these data clearly demonstrate that GADD45 β plays important roles in G-CSF-triggered granulocytic differentiation and the regulation of neutrophil functions.

GADD45 β -dependent active gene demethylation during G-CSF-triggered granulocytic differentiation of HSPCs

GADD45 proteins, including GADD45 β , regulate active DNA demethylation by promoting the coupling of deamination, glycosylation, and the recruitment of the DNA demethylation machinery to specific genomic loci^{37-40,53}. We therefore investigated whether

the G-CSF-triggered granulocytic differentiation of HSPCs requires active gene demethylation mediated by GADD45 β . We assessed methylation changes in control and GADD45 β -KO CD34⁺ HSPCs treated or not with G-CSF, using an Infinium MethylationEPIC array (Illumina, Inc.) and subsequent data analysis with the R packages, *minfi*, *limma*, and *DMRcate*⁵⁴⁻⁵⁷.

G-CSF treatment of control CD34⁺ HSPCs triggered robust changes of DNA methylation: we detected 13.516 hypomethylated and 6.236 hypermethylated CpGs (adjusted p -value < 0.05) (**Figure 6A, left part, Supplemental Table 2**). In contrast, GADD45 β KO markedly attenuated the G-CSF-induced demethylation: we detected only 8.440 hypomethylated and 4.674 hypermethylated CpGs (χ^2 test: $p = 0.0001$, **Figure 6A, right part**). We found that 5.704 CpGs and 628 were hypomethylated in G-CSF-treated WT and GADD45 β -KO cells, respectively (**Figure 6B**). In contrast, hypermethylation was seen for 2.878 sites in WT cells and 1.316 sites in GADD45 β -KO cells upon G-CSF treatment (**Figure 6B**). The highest number of differentially methylated CpGs among the studied groups can be assigned to open sea regions (χ^2 test: $p < 0.05$, **Figure 6C, left**). Gene-specific annotations of CpGs show that 5'UTR and 3'UTR are the preferential places for differentially methylated CpGs (χ^2 test: $p < 0.05$, **Figure 6C, right**).

Consistent with the gene expression changes discussed above, Genomatix analysis of methylation data revealed that GADD45 β and G-CSF significantly regulated various biological processes, including myeloid leukocyte differentiation, neutrophil activation, cell migration, and chemotaxis (**Supplemental Figure 7A**). G-CSF-dependent signaling pathways regulated by GADD45 β -mediated hypomethylation were identified, including hematopoietic cell kinase, SRC, CXCR1, G-CSFR, and RARA signaling (**Supplemental Figure 7B**). Again, diseases associated with defective G-CSF-triggered hypomethylation upon GADD45 β KO

were immune system diseases, AML, leukocyte disorders, leukopenia, pre-leukemia, and neutropenia (**Figure 6D**).

The top genes with differentially methylated regions (DMRs) were *RXRA*, *MEFV*, *FPR2*, *CSF3R*, and several genes encoding neutrophil granule proteins (e.g., *ELANE*, *MPO*, *AZU1*, and *CTPSG*) (**Figure 6E and Supplemental Figure 8A**).

Genomic locus overlap enrichment analysis⁵⁸ showed that the DMRs were associated with top-ranked datasets representing regions occupied by H3K9K14ac in ATRA-treated NB4 cells, the RARA binding sites in the PML-RAR α zinc-inducible cell line, UPR9, and SPI-associated regions (**Supplemental Table 3**).

Activation of the retinoic acid signaling by ATRA rescued defective granulocytic differentiation of CN HSPCs

We further evaluated whether the GADD45 β -mediated regulation of active DNA demethylation correlated with the mRNA expression differences that we observed between control and GADD45 β -KO cells treated with G-CSF. We selected genes that exhibited significantly reduced mRNA expression in G-CSF-treated GADD45 β -KO cells but not in G-CSF-exposed control samples, and assessed their association with differentially methylated CpGs. We found that G-CSF regulates the methylation and expression of genes essential for myeloid differentiation or neutrophil activation (e.g., *RXRA*, *MEFV*, *CXCR1*, *FPR2*, and *SERPINA1*) via GADD45 β (**Figure 7A**). Hypomethylated CpGs in these genes were located in regions with regulatory activity, such as the transcriptional start sites (TSS), first exon, and untranslated regions (UTRs). Genomatix analysis revealed that GADD45 β -deficient G-CSF-treated HSPCs exhibited dysregulation of biological processes and signal transduction cascades that regulate granulopoiesis and neutrophil functions, as well as those associated with disease entities, such as phagocyte bactericidal dysfunctions, neutropenia, leukocyte disorders, and myeloid leukemia (**Figure 7B,C, Supplemental Figure 9A**).

We identified the retinoic acid pathway as one of the top hits regulated by GADD45 β during G-CSF-triggered *in vitro* granulopoiesis (**Figures 4 and 5**). We, therefore, assumed that in the absence of GADD45 β activation in CN patients HSPCs, the retinoic acid pathway could not be induced leading to diminished granulocytic differentiation. We evaluated whether activation of the retinoic acid signaling by ATRA will bypass missing activation of GADD45 β downstream of G-CSF. We treated CN HSPCs with ATRA or DMSO during the *in vitro* liquid culture granulocytic differentiation. Strikingly, in all treated CN patient's HSPCs, (five CN patients: *ELANE*-CN n = 3 and *HAXI*-CN n = 2), we observed markedly improved granulocytic differentiation, as assessed by a drastic reduction of myeloblasts/promyelocytes and increase of neutrophils on cytopsin slides of cells assessed on day 14 of culture (**Figure 7D, E**).

These data strongly argue that both granulocytic differentiation and neutrophil functions are regulated by GADD45 β -mediated DNA demethylation upon G-CSF treatment of CD34⁺ cells via activation of retinoic acid signaling. Moreover, the treatment of CN HSPCs with ATRA rescued the GADD45 β deficiency and induced granulopoiesis.

Discussion

Granulopoiesis is a highly complex and coordinated process of differentiation of HSPCs into mature neutrophils. It is controlled by a network of regulatory mechanisms and factors, including transcription factors, epigenetic modifiers, receptors, cytokines, and protein kinases. In the present study, we demonstrated that GADD45 β plays an essential role in the G-CSF-triggered granulopoiesis. We were able to link diminished GADD45 β expression in HSPCs to CN, which is an inherited bone marrow failure syndrome with severe neutrophil differentiation defects. Rescue experiments in CN HSPCs confirmed that GADD45 β plays an important role in G-CSF-mediated granulopoiesis. Moreover, ectopic expression of Gadd45 β in murine HSPCs resulted in the elevated myelopoiesis. These data are in line with previous observations that neutrophils exhibit defects in their numbers and functions in *Gadd45 β ^{-/-}* mice under stress conditions^{27,34,43,59}. We herein observed elevated DNA damage in bone marrow HSPCs of G-CSF treated CN patients. We and others previously demonstrated that inherited CN-associated mutations deregulate intracellular signaling cascades^{1-11,60}. This may lead to replicative stress, DNA damage, and ultimately deregulated commitment of HSPCs resulting in defective granulopoiesis. GADD45 β expression is activated upon stress (e.g. DNA damage or cytokine exposure^{27,34,43}), regulating gene expression programs specific for granulopoiesis and neutrophil functions. In CN patients, in contrast, GADD45 β expression is not activated, and granulopoiesis is therefore not initiated.

Severe defects in the expression levels of the transcription factors, LEF-1 and C/EBP α , were previously described by our group in myeloid cells of CN patients harboring either *ELANE* or *HAXI* mutations and were suggested to explain the defective granulopoiesis seen in this disorder². LEF-1 binds to and activates the *C/EBPA* gene promoter under normal circumstances². We herein show that C/EBP α binds to and activates *GADD45B* promoter. Therefore, we hypothesized that GADD45 β is not activated in CN HSPCs due to the

downregulation of LEF-1 and C/EBP α . Since both investigated CN patient groups (with *ELANE* or *HAXI* mutations) showed defective GADD45 β expression upon G-CSF treatment, we assume that this results from common dysfunctional pathways downstream of the inherited mutations. The mechanism of GADD45 β deregulation in CN HSPCs downstream of e.g. UPR triggered by mutated *ELANE* or mitochondrial dysfunctions triggered by *HAXI* mutations remains to be investigated. We previously described compensatory G-CSF/NAMPT/SIRT1-mediated activation of C/EBP β -triggered granulopoiesis in CN patients in the absence of LEF-1 and C/EBP α ¹⁰. Based on these observations, we assume that G-CSF - C/EBP β - GADD45 β axis is not active in CN, and G-CSF induces granulopoiesis via NAMPT/SIRT1/C/EBP β pathway, that is GADD45 β independent. Future work will be needed to examine why C/EBP β cannot induce GADD45 β expression in CN HSPCs.

The GADD45 protein family consists of three members that have similar structures and partially redundant functions⁶¹. The expression levels of the other GADD45 proteins are not affected in CN (data not shown), but the presence of these proteins does not appear to compensate for the abrogation of GADD45 β . This might reflect that GADD45 β has tissue-specific functions and/or a specific affinity for particular stimuli, such as G-CSFR signaling. *Gadd45b*^{-/-} mice also have a neutropenic phenotype with markedly diminished stress-induced neutrophil functions^{27,34,43,59}. The role of GADD45 β in G-CSF triggered granulopoiesis appears to be evolutionarily important, given our observation that *gadd45bb*-deficient zebrafish also exhibit markedly reduced neutrophil numbers. Since *Elane*- or *Hax1*-KO mice do not develop neutropenia, we suggest that *gadd45bb*-KO zebrafish could be used as an experimental model to investigate neutropenia associated with these mutations.

The signal transduction pathways that are specifically regulated by GADD45 β in human HSCs have not yet been fully elucidated. NF κ B, p38, and MKK7 signaling have been described to be regulated by GADD45 β in mice^{27,34,43,59,62}. Our RNA-seq analysis

demonstrated that G-CSF induces e.g. *RXRA*, *ITGAM* (CD11b), *FPR1/2*, *MEFV*, *BATF*, and *FGR* in a GADD45 β dependent manner. Intriguingly, these factors were also upregulated in bone marrow myeloid progenitor cells from G-CSF-treated healthy donors, but not in those from CN patients. All these genes are key hematopoietic- and myeloid-lineage factors. For example, endogenous retinoic acid (RA) receptors are upregulated in mouse HSPCs upon G-CSF treatment⁶³ and RARA/RXRA signaling plays an important role during granulopoiesis^{64,65}. Vitamin A and D both require RARA/RXRA for proper intracellular signal transduction and, interestingly, our RNA seq and methylation analyses identified disease entities associated with neutropenia and other immunological bone marrow failure syndromes, as well as vitamin A or D deficiency among the diseases significantly correlated with GADD45 β deficiency.

GADD45 β regulates active DNA demethylation that involves the base excision repair^{38,66,67}. The GADD45 proteins remove 5-hydroxymethylcytosine (5HMC) and 5-methylcytosine (5MC) and act as a scaffold for recruited cytidine deaminases or DNA glycosylases^{39,40,68-70}. GADD45 proteins are also essential for targeting promoters for 5HMC/5MC removal through direct interactions with nuclear hormone receptors⁷¹ or hyperacetylated nucleosomes²⁵. We found here, that in GADD45 β -KO cells treated with G-CSF, the number of hypomethylated CpGs was markedly reduced, whereas much less alteration was seen for hypermethylated CpGs. Consistent with the profiles of differentially expressed genes, our analysis of DNA hypomethylated sites revealed an association with defects in myeloid cell differentiation, hematopoiesis, neutrophil activation, regulation of cell adhesion, chemotaxis, and phagocytosis in these cells. The G-CSFR, RARA/RXRA, vitamin D, and FPR1 signaling pathways were among top regulated pathways, and neutropenia was among the significant disease entities correlated with GADD45 β -dependent methylation changes in G-CSF-stimulated HSPCs. By comparing our RNA seq data with the observed DNA methylation changes, we were able to identify candidate factors whose expression

levels are regulated by GADD45 β -mediated active demethylation. These factors included *RXRA*, *MEFV*, *FPR2*, *CSF3R* and genes encoding the neutrophil granule proteins, NE, AZU1, MPO, and CTSG.

In addition, genomic locus overlap enrichment analysis showed that DMRs were associated with the top-ranked regions occupied by H3K9K14ac in ATRA-treated NB4 cells, RARA binding sites in the PML-RAR α zinc-inducible cell line, UPR9, and *SPII*/PU.1 binding sites. H3K9K14ac marks active inducible gene regulatory elements establishing a chromatin conformation that is compatible with transcription⁷². Martens et al.⁷³ demonstrated that ATRA treatment of acute promyelocytic leukemia (APL) cells strongly increases H3K9K14ac at PML-RARA/RXR target sites. The increased methylation observed in most DMRs upon GADD45 β KO might affect the induction of local DNA histone modifications, perhaps accounting for the deregulation of the myeloid differentiation program in GADD45 β -KO HSPCs.

Strikingly, to functionally validate our observations from the RNA-seq and methylation array analyses, we activated retinoic acid signaling in GADD45 β -deficient HSPCs of CN patients. Indeed, we could circumvent the induction of GADD45 β by treating CN HSPCs with ATRA to trigger granulopoiesis by activating retinoic acid signaling. ATRA is an FDA-approved drug for the treatment of human promyelocytic leukemia⁷⁴ and myelodysplastic syndrome⁷⁵ and could offer a potential therapy option for CN patients.

Gene expression and methylation changes detected in our patients were associated with pre-leukemia, MDS, and AML. Since CN is a pre-leukemic bone marrow syndrome, it would be interesting to investigate the role of diminished GADD45 β expression in leukemia development in CN. There is some controversy regarding the role of GADD45 β in tumorigenesis and leukemogenesis, with GADD45 proteins reportedly acting as tumor suppressors in some tumors (e.g., breast and prostate cancer), but as tumor-promoting factors in others (e.g., colorectal cancer)⁷⁶⁻⁸⁷. In leukemia, GADD45 β was reported to induce

apoptosis in AML³⁰, and GADD45 β deficiency was shown to accelerate BCR-ABL-driven chronic myeloid leukemia⁸⁸.

In summary, we herein show that GADD45 β plays essential roles in G-CSF-triggered granulopoiesis by regulating the active demethylation and expression of genes essential for these processes, including components of the retinoic acid signaling (**Figure 7E**). G-CSF activates GADD45 β expression via C/EBP α and since the myeloid cells of CN patients are deficient for C/EBP α , GADD45 β and downstream retinoic acid signaling are not activated leading to severe diminished granulocytic differentiation (**Figure 7E**). Strikingly, ATRA treatment rescues defective granulocytic differentiation of CN HSPCs. These data clearly demonstrate how investigations combining basic and translational science may lead to the identification of novel therapeutic opportunities. In our case, patients with severe congenital neutropenia, especially patients who do not respond to the standard G-CSF therapy may benefit from this scientific approach.

Figure legends

Figure 1. Diminished GADD45 β expression in line with elevated gH2AX levels in HSCs of CN patients may lead to “decision shift” from myeloid to lymphoid progenitors

A, Bone marrow mononuclear cells were stained for surface markers to detect human stem and progenitor cell subsets, gH2AX was included into the panel (healthy controls treated with G-CSF n = 4, *ELANE*-CN n = 8, *HAXI*-CN n = 7). The cell populations are as followed: multipotent progenitors (MPP), common myeloid progenitors (CMP), granulocyte-macrophage progenitors (GMP), multi-lymphoid progenitors (MLP) and B- and NK-cell progenitors (B/NK). Data represent means \pm SEM; analyzed using unpaired nonparametric t-test (Mann-Whitney *U*): *, $p < 0.05$. **B**, The composition of HSPCs was assessed by multicolor FACS panels (healthy controls (n = 7), healthy control + G-CSF (n = 5,) *ELANE*-CN (n = 12), *HAXI*-CN (n = 10). Data represent means \pm SEM; analyzed using unpaired nonparametric t-test (Mann-Whitney *U*): *, $p < 0.05$; **, $p < 0.01$; ***, $p < 0.001$; ns, not significant. **C**, GADD45 β expression was measured by qRT-PCR in CD33⁺ progenitors of healthy individuals (n = 3), healthy individuals treated with G-CSF (n = 2), patient with metabolic neutropenia (MN, n = 3) and congenital neutropenia patients (CN, n = 7). Data represent means \pm SEM from duplicates. **D**, GADD45 β protein expression was investigated by DUOLINK proximity ligation assay in healthy donor CD33⁺ cells treated with G-CSF and *ELANE*-CN patients CD33⁺ cells. Representative images are depicted.

Figure 2. Ectopic expression of GADD45 β rescues neutrophilic differentiation of CD34⁺ HSPCs of CN patients and accelerates granulopoiesis in mice

A, Schematic of the experimental procedure: CD34⁺ HSPCs of two *ELANE*-CN patients were expanded *in vitro*, transduced with lentivirus containing GADD45 β construct or a control virus with the fluorescent marker Venus and differentiated in liquid culture for 14 days. **B**, Neutrophilic surface marker expression was measured by FACS. Only Venus⁺CD45⁺ cell

fraction was considered for analysis. In both patients the ectopic GADD45 β expression led to the increased percentage of CD11b⁺CD15⁺, CD11b⁺CD16⁺ and CD15⁺CD16⁺ cells significantly. Data represent means \pm S.D.; *, $p < 0.05$; **, $p < 0.01$; ***, $p < 0.001$. **C,D**, Murine LT-HSCs were transduced with *Gadd45b*, differentiated for 8 days in liquid culture. **C**, Surface marker expression was evaluated at different time points of culture by FACS, as described in material and methods. Transduced cells were gated for immature HSPCs, GMP-like cells, mature neutrophils and macrophages, means \pm S.D. of 3 independent experiments; *, $p < 0.05$; **, $p < 0.01$. Representative FACS images of cells on day 8 of differentiation stained for granulocyte/monocyte surface markers CD11b and CD16/32 are depicted in **D**. **E**, CFU assay of mouse LT-HSCs transduced with either control or *Gadd45b* virus under permissive cytokine conditions, as described in material and methods. Colonies generated from transduced cells were counted, data represent means \pm S.D. of 3 independent experiments (left image). 2×10^4 cells isolated from CFUs were re-plated in the secondary CFUs, as described in material and methods ($n = 1$, right image).

Figure 3. Diminished *in vitro* granulocytic differentiation of HSPCs and iPSCs upon GADD45 β knockout

A, Bone marrow CD34⁺ HSPCs were nucleofected with *GADD45B*-specific CRISPR/Cas9-gRNA RNP. Granulocytic differentiation was evaluated in liquid culture differentiation for 14 days. Neutrophilic surface marker expression was assessed by FACS. **B-E**, Evaluation of granulocytic differentiation of GADD45 β -deficient iPSCs; **B**, CFU assay; **C**, EB-based myeloid differentiation; **D,E**, morphological assessment of differentiated iPSCs on day 28 of culture was conducted on Wright-Giemsa stained cytospin preparations (MB/ProM: Myeloblasts/Promyelocytes; Myelo/Meta: Myelocytes/Metamyelocytes; Band/Seg: Band/Segmented cells; MF: Macrophages); representative cytospin images (60 X magnification) of

three experiments are depicted in **E**. **A-E** show data from 3 experiments. Data represent means \pm S.D.; *, $p < 0.05$; **, $p < 0.01$; ***, $p < 0.001$.

Figure 4. Knockout of *gadd45bb* in zebrafish resulted in drastically low neutrophil numbers

A, Quantification of GFP⁺ neutrophils in uninjected controls and *gadd45bb* sgRNAs injected Tg(mpo:gfp) zebrafish embryos at 3 dpf. Each dot represents an individual embryo at 3 dpf (N). Data are mean \pm S.D., ****, $p < 0.0001$. Representative images are shown in the right panel. **B**, Number of mpo-expressing cells in the hematopoietic site of embryos in different experimental setups at 1 dpf is indicated. Each dot represents an individual embryo at 1 dpf (N). Data are mean \pm S.D., **** $p < 0.0001$, ** $p < 0.001$, n.s., not significant. Representative images are shown in the right panel. **C**, In silico promoter analysis of *GADD45B* promoter region by Genomatix with four predicted binding sites for C/EBP transcription factors. C/EBP α binding sites on *GADD45 β* promoter were analyzed by chromatin immunoprecipitation. C/EBP α binding was confirmed for binding site 1, 3 and 4. **D**, Binding of C/EBP α to promoter region (1.2 kb) of *GADD45 β* was assessed by dual luciferase reporter gene assay with different concentrations of C/EBP α -expressing construct, representative data from 3 experiments. Data represent means of 3 experiments \pm S.D.; *, $p < 0.05$; **, $p < 0.01$; ***, $p < 0.001$; ****, $p < 0.0001$.

Figure 5. CRISPR/Cas9-mediated knockout of *GADD45 β* in CD34⁺ HSPCs repressed G-CSF-triggered granulocytic differentiation program

A, Schematic of the experimental approach. **B**, Comparison between wild-type and *GADD45 β* -KO CD34⁺ HSPCs both treated with G-CSF revealed 94 significantly differentially expressed genes (adjusted p -value < 0.05), most of them having roles in myeloid differentiation (indicated with *). **C**, candidate genes of which the expression was regulated

similarly in current RNA seq data and in microarray experiments conducted and published previously on healthy individual and CN patient promyelocytes treated with G-CSF. **D-F**, Genomatix-based gene ontology analysis using a list of significantly upregulated genes in G-CSF treated GADD45 β WT HSPCs, in comparison to GADD45 β -KO HSPCs revealed top significantly enriched biological processes (**D**), signal transduction pathways (**E**) and disease entities (**F**) that are GADD45 β dependent. **G**, iRegulon transcription factor motif enrichment analysis using a list of significantly upregulated genes in G-CSF treated GADD45 β WT HSPCs, in comparison to GADD45 β -KO HSPCs, revealed enrichment of genes (Normalized Enrichment Score (NES) > 3.0 and Area Under the cumulative Recovery Curve (AUC) > 0.03) with myeloid-specific transcription motifs in control but not in knockout cells.

Figure 6. GADD45 β is essential for active DNA demethylation in response to G-CSF

A-F, DNA methylation of G-CSF-treated control or GADD45 β -KO cells was evaluated using methylation EPIC array and was analyzed using R packages *minfi* and *limma*. **A**, G-CSF treatment induced the hypomethylation of 13.516 CpGs and hypermethylation of 6.236 CpGs in control cells (left). In *GADD45B*-KO cells (right), G-CSF induced hypomethylation of 8.440 and hypermethylation of 4.674 CpGs. **B**, Venn diagram of hypo- or hypermethylated CpGs in indicated groups. **C**, Evaluation of the numbers of differentially methylated CpGs per gene region (left) revealed that top significant differentially methylated CpGs (adjusted p -value < 0.05) were located mainly in open sea and island regions of genes. N: upstream and S: downstream of CpG island, shore: 0-2 kb from island, shelf: 2-4 kb from island. Gene-oriented annotation of CpGs (CpG feature, right) revealed that the most significant differences preferentially located in intragenic regions, 5'UTR and 3'UTR. Significance was calculated with the χ^2 test: $p < 0.05$. **D**, Genomatix-based gene ontology analysis using a list of significantly differentially hypomethylated CpGs in G-CSF treated GADD45 β -WT HSPCs, in comparison to GADD45 β -KO HSPCs revealed top significantly enriched disease

entities that are GADD45 β dependent. **E**, Differentially methylated regions (DMRs) in top genes that are hypomethylated upon G-CSF but not in GADD45 β -KO cells are shown (*minfdr* <10⁻⁶).

Figure 7. Regulation of G-CSF-triggered granulopoiesis by GADD45 β -mediated gene demethylation

A, List of significant genes differentially expressed and methylated (adjusted *p*-value < 0.05) with differentially hypomethylated CpGs (adjusted *p*-value < 0.05) upon G-CSF treatment of healthy control HSPCs, as compared to GADD45 β -KO cells. For all genes, CpGs are located in essential gene regulatory regions. **B,C**, Genomatix-based gene ontology analysis using the list of genes from **A** revealed top significantly enriched biological processes (**B**) and diseases entities (**C**) that are GADD45 β dependent. **D, E**, Five CN patient HSPCs (*HAXI*-CN n =2 and *ELANE*-CN n = 3) were treated with either DMSO or ATRA during *in vitro* liquid culture granulocytic differentiation. Bar chart of the morphological analysis (**D**) and representative cytopsin images (**E**) of the cytopsin slides of cells derived on day 14 of culture are presented, MB/ProM: Myeloblasts/Promyelocytes; Band/Seg: Band/ Segmented cells, 60 X magnification. Data represent percentages of respective populations from five CN patients \pm S.D.; **, *p* < 0.01. **F**, Mechanism of “maturation arrest” of G-CSF-triggered granulopoiesis in CN patients via diminished GADD45 β -mediated regulation of granulopoiesis-activating genes, including components of the RA signaling. Treatment of cells with ATRA restored granulopoiesis in CN.

Acknowledgments

This work was supported by the J. Carreras Leukemia Foundation (J.S., P.M.), Madeleine Schickedanz Kinderkrebsstiftung (J.S., K.W., M.K.), DFG (J.S., M.K.), intramural Fortüne program of the Medical Faculty of the UKT (M.K., J.S.), GIF (K.W., B.D.), German Cancer Consortium (P.M., J.S., M.A.R.), Else Kröner-Fresenius Stiftung (M.K.), Fritz Thyssen Foundation (J.S.). We thank Hans-Georg Rammensee for the financial support of the RNA seq and methylation arrays; E. Trompouki (MPI of Immunobiology and Epigenetics, Freiburg) and P. Müller (Friedrich-Miescher Laboratory, Tübingen) for providing zebrafish wild-type TE strain and the Tg(*mpo:gfp*) fish; J. Wittbrodt (Centre for Organismal Studies, Heidelberg) for the support with CRISPR-Cas9 experiments in zebrafish. We thank K. Hähnel and R. Bernhard for the excellent technical support. We also thank A. Dick for support with zebrafish experiments; the microarray and high-throughput sequencing units of the DKFZ Genomics and Proteomics Core Facility for providing the Illumina Human Methylation EPIC array and mRNA sequencing services.

Author contributions

J.S. and K.W. made initial observations and supervised experimentation; J.S. and P.M. designed the experiments, analyzed the data and wrote the manuscript (with the assistance of M.K., B.B. and K.W.); P.M. and M.K. designed GADD45 β gRNA, P.M., M.K., S.K. and M.N. analyzed RNA seq and methylation array data; P.M. and M.N. performed CRISPR/Cas9-mediated GADD45 β knockout in iPSCs and primary HSPCs; B.D. performed differentiation of iPSCs; N.A., B.B., L.D. and P.M. performed zebrafish experiments; B.B. performed analysis and data summary of zebrafish experiments; T.T. made the *gadd45bb* CRISPR constructs; P.M. and B.F. performed CHIP and reporter gene assay; F.B.T., S.W. and M.A.R. generated Gadd45 β construct and performed *in vitro* differentiation of mouse HSCs; C.Z. and K.W. provided patients material; M.K. and M.U.R. assisted with the data analysis and provided insightful comments.

References

1. Skokowa, J., Dale, D.C., Touw, I.P., Zeidler, C. & Welte, K. Severe congenital neutropenias. *Nature reviews. Disease primers* **3**, 17032 (2017).
2. Skokowa, J., et al. LEF-1 is crucial for neutrophil granulocytopoiesis and its expression is severely reduced in congenital neutropenia. *Nat Med* **12**, 1191-1197 (2006).
3. Cario, G., et al. Heterogeneous expression pattern of pro- and anti-apoptotic factors in myeloid progenitor cells of patients with severe congenital neutropenia treated with granulocyte colony-stimulating factor. *Br J Haematol* **129**, 275-278 (2005).
4. Gupta, K., et al. Bortezomib inhibits STAT5-dependent degradation of LEF-1, inducing granulocytic differentiation in congenital neutropenia CD34(+) cells. *Blood* **123**, 2550-2561 (2014).
5. Klimentkova, O., et al. A lack of secretory leukocyte protease inhibitor (SLPI) causes defects in granulocytic differentiation. *Blood* **123**, 1239-1249 (2014).
6. Nustede, R., et al. ELANE mutant-specific activation of different UPR pathways in congenital neutropenia. *Br J Haematol* **172**, 219-227 (2016).
7. Skokowa, J. & Welte, K. Dysregulation of myeloid-specific transcription factors in congenital neutropenia. *Ann N Y Acad Sci* **1176**, 94-100 (2009).
8. Skokowa, J. & Welte, K. Defective G-CSFR signaling pathways in congenital neutropenia. *Hematol Oncol Clin North Am* **27**, 75-88, viii (2013).
9. Skokowa, J. & Welte, K. LEF-1 is a decisive transcription factor in neutrophil granulopoiesis. *Ann N Y Acad Sci* **1106**, 143-151 (2007).
10. Skokowa, J., et al. NAMPT is essential for the G-CSF-induced myeloid differentiation via a NAD(+)-sirtuin-1-dependent pathway. *Nat Med* **15**, 151-158 (2009).
11. Skokowa, J., et al. Interactions among HCLS1, HAX1 and LEF-1 proteins are essential for G-CSF-triggered granulopoiesis. *Nat Med* **18**, 1550-1559 (2012).
12. Dannenmann, B., et al. Human iPSC-based model of severe congenital neutropenia reveals elevated UPR and DNA damage in CD34(+) cells preceding leukemic transformation. *Exp Hematol* **71**, 51-60 (2019).
13. Gupta, K., et al. Bortezomib inhibits STAT5-dependent degradation of LEF-1, inducing granulocytic differentiation in congenital neutropenia CD34+ cells. *Blood* **123**, 2550-2561 (2014).
14. Kollner, I., et al. Mutations in neutrophil elastase causing congenital neutropenia lead to cytoplasmic protein accumulation and induction of the unfolded protein response. *Blood* **108**, 493-500 (2006).
15. Grenda, D.S., et al. Mutations of the ELA2 gene found in patients with severe congenital neutropenia induce the unfolded protein response and cellular apoptosis. *Blood* **110**, 4179-4187 (2007).
16. Nanua, S., et al. Activation of the unfolded protein response is associated with impaired granulopoiesis in transgenic mice expressing mutant Elane. *Blood* **117**, 3539-3547 (2011).
17. Nayak, R.C., et al. Pathogenesis of ELANE-mutant severe neutropenia revealed by induced pluripotent stem cells. *J Clin Invest* **125**, 3103-3116 (2015).
18. Xia, J. & Link, D.C. Severe congenital neutropenia and the unfolded protein response. *Curr Opin Hematol* **15**, 1-7 (2008).
19. Klein, C., et al. HAX1 deficiency causes autosomal recessive severe congenital neutropenia (Kostmann disease). *Nat Genet* **39**, 86-92 (2007).
20. Wang, J., et al. A differentiation checkpoint limits hematopoietic stem cell self-renewal in response to DNA damage. *Cell* **148**, 1001-1014 (2012).
21. van Galen, P., et al. The unfolded protein response governs integrity of the haematopoietic stem-cell pool during stress. *Nature* **510**, 268-272 (2014).
22. Matatall, K.A., et al. Chronic Infection Depletes Hematopoietic Stem Cells through Stress-Induced Terminal Differentiation. *Cell Rep* **17**, 2584-2595 (2016).
23. Wang, X.W., et al. GADD45 induction of a G2/M cell cycle checkpoint. *Proc Natl Acad Sci U S A* **96**, 3706-3711 (1999).

24. Vairapandi, M., Balliet, A.G., Hoffman, B. & Liebermann, D.A. GADD45b and GADD45g are cdc2/cyclinB1 kinase inhibitors with a role in S and G2/M cell cycle checkpoints induced by genotoxic stress. *J Cell Physiol* **192**, 327-338 (2002).
25. Carrier, F., *et al.* Gadd45, a p53-responsive stress protein, modifies DNA accessibility on damaged chromatin. *Mol Cell Biol* **19**, 1673-1685 (1999).
26. Hollander, M.C., *et al.* Genomic instability in Gadd45a-deficient mice. *Nat Genet* **23**, 176-184 (1999).
27. Gupta, M., *et al.* Hematopoietic cells from Gadd45a- and Gadd45b-deficient mice are sensitized to genotoxic-stress-induced apoptosis. *Oncogene* **24**, 7170-7179 (2005).
28. Liebermann, D.A. & Hoffman, B. Gadd45 in stress signaling. *J Mol Signal* **3**, 15 (2008).
29. Magimaidas, A., *et al.* Gadd45b deficiency promotes premature senescence and skin aging. *Oncotarget* **7**, 26935-26948 (2016).
30. Selvakumaran, M., *et al.* The novel primary response gene MyD118 and the proto-oncogenes myb, myc, and bcl-2 modulate transforming growth factor beta 1-induced apoptosis of myeloid leukemia cells. *Mol Cell Biol* **14**, 2352-2360 (1994).
31. Zhan, Q., *et al.* The gadd and MyD genes define a novel set of mammalian genes encoding acidic proteins that synergistically suppress cell growth. *Mol Cell Biol* **14**, 2361-2371 (1994).
32. Wingert, S., *et al.* DNA-damage response gene GADD45A induces differentiation in hematopoietic stem cells without inhibiting cell cycle or survival. *Stem Cells* **34**, 699-710 (2016).
33. Thalheimer, F.B., *et al.* Cytokine-regulated GADD45G induces differentiation and lineage selection in hematopoietic stem cells. *Stem Cell Reports* **3**, 34-43 (2014).
34. Gupta, M., Gupta, S.K., Hoffman, B. & Liebermann, D.A. Gadd45a and Gadd45b protect hematopoietic cells from UV-induced apoptosis via distinct signaling pathways, including p38 activation and JNK inhibition. *J Biol Chem* **281**, 17552-17558 (2006).
35. De Smaele, E., *et al.* Induction of gadd45beta by NF-kappaB downregulates pro-apoptotic JNK signalling. *Nature* **414**, 308-313 (2001).
36. Nasri, M., *et al.* Fluorescent labeling of CRISPR/Cas9 RNP for gene knockout in HSPCs and iPSCs reveals an essential role for GADD45b in stress response. *Blood advances* **3**, 63-71 (2019).
37. Ma, D.K., *et al.* Neuronal activity-induced Gadd45b promotes epigenetic DNA demethylation and adult neurogenesis. *Science* **323**, 1074-1077 (2009).
38. Gavin, D.P., *et al.* Growth arrest and DNA-damage-inducible, beta (GADD45b)-mediated DNA demethylation in major psychosis. *Neuropsychopharmacology* **37**, 531-542 (2012).
39. Rai, K., *et al.* DNA demethylation in zebrafish involves the coupling of a deaminase, a glycosylase, and gadd45. *Cell* **135**, 1201-1212 (2008).
40. Cortellino, S., *et al.* Thymine DNA glycosylase is essential for active DNA demethylation by linked deamination-base excision repair. *Cell* **146**, 67-79 (2011).
41. Guidotti, A., *et al.* Epigenetic GABAergic targets in schizophrenia and bipolar disorder. *Neuropharmacology* **60**, 1007-1016 (2011).
42. Brinkman, E.K., Chen, T., Amendola, M. & van Steensel, B. Easy quantitative assessment of genome editing by sequence trace decomposition. *Nucleic Acids Res* **42**, e168 (2014).
43. Gupta, S.K., Gupta, M., Hoffman, B. & Liebermann, D.A. Hematopoietic cells from gadd45a-deficient and gadd45b-deficient mice exhibit impaired stress responses to acute stimulation with cytokines, myeloablation and inflammation. *Oncogene* **25**, 5537-5546 (2006).
44. Bagger, F.O., Kinalis, S. & Rapin, N. BloodSpot: a database of healthy and malignant haematopoiesis updated with purified and single cell mRNA sequencing profiles. *Nucleic Acids Res* **47**, D881-D885 (2019).

45. Robertson, A.L., Avagyan, S., Gansner, J.M. & Zon, L.I. Understanding the regulation of vertebrate hematopoiesis and blood disorders - big lessons from a small fish. *FEBS Lett* **590**, 4016-4033 (2016).
46. de Pater, E. & Trompouki, E. Bloody Zebrafish: Novel Methods in Normal and Malignant Hematopoiesis. *Frontiers in cell and developmental biology* **6**, 124 (2018).
47. Kawahara, A., Che, Y.S., Hanaoka, R., Takeda, H. & Dawid, I.B. Zebrafish GADD45beta genes are involved in somite segmentation. *Proc Natl Acad Sci U S A* **102**, 361-366 (2005).
48. Renshaw, S.A., *et al.* A transgenic zebrafish model of neutrophilic inflammation. *Blood* **108**, 3976-3978 (2006).
49. Bajoghli, B., Aghaallaei, N., Heimbucher, T. & Czerny, T. An artificial promoter construct for heat-inducible misexpression during fish embryogenesis. *Dev Biol* **271**, 416-430 (2004).
50. Stachura, D.L., *et al.* The zebrafish granulocyte colony-stimulating factors (Gcsfs): 2 paralogous cytokines and their roles in hematopoietic development and maintenance. *Blood* **122**, 3918-3928 (2013).
51. Janky, R., *et al.* iRegulon: from a gene list to a gene regulatory network using large motif and track collections. *PLoS Comput Biol* **10**, e1003731 (2014).
52. Verfaillie, A., Imrichova, H., Janky, R. & Aerts, S. iRegulon and i-cisTarget: Reconstructing Regulatory Networks Using Motif and Track Enrichment. *Curr Protoc Bioinformatics* **52**, 2 16 11-39 (2015).
53. Labonte, B., *et al.* Gadd45b mediates depressive-like role through DNA demethylation. *Sci Rep* **9**, 4615 (2019).
54. Peters, T.J., *et al.* De novo identification of differentially methylated regions in the human genome. *Epigenetics Chromatin* **8**, 6 (2015).
55. Aryee, M.J., *et al.* Minfi: a flexible and comprehensive Bioconductor package for the analysis of Infinium DNA methylation microarrays. *Bioinformatics* **30**, 1363-1369 (2014).
56. Fortin, J.P., Triche, T.J., Jr. & Hansen, K.D. Preprocessing, normalization and integration of the Illumina HumanMethylationEPIC array with minfi. *Bioinformatics* **33**, 558-560 (2017).
57. Ritchie, M.E., *et al.* limma powers differential expression analyses for RNA-sequencing and microarray studies. *Nucleic Acids Res* **43**, e47 (2015).
58. Sheffield, N.C. & Bock, C. LOLA: enrichment analysis for genomic region sets and regulatory elements in R and Bioconductor. *Bioinformatics* **32**, 587-589 (2016).
59. Salerno, D.M., Tront, J.S., Hoffman, B. & Liebermann, D.A. Gadd45a and Gadd45b modulate innate immune functions of granulocytes and macrophages by differential regulation of p38 and JNK signaling. *Journal of cellular physiology* **227**, 3613-3620 (2012).
60. Koch, C., *et al.* GM-CSF treatment is not effective in congenital neutropenia patients due to its inability to activate NAMPT signaling. *Ann Hematol* **96**, 345-353 (2017).
61. Moskalev, A.A., *et al.* Gadd45 proteins: relevance to aging, longevity and age-related pathologies. *Ageing Res Rev* **11**, 51-66 (2012).
62. Papa, S., *et al.* Gadd45 beta mediates the NF-kappa B suppression of JNK signalling by targeting MKK7/JNK2. *Nature cell biology* **6**, 146-153 (2004).
63. Niu, H., *et al.* Endogenous retinoid X receptor ligands in mouse hematopoietic cells. *Science signaling* **10**(2017).
64. Johnson, B.S., *et al.* Retinoid X receptor (RXR) agonist-induced activation of dominant-negative RXR-retinoic acid receptor alpha403 heterodimers is developmentally regulated during myeloid differentiation. *Mol Cell Biol* **19**, 3372-3382 (1999).
65. Lawson, N.D. & Berliner, N. Neutrophil maturation and the role of retinoic acid. *Exp Hematol* **27**, 1355-1367 (1999).
66. Gavin, D.P., *et al.* Gadd45b and N-methyl-D-aspartate induced DNA demethylation in postmitotic neurons. *Epigenomics* **7**, 567-579 (2015).

67. Grassi, D., *et al.* Neuronal Activity, TGFbeta-Signaling and Unpredictable Chronic Stress Modulate Transcription of Gadd45 Family Members and DNA Methylation in the Hippocampus. *Cereb Cortex* **27**, 4166-4181 (2017).
68. Guo, J.U., Su, Y., Zhong, C., Ming, G.L. & Song, H. Hydroxylation of 5-methylcytosine by TET1 promotes active DNA demethylation in the adult brain. *Cell* **145**, 423-434 (2011).
69. Morgan, H.D., Dean, W., Coker, H.A., Reik, W. & Petersen-Mahrt, S.K. Activation-induced cytidine deaminase deaminates 5-methylcytosine in DNA and is expressed in pluripotent tissues: implications for epigenetic reprogramming. *J Biol Chem* **279**, 52353-52360 (2004).
70. Spruijt, C.G., *et al.* Dynamic readers for 5-(hydroxy)methylcytosine and its oxidized derivatives. *Cell* **152**, 1146-1159 (2013).
71. Yi, Y.W., *et al.* Gadd45 family proteins are coactivators of nuclear hormone receptors. *Biochemical and biophysical research communications* **272**, 193-198 (2000).
72. Karmodiya, K., Krebs, A.R., Oulad-Abdelghani, M., Kimura, H. & Tora, L. H3K9 and H3K14 acetylation co-occur at many gene regulatory elements, while H3K14ac marks a subset of inactive inducible promoters in mouse embryonic stem cells. *BMC Genomics* **13**, 424 (2012).
73. Martens, J.H., *et al.* PML-RARalpha/RXR Alters the Epigenetic Landscape in Acute Promyelocytic Leukemia. *Cancer Cell* **17**, 173-185 (2010).
74. Huang, M.E., *et al.* Use of all-trans retinoic acid in the treatment of acute promyelocytic leukemia. *Blood* **72**, 567-572 (1988).
75. Baldus, M., Walter, H., Moller, M., Schurfeld, C. & Brass, H. All-Trans-Retinoic Acid (Atra) in the Treatment of Myelodysplastic-Syndromes - Results in 5 Cases. *Onkologie* **17**, 515-520 (1994).
76. Tront, J.S., Hoffman, B. & Liebermann, D.A. Gadd45a suppresses Ras-driven mammary tumorigenesis by activation of c-Jun NH2-terminal kinase and p38 stress signaling resulting in apoptosis and senescence. *Cancer Res* **66**, 8448-8454 (2006).
77. Tront, J.S., Huang, Y., Fornace, A.J., Jr., Hoffman, B. & Liebermann, D.A. Gadd45a functions as a promoter or suppressor of breast cancer dependent on the oncogenic stress. *Cancer Res* **70**, 9671-9681 (2010).
78. Tront, J.S., Willis, A., Huang, Y., Hoffman, B. & Liebermann, D.A. Gadd45a levels in human breast cancer are hormone receptor dependent. *J Transl Med* **11**, 131 (2013).
79. Wang, W., *et al.* Analysis of methylation-sensitive transcriptome identifies GADD45a as a frequently methylated gene in breast cancer. *Oncogene* **24**, 2705-2714 (2005).
80. Yamasawa, K., Nio, Y., Dong, M., Yamaguchi, K. & Itakura, M. Clinicopathological significance of abnormalities in Gadd45 expression and its relationship to p53 in human pancreatic cancer. *Clin Cancer Res* **8**, 2563-2569 (2002).
81. Ying, J., *et al.* The stress-responsive gene GADD45G is a functional tumor suppressor, with its response to environmental stresses frequently disrupted epigenetically in multiple tumors. *Clin Cancer Res* **11**, 6442-6449 (2005).
82. Zerbini, L.F., *et al.* JunD-mediated repression of GADD45alpha and gamma regulates escape from cell death in prostate cancer. *Cell Cycle* **10**, 2583-2591 (2011).
83. Ramachandran, K., *et al.* Methylation-mediated repression of GADD45alpha in prostate cancer and its role as a potential therapeutic target. *Cancer Res* **69**, 1527-1535 (2009).
84. Michaelis, K.A., *et al.* Identification of growth arrest and DNA-damage-inducible gene beta (GADD45beta) as a novel tumor suppressor in pituitary gonadotrope tumors. *Endocrinology* **152**, 3603-3613 (2011).
85. Na, Y.K., *et al.* Hypermethylation of growth arrest DNA-damage-inducible gene 45 in non-small cell lung cancer and its relationship with clinicopathologic features. *Mol Cells* **30**, 89-92 (2010).
86. Li, Y., *et al.* Adenoviral-mediated gene transfer of Gadd45a results in suppression by inducing apoptosis and cell cycle arrest in pancreatic cancer cell. *J Gene Med* **11**, 3-13 (2009).

87. Zhao, Z., *et al.* GADD45B as a Prognostic and Predictive Biomarker in Stage II Colorectal Cancer. *Genes* **9**(2018).
88. Sha, X., Hoffman, B. & Liebermann, D.A. Loss of Gadd45b accelerates BCR-ABL-driven CML. *Oncotarget* **9**, 33360-33367 (2018).

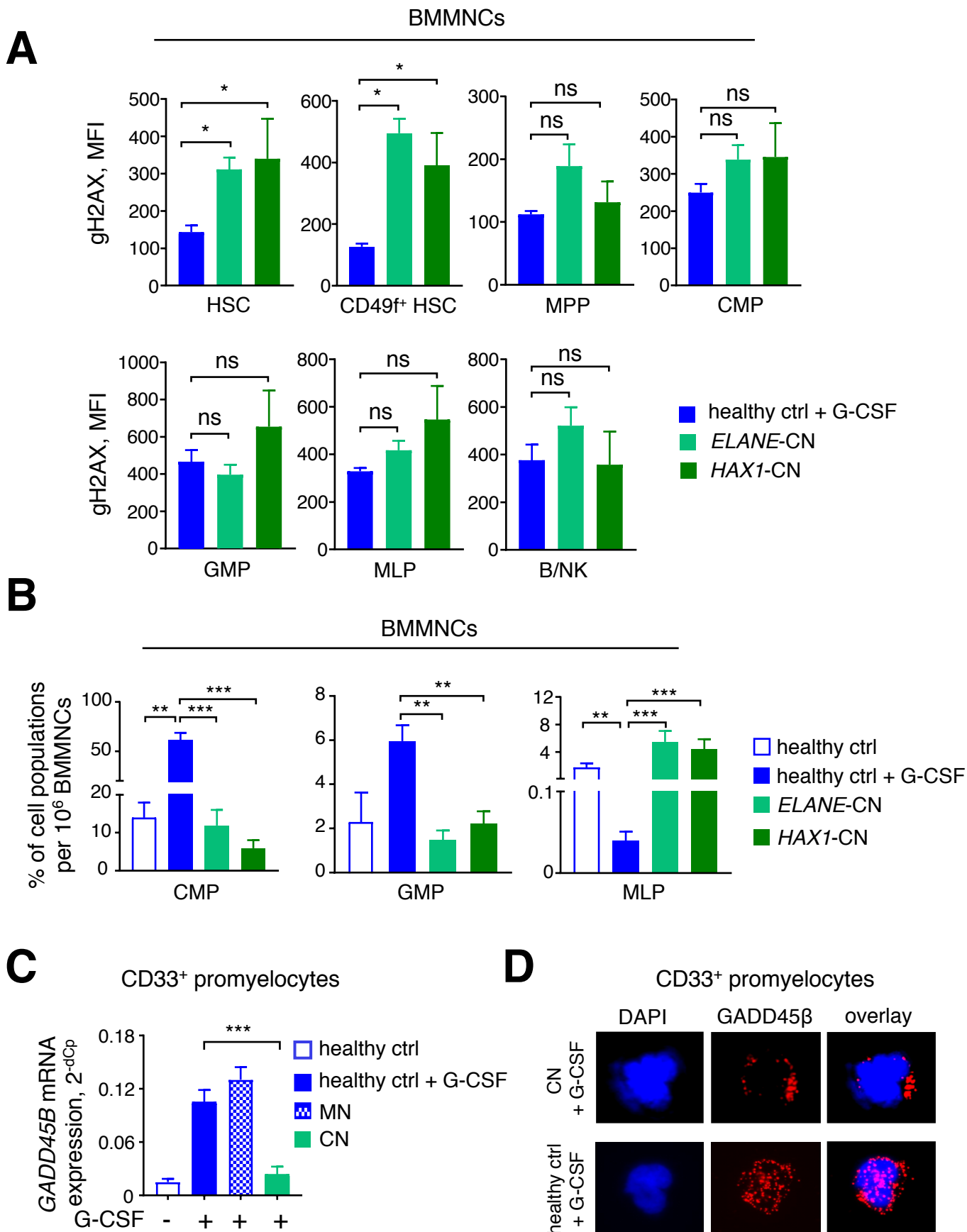
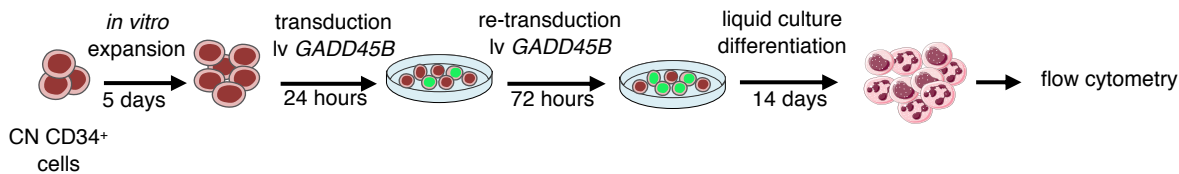
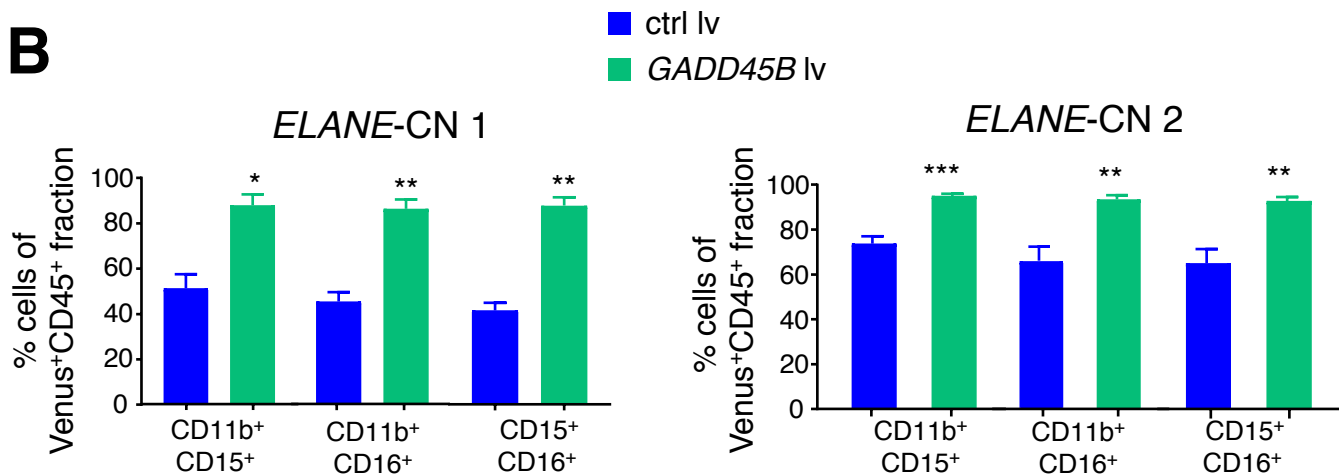
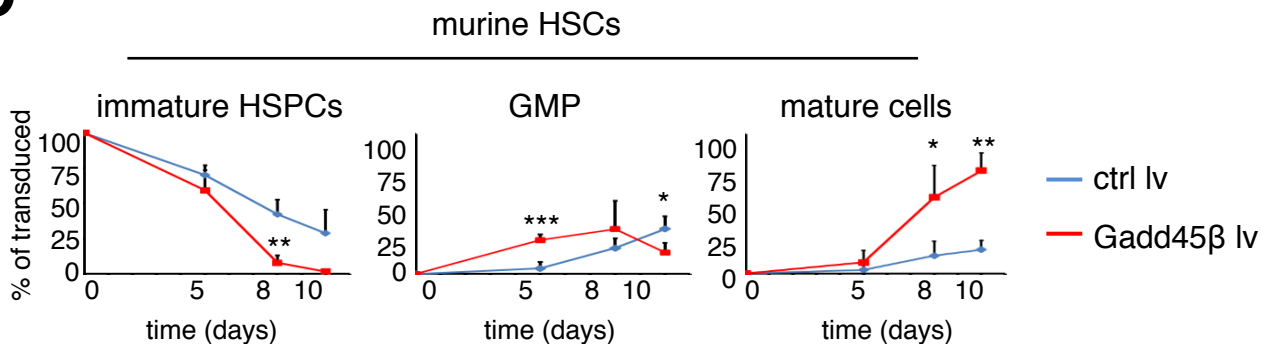
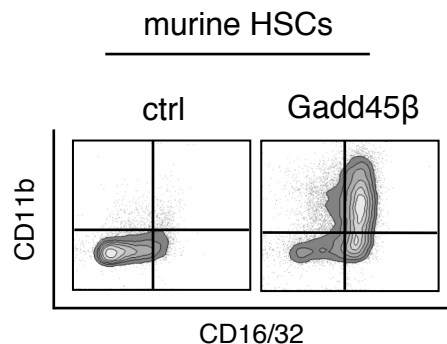
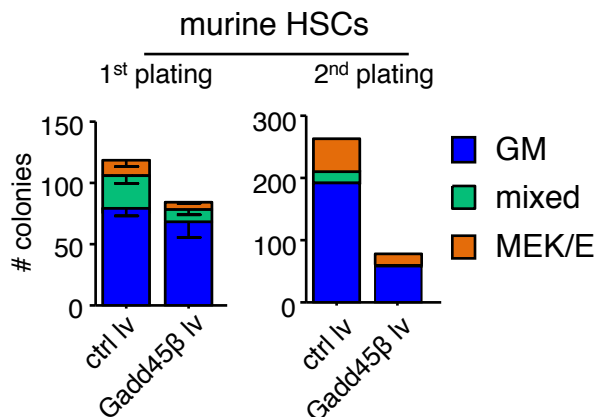
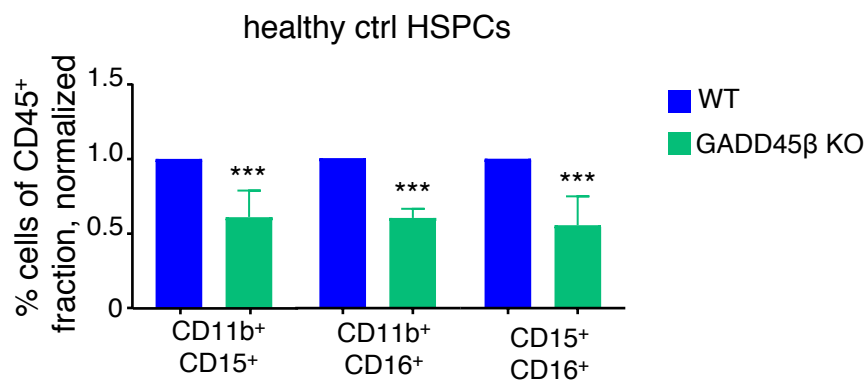
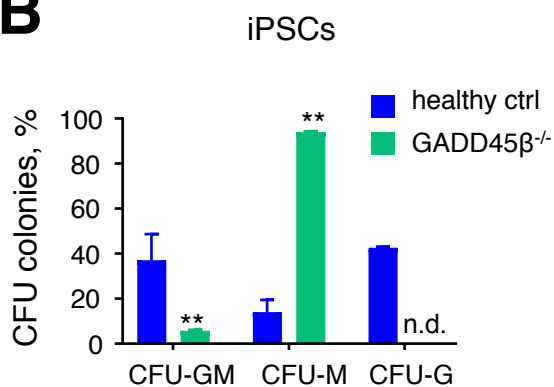
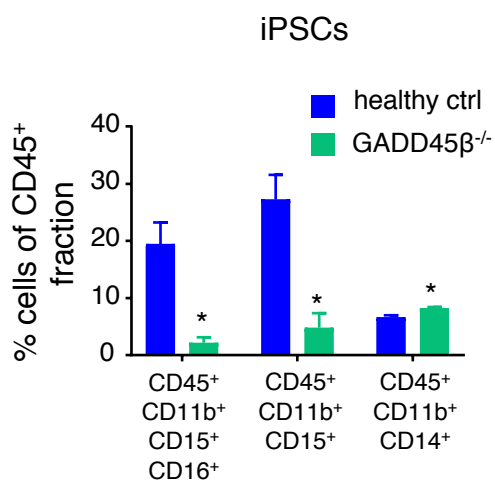
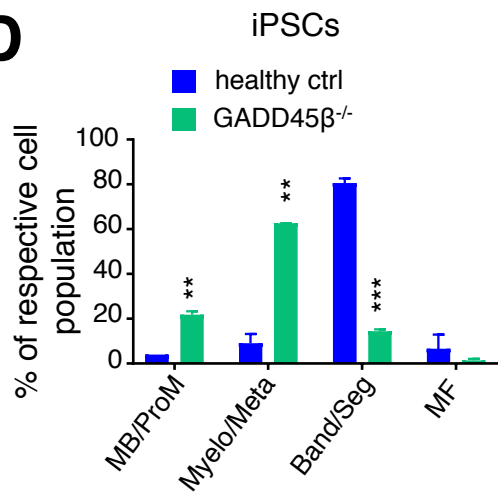
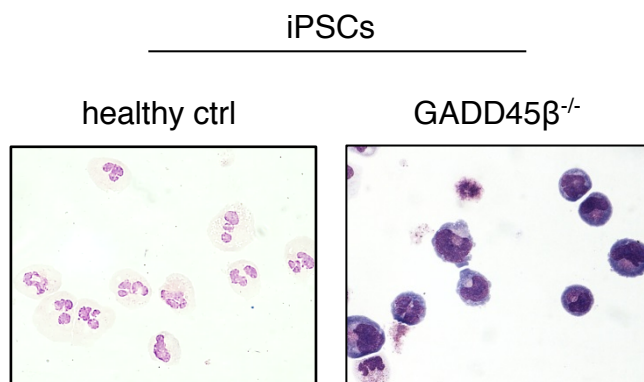
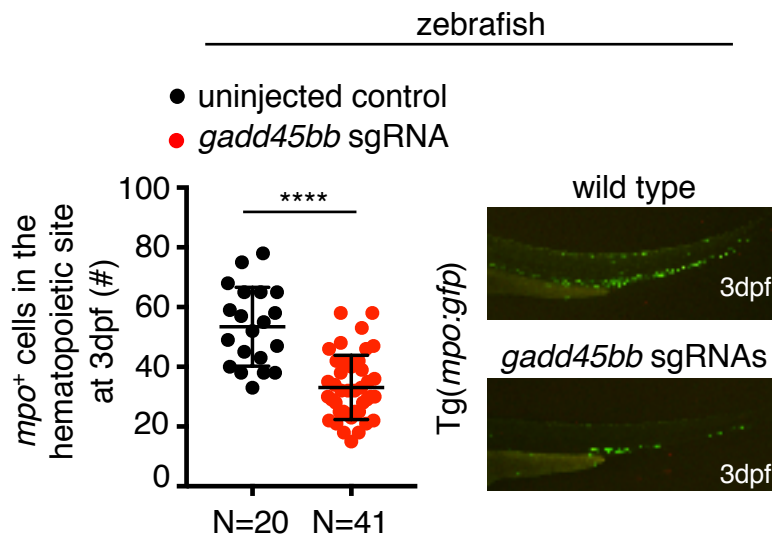
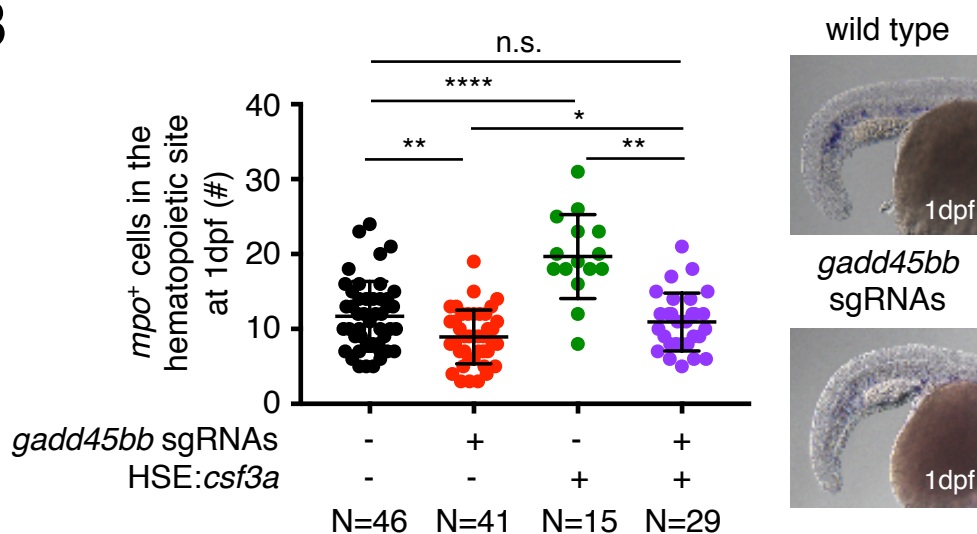
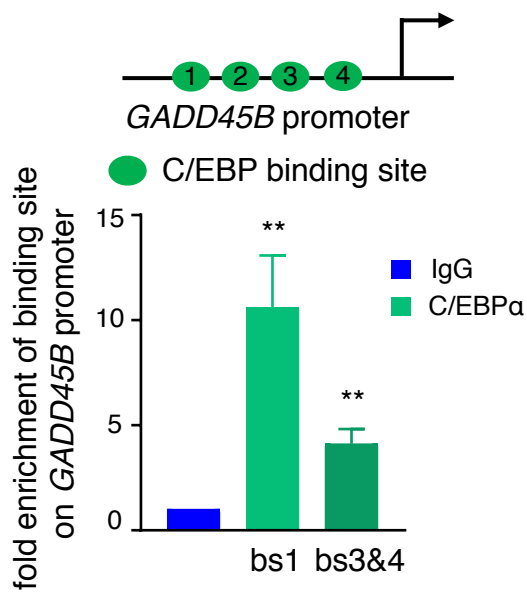
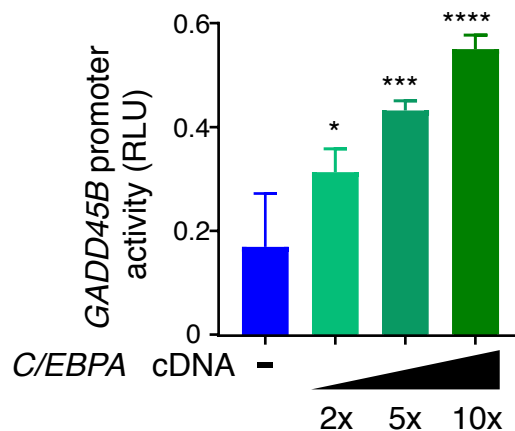


Figure 1

A**B****C****D****E****Figure 2**

A**B****C****D****E****Figure 3**

A**B****C****D****Figure 4**

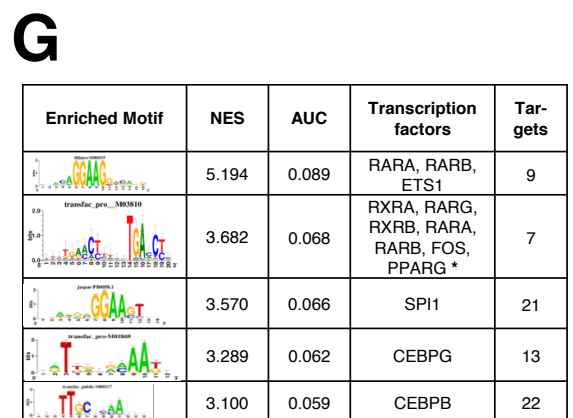
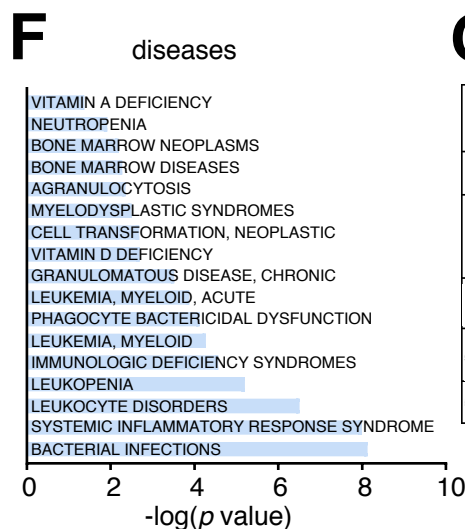
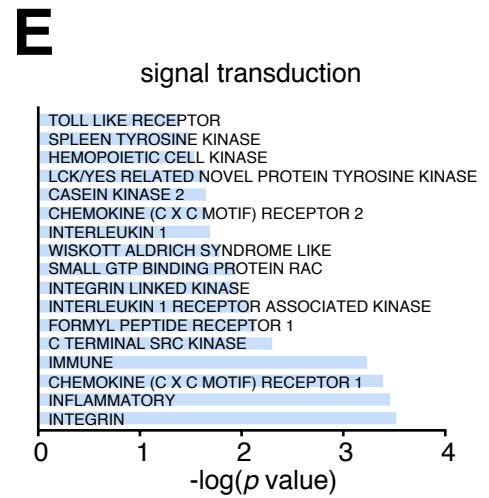
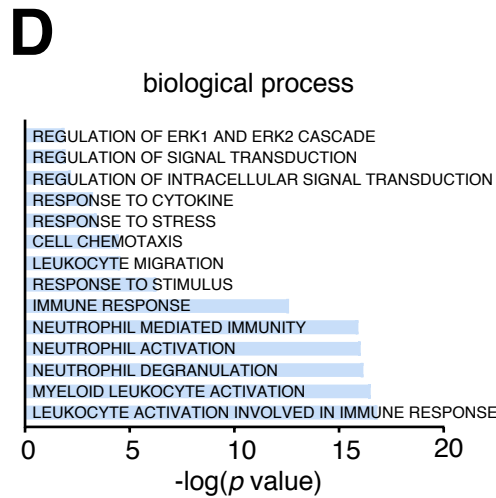
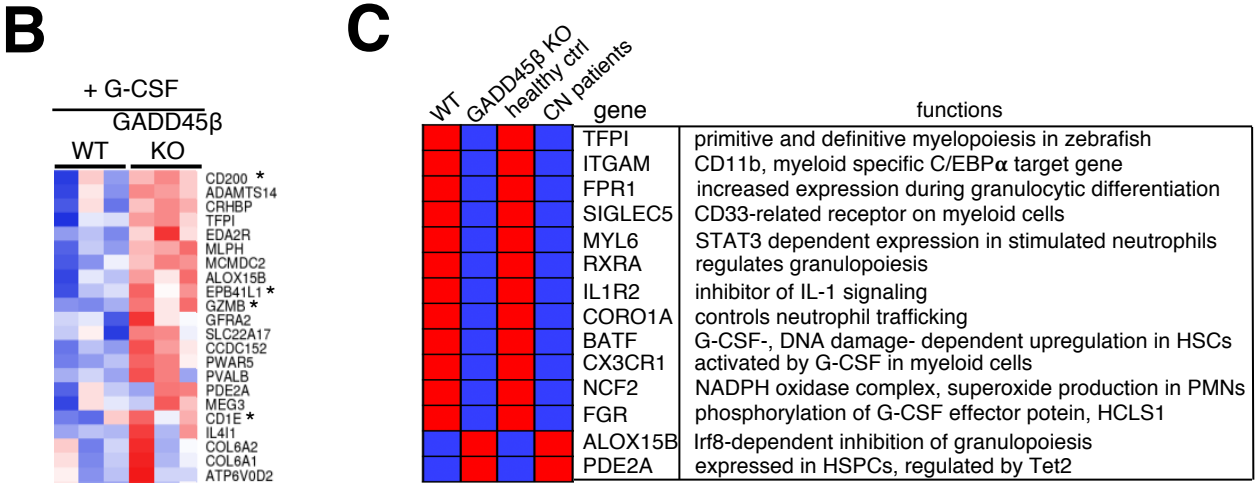
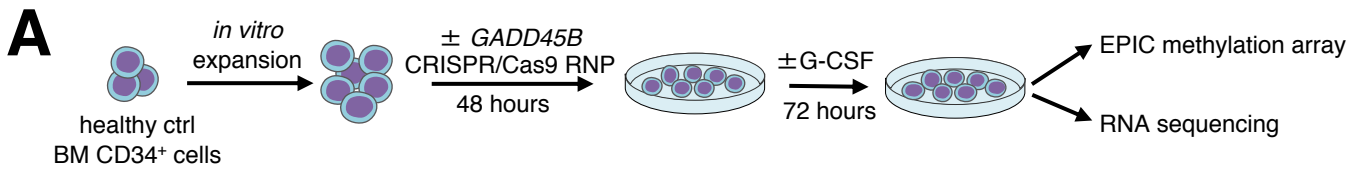


Figure 5

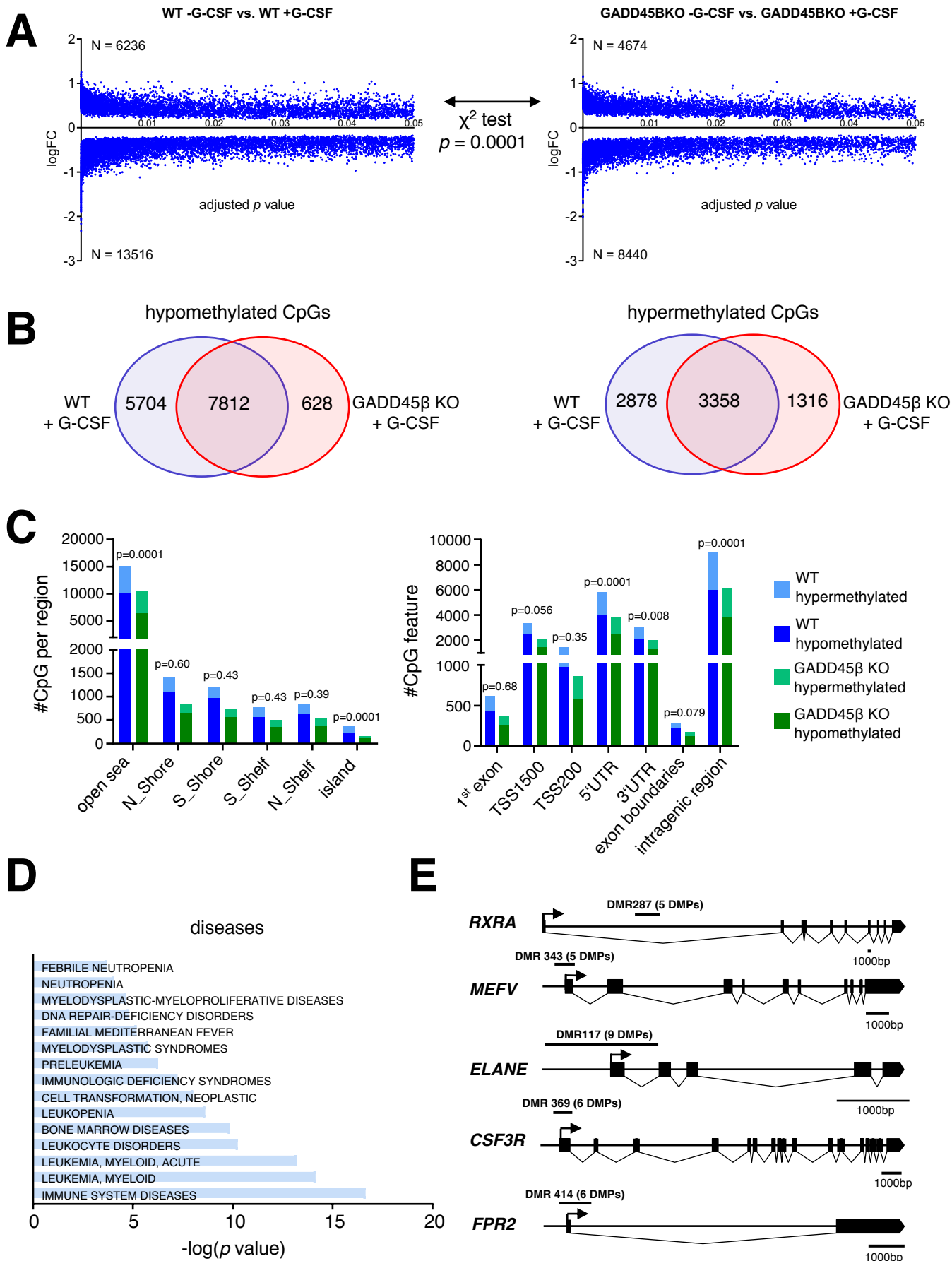


Figure 6

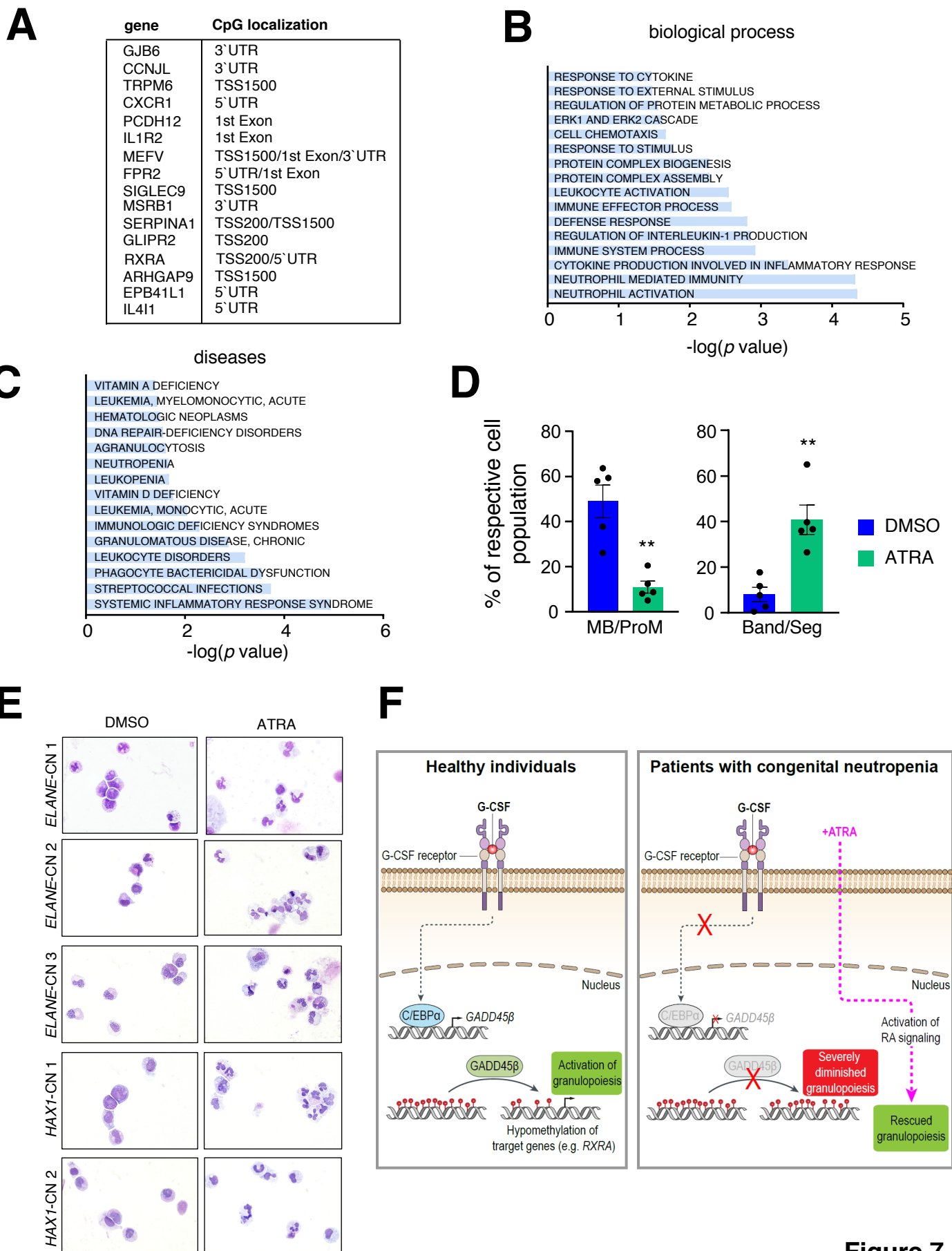


Figure 7

Supplemental information

Supplemental material and methods

Cell culture

The human embryonic kidney 293T (HEK293T) cell line was cultured under standard conditions (37 °C, 5 % CO₂, 20 % O₂) using DMEM high glucose for HEK293T cells (Gibco, #41966-052).

Human CD34⁺ hematopoietic stem and progenitor cells (HSPCs) and CD33⁺ myeloid progenitor cells were isolated from bone marrow- or peripheral blood mononuclear cell fraction by magnetic bead separation using Human CD34 Progenitor Cell Isolation kit, (#130-046-703) and Human CD33 Myeloid Progenitor Cell Isolation kit (#130-045-501) (Miltenyi Biotech, Germany). CD34⁺ cells were cultured in a density of 2 x 10⁵ cells/ml in Stemline II Hematopoietic Stem Cell Expansion medium (Sigma Aldrich, #50192) supplemented with 10 % FBS, 1 % penicillin/streptomycin, 1 % L-glutamine and a cytokine cocktail consisting of 20 ng/ml IL-3, 20 ng/ml IL-6, 20 ng/ml TPO, 50 ng/ml SCF and 50 ng/ml FLT-3L.

Human induced pluripotent stem cells (iPSCs) were cultured on Geltrex LDEV-free reduced growth factor basement membrane matrix (Thermo Fisher Scientific, #A1413201) coated plates in a density of 2 x 10⁵ cells/ml in StemFlex medium (Thermo Fisher Scientific, #A3349401) supplemented with 1 % penicillin/streptomycin.

FACS analysis of HSPCs composition

10⁵ CD34⁺ HSPCs or 10⁶ bone marrow mononuclear cells were washed with PBS and stained with corresponding surface marker antibodies in PBS containing 2% FBS and 0.02% sodium azide. For HSPC surface marker analysis (panel adapted from van Galen et al.¹), following antibodies were used: mouse anti-human CD38 (BD, #563964), mouse anti-human CD34 (BD, #348811), rat anti-human CD49f (BD, #563271), mouse anti-human CD90 (BD, #562685), mouse anti-human CD45RA (BD, #560673), mouse anti-human CD10 (BD, #563734), mouse anti-human CD135 (BD, #564708). For the analysis of nuclear H2AX

protein, cells were subsequently permeabilized and fixed using IntraSure kit (BD #641776) followed by incubation with mouse anti-human gamma H2AX (BD, #560447 or #560445) antibody.

Pure knockout clone isolation and embryoid body (EB)-based iPSC differentiation

Human healthy donor iPSCs were nucleofected with CRISPR/Cas9-gRNA RNP complexes against *GADD45B* (150 pmol per 10^6 cells, program CA-137) and afterwards plated on a Geltrex-coated 10-cm dish (15×10^3 cells/dish) in StemFlex medium (ThermoFisher, #A3349401) with RevitaCell supplement (Thermo Fisher Scientific, #A2644501). Media was changed every 24 hours without RevitaCell supplement. After 9 to 12 days, iPSC colonies were picked and transferred on a Geltrex-coated 96 well plate. Knockout was assessed for each clone by Cas9 *in vitro* digestion and confirmed by Sanger sequencing. The knockout clone was expanded and cultured on feeder cells. The expanded iPSC clones were dissociated from SNL-feeders or Geltrex LDEV-free reduced growth factor basement membrane matrix (Thermo Fisher Scientific, #A1413201) coated plates using PBS/EDTA (0.02%) for 5 min. As described in Dannenmann et al.² EB induction was done via spin EBs (2×10^4 cells/EB) in 96-well plates using APEL serum-free differentiation medium (Stemcell Technologies, #5270) supplemented with bFGF (20 ng/ml) and ROCK inhibitor (Y-27632 dihydrochloride, R&D Systems, #1254). On day 1, BMP4 (40 ng/ml) was added to induce mesodermal differentiation. On day 4, EBs were plated on Geltrex coated 6-well-plates (10 EBs/well) in APEL medium supplemented with VEGF (40 ng/ml), SCF (50 ng/ml) and IL-3 (50 ng/ml). For neutrophilic differentiation, the medium was changed 3 days later to APEL supplemented with IL-3 (50 ng/ml) and G-CSF (50 ng/ml). First hematopoietic floating cells appeared on day 12 – 14. Floating cells were harvested starting from day 14 to day 32 every 3 - 4 days and used for FACS analysis and Wright-Giemsa staining for morphologic discrimination.

Colony forming unit (CFU) assay

As described previously³, CD34⁺ cells were resuspended in Iscove's MDM with 2 % FBS (Stemcell Technologies, #07700) and enriched Methocult (Stemcell Technologies, #H4435). Cell suspension was plated on 3.5 cm dishes (1 x 10³ cells/dish) followed by colony counting at day 14.

Murine *Gadd45b* expression vector

The open reading frame (ORF) of a fluorescent reporter protein (either VENUS-hImportin subunit α 1 (AA2-67) or tdTOMATO-hImportin subunit α 1 (AA2-67)) was cloned into the third generation self-inactivating lentiviral vector pRRL.PPT.SFFV.IRES.eGFP.wPRE by replacing the ORF of green fluorescent protein⁴. A multiple cloning site (MCS) was inserted after the SFFV promoter. The ORF of murine *Gadd45b* was amplified by RT-PCR (forward 5'-TTGGCCGGCCTGCATCATGACCCTGGAAGAG-3', reverse 5'-TTACTAGTCACGGGTAGGGTAGCCTTTGA-3') and then cloned into the MCS.

Lentivirus production and transduction

Human GADD45 β cDNA expressing and empty control lentiviruses were produced in HEK293T cells⁵. For this, HEK293T were transfected with lentiviral envelope plasmid pMD2.G, the lentiviral packaging plasmid psPAX2 and donor plasmid using *TransIT-LT1* transfection reagent (Mirus, #MIR2300) according to the manufacturer's protocol. Two days after transfection, the supernatant containing the virus was harvested and concentrated using Lenti-X Concentrator (Takara Clontech, #631232). Viral titers were determined by transduction of HEK293T cells with different concentrations of virus supernatant and FACS.

Vesicular Stomatitis Virus-G (VSVG)-pseudotyped lentiviral particles containing murine *Gadd45 β* cDNA were produced in a split genome approach by calcium-phosphate-mediated transient transfection of human embryonic kidney 293T producer cells⁵. After 48 hours, supernatant was collected, filtered (45 μ m), and enriched by ultracentrifugation

(50.000 g, 2 hours). Viral titers were determined by transduction of NIH3T3 cells with different concentrations of virus supernatant and FACS.

CD34⁺ cells were transduced with a multiplicity of infection (MOI) of 6 to 10 using 5 µg/ml polybrene by spinoculation at 500 x g at 4 °C for 10 minutes. Cells were re-transduced after 24 hours. One day after re-transduction medium was exchanged and cells were incubated for two more days before differentiation experiments were started.

GADD45β shRNA and control shRNA were produced in HEK293T cells and concentrated with Lenti-X Concentrator as described above. NB4 cells were transduced with MOI 5 using 5µg/ml polybrene. Medium was exchanged after 24 hours. NB4 cells were differentiated using 1 µM ATRA for 14 days.

***In vitro* differentiation of murine LT-HSCs**

Mouse BM cells from femurs, tibiae, coxae and sternum of 12-16 week old C57BL/6 mice were isolated by crushing the bones and LT-HSCs were sorted with a FACS Aria (BD) after staining with antibodies against CD117, Sca1, CD150, CD48, CD34, CD16/32, and Streptavidin. Details are explained elsewhere²⁸. 100 murine LT-HSCs were lentivirally transduced (MOI 100) and cultured in SFEM (Stemcell Technologies) supplemented with 100 ng/ml SCF and TPO (PeproTech). Cells were analyzed by FACS (antibodies against CD48, CD117, CD16/32, CD11b) at indicated time points²⁸. To read out colony-formation, LT-HSCs were lentivirally transduced (MOI 100), seeded 24 hours later in M3434 medium (Stemcell Technologies) and scored microscopically after 9 to 12 days for transduction and colony formation. After counting the cells, defined cell numbers after primary colony formation were replated to fresh M3434 medium and scored for secondary colony formation after 9 to 12 days.

Genomic DNA isolation and *GADD45B* Sanger sequencing

Genomic DNA was isolated using the QIAamp DNA Mini Kit (Qiagen, #51306) according to the manufacturer's instructions. PCR to amplify CRISPR/Cas9 sgRNA RNP-

edited region of *GADD45B* was conducted using GoTaq Hot Start Polymerase Kit (Promega, #M5006). PCR products were purified using the QIAquick PCR Purification Kit (Qiagen, #28106), and Sanger sequencing was performed at Eurofins Genomics.

qRT-PCR

RNA was isolated using the RNeasy Mini Kit (Qiagen, #74106) according to the manufacturer's instructions. Reverse transcription was conducted with the Omniscript RT kit (Qiagen, #205113) according to the protocol using a mix of random hexamers (Thermo Fisher Scientific, #S0142) and oligo-dT (Thermo Fisher Scientific, #S0132) primers. The mRNA expression of mRNA was measured with the SYBR Green quantitative PCR kit (Roche, #04887352001) and primers against *GADD45B* mRNA (forward 5'-TGCTGTGACAACGACATCAAC-3' and reverse 5'-GTGAGGGTTCGTGACCAGG-3'). *GADD45B* mRNA expression was normalized to *GAPDH* and is presented as $2^{-\Delta C_p}$ values.

Duolink *in situ* proximity ligation assay

Proximity ligation assay was described in detail elsewhere^{3,6}. Cytospin slides (1×10^4 cells per slide) were fixed in ice-cold methanol for 5 min, washed with PBS twice, permeabilized using 0.5% Triton X-100 for 10 min, washed with PBS twice and stained using primary anti-GADD45 β antibody followed by Duolink[®] *in situ* PLA probes and Duolink[®] *in situ* Detection Reagents Orange (Olink Bioscience) following the manufacturer's protocol (Olink Bioscience, Uppsala, Sweden). After staining, samples were air-dried, mounted with Duolink[®] *In Situ* Mounting Medium with DAPI (Olink Bioscience) and examined using an Axio Observer.Z1 fluorescence microscope (ZEISS, Oberkochen, Germany).

Dual luciferase reporter gene assay

GADD45B promoter (1.2 kb upstream of ATG) predicted to contain four C/EBP binding sites was cloned into the pGL4.10 [*luc2*] firefly luciferase reporter vector (Promega, #E6651). HEK293T cells were transfected with the *GADD45B* firefly luciferase reporter vector, *Renilla* vector and *C/EBPA* plasmid in different concentrations using *TransIT-LT1*

transfection reagent (Mirus, #MIR2300). Lysates were harvested 60 hours post transfection and activity of both firefly and *Renilla* luciferase was measured using a GloMax Multi Detection System (Promega).

Chromatin immunoprecipitation assay

THP1 cells (15×10^6) were fixed using 1 % formaldehyde for 5 min at room temperature, fixation reaction was stopped by adding 0.125 M glycine. Cells were rinsed twice with ice-cold PBS and resuspended in 1 mL Farnham lab (FL) buffer (5 mM PIPES pH 8, 85 mM KCl, 0.5% Igepal CA-630) containing protease inhibitors. Covaris M220 focused ultrasonicator was used to isolate nuclei (peak power 75 W, duty factor 15 % and 200 cycles/burst at 4 °C). Nuclei were centrifuged at 1000 xg for 5 min at 4 °C and washed once in FL buffer. To shear the chromatin nuclei were taken up in resuspension buffer D3 (1 mM EDTA, 10 mM Tris-HCl pH 7.6, 0.1 % SDS) containing protease inhibitors and sonicated for 25 min, at peak power 75 W, duty factor 15 % and 200 cycles/burst. Sheared chromatin was pre-cleaned with mixed Dynabeads (protein A and G, Thermo Fisher Scientific, #10001D and #10003D) and precipitated using either C/EBP α monoclonal antibody (sc-166258) or input control antibody (sc-2025). After several washing steps immunoprecipitated protein-DNA crosslinked complexes were eluted, the cross-links were reversed over night by incubation with 0.2 M NaCl and 20 μ g RNase A (Macherey Nagel, #740505) at 65 °C and de-proteinated with 40 μ g proteinase K (Qiagen, #19131). We detected C/EBP α bound fraction of DNA was measured by qRT-PCR. The protocol was adapted from Arrigoni *et al.*⁷.

Zebrafish experiments

All zebrafish experiments described in the present study were conducted on embryos younger than 5 days post-fertilization under the guidelines of the European Commission, Directive 2010/63/EU. Zebrafish husbandry was performed in accordance with European Union animal welfare guidelines⁸ and under the supervision of the local representative of the animal welfare agency (permit 35/9185.46/Uni Tü). The zebrafish strain used in this study

was *Danio rerio* wild type TE. The stable transgenic line Tg(*mpo:gfp*) was described previously⁹.

sgRNA target site selection

sgRNAs for zebrafish *gadd45bb* were designed with CCTop as described in Stemmer et al.¹⁰. Four sgRNAs were used (PAM in brackets): CGAGACAGTGTCTGCTGCAAG (AGG), CTGTGCCAGACGCCTCATGC(CGG), AGACCAAAGGAGCATCTGGG(TGG) and CTACGCTTTGCACTCCACGT(GGG). Cloning of sgRNA templates and in vitro transcription was performed as detailed in Stemmer et al.¹⁰.

Whole-mount *in situ* hybridization

RNA *in situ* hybridization of zebrafish embryos was performed as described previously¹¹ using digoxigenin-labeled RNA antisense probe for *gadd45bb* (accession number NM001012386, nucleotides 484-968) and *myeloperoxidase*, *mpo* (accession number BC056287, nucleotides 225-938).

In vitro transcription of mRNA

The pCS2+Cas9 plasmid was linearized using NotI and the mRNA was transcribed in vitro using the mMessage_mMachine SP6 Kit (ThermoFisher Scientific, AM1340).

Microinjection and heat treatment of zebrafish embryos

Zebrafish zygotes were co-injected with 15 ng/μl of the sgRNAs and 150 ng/μl of Cas9 mRNA. As negative control, 150 ng/μl of Cas9 mRNA without sgRNAs was injected into wild type embryos. Embryos were kept at 28°C in E3 medium with 200 μM 1-phenyl 2-thiourea (PTU) to prevent pigmentation. To ectopically express *csf3a*, full-length cDNA of zebrafish *csf3a* was cloned in a plasmid containing a bi-directional heat-inducible promoter¹² and Tol2 binding sites. The resulting plasmid, HSE:*csf3a*, was then co-injected at 20 ng/μl with 10 ng/μl of mRNA of Tol2 transposase. Embryos were then heat treated for 1 hour at 39 °C after one day. GFP-positive embryos were selected for whole-mount *in situ* hybridization analysis and genotyping.

Genotyping of gadd45bb crispants

To genotype gadd45bb crispants, genomic DNA was extracted from individual embryos after whole-mount in situ hybridization analysis using the QuickExtract™ DNA extraction solution (Epicentre, USA) according to the manufacturer's protocol. PCR with specific forward (5'-TTGCAAGATTTCACTGCGGC-3') and reverse (5'-ACGAAAGGTAAACATGTGCAA A-3') primers was used for subsequent sequence analysis. The investigators were blinded to allocation during experiments and outcome assessment.

RNA sequencing

RNA was isolated using the RNeasy Mini kit (Qiagen, #74106). The RNA concentration was determined by Qubit RNA High Sensitivity kit (Thermo Fisher Scientific, #Q32855). Library preparation and RNA sequencing on a HiSeq 4000 (single-read 50bp) were performed at the DKFZ Genomics and Proteomics Core Facility. RNA seq data analysis was performed on an input matrix of raw read counts loaded in R package DESeq2¹³. The counts from technical replicates were combined using the *collapseReplicates* function of DESeq2. Differences in gene expression between groups were quantified while controlling for individuals effects. The identified list of differently expressed genes was further characterized by performing analysis in Genomatix (Intrexon Bioinformatics, Germany), iRegulon^{14,15} and Heatmapper¹⁶.

Methylation analysis

DNA was isolated using QIAamp DNA Mini kit (Qiagen, #51306). The DNA concentration was determined by Qubit dsDNA High Sensitivity kit (Thermo Fisher Scientific, #Q32854). Methylation analysis using the Infinium Human MethylationEPIC beadchip, which covers 866.895 genome-wide CpGs, was performed at the DKFZ Genomics and Proteomics Core Facility. The analysis of methylation data was conducted using R packages *minfi*^{17,18} and *limma*¹⁹. Next, R packages *DMRcate* and *limma* were applied for the

identification of differentially methylated regions between groups²⁰. Genomatix and iRegulon analysis were performed to gain an insight into biological processes and gene pathways that differentially methylated CpGs might be involved in.

Supplemental figure legends

Supplemental Figure 1. GADD45 β expression is increased during granulopoiesis with highest levels in granulocytes. **A**, Analysis of GADD45 β expression using the public database *Bloodspot*²¹ revealed that early progenitors do not express much GADD45 β and during granulopoiesis it is increased with an expression peak in granulocytes (PMN).

Supplemental Figure 2. Gene modification efficiency of CRISPR/Cas9-mediated GADD45 β knockout in CD34⁺ HSPCs from three healthy donors that were used for RNA seq and EPIC methylation array

A-C, Gene modification efficiency of *GADD45B*-targeting CRISPR/Cas9 RNP was determined by Sanger sequencing (left) and indel percentage was determined by ICE webtool, Synthego (right). Representative chromatograms are depicted.

Supplemental Figure 3. EB-based myeloid differentiation of GADD45 β ^{-/-} iPSCs revealed an increased amount of immature and decreased amount of mature cells compared to control iPSCs

A, EB-based myeloid differentiation of GADD45 β -deficient iPSCs was performed and floating cells generated on day 14 of culture were analysed by FACS. **B**, Morphological evaluation using Wright-Giemsa stained cytopsin preparations of differentiated iPSCs on day 21 of culture. **A, B** Data from 3 independent experiments are depicted, means \pm SD; *, $p < 0.05$; **, $p < 0.01$; ***, $p < 0.001$.

Supplemental Figure 4. Injection of Cas9 mRNA alone does not affect neutrophil numbers. **A**, Cas9 mRNA was injected into wild-type embryos. After one day, the numbers of neutrophils were determined by whole-mount in situ hybridization using a mpo antisense

probe. The number of mpo-expressing cells in the trunk region was then compared to uninjected embryos. N indicates number of embryos. Data are means \pm SD.

Supplemental Figure 5. *GADD45 β* promoter has four putative C/EBP binding sites

A, 654 bp sequence of the *GADD45 β* gene till ATG start codon with four predicted C/EBP binding sites (b.s.1-4, indicated in red) is depicted.

Supplemental Figure 6. iRegulon motif enrichment analysis of genes upregulated after G-CSF treatment of healthy control HSPCs, but not *GADD45 β* -KO cells

A, List of significantly enriched motifs and transcription factors binding to these motifs are presented.

Supplemental Figure 7. Gene ontology and motif enrichment analysis of differentially hypomethylated CpGs upon *GADD45 β* KO

A,B, Genomatix gene ontology analysis of biological processes (**A**) and signal transduction pathways (**B**) related to *GADD45 β* -dependent DNA demethylation. **C**, Significantly enriched motifs of hypomethylated genes were identified using iRegulon motif enrichment analysis.

Supplemental Figure 8. Differentially methylated regions (DMRs) related to myeloid-specific genes are hypomethylated upon G-CSF treatment of control but not *GADD45 β* -KO cells. Presented are DMRs of *HDAC5*, *AZU1*, *MPO*, *CTSG*, *SLPI*, *CXCR2*, *GF11*, *PRTN3* and *IL1R2*. The number of DMPs in each DMR is indicated in parenthesis.

Supplemental Figure 9. Gene ontology analysis of genes that are differentially expressed and methylated in G-CSF-treated HSPCs upon *GADD45 β* knockout

A, Gene ontology analysis was performed using Genomatix software. Selected significant signal transduction pathways are presented.

Supplemental tables

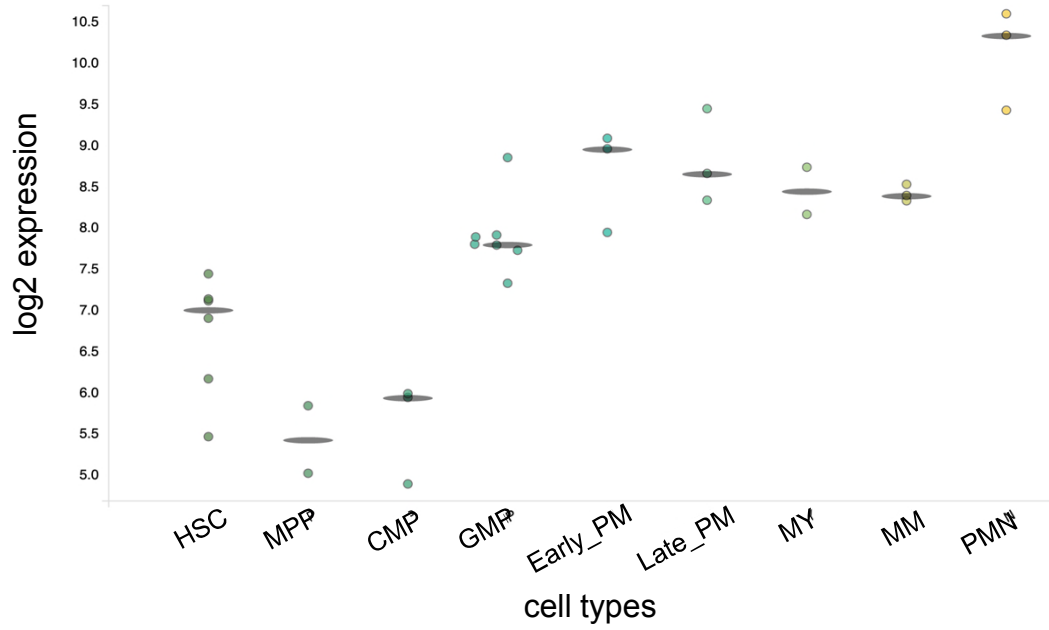
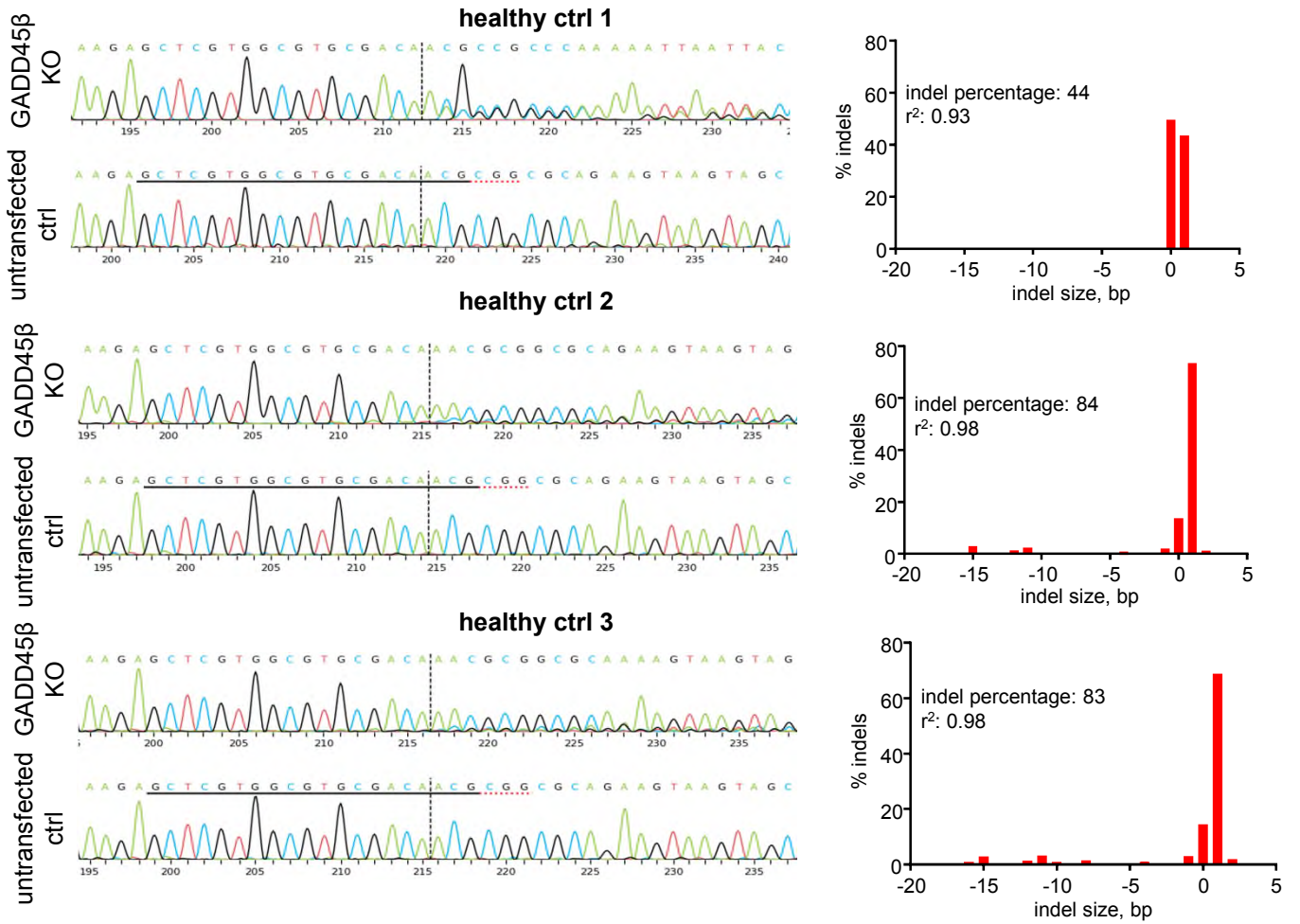
Supplemental table 1. Differentially expressed genes between G-CSF treated control and GADD45 β -KO group

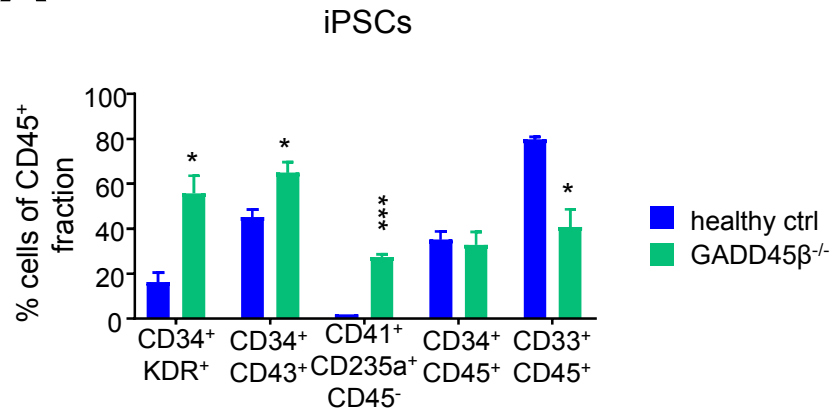
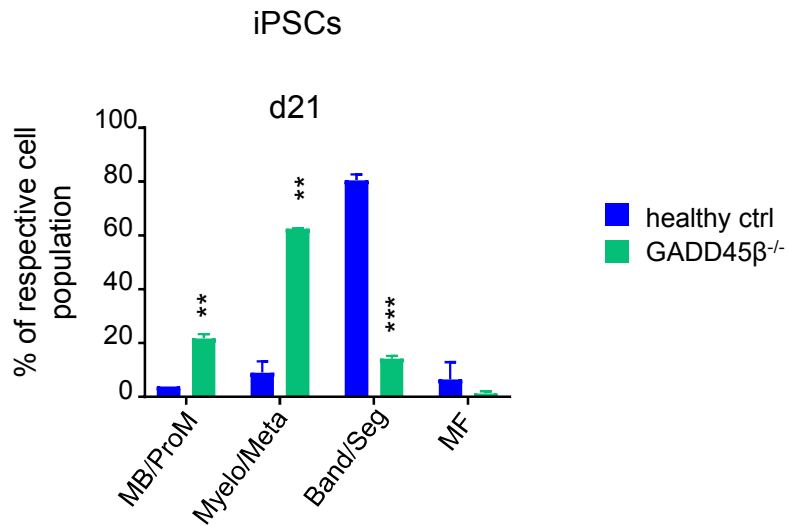
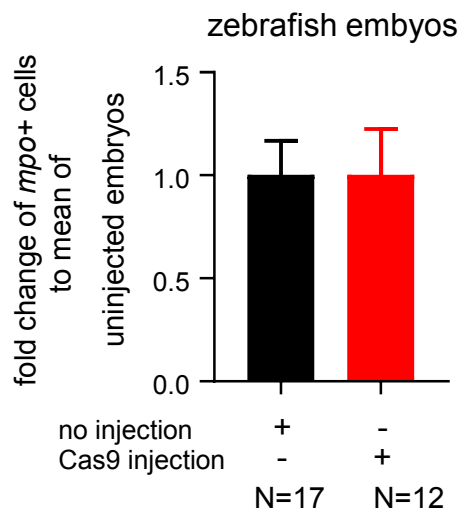
Supplemental table 2. Differentially methylated sites (DMPs) between G-CSF treated and untreated control cells

Supplemental table 3. Genomic locus enrichment analysis of differentially methylated regions between G-CSF treated control and GADD45 β -KO groups

Supplemental references

1. van Galen P, Kreso A, Mbong N, et al. The unfolded protein response governs integrity of the haematopoietic stem-cell pool during stress. *Nature*. 2014;510(7504):268-272.
2. Dannenmann B, Zahabi A, Mir P, et al. Human iPSC-based model of severe congenital neutropenia reveals elevated UPR and DNA damage in CD34(+) cells preceding leukemic transformation. *Exp Hematol*. 2019;71:51-60.
3. Skokowa J, Klimiankou M, Klimenkova O, et al. Interactions among HCLS1, HAX1 and LEF-1 proteins are essential for G-CSF-triggered granulopoiesis. *Nat Med*. 2012;18(10):1550-1559.
4. Schambach A, Mueller D, Galla M, et al. Overcoming promoter competition in packaging cells improves production of self-inactivating retroviral vectors. *Gene Ther*. 2006;13(21):1524-1533.
5. Naldini L. Lentiviruses as gene transfer agents for delivery to non-dividing cells. *Curr Opin Biotechnol*. 1998;9(5):457-463.
6. Soderberg O, Gullberg M, Jarvius M, et al. Direct observation of individual endogenous protein complexes in situ by proximity ligation. *Nat Methods*. 2006;3(12):995-1000.
7. Arrigoni L, Richter AS, Betancourt E, et al. Standardizing chromatin research: a simple and universal method for ChIP-seq. *Nucleic Acids Res*. 2016;44(7):e67.
8. Bert B, Chmielewska J, Bergmann S, et al. Considerations for a European animal welfare standard to evaluate adverse phenotypes in teleost fish. *EMBO J*. 2016;35(11):1151-1154.
9. Renshaw SA, Loynes CA, Trushell DM, Elworthy S, Ingham PW, Whyte MK. A transgenic zebrafish model of neutrophilic inflammation. *Blood*. 2006;108(13):3976-3978.
10. Stemmer M, Thumberger T, Del Sol Keyer M, Wittbrodt J, Mateo JL. CCTop: An Intuitive, Flexible and Reliable CRISPR/Cas9 Target Prediction Tool. *PLoS One*. 2015;10(4):e0124633.
11. Aghaallaei N, Bajoghli B, Czerny T. Distinct roles of Fgf8, Foxi1, Dlx3b and Pax8/2 during otic vesicle induction and maintenance in medaka. *Dev Biol*. 2007;307(2):408-420.
12. Bajoghli B, Aghaallaei N, Heimbucher T, Czerny T. An artificial promoter construct for heat-inducible misexpression during fish embryogenesis. *Dev Biol*. 2004;271(2):416-430.
13. Love MI, Huber W, Anders S. Moderated estimation of fold change and dispersion for RNA-seq data with DESeq2. *Genome Biol*. 2014;15(12):550.
14. Janky R, Verfaillie A, Imrichova H, et al. iRegulon: from a gene list to a gene regulatory network using large motif and track collections. *PLoS Comput Biol*. 2014;10(7):e1003731.
15. Verfaillie A, Imrichova H, Janky R, Aerts S. iRegulon and i-cisTarget: Reconstructing Regulatory Networks Using Motif and Track Enrichment. *Curr Protoc Bioinformatics*. 2015;52:2 16 11-39.
16. Babicki S, Arndt D, Marcu A, et al. Heatmapper: web-enabled heat mapping for all. *Nucleic Acids Res*. 2016;44(W1):W147-153.
17. Aryee MJ, Jaffe AE, Corrada-Bravo H, et al. Minfi: a flexible and comprehensive Bioconductor package for the analysis of Infinium DNA methylation microarrays. *Bioinformatics*. 2014;30(10):1363-1369.
18. Fortin JP, Triche TJ, Jr., Hansen KD. Preprocessing, normalization and integration of the Illumina HumanMethylationEPIC array with minfi. *Bioinformatics*. 2017;33(4):558-560.
19. Ritchie ME, Phipson B, Wu D, et al. limma powers differential expression analyses for RNA-sequencing and microarray studies. *Nucleic Acids Res*. 2015;43(7):e47.
20. Peters TJ, Buckley MJ, Statham AL, et al. De novo identification of differentially methylated regions in the human genome. *Epigenetics Chromatin*. 2015;8:6.
21. Bagger FO, Kinalis S, Rapin N. BloodSpot: a database of healthy and malignant haematopoiesis updated with purified and single cell mRNA sequencing profiles. *Nucleic Acids Res*. 2019;47(D1):D881-D885.

A**B****Supplemental Figure 1**






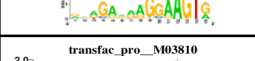
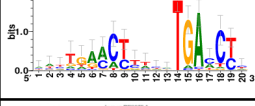


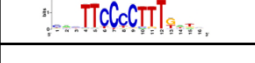
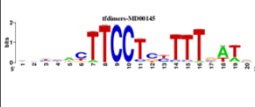
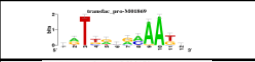

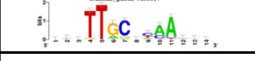
A**B****C**

A

b.s. 1
CCTTCCCGGTGCAGCCCCTCCACCCCCAGCAGAACTTGGGAAAGGCGCG
GTCCGGGACTCTCCGCGGATCGGGAGGGGATTCCAGGCCCCCCCGAAA
GTCCGGGCCGCCTCGCGCGCTGGAAATCCCGCGCGCGCCCCGAACCGC
GGCTCGGCTGCCGGGAAATCAGGAGAAAAAACTTCTGCTTTTTTTTCTTT
TCTGGCATTGCGGGTACCTACCCGGCCCCCGCGCGCCCTCCTCCCGGT
TCTCGCCCCACGTGGGGCGCCCCCGCACGCCGCTCCTCCCCCTCCCC
TCCGTCCGCCAACCGCAGAGCTAGCTGCACTCGCCCTGTCTTTCCACC
b.s. 2
AATAGGAGGGGCGAATGACTCCACTGAGGCCACGCCCAATGTTCAAGTC
TATAAAAGTCGGTGCCGGAGGCTCCCAGCTCAGATCGCCGAAGCGTCGG
b.s. 3
ACTACCGTTGGTTTCCGCAACTTCCTGGATTATCCTCGCCAAGGACTTTG
CAATATATTTTTCCGCCTTTTTCTGGAAGGATTTGCTGCTTCCCGAAGGTC
TTGGACGAGCGCTCTAGCTCTGTGGGAAGGTTTTGGGCTCTCTGGCTCG
b.s. 4
GATTTTCAATTTCTCCCTGGGACTGCCGTGGAGCCGCATCCACTGTGG
ATTATAATTGCAACATG

A

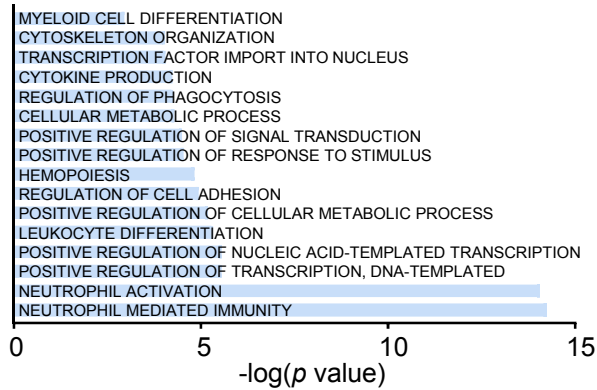
HSPCs

Enriched Motif	NES	AUC	Transcription factors	Targets
	5.194	0.089	RARA, RARB, ETS1	9
	5.117	0.088	ELF1, CBFB, RUNX2	8
	4.496	0.079	ETS1	4
	4.289	0.076	LTF	7
	4.136	0.074	NR3C1, STAT1	8
	3.947	0.071	TAL1	4
transfac_pro_M03810 	3.682	0.068	RXRA, RARG, RXRB, RARA, RARB, FOS, PPARG *	7
	3.570	0.066	SPI1	21
	3.471	0.065	NFKB1, NFKB2	5
	3.393	0.064	STAT1, LEF1	5
	3.358	0.063	ELK4, ELF2, GABPB1, TCF4, FLI1, ELK1, ELF4, ETV6, ETV7	10
	3.289	0.062	CEBPG	13
	3.219	0.061	IRF4, SPI1, ETS1, GABPB1	26
	3.100	0.059	CEBPB	22
* Binding with FDR < 2.5x10 ⁻⁵				

A

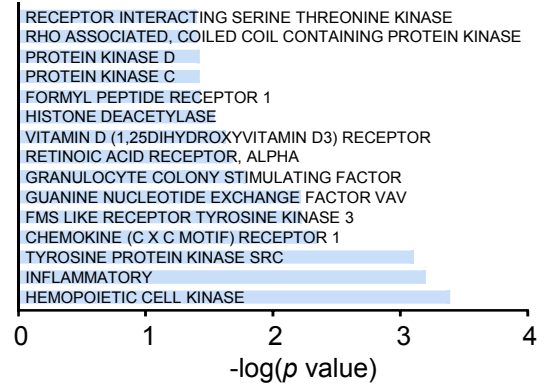
HSPCs

biological process


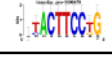
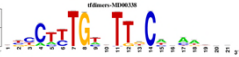
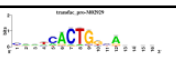

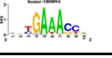
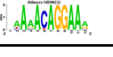
**B**

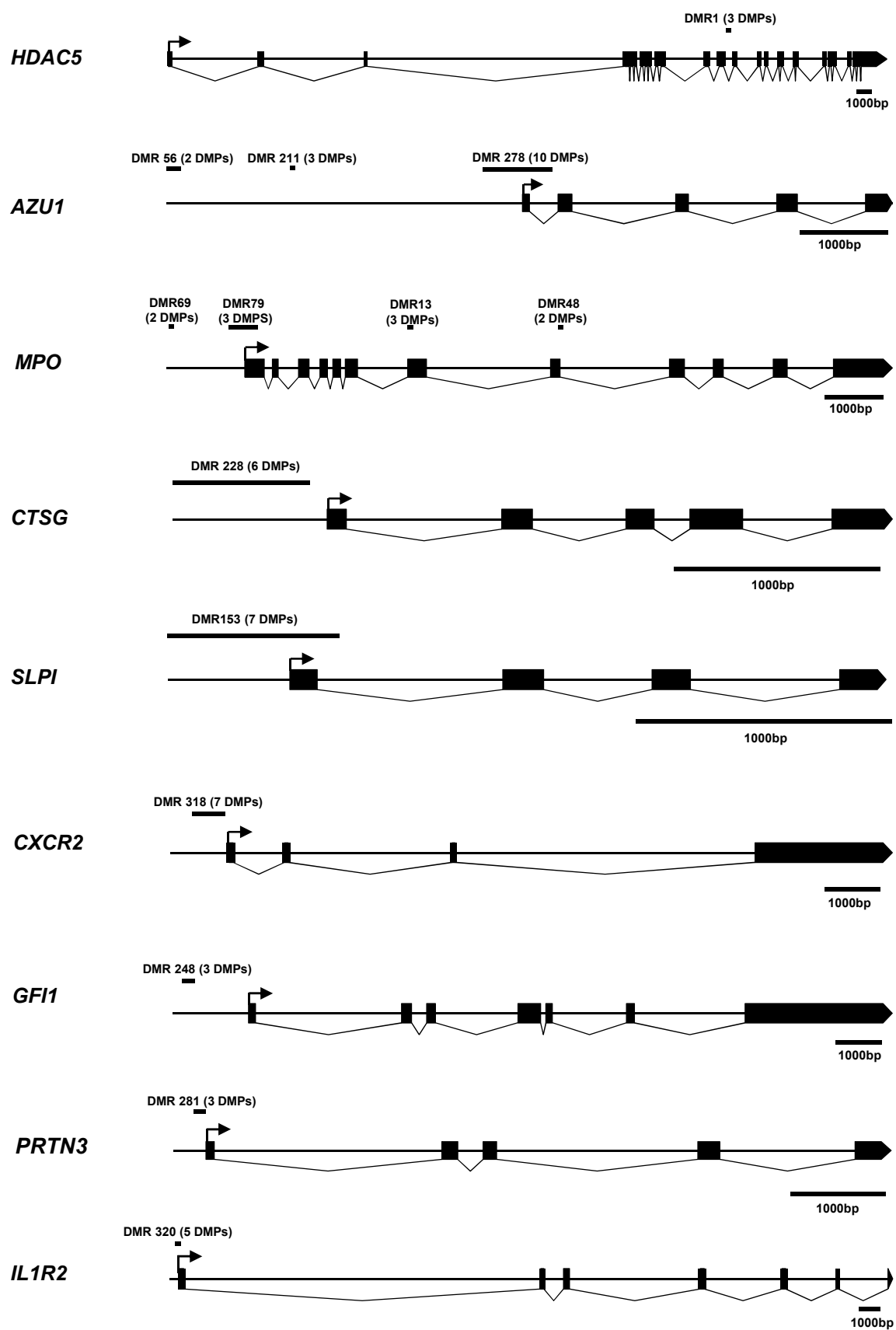
HSPCs

signal transduction

**C**

HSPCs

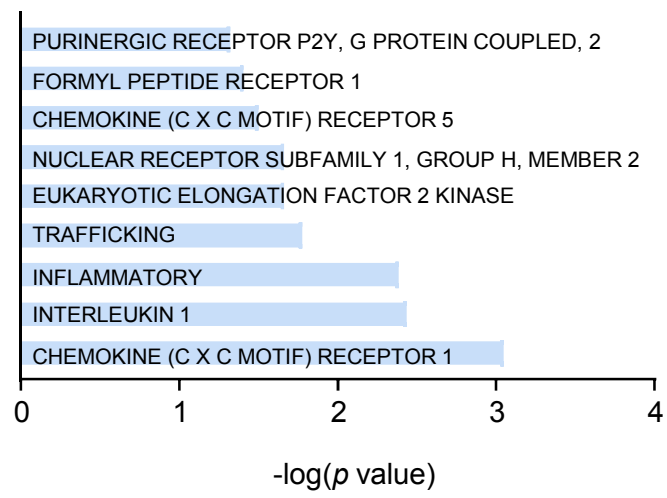
Enriched Motif	NES	AUC	Transcription factors	Targets
	3.297	0.04	FOXP3	74
	3.226	0.04	ETV7	100
	3.214	0.04	CEBPE, CEBPG, CEBPD, SOX9, CEBPB, CEBPA	111
	3.152	0.039	ZBTB3	164
	3.061	0.039	EP300	85
	3.047	0.039	IRF4	127
	3.029	0.039	FOXO1, GABPA	64

A**Supplemental Figure 6**

A

HSPCs

signal transduction



Lebenslauf

PERSÖNLICHE DATEN 		Geburtsdatum: 20.09.1987 Geburtsort: Kerkuk – Irak Geburtsname: Mardan Familienstand: verheiratet Staatsangehörigkeit: Deutsch
PROMOTION 	08/2015- 07/2020	Promotion (Dr. rer. Nat.) im Labor für Translationale Onkologie unter der Betreuung von Prof. Dr. Julia Skokowa (Innere Medizin II, Universitätsklinikum Tübingen) zum Thema: „ <i>GADD45b plays an essential role in the G-CSF triggered granulocytic differentiation of human hematopoietic stem cells</i> “
STUDIUM 	2013- 2015	Beginn des Studiengangs „Biochemistry“ (M.Sc) im SS13 an der Eberhard Karls Universität Tübingen, Abschluss mit dem <i>Master of Science im Mai 2015</i> mit der Gesamtnote 1,4 Schwerpunktfächer: Molecular Oncology, Molecular Medicine, Biochemistry of cell organelles, Pathobiochemistry
	10/2014- 05/2015	Masterarbeit mit dem Thema: „ <i>Impact of Akt knockout on reprogramming of mouse embryonic fibroblasts to induced pluripotent stem cells</i> “ im Labor für Molekulare Medizin unter der Leitung von Prof. Klaus Schulze-Osthoff (Universitätsklinikum & Interfakultäres Institut für Biochemie Tübingen) unter der Betreuung von PD Dr. Frank Essmann, Abschluss der Masterarbeit mit Note 1,0
	2009- 2012	WS 09/10 Studium der Biochemie an der Eberhard Karls Universität Tübingen, <i>Bachelor of Science</i> -Abschluss mit der Gesamtnote 2,3 Schwerpunktfächer: Immunologie, Zellbiochemie, Molekular-biologie, Toxikologie, Infektionsbiologie
	03-08/ 2012	Bachelorarbeit zum Thema „ <i>Molekulare Regulation des Transkriptionsfaktors SOX2 in Tumor-Stammzellen</i> “ im Labor für Entwicklungsbiologie unter der Leitung von Prof. Dr. Claudia Lengerke (Basel), Abschluss der Bachelorarbeit mit der Note 1,0
PUBLIKATIONEN 	2020	P. Mir , M. Ritter, K. Welte, J. Skokowa and M. Klimiankou, ‘ <i>Gene Knockout in Hematopoietic Stem and Progenitor Cells Followed by Granulocytic Differentiation</i> ’, RNA Interference and CRISPR Technologies, Methods in Molecular Biology, vol. 2115, p. 455-469, February 2020 P. Mir , M. Klimiankou, B. Findik, K. Haehnel, S. Mellor-Heineke, C. Zeidler, J. Skokowa, K. Welte, ‘ <i>New insights into the pathomechanism of cyclic neutropenia</i> ’, Annals of the New York Academy of Science, accepted January 2020. P. Mir , M. Klimiankou, B. Dannenmann, N. Aghaallaei, M. Nasri, S. Wingert, F. Thalheimer, B. Findik, L. Doll, M. Ritter, T. Thumberger, S. Kandabarau, C. Zeidler, M. Rieger, B. Bajoghli, K. Welte and J. Skokowa, ‘ <i>Retinoic acid restores granulocytic differentiation in severe congenital neutropenia: Role of GADD45b-dependent gene demethylation</i> ’, in revision.

B. H. Alvarez*, J. Skokowa*, M. Coles* , **P. Mir**, L. Weidmann, K. W. Rogers, K. Welte, A. Lupas, P. Müller, M. ElGamacy, '*Design of novel granulopoietic proteins by topological resccaffolding*', manuscript in revision. (*equal contribution)

B. H. Alvarez*, J. Skokowa*, M. Coles , **P. Mir**, K. W. Rogers, K. Maksymenko, M. Nasri, K. Welte, A. Lupas, P. Müller, M. ElGamacy, '*A topological refactoring design strategy yields highly stable granulopoietic proteins*', in revision. (*equal contribution)

Y. Xu, M. Nasri, B. Dannenmann, **P. Mir**, A. Zahabi, K. Welte, Tatsuya Morishima*, Julia Skokowa*, '*NAMPT/SIRT2-mediated inhibition of the p53-p21 signaling pathway is indispensable for maintenance and hematopoietic differentiation of human iPSC cells*', in revision. (*equal contribution)

2019 B. Dannenmann, A. Zahabi, **P. Mir**, B. Oswald, R. Bernhard, M. Klimiankou, T. Morishima, K. Schulze-Osthoff, C. Zeidler, L. Kanz, N. Lachmann, T. Moritz, K. Welte and J. Skokowa, '*Human iPSC-based model of severe congenital neutropenia reveals elevated UPR and DNA damage in CD34+ cells preceding leukemic transformation*', *Experimental Hematology*, vol. 71, p. 51-60, January 2019.

M. Nasri*, **P. Mir***, B. Dannenmann, D. Amend, T. Skroblyn, Y. Xu, K. Schulze-Osthoff, M. Klimiankou, K. Welte and J. Skokowa, '*Fluorescent labeling of CRISPR/Cas9 RNP for gene knockout in HSPCs and iPSCs reveals an essential role for GADD45b in stress response*', *Blood Advances*, vol. 3, no. 1, p. 63-71, January 2019. (*equal contribution)

M. Nasri, M. Ritter*, **P. Mir***, B. Dannenmann*, N. Aghaallaei, D. Amend, V. Makaryan, Y. Xu, B. Fletcher, R. Bernhard, I. Steiert, K. Hähnel, J. Berger, I. Koch, B. Sailer, K. Hipp C. Zeidler, M. Klimiankou, B. Bajoghli, D. C. Dale, K. Welte and J. Skokowa, '*CRISPR/Cas9 mediated ELANE knockout enables neutrophilic maturation of primary hematopoietic stem and progenitor cells and induced pluripotent stem cells of severe congenital neutropenia patients*', *Haematologica*, vol. 105, no. 3, p. 598-609, June 2019. (*equal contribution)

2016 T. Schaefer*, H. Wang*, **P. Mir**, M. Konantz, T. Pereboom, B. Merz, T. Fehm, S. Perner, O. Rothfuss, L. Kanz, K. Schulze-Osthoff, C. Lengerke. '*Molecular and functional interactions between AKT and SOX2 in breast carcinoma*', *Oncotarget* 2016. (*equal contribution)

AUSZEICHNUNGEN | 2019 **P. Mir**, '*GADD45b plays an essential role in the G-CSF triggered granulocytic differentiation of human hematopoietic cells*', Vortrag, Auszeichnung mit dem **Best Abstract Award, Best of DGHO** 'Translational Medicine', Annual meeting of German Society of Hematology and Oncology (DHGO), Berlin

P. Mir, '*Active DNA demethylation mediated by GADD45 β is essential during G-CSF triggered granulocytic differentiation*', Vortrag, winner of Auszeichnung mit dem **ASH Abstract Achievement Award**, Annual meeting of the American Society of Hematology (ASH), Orlando

2018 **P. Mir**, '*GADD45b plays an essential role in the G-CSF triggered granulocytic differentiation of human hematopoietic cells*', Vortrag, Auszeichnung mit dem **ASH Abstract Achievement Award**, ASH annual meeting, San Diego

	2017	P. Mir , ' <i>Abrogated GADD45b-mediated integrity control of hematopoietic stem cells upon ER stress and DNA damage triggers lymphopoiesis over granulopoiesis in congenital neutropenia</i> ', Vortrag, Auszeichnung mit dem ASH Abstract Achievement Award , ASH annual meeting, Atlanta
	2013	P. Mardan , ' <i>Interactions between the embryonic stem cell protein SOX2 and the AKT signaling pathway regulate breast cancer stem cells</i> ' Vortrag, Auszeichnung mit dem Young Investigator's Award und Best of congress – translational research “ DGHO, Wien
WISSENSCHAFTLICHE ERFAHRUNGEN 	2015	Mai – Juli Wissenschaftliche Hilfskraft im Labor von Prof. Dr. Schulze-Osthoff (UKT/IFIB)
	2014	Zweimonatiges Praktikum bei <i>Immatics Biotechnologies GmbH</i> , Betreuung durch Dr. Toni Weinschenk
	2012– 2013	Wissenschaftliche Hilfskraft in der Arbeitsgruppe von Prof. Dr. Claudia Lengerke mit eigenständigem Projekt: ' <i>Interactions between the embryonic stem cell protein SOX2 and the AKT signaling pathway regulate breast cancer stem cells</i> '
	2008/ 2010	Stipendium zur Teilnahme an der 125. & 126. Tagung der Gesellschaft deutscher Naturforscher und Ärzte (GDNÄ)

Tübingen, den 05.08.2020